

**HOST-GUEST CHEMISTRY BETWEEN CUCURBIT[7]URIL AND
CATIONIC AND NEUTRAL GUESTS**

by

Brendan C. MacGillivray

A thesis submitted to the Department of Chemistry
in conformity with the requirements for
the degree of Master of Science

Queen's University
Kingston, Ontario, Canada
(September 2012)

Copyright © Brendan C. MacGillivray, 2012

Abstract

This thesis describes the use of electrospray mass spectrometry, ^1H NMR, and UV-visible spectroscopy, along with molecular modeling studies, to characterize the host-guest complexes that are formed between the cucurbit[7]uril (CB[7]) host molecule and a series of cationic alkylammonium (benzethonium), biguanidinium (metformin, phenformin, chlorhexidine and alexidine), amidinium (berenil, pentamidine, and 4-hydroxy- and 4-aminobenzamidines), and flavylum (4'- and 6-methoxyflavylium and 6,4'-dimethoxyflavylium) guests in aqueous solution. The stoichiometries and binding strengths of the CB[7] host-guest complexes with these series of drug and dye molecules were determined, and have been rationalized in terms of the specific ion-dipole interactions and hydrophobic effects involved. The potential uses of CB[7] as a slow-release drug delivery agent and molecular stabilizing agent are indicated from kinetic and spectroscopic studies on the reactivities of the host-guest complexes.

CB[7] forms 1:1 and 2:1 host-guest complexes with the benzethonium cation by sequential binding to the hydrophilic benzyldimethylammonium group and the hydrophobic 2,4,4-trimethylpentyl group, respectively. The binding strength at the former site is consistent with data for other CB[7]-benzylammonium guests, while the strength of binding of the neutral hydrophobic group results from efficient packing within the inner CB[7] cavity.

Each of the biguanidinium guests was shown to form strong 1:1 host-guest complexes with CB[7]. Metformin proved to be small enough to form 1:2 host-guest complexes at low concentrations of CB[7], while chlorhexidine and alexidine were shown to be large enough

to form sequential 2:1 and 3:1 host-guest complexes with CB[7]. UV-visible pH titrations showed that CB[7] binds more strongly to mono-protonated metformin than the di-protonated form of this guest.

Both pentamidine and berenil formed tightly bound complexes with CB[7], indicating that this host could potentially act as carrier for these drug molecules. CB[7] catalyzes the acid decomposition of berenil and each of the decomposition products, 4-hydroxy- and 4-aminobenzamidinium, bind to CB[7] with increases in their pK_a values in the presence of CB[7].

The three flavylum dyes, with cationic oxonium centers, were shown to complex strongly with CB[7], resulting in a stabilization of the flavylum cation, with respect to the ring-opened 2-hydroxychalcones in neutral solutions.

Acknowledgements

I would, first and foremost, like to thank my supervisor, Dr. Donal Macartney for giving me the opportunity to conduct research in his lab. While I cannot adequately express my gratitude for all that he has done for me, I will say that working for him has been a true pleasure and that he has been an incredible supervisor, mentor, and friend. I will be forever grateful for his support, guidance and patience during my time here.

I would especially like to thank my parents Keith and Rhonda, and my sisters Chelsea and Breanna for all their love and support. I would be nowhere without you guys, and I am eternally gratefully for everything you have done for me.

I would like to thank everyone in the Department of Chemistry for the lessons they have taught me and the guidance they have given me. In particular, I'd like to thank Dr. Françoise Sauriol for her guidance in every aspect of NMR, Dr. Jiayi Wang for his assistance with mass spectrometry, and Dr. Lyndsay Hull for loaning me equipment and chemicals as needed. I would also like to thank my committee members, Dr. Anne Petitjean and Dr. Simon Hesp for their valuable time and helpful suggestions during the course of my research. Finally, I would like to thank Dr. Henryka Tilk for helping to build and inspire my love of teaching, and for setting an incredible example of what an excellent teacher should be.

While working in the Macartney lab, I have had the opportunity to work with a number of devoted colleagues, mentors, and friends. Thanks for everything, Ian Wyman, Mona Gamal Eldin, Julian Kwok, Kristina Stevenson, Alex Love, Jason Rygus and Jen Adams (honorary member).

I would be remiss, if I failed to thank all of the friends in my personal life who have made my time at Queen's legendary! You have all been an endless source of kindness, patience and support, and from the bottom of my heart I'd like to thank-you Heather Mowatt, Virginia Dafoe, Hope Hutchins, Tim Clutton, Gillian Besco, James Beattie, Eileen McEwen, Andrew Engbretson, Sarah Fong, Heidi Manicke, Chi Yan Lam, Ioana Cozma, Zach Chan, Catherine Jee, Kayleigh Campbell, Josh McCaul, Rakesh Rajdev, Andrew Labaj and anyone else who I may have forgotten.

Finally, I'd like to thank the person who I couldn't place in any other category because he fits into almost all of them. Andrew Fraser (the good one, not the other one), I don't know how of you put up with me for over 20 years, but I'm thankful that you have. As we part company, I'd like to leave you with quote from Beethoven (the guy, not the dog) "Never shall I forget the time I spent with you. Please continue to be my friend, as you will always find me yours." Thank you so much for everything!

TABLE OF CONTENTS

Abstract.....	ii
Acknowledgements.....	iv
Table of Contents.....	vi
List of Figures.....	xii
List of Tables.....	xix
List of Abbreviations.....	xx

Chapter 1

INTRODUCTION.....	1
1.1 Supramolecular Chemistry.....	1
1.1.1 Non-Covalent Interactions of Supramolecular Complexes.....	1
1.1.1.1 Electrostatic Interactions.....	2
1.1.1.2 Hydrogen Bonding.....	4
1.1.1.3 π -Bonding.....	6
1.1.1.4 Dispersion Forces.....	8
1.1.1.5 Hydrophobic Effect.....	9
1.1.2 Concepts in Supramolecular Chemistry.....	9
1.1.2.1 Complementarity.....	10
1.1.2.2 Preorganization.....	12
1.1.2.3 Molecular Recognition.....	14
1.2 Classification of Supramolecular Complexes.....	15
1.2.1 Molecular Self-Assembly.....	15

1.2.2	Host-Guest Chemistry.....	16
1.2.2.1	Crown Ethers.....	18
1.2.2.2	Cryptands.....	20
1.2.2.3	Calixarenes.....	21
1.2.2.4	Cyclodextrins.....	24
1.3	Cucurbituril.....	27
1.3.1	Properties of Cucurbiturils.....	29
1.3.2	Homologues of Cucurbituril.....	30
1.3.3	Cucurbit[<i>n</i>]uril Host-Guest Complexes.....	31
1.3.4	Applications of Cucurbit[7]uril.....	33
1.3.4.1	Molecular Catalysis.....	33
1.3.4.2	Drug Delivery.....	35
1.3.4.3	Chemical Sensors.....	36
1.4	Research Aims.....	38
	References.....	39

Chapter 2

	EXPERIMENTAL SECTION.....	42
2.1	Preparation of Materials.....	42
2.1.1	Synthesis of the CB[7] Host Compound.....	42
2.1.2	Synthesis of the Guest Compound.....	43
2.2	Experimental Methods and Apparatus.....	47
2.2.1	Mass Spectrometry.....	47

2.2.2	Nuclear Magnetic Resonance Spectroscopy.....	48
2.2.3	NMR Chemical Shift Titrations.....	49
2.2.4	UV-Visible Spectroscopy.....	52
2.2.5	Chemical Structures & Molecular Modeling Studies.....	53
2.3	Determination of Binding Constants.....	53
2.3.1	Fitting a Binding Curve.....	55
2.3.2	Competitive Binding Studies.....	57
2.3.3	Statistical Binding.....	60
2.4	Complexation-Induced pK_a Shifts.....	62
2.5	Complexation-Induced Changes in Rate Constant	62
	References.....	64

Chapter 3

	HOST-GUEST COMPLEXATION BETWEEN CB[7] AND BENZETHONIUM.....	66
3.1	Introduction.....	66
3.2	Results and Discussion.....	69
3.2.1	ESI Mass Spectrometry and 1H NMR Spectroscopy.....	69
3.2.2	Determination of Binding Constants.....	75
3.2.2.1	Binding of the Hydrophilic Moiety.....	75
3.2.2.2	Binding of the Hydrophobic Moiety.....	76
3.2.3	Potential Applications of CB[7]·Benzethonium Host-Guest Complexes.....	79
3.3	Conclusions.....	80
	References.....	81

Chapter 4

HOST-GUEST COMPLEXATION BETWEEN

CUCURBIT[7]URIL AND BIGUANIDIUM GUESTS.....	83
4.1 Introduction.....	83
4.2 Results and Discussion.....	88
4.2.1 ESI Mass Spectrometry.....	88
4.2.2 ¹ H NMR Spectroscopy.....	90
4.2.2.1 Metformin.....	91
4.2.2.2 Phenformin.....	95
4.2.2.3 Chlorhexidine.....	97
4.2.2.4 Alexidine.....	101
4.2.3 Determination of Binding Constants.....	106
4.2.3.1 Metformin.....	106
4.2.3.2 Phenformin.....	108
4.2.3.3 Chlorhexidine.....	109
4.2.3.4 Alexidine.....	112
4.3 Comparison of the Binding Modes of CB[7] with the Bis(biguanidinium) Guests and other Polycationic Guests.....	115
4.4 Effect of Complexation of Metformin by CB[7] on the Guest pK _a value.....	118
4.5 Conclusions.....	120
References.....	121

Chapter 5

HOST-GUEST COMPLEXATION BETWEEN CB[7] AND AMIDINIUM GUESTS....	124
5.1 Introduction.....	124
5.2 Results and Discussion.....	128
5.2.1 ESI Mass Spectrometry and ¹ H NMR Spectroscopy.....	128
5.2.2 Determination of Binding Constants.....	139
5.2.3 Kinetics of Berenil Decomposition.....	143
5.3 Conclusions.....	147
References.....	148

Chapter 6

HOST-GUEST COMPLEXATION BETWEEN CB[7] AND FLAVYLIUM GUESTS...	149
6.1 Introduction.....	149
6.2 Results and Discussion.....	152
6.2.1 ESI Mass Spectrometry and ¹ H NMR Spectroscopy.....	152
6.2.2 Determination of Binding Constants.....	160
6.2.3 UV-visible Spectroscopy.....	161
6.2.3.1 Flavylium/2-Hydroxychalcone Hydrolysis Equilibrium.....	161
6.2.3.2 <i>Cis-</i> to <i>Trans</i> -hydroxychalcone Isomerization.....	168
6.2.3.3 Thermal <i>Cis-</i> to <i>Trans</i> -hydroxychalcone Isomerization in Basic Solution...	170
6.3 Conclusions.....	172
References.....	173

Chapter 7

CONCLUSIONS AND SUGGESTIONS FOR FUTURE WORK.....	174
7.1 Introduction.....	174
7.2 The Benzethonium Guest.....	174
7.3 The Biguanidinium Guests.....	177
7.4 The Amidinium Guests.....	179
7.5 The Flavylum Guests.....	182
References.....	184

LIST OF FIGURES

Figure 1.1	(a) An optimal ion-dipole alignment (b) A slightly misaligned ion-dipole interaction (c) A misaligned ion-dipole interaction.....	3
Figure 1.2	(a) A perpendicular dipole-dipole interaction (b) A parallel dipole-dipole interaction.....	4
Figure 1.3	The formation of a hydrogen bond between a proton donor and proton acceptor.....	5
Figure 1.4	A depiction of a cation- π interaction.....	7
Figure 1.5	An edge-to-face and face-to-face π - π stacking interaction.....	8
Figure 1.6	The complementarity between molecules with (a) good shape fit and poor size fit (b) good size fit and poor shape fit (c) good shape and size fit.....	10
Figure 1.7	A depiction of two complementary molecules interacting with one another through a variety of non-covalent interactions.....	11
Figure 1.8	The addition of ammonia or ethylenediamine to a hydrated nickel complex.....	13
Figure 1.9	The binding of an acyclic ligand and macrocyclic ligand to zinc(II).....	14
Figure 1.10	A set of self-assembling DNA bases.....	16
Figure 1.11	An illustration of 18-crown-6.....	18
Figure 1.12	The binding of 18-crown-6 and its acyclic counterpart.....	19
Figure 1.13	An example of a cryptand host molecule, specifically [2.2.2]cryptand.....	20
Figure 1.14	The calix[4]arene and calix[6]arene homologues in their cone configurations.....	22

Figure 1.15	Calix[4]arene in the 1-2-alternate, 1-3-alternate, and partial cone configurations.....	23
Figure 1.16	The structures of α , β and γ -cyclodextrins.....	25
Figure 1.17	The reaction scheme for the synthesis of cucurbituril.....	28
Figure 1.18	A stick side-view and space-filling top-view diagram of the first synthesized cucurbituril molecule.....	28
Figure 1.19	The cyclization of omeprazole from its in-active form to its active form.....	34
Figure 1.20	The base-on/base-off equilibrium of vitamin B ₁₂ and the effect of CB[7] binding.....	37
Figure 2.1	The mechanism used to convert 2-hydroxybenzaldehyde and acetophenone into a flavylum salt.....	44
Figure 2.2	The acid-catalyzed formation of 6-methoxyflavylium, 4'-methoxyflavylium, and 6,4'-dimethoxyflavylium.....	45
Figure 2.3	A summary of the effects exhibited by a guest, when binding to CB[7].....	50
Figure 3.1	The structure of the conjugate acid of amantadine.....	67
Figure 3.2	The structure of the benzethonium cation.....	68
Figure 3.3	¹ H NMR proton resonance assignments for the benzethonium cation.....	70
Figure 3.4	A stack plot of the ¹ H NMR spectra of benzethonium.....	72
Figure 3.5	¹ H NMR $\Delta\delta_{lim}$ values for the titration of benzethonium with CB[7].....	73
Figure 3.6	Energy-minimized gas-phase structure of the 2:1 host-guest complex of CB[7] and the benzethonium cation.....	73
Figure 3.7	The CB[7] complexation-induced chemical shift changes for cationic guests containing benzylammonium and related binding sites.....	74

Figure 3.8	Binding curves for the 1:1 and 2:1 CB[7]·benzethonium complexes.....	76
Figure 4.1	The structures of (a) the guanidinium cation (b) the biguanidinium cation...	84
Figure 4.2	The chemical structures of (a) metformin (b) phenformin.....	84
Figure 4.3	The chemical structures of chlorhexidine and alexidine.....	86
Figure 4.4	The ESI mass spectrum of chlorhexidine in the presence of excess CB[7]...	89
Figure 4.5	The CB[7] complexation-induced chemical shift changes for the biguanidinium and bis(biguanidinium) guests.....	91
Figure 4.6	A stack plot of the ¹ H NMR spectra of metformin.....	92
Figure 4.7	Binding curves for the 1:2 and 1:1 CB[7]·metformin complexes.....	93
Figure 4.8	Host-guest equilibria between CB[7] and metformin.....	94
Figure 4.9	A stack plot of the ¹ H NMR spectra of phenformin.....	96
Figure 4.10	Host-guest stability constants and $\Delta\delta_{lim}$ values for the CB[7] complexations of cationic guests containing benzyl functional groups.....	97
Figure 4.11	A stack plot of the ¹ H NMR spectra of chlorhexidine.....	99
Figure 4.12	Stepwise formation of the 1:1, 2:1, and 3:1 host-guest complexes formed between CB[7] and chlorhexidine.....	100
Figure 4.13	A stack plot of the ¹ H NMR spectra of alexidine.....	102
Figure 4.14	Stepwise formation of the 1:1, 2:1, and 3:1 host-guest complexes formed between CB[7] and alexidine.....	104
Figure 4.15	Alternative stepwise formation of the 1:1, 2:1, and 3:1 host-guest complexes formed between CB[7] and alexidine.....	105
Figure 4.16	The chemical structures of (a) the tetramethylammonium cation and (b) <i>p</i> -toluidinium cation competitor guests.....	107

Figure 4.17	Speciation diagram for the host-guest complexes of chlorhexidine with CB[7].....	110
Figure 4.18	The pH dependences of the absorbances of metformin in the absence and presence of CB[7]	119
Figure 5.1	The structure of an amidinium cation.....	124
Figure 5.2	The chemical structures of berenil, pentamidine, and DAPI.....	125
Figure 5.3	The acid-catalyzed cleavage of central triazene group of berenil.....	127
Figure 5.4	A stack plot of the ^1H NMR spectra of pentamidine.....	130
Figure 5.5	A stack plot of the ^1H NMR spectra of berenil.....	131
Figure 5.6	Stack plots of the ^1H NMR spectra of 4-aminobenzamidine and 4-hydroxybenzamidine	132
Figure 5.7	The ^1H NMR $\Delta\delta_{\text{lim}}$ values are shown for the titration of (a) DAPI, (b) pentamidine, (c) berenil, (d) 4-aminobenzamidine, and (e) 4-hydroxybenzamidine with CB[7].....	134
Figure 5.8	The energy-minimized gas-phase structures of the 1:1 and 2:1 host-guest complexes formed between CB[7] and pentamidine.....	135
Figure 5.9	The energy-minimized gas-phase structure of the 1:1 host-guest complex formed between CB[7] and berenil.....	137
Figure 5.10	The energy minimized structures of the CB[7] host-guest complexes with 4-aminobenzamidine and 4-hydroxybenzamidine.....	138
Figure 5.11	The chemical structure of the <i>p</i> -toluidinium cation.....	140
Figure 5.12	The absorbance spectra of berenil over time in an aqueous solution at pH 2.5 in the absence and presence of CB[7].....	144

Figure 5.13	The time-dependent absorbance of berenil at 370 nm in an aqueous solution at pH 2.00 in the absence and presence of CB[7].....	145
Figure 5.14	A first-order plot of the degradation of berenil in the absence and presence of CB[7] at pH 2.00.....	145
Figure 5.15	A plot of the log of the rate constants for the berenil degradation against pH in the absence and presence of CB[7].....	146
Figure 6.1	The chemical and space-filling structures of a flavylum cation.....	149
Figure 6.2	The chemical structures of the (a) 4'-methoxyflavylium, (b) 6-methoxyflavylium, and (c) 6,4'-dimethoxyflavylium cations.....	150
Figure 6.3	The base-catalyzed conversion of a flavylum cation to a <i>trans</i> -2-hydroxychalcone in aqueous solution.....	151
Figure 6.4	A stack plot of the ¹ H NMR spectra of the 4'-methoxyflavylium cation....	154
Figure 6.5	A stack plot of the ¹ H NMR spectra of the 6-methoxyflavylium cation.....	155
Figure 6.6	A stack plot of the ¹ H NMR spectra of the 6,4'-dimethoxyflavylium cation.....	156
Figure 6.7	Plots of $-\Delta\delta_{\text{obs}}$ against [CB[7]]/[Guest] for the titrations of the 4'-methoxyflavylium, 6-methoxyflavylium and 6,4'-dimethoxyflavylium cations in D ₂ O.....	157
Figure 6.8	The ¹ H NMR $\Delta\delta_{\text{lim}}$ values are shown for the titration of the (a) 6-methoxyflavylium, (b) 4'-methoxyflavylium, and (c) 6,4'-dimethoxyflavylium cations with CB[7].....	158
Figure 6.9	The possible structures of host-guest complexes of the 6,4'-dimethoxyflavylium cation with the CB[7] host.....	159

Figure 6.10	The energy-minimized gas phase structures of two potential 1:1 host-guest complexes formed between CB[7] and the 6,4'-dimethoxyflavylium cation.....	159
Figure 6.11	The chemical structure of the tetraethylammonium cation.....	161
Figure 6.12	A UV-visible titration of 6,4'-dimethoxyflavylium.....	162
Figure 6.13	A plot of the absorbance as a function of the CB[7]/6,4'-dimethoxyflavylium ratio.....	163
Figure 6.14	The pH dependent absorbance spectra of the 6,4'-dimethoxyflavylium cation at in the absence and presence of CB[7].....	164
Figure 6.15	The absorbance spectra of the 4'-methoxyflavylium cation in the absence and presence of CB[7] as a function of pH.....	165
Figure 6.16	The absorbance spectra of the 6-methoxyflavylium cation in the absence and presence of CB[7] as a function of pH.....	165
Figure 6.17	The absorbance spectra of the 6,4'-dimethoxyflavylium cation in the absence and presence of CB[7] as a function of pH.....	166
Figure 6.18	The UV-visible spectra of neutral solutions of the 4'-methoxyflavylium, 6-methoxyflavylium, and 6,4'-dimethoxyflavylium immediately after dissolution and after 24 hours in the dark and after 24 hours under light in the absence and presence of CB[7].....	160
Figure 6.19	Time-dependent spectra of the reaction of a solution of the 6,4'-dimethoxyflavylium cation containing CB[7] upon addition of NaOH.....	170

Figure 6.20	Plot of the absorbance as a function of time for the reaction of the 6,4'-dimethoxyflavyium cation with and without CB[7] upon addition of NaOH.....	171
Figure 6.21	Plots of $\ln(A_{inf} - A_t)$ against time for the reaction of the 6,4'-dimethoxyflavyium cation with and without CB[7] upon addition of NaOH.....	171
Figure 7.1	Structure of 1-hydroxy-4-methyl-6-(2,4,4-trimethylpentyl)-2(1H)-pyridinone.....	177
Figure 7.2	Structure of the 4-aminobenzamidinium cation appended to agarose beads (R) with a glycine-glycine spacer.....	181
Figure 7.3	The structure of bis-(7-hydroxyflavylium) compound containing a methyl viologen bridge.....	183

LIST OF TABLES

Table 1.1	The dimensions and volumes of cucurbit[<i>n</i>]urils.....	31
Table 2.1	The host and guest concentrations used to conduct the titrations.....	50
Table 4.1	High resolution ESI-MS data for the host-guest complexes of CB[7] with the metformin, phenformin, chlorhexidine, and alexidine guests.....	88
Table 4.2	The host-guest stability constants for CB[7] complexes with metformin, phenformin, chlorhexidine and alexidine.....	114
Table 4.3	Stability constants and $\Delta\delta_{\text{lim}}$ values for guest hexamethylene chain proton resonances for the 1:1 and 2:1 CB[7] host-guest complexes.....	117
Table 5.1	High resolution ESI-MS data for the host-guest complexes of CB[7] with pentamidine, berenil, 4-aminobenzamidine, and 4-hydroxybenzamidine...	129
Table 5.2	The host-guest stability constants for CB[7] complexes with pentamidine, berenil, DAPI, 4-aminobenzamidine, and 4-hydroxybenzamidine.....	141
Table 6.1	High resolution ESI-MS data for the host-guest complexes of CB[7] with the 4'-methoxyflavylium, 6-methoxyflavylium, and 6,4'-dimethoxyflavylium cations in aqueous solution.....	152
Table 6.2	The calculated pK_{H} values for the flavylium cations in the absence and presence of CB[7] in aqueous solution.....	166

LIST OF ABBREVIATIONS

α -CD	alpha-cyclodextrin
α -DMB	α -axial-5,6-dimethylbenzimidazole
β -CD	beta-cyclodextrin
γ -CD	gamma-cyclodextrin
δ	chemical shift
δ^-	partially negatively charged
δ^+	partially positively charged
δ_{bound}	bound chemical shift
δ_{free}	free chemical shift
$\Delta\delta$	change in chemical shift
$\Delta\delta_{\text{obs}}$	observed change in chemical shift
λ_{max}	wavelength of maximum absorbance
$^{\circ}\text{C}$	degrees Celsius
$^1\text{H NMR}$	proton nuclear magnetic resonance
\AA	angstrom
A_{G}	absorbance of guest
A_{HG}	absorbance of host-guest complex
A_{obs}	observed absorbance
A_0	absorbance at time 0
A_t	absorbance at time t
AMPK	adenine monophosphate-activated protein kinase

CB	cucurbituril
CB[<i>n</i>]	cucurbit[<i>n</i>]uril
CB[5]	cucurbit[5]uril
CB[6]	cucurbit[6]uril
CB[7]	cucurbit[7]uril
CB[8]	cucurbit[8]uril
CB[10]	cucurbit[10]uril
CD	cyclodextrin
CGTase	cyclodextrin transferase
C	competitor
C _b	bound competitor
C _f	free competitor
C _{Tot}	total competitor
cm	centimeter
D ₂ O	deuterium oxide
DABCO	1,4-diazabicyclo[2,2,2]octane
DAPI	4',6-diamidino-2-phenylindole
DCI	deuterium chloride
DMSO- <i>d</i> ₆	deuterated dimethyl sulfoxide
DNA	deoxyribonucleic acid
d	doublet
dd	doublet of doublets
ESI	electrospray ionization

en	ethylenediamine
FV	flavylium
G_b	bound guest
G_f	free guest
G_{Tot}	total guest
g	gram
H_b	bound host
H_f	free host
H_{Tot}	total host
H·C	host-competitor complex
H·G	host-guest complex
HOD	deuterium hydroxide
Hz	hertz
IR	infrared
imid	imidazolium
isoquin	isoquinolinium
J	coupling constant
K	association constant, binding constant, or equilibrium constant
K_H	hydrolysis equilibrium constant
K_I	photochemical isomerization equilibrium constant
K_{rel}	relative binding constant
K_{obs}	observed binding constant
K_T	ring-opening tautomerization equilibrium constant

k	rate constant
k_{bound}	rate constant for bound guest
k_{free}	rate constant for free guest
k_{on}	rate constant for host-guest complex formation
k_{off}	rate constant for host-guest complex dissociation
kg	kilogram
kJ	kilojoule
L	litre
LKB1	liver kinase B1
LPS	lipopolysaccharide
M	molar
Mebpy	methyl bipyridinium
Mepyr	methyl pyridinium
MHz	megahertz
MS	mass spectrometry
m	multiplet
mg	milligram
min	minute
mM	millimolar
mmol	millimole
mL	millilitre
mol	mole
m/z	mass to charge ratio

NMR	nuclear magnetic resonance
n	number of polymeric subunits
nm	nanometer
pD	$-\log [D^+]$
pH	$-\log [H^+]$
pK_a	$-\log K_a$
ppm	parts per million
r	the distance between two ions
SDS	sodium dodecyl sulfate
s	second or singlet
TOF	time of flight
t	time or triplet
<i>t</i> -Bupyr	tert-butylpyridinium
td	triplet of doublets
UV	ultraviolet
vis	visible

Chapter 1

INTRODUCTION

1.1 Supramolecular Chemistry

Supramolecular chemistry has been described by one its forefathers, Jean-Marie Lehn, as the “chemistry beyond the molecule”.^{1,2,3} This definition arose because, unlike the traditional fields in chemistry, which exclusively examine the properties of a single molecule or complex, supramolecular chemistry focuses on the interaction between several molecules and the effect of that interaction on their properties.¹ In order to understand the interaction between two molecules, it is necessary to examine the forces that attract molecules to each other and hold them in place. In supramolecular systems, these forces are called non-covalent interactions, which are described as follows.^{2,3}

1.1.1 Non-covalent Interactions of Supramolecular Complexes

Supramolecular chemistry has also been described by Lehn as the “chemistry of the non-covalent bond”.^{3,4} This characterization came about because non-covalent bonds are the intermolecular glue that hold supramolecular complexes together.² Although non-covalent bonds (with bond strengths of 2 – 300 kJ/mol) are considered weaker than their covalent counterparts (with bond strengths in the range of 150 – 450 kJ/mol for single bonds), it is not the strength of any one bond that imparts stability.^{2,4,5} The true power of supramolecular chemistry arises when weak non-covalent interactions act in combination to hold two or more molecules together.^{2,3,4} By examining the forces that drove the formation of the non-covalent bond, it was determined that these weak interactions could be divided into five

categories. These categories include electrostatic interactions, hydrogen bonding, π -bonding, dispersion forces and hydrophobic effects.^{2,3,4,5}

1.1.1.1 Electrostatic Interactions

Electrostatic interactions are formed by Coulombic attractions between oppositely charged ions or dipoles.^{2,5} The strength of these interactions can vary greatly depending on the distance between the charges, the orientation of the charged molecules, and the dispersion of the charge across each molecule. That being said, however, one of the most important factors in determining the strength of an electrostatic interaction is determining whether an ion-ion interaction, ion-dipole interaction or dipole-dipole interaction is involved.^{3,4,5}

Ion-ion interactions possess bond energies on the order of 100 – 350 kJ/mol, which is comparable in strength to the bond energies of covalent single bonds.^{4,5} There are two factors affecting the strength of this type of interaction. The first factor is the distance between the two ions (r).^{3,4,5} The energy of the bond formed between the ions is proportional to $1/r^2$, so as the ions approach each other, the bond formed between them grows increasingly stronger.⁵ This trend continues until the repulsion of the ions' electron clouds are equal to the attractive forces caused by their charges. At this point the distances between the charges and the bond strength have been optimized. The other factor affecting bond strength is the degree of charge delocalization across the molecular structure of the ion.^{3,4,5} The strongest ion-ion interaction occurs when the charges are localized to a single atom on each of the ions.⁵ If one or both of the charges is able to delocalize across several atoms on one or both of the ions,

then the bond between them weakens. Thus, two ions which are close to each other in space and have localized charges form the strongest type of non-covalent bond.

Ion-dipole interactions form the next strongest type of non-covalent bond, with bond energies ranging from 50 – 200 kJ/mol.^{3,4,5} As in ion-ion interactions, the distance between the charges and the charge distribution across the molecules both play roles in the strength of this bond.⁵ However, two additional factors, the strength of the dipole and the directionality of the dipole, can have a major impact on the strength of an ion-dipole interaction. To form a dipole, two adjacent atoms must possess a difference in electronegativity, with one atom being more negative (δ^-) and the other more positive (δ^+). The greater the difference in electronegativity, the stronger the dipole and the stronger the ion-dipole interaction formed by that dipole. The line formed by the bond connecting these two atoms represents the directionality of the dipole. The strongest ion-dipole interactions form when the ion is in position along this line (Figure 1.1A).^{3,5} As the ion moves out of alignment, the ion-dipole interaction weakens (Figure 1.1B) and ceases to exist once the ion reaches a position perpendicular to directionality of the dipole (Figure 1.1C).^{3,5} Thus, strong ion-dipole interactions occur when a strong dipole is directly aligned with a nearby ion.⁵

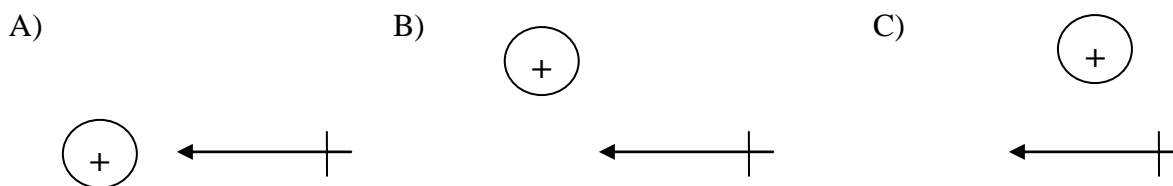
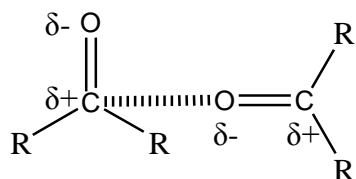


Figure 1.1 A) The ion is in optimal alignment with the dipole. B) The ion has moved out of alignment, but can still interact with the dipole. C) The ion is perpendicular to the dipole, out of alignment and does not form a non-covalent bond.

Dipole-dipole interactions are the weakest form of electrostatic interaction, with bond strengths of 5 - 50 kJ/mol.^{3,4,5} As with ion-dipole interactions, the strength, directionality and distance between each dipole play a role in the overall strength of this interaction.^{3,5} However, unlike ion-dipole interactions, the alignment of each of the dipoles with one another can play a large role in the strength of the non-covalent bond that forms between them.⁵ There are two forms of optimal dipole-dipole alignments, a perpendicular alignment (Figure 1.2A) and a parallel alignment (Figure 1.2B).^{3,4} The further a pair of dipoles is from those alignments, the weaker the dipole-dipole interaction.

A)



B)

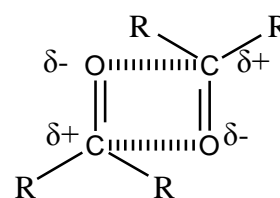


Figure 1.2 A) A perpendicular dipole-dipole interaction between the negative end (δ^-) of one dipole and the positive end (δ^+) of another dipole.^{3,4} B) A parallel dipole-dipole interaction, where both the positive and negative ends of one dipole interact with the negative and positive ends, respectively, of another dipole.

Supramolecular chemists often employ electrostatic interactions to ensure strongly bound complexes, which has resulted in a broad range of supramolecular systems that rely primarily on ions and dipoles in order to bind complexes.²

1.1.1.2 Hydrogen Bonding

Hydrogen bonds have been termed “the master key interaction of supramolecular chemistry” because they are the most flexible form of non-covalent interaction.⁴ This

specific class of dipole-dipole interaction is characterized by the formation of a non-covalent bond between a proton donor and proton acceptor (Figure 1.3).^{3,4}

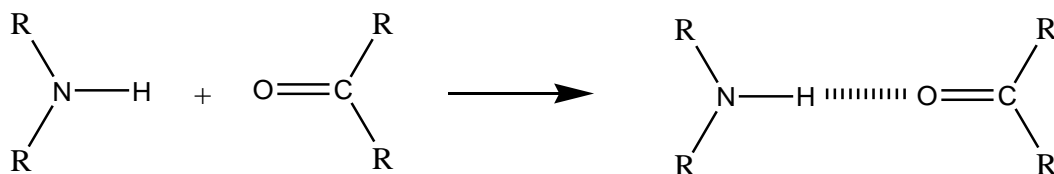


Figure 1.3 Hydrogen bonds are formed between proton donors and protons acceptor. The proton donor groups are electronegative atoms, such as nitrogen, oxygen or fluorine, which are bound to a hydrogen atom (left). The proton acceptors are electronegative atoms on groups such as carbonyls (center). If these two groups are brought close enough together and in the correct orientation, then they form a hydrogen bond (right).^{3,4}

The properties of hydrogen bonds are highly varied in terms of inter-atom bond distance, bond angle and binding energy.^{3,4,5} As a result of this variability, hydrogen bonds are often classified as strong, moderate, or weak, based on their properties.

Strong hydrogen bonds are considered the most rigid, with short bond distances of 2.2 - 2.5 Å and restricted bond angles of 175° – 180°.^{3,5} However, this same rigidity allows for the formation of hydrogen bonds with binding energies of 60 – 120 kJ/mol.^{3,5} This type of hydrogen bond is often essential for attracting the components of supramolecular complexes and keeping them in close proximity to one another.⁴

Moderate hydrogen bonds have longer bond distances of 2.5 – 3.2 Å and broader bond angles of 130° – 180°, which results in reduced rigidity and a binding energy correspondingly lower at 15 – 60 kJ/mol.^{3,5} This type of hydrogen bond often works in combination with strong hydrogen bonds to help lock the components of supramolecular complexes in place.

Weak hydrogen bonds have the longest bond distances of 3.2 – 4.0 Å and the broadest bond angles of 90° – 150°. They also possess the lowest binding energies of less than 15 kJ/mol.^{3,5} Although these hydrogen bonds are too weak to anchor the components of a complex together, they still serve an essential purpose. They act to refine the exact position of the complex components relative to one another, adding an extra degree of selectivity and stability.^{2,4}

The broad range of potential hydrogen bond configurations, when combined with the ease of integrating this type of bond into molecular structures, allows for the formation of structures that are both strongly bound to and highly selective for one another.² As a result, hydrogen bonds are often used to bind molecules together in both natural biological systems and artificial supramolecular complexes.^{2,3,4,5}

1.1.1.3 π -Bonding

π -Bonding occurs when one or more components of a supramolecular complex contain an aromatic π -system.² This π -system can interact non-covalently with either cations or other π -systems to form cation- π interactions and π - π stacking interactions, respectively.⁵ Each of these interactions possess different orientations and strengths, which are described in detail below.

Cation- π interactions form due to a variation of a quadrupole moment which has a partially positive σ -scaffold along the plane of the aromatic ring and a partially negative π -cloud just above and below the plane of the aromatic ring.⁵ A positively charged cation will interact with this negative π -cloud and settle into a position directly above or below the center of the aromatic ring (Figure 1.4). The strength of a cation- π interaction is dependent

on the size and charge distribution of the cation, but usually falls in the range of 5 – 80 kJ/mol.^{4,5}

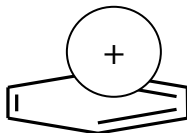


Figure 1.4 Aromatic rings, like the benzene molecule depicted above, participate in cation- π interactions. When the positively charged cation interacts with the partially negative region that is located above or below the plane of an aromatic ring, it causes the cation to settle into a position directly above or below the center of that aromatic ring.⁴

π - π Stacking interactions occur when two aromatic π -systems interact with one another in either an edge-to-face or face-to-face manner (Figure 1.5).^{4,5} In either case, one aromatic π -system interacts with the center of the other aromatic π -system. In the edge-to-face interaction, the negative π -cloud of one ring interacts with the positive σ -scaffold of the other ring.^{4,5} In the face-to-face interaction, the repulsion from both negative π -clouds prevents both rings from aligning in a direct face-to-face manner.⁵ However, since the σ -scaffold protrudes further than the π -cloud at the side of the aromatic ring, therefore the center and outer edge of one ring can interact with the outer edge and center of the other ring system in an offset face-to-face manner.^{4,5} Both the edge-to-face and face-to-face ring systems result in π - π stacking interactions with binding energies of 0 – 50 kJ/mol.^{4,5} These interactions have been built into a number of supramolecular receptors, such as calixarenes, which contain phenyl rings in their subunits.²



Figure 1.5 An edge-to-face interaction between the σ -scaffold of one ring and the π -cloud of the other ring (left). An offset face-to-face interaction between the outer σ -scaffold and center of both aromatic ring systems (right).^{3,4,5}

1.1.1.4 Dispersion Forces

Dispersion forces, or induced dipole-induced dipole forces, are formed between two molecules experiencing induced dipoles.² An induced dipole occurs when a molecule's electron cloud is perturbed by a passing ion or molecule.^{3,4,5} The perturbation creates a temporary imbalance in the molecule's electronic structure, resulting in a weak dipole across the molecule. This weak, induced dipole on one molecule can interact with a similar, but oppositely induced dipole on another molecule forming a weak non-covalent interaction. Although these forces are very common, they are also very weak in comparison to other non-covalent interactions. Dispersion forces are similar to dipole-dipole interactions in that the orientation of the dipoles and the distance between the molecules both play a role in the strength of the interaction that forms.⁴ However, unlike dipole-dipole interactions, induced-dipole interactions possess strengths of less than 5 kJ/mol, making them the weakest type of non-covalent interaction.^{4,5} This inherent weakness, coupled with the fact that induced-dipoles are so unspecific, makes it difficult to design supramolecular complexes that are formed solely by this type of interaction.^{2,3} Therefore, the role of dispersion forces in supramolecular chemistry is limited to strengthening complexes whose formation is driven by other stronger non-covalent forces.²

1.1.1.5 Hydrophobic Effect

Although the hydrophobic effect results from enthalpic and entropic effects, it cannot be considered a force on its own.⁴ While other non-covalent interactions rely on the attraction of oppositely charged molecules, the hydrophobic effect relies on the fact that polar solvent molecules are more strongly attracted to themselves than to a non-polar surface, pocket, or cavity on a supramolecular complex.^{2,4,5,6} Once another molecule with a non-polar region is introduced into solution, it will bind to the non-polar surface and release the water molecules, allowing them to interact with one another, increasing the enthalpy of the system.^{2,4,5} Also, if the non-polar molecule is larger than water, it will likely release several water molecules upon binding, increasing the disorder of the system and, thereby, also increase the entropy of the system.^{2,4,5} Several supramolecular complexes have been designed to take advantage of the hydrophobic effect.^{2,6} One such system is the cyclodextrin host molecule, which contains a central hydrophobic cavity for binding neutral molecules.^{2,6}

1.1.2 Concepts in Supramolecular Chemistry

In supramolecular chemistry, a number of forces act to attract and hold molecules together. Non-covalent bonds, as described in the previous section, act in combination with one another to create and maintain supramolecular complexes.^{2,3,4,5,6} However, there are additional considerations, such as complementarity, preorganization, and molecular recognition that can influence the strength and selectivity of binding sites.^{1,2,3,4,5,6,7} These concepts are described as follows.

1.1.2.1 Complementarity

Emil Fischer, a forefather of modern biochemistry, first described complementarity in 1894 while studying enzyme-substrate complexes.² His work demonstrated that substrates need to match enzymes in terms of size and shape in much the same way keys need to match their locks. This became known as the lock and key principle and was an essential component in the development of molecular biology.^{2,5} Over time, and with a few modifications, this principle was also applied to supramolecular chemistry.⁵

As the lock and key model describes, when two molecules come together to form a supramolecular complex, there must be a match in both size and shape before a tightly bound complex can form (Figure 1.6).^{2,5} If there is a large discrepancy between the two molecules in terms of either size or shape at the binding site, then they will either bind to each other very weakly or will not bind at all.⁵

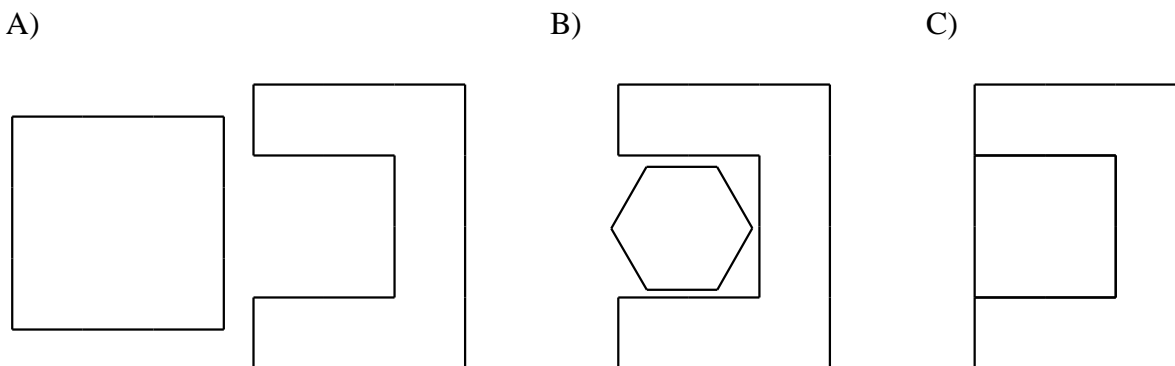


Figure 1.6 A depiction of the lock and key effect. A) One molecule is a good shape fit, but poor size fit for the other, preventing the formation of a complex with strong or selective binding. B) One molecule is a poor shape fit, but good size fit for the other, allowing the formation of a weakly bound complex. C) One molecule is an excellent size and shape fit for the other, allowing for the formation of tightly bound complex.

In addition to the steric matching described above, for two molecules to form a strong complex they must also match each other in terms of their electronic structures.^{2,3,4,5} This electronic match can involve any type of non-covalent interaction, as long as the interacting elements align in a complementary manner along the surface of each molecule (Figure 1.7).^{3,4,5} If each of the interacting components aligns correctly, then a tightly bound complex will result.

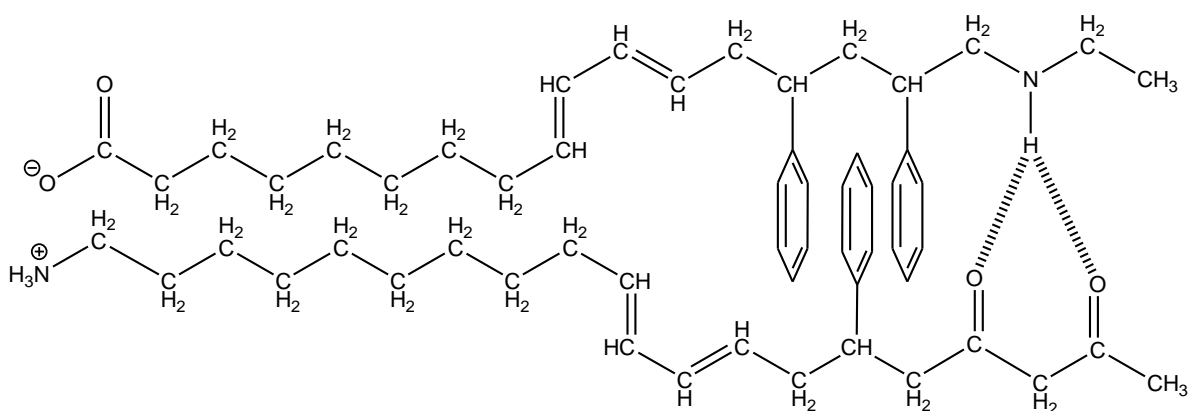


Figure 1.7 A depiction of two complementary molecules interacting with one another via, from left to right, electrostatic interactions, hydrophobic effects, π - π stacking and hydrogen bonding.

Thus, the lock and key model demonstrates that through spatial and electronic complementarity, two molecules can maximize the attractive forces between them and form a strong and selective supramolecular complex.^{2,3,4,5} However, this model fails to take into account one fundamental aspect of supramolecular binding: as molecules increase in size, their structures tend to become more flexible and are able to contort in order to bind to one another.⁵ This increased flexibility falls outside of the model that is based on rigidly defined

components, such as a lock and key. In order to overcome this pitfall, the preorganization principle was introduced.^{5,7}

1.1.2.2 Preorganization

The preorganization principle was first described by Donald Cram during his work on supramolecular host molecules.^{5,7} In order to create his principle, Cram drew inspiration from the chelate effect and the macrocyclic effect, which were known principles of coordination chemistry.^{5,7}

The chelate effect refers to the fact that multidentate ligands form complexes that are more stable than complexes formed by their monodentate counterparts.^{2,3,4,5} An example of this effect is the addition of ammonia or ethylenediamine (en) to a hydrated nickel complex (Figure 1.8).² The resulting Ni(en)_3^{2+} complex has a $\log\beta$ value of 18.28 making it ten orders of magnitude more stable than the $\text{Ni(NH}_3)_6^{2+}$ complex, which has a $\log\beta$ of 8.61.² This effect is a result of both entropic and enthalpic influences. The ammonia addition involves six ammonias replacing six waters, so there is very little entropic benefit to this reaction. Also, the process of bringing six polar ammonia groups together to form a complex has some enthalpic costs. The ethylenediamine addition, however, involves three ethylenediamines replacing six waters, so the net release of water increases disorder, and, therefore increases entropy. Also, ethylenediamine has already paid some of the enthalpic costs by having three sets of molecules with two polar groups already in close proximity to one another. As a result, the ethylenediamine complex is much more stable than its ammonia counterpart. It was this increase in complex stability that intrigued Cram and led him to integrating this effect into his preorganization principle.^{2,5}

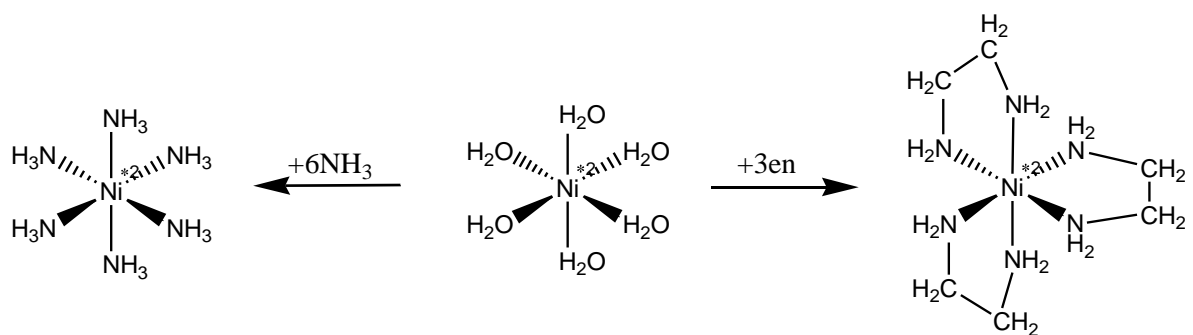


Figure 1.8 The addition of ammonia or ethylenediamine to a hydrated nickel complex (center) to form octahedral nickel ammonia complex (left) or octahedral ethylenediamine complex (right).²

The other effect that drew Cram's attention was the macrocyclic effect.⁵ This effect arises from the fact that cyclic systems usually form stronger complexes than their acyclic counterparts.^{2,3,4,5} An example of this is the complexation of zinc(II) by two ligands, one acyclic and one macrocyclic (Figure 1.9). The resulting macrocyclic complex has a $\log K$ value of 15.34, which is a 10^4 greater binding stability than its acyclic counterpart with a $\log K$ of 11.25.² This effect can be accounted for by entropic and enthalpic influences. Entropically, the macrocyclic complex is more stable because it has a more rigid structure than its flexible acyclic counterpart, and therefore loses less disorder on binding. The macrocycle has also already paid the enthalpic cost of bringing the four polar amine groups into close proximity with one another.^{2,4} Furthermore, the macrocyclic system is less solvated than the acyclic system, further reducing the enthalpic costs associated with desolvation.² This additional increase in stability was also noted by Cram and taken into account in his preorganization principle.^{5,7}

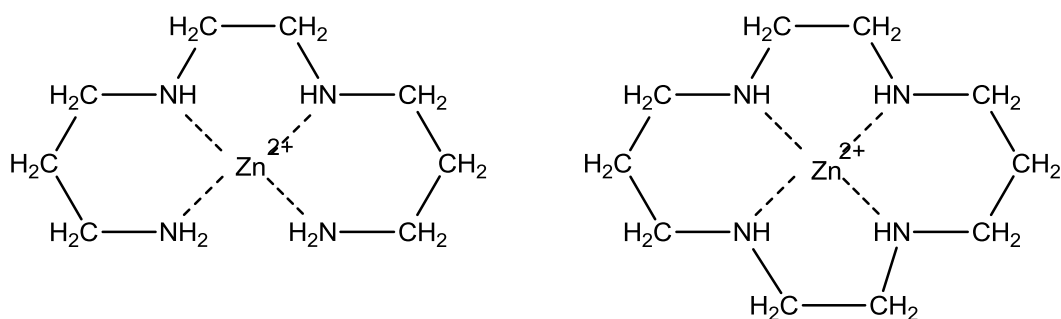


Figure 1.9 The binding of an acyclic ligand (left) and macrocyclic ligand (right) to zinc(II).²

Based on the chelate and macrocyclic effects, Cram⁵ created his preorganization principle, which states that “the more highly two molecules are organized for binding and low solvation prior to their complexation, the more stable will be their complexes.” Thus, if two molecules bind to each other strongly and selectively, with minimal reorganization in structure or uptake of energy, then they are said to be preorganized.^{2,3,4,5,7}

1.1.2.3 Molecular Recognition

When describing molecular recognition it is important not to confuse it with complementarity or preorganization, as often occurs in the literature.¹ While both of these principles improve the recognition of molecules for one another, true molecular recognition requires more. Lehn described molecular recognition “as a process involving both binding and selection of a substrate by a given receptor molecule, as well as possibly a specific function.”¹ He also went on to point out that a binding event is not sufficient to define recognition. The key to defining molecular recognition is binding with a purpose, in the way that enzymes bind substrates for the purpose of catalysis or receptors bind hormones for the purpose of cell signaling.^{1,3,4} Thus, molecules are said to recognize one another if they select for one another and bind to one another with a purpose.¹

1.2 Classification of Supramolecular Complexes

Supramolecular complexes can be created using many combinations of the interactions and principles discussed in the previous section. Once formed, however, these complexes can be divided into two distinct categories, self-assembly and host-guest chemistry.^{3,5} While both categories are described briefly below, emphasis will be placed on host-guest chemistry, as the work that follows herein, falls into that category.

1.2.1 Molecular Self-Assembly

Self-assembly is defined as a reversible and spontaneous interaction between two or more molecules, resulting in the formation of a molecular aggregate.³ This definition is a simple one, and as such, there are many types of natural and synthetic interactions that fall into this category.⁸ Even before the development of supramolecular chemistry as a field, self-assembly was recognized as crucial to the existence of all life on earth.² One of the most common examples of a natural self-assembly process is the non-covalently bound DNA double helix.^{1,2} This structure is made up of two polymeric strands that are strongly and reversibly bound to one another by a series of highly ordered hydrogen bonds.² These hydrogen bonds form between a set of complementary subunits called nucleotide bases.^{1,2} Since each base will only bind to its complementary partner due to the number of hydrogen bonds that can form between them (Figure 1.10), the two strands of DNA are considered highly selective for one another.^{1,2} It is this type of selectivity that supramolecular chemists often attempt to mimic when designing their own self-assembling architectures.^{2,5,8}

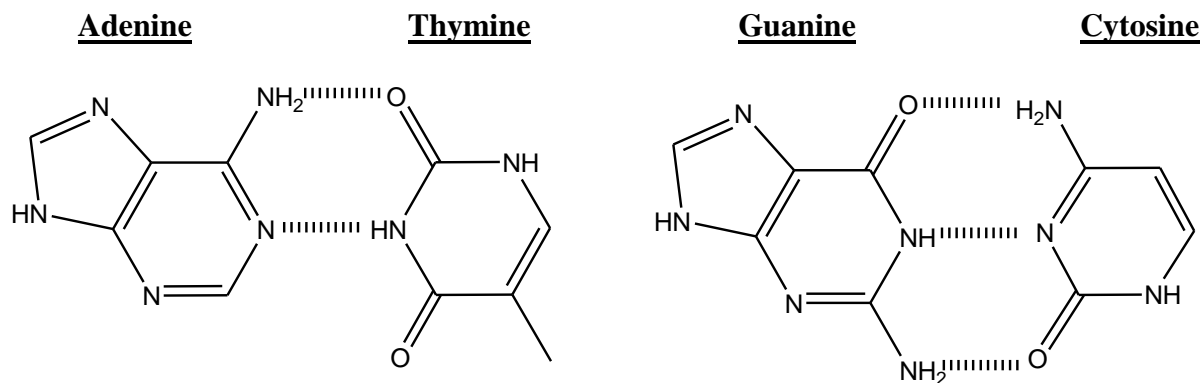


Figure 1.10 A set of self-assembling DNA bases. Adenine will only bind to thymine, and does so selectively with two hydrogen bonds (left). Guanine will only bind to cytosine, and does so selectively with three hydrogen bonds (right).²

There are a wide variety of paradigms in synthetic chemistry and supramolecular chemistry that are dependent on self-assembly.^{2,5,8} Many of these systems represent attempts by supramolecular chemists to produce aggregates that are either too complicated or too tedious to be formed by covalent syntheses.^{5,8} While a full account of these systems is beyond the scope of this thesis, some examples include films, gels, liquid crystals, nanostructures and certain types of polymers.⁸

1.2.2 Host-Guest Chemistry

Host-guest chemistry involves a binding event between a large molecule, termed the host, and a smaller molecule, termed the guest.⁴ Many hosts are a form of cavitand, meaning that their molecular structure contains a large cavity, such as a pocket or hole. This cavity allows the host to encapsulate and non-covalently bind a guest. Guests can range in size and complexity, from small, charged metal ions to complex organic compounds, such as drug molecules.^{2,4} One common requirement for a guest, however, is that it must possess

properties complementary to that of its host. When a host binds to a guest, the result is 1:1 inclusion complex as described by the general equation below.^{2,4}



This equation represents the equilibrium that forms between the free host, free guest and host-guest complex.^{2,4} The equilibrium has an association constant, K , which can be defined by the following relationship.^{2,4}

$$K = \frac{[H \cdot G]}{[H_f][G_f]} \quad (1.2)$$

Association constants are frequently used to measure how strongly a host is bound to a guest.⁴ Thus, K can be a useful tool in comparing the affinity of two hosts for a guest, which will be useful when examining the different types of hosts described below.

Supramolecular host molecules have been designed to accommodate a wide variety of cationic, neutral, and anionic guests. While a broad range of these host complexes have been characterized, the work that follows will focus primarily on cucurbituril, a macrocyclic host molecule that complexes with both cationic and neutral guests.⁴ In order to understand the unique characteristics of cucurbituril, its properties need to be compared with the properties of other macrocyclic host molecules capable of complexing cationic or neutral guests. As a result, a number of these macrocyclic hosts, including crown ethers, cryptands, calixerenes, cyclodextrins, and cucurbiturils, are described below.^{2,4}

1.2.2.1 Crown Ethers

Crown ethers (Figure 1.11), also called corands, were first discovered by Charles Pedersen in 1967.^{2,9} While working on a novel ligand to bind vanadium, Pedersen isolated a small amount of white impurity.² He conducted some simple lab tests on this compound and discovered, to his surprise, that its solubility increased in methanol, in the presence of sodium hydroxide.^{2,10} This result was strange since none of his starting materials or expected products should have been affected by alkalinity.¹⁰ After further analysis, Pedersen determined that the material he had synthesized was, in fact, interacting with the sodium ions in solution and not the hydroxide ions.¹⁰ Pedersen had discovered the first artificial ligand that could complex with alkali metals.^{2,10} It was also later recognized that he had discovered the first artificial host molecule, a discovery which earned him a Nobel Prize in Chemistry in 1987.^{2,10}

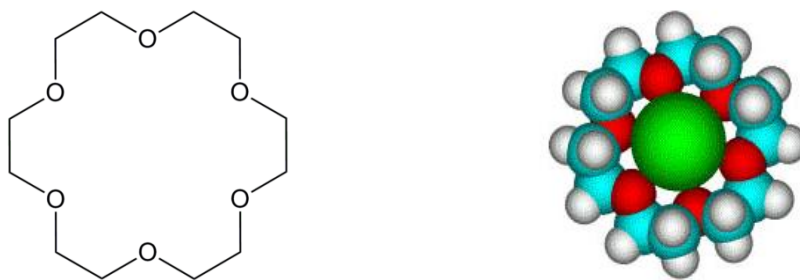


Figure 1.11 An example of a crown ether host molecule, specifically 18-crown-6 (left). A space filling model of 18-crown-6 bound to a potassium ion (right). The carbon atoms are shown in light blue, hydrogen in white, oxygen in red, and potassium in green.

After his initial discovery, Pedersen went on to synthesize a whole family of crown ether type complexes and, due to the length of their IUPAC names, even created a crown ether naming system.¹⁰ His system involved placing the total number of atoms in the ring

first, followed by “crown” and ending in the total number of oxygens in the ring. Thus, in Figure 1.11 there are eighteen atoms total and six oxygen atoms, so it is named 18-crown-6.

Crown ethers are able to use their oxygens to form ion-dipole interactions with alkali metal cations, and the closer the size match between the diameter of the cation and the diameter of the cavity, the stronger the complex that will form between them (Figure 1.11).² Preorganization also performs an essential role in the success of crown ethers as hosts, as evidenced by the fact that unidentate ethers, such as diethyl ether, show very poor metal binding ability.⁴ Additionally, while 18-crown-6 has a fairly high binding constant with K^+ in methanol, with a $\log K$ of 6.08, its linear counterpart, pentaethyleneglycoldimethylether, is 10^4 times weaker in binding stability, with a $\log K$ of 2.30 (Figure 1.12).⁴

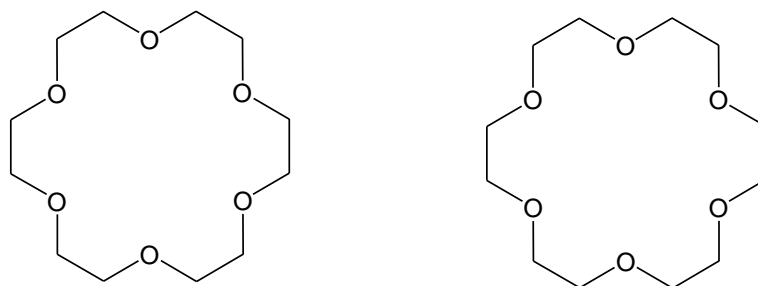


Figure 1.12 While 18-crown-6 (left) has a $\log K$ of 6.08 for binding K^+ in methanol, its acyclic counterpart pentaethyleneglycoldimethylether (right) has a $\log K$ of only 2.30.⁴

The example above demonstrates the importance of the macrocyclic effect in the binding effectiveness of crown ether hosts.⁴ However, most crown ethers only bind cations in a two dimensional fashion, reducing their potential binding strength.^{2,10} While several attempts were made to add a third arm to crown structures, via a bridging nitrogen atom in the place of an oxygen atom, these attempts proved to have few benefits.² In order to

understand the potential power of binding a cation in three dimensions, another series of host molecules, called cryptands, needed to be examined.^{2,4}

1.2.2.2 Cryptands

Cryptands (Figure 1.13) were first synthesized by Jean-Marie Lehn in 1969.^{2,9} This family of bicyclic hosts earned Lehn his share of the 1987 Nobel Prize, alongside Pedersen and Cram.^{9,10} The name cryptand was assigned to this family of hosts because, similar to a crypt, they “entomb” cations in a cage-like structure.^{2,4} As with crown ethers, cryptands have their own naming system that is based on the number of oxygens between the bridgehead nitrogens.² As Figure 1.13 demonstrates, there are two oxygens on each arm of the cryptand, so it is named [2.2.2] cryptand.^{4,11}

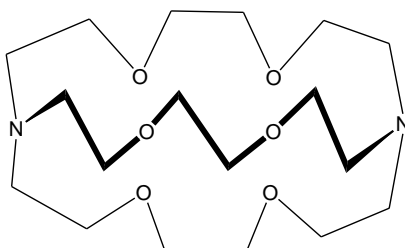


Figure 1.13 An example of a cryptand host molecule, specifically [2.2.2] cryptand.

Cryptands bind guests in the same manner as crown ethers, through ion-dipole interactions between their oxygens and the cationic guest.^{2,4} In addition, cryptands also employ a three dimensional extension of the macrocyclic effect, called spherical recognition, to bind guests.^{2,4,11} This spherical recognition adds an extra degree of preorganization to the complex and allows it to bind cations with much greater binding stabilities than crown ethers.^{4,11} An example of this increased stability occurs when [2.2.2] cryptand binds a

potassium ion.^{4,11} The complex formed between the cryptand and the metal cation has a $\log K$ of 10.40 in methanol, which is several orders of magnitude more stable than the strongest crown ether-potassium complex, formed by 18-crown-6.^{4,11}

While cryptands do form stronger complexes with metal cations than crown ethers, this series of guests does have a number of limits. One such limit is the maximum size of the cryptands. The result of this limitation is that cryptands can only bind to metal cations and very small organic cations.² Also, since the main driving force of cryptand binding is an electrostatic ion-dipole interaction, this host will bind almost exclusively to cations and polar molecules with strong dipoles.^{2,4,11} In order to bind a wider range of guests, a family of hosts with a wider set of homologs, larger set of cavity sizes and greater range of non-covalent interactions was examined.^{2,4} This set of host molecules are referred to as calixarenes.

1.2.2.3 Calixarenes

The term calixarene was coined by C. David Gutsche, who likened the molecule to a “calix” (an Ancient Greek chalice or vase).^{4,12} Although Gutsche was the first person to study the host-guest properties of calixarenes in 1972, he did so by drawing on work from the previous hundred years.⁴ Calixarenes are formed by the base catalyzed condensation reaction between *p*-tert-butylphenol groups and formaldehyde.^{2,12} The macrocyclic hosts that are formed by this reaction are highly flexible and easily modified.

Calixarenes are an important and powerful family of host molecules because of their high-degree of variability in terms of size, configuration, and binding functional group.^{2,12} During his early research, Gutsche determined that by varying the conditions of the calixarene synthesis reaction, he could produce a series of homologues with varying ring

sizes. In order to differentiate between these different homologues, Gutsche introduced a special notation system for calixarenes.¹² This system involves referring to “calix[*n*]arenes”, where *n* refers to the number of phenol subunits found in the ring.^{4,12} Calix[*n*]arenes where *n* = 4,5,6,7 and 8 have been identified, however, calix[4]arene, calix[6]arene (Figure 1.14) and calix[8]arene are the most frequently studied homologues.^{2,4,12}

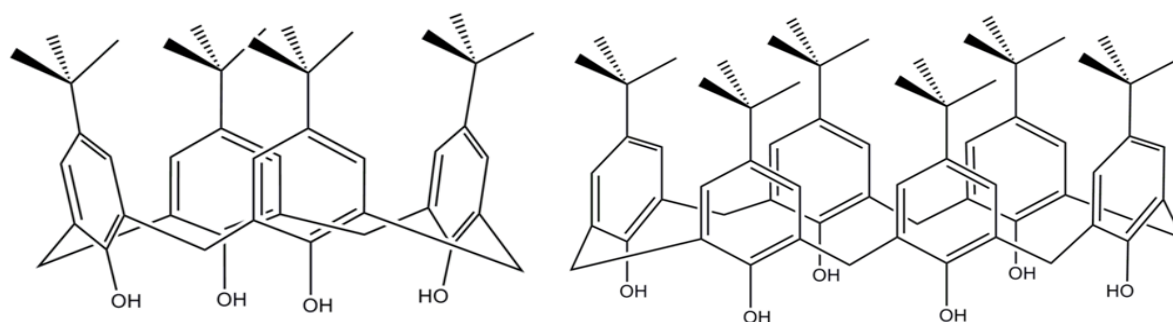


Figure 1.14 The calix[4]arene (left) and calix[6]arene (right) homologues in their cone configurations.

While there are differences among the various homologues, each individual homologue is also capable of adopting several distinct configurations.^{2,12} For example, calix[4]arene, the simplest homologue, can assume four configurations: cone (Figure 1.14), 1-2-alternate, 1-3-alternate, and partial cone (Figure 1.15). The prevalence of these configurations is mainly determined by the functional groups found on the calixarene; however, the chemical nature of a bound guest can also have an impact.

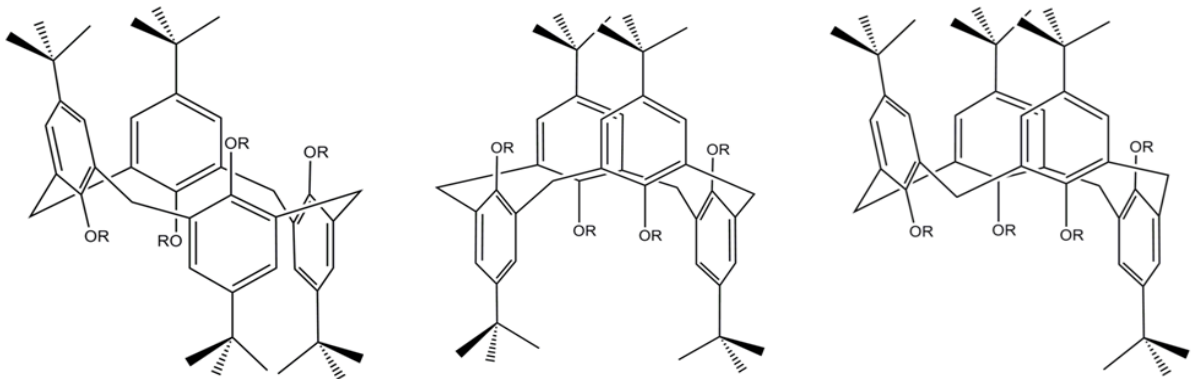


Figure 1.15 Calix[4]arene in the 1-2-alternate (left), 1-3-alternate (center), and partial cone (right) configurations.

The functional groups found on the phenyl ring system can affect a wide variety of the host's properties including: the conformation of the calixarene, the guests that it is able to bind to, and the strength with which it is able to bind them.^{2,12} The parent calixarenes possess tert-butyl groups *para* to hydroxyl groups on the phenyl residues. In solution, these calixarenes exist in the cone conformation, due to the intramolecular hydrogen bonds that form between the phenolic hydroxyl groups.¹² This variation of the host, can bind a broad range of guests in a number of ways.^{2,12} Metal cations, for example, can be bound through either cation- π interactions with the phenyl residues or electrostatic interactions with the deprotonated phenolic hydroxyl groups. These sorts of interactions have been used to carry metal cations such as cesium across organic membranes.¹² Calixarenes are also able to bind small neutral guests, such as toluene, in their central aromatic cavities.^{2,12} Furthermore, through the use of larger analogues, such as calix[8]arene, it is even possible to bind large non-polar molecules, such as C₆₀.² While these parent calixarene hosts cannot bind all forms

of cationic and neutral guests, it is possible to modify them to better accommodate an even wider variety of guests.^{2,12}

Parent calixarenes can undergo modification in one of two ways.¹² The first way involves introducing functional groups, such as esters, at the phenolic hydroxyl group.^{2,12} This sort of modification permits stronger binding to a wider range of metal cations.¹² The other potential modification, involves the elimination of the *tert*-butyl groups from the phenyl residues and the addition of new functional groups, such as *p*-sulfonic acids, via electrophilic aromatic substitution. This sort of modification allows the calixarenes to strongly bind organic cations with ammonium groups via ion-ion interactions. These modifications have also been used to increase the solubility of calixarenes in aqueous solution, allowing them to bind to neutral guests with their central cavity via hydrophobic interactions.

While calixarenes are highly varied and capable of undergoing modification to bind a broad range of guests, they also possess a number of drawbacks. One such drawback is that calixarene subunits are each held together by a single methylene bridge.^{2,4,12} This makes calixarenes floppy and costs a degree of preorganization that would allow this family of hosts to form stronger host-guest complexes. This is also a problem in other host families, such as the cyclodextrins.

1.2.2.4 Cyclodextrins

Cyclodextrins (CD) are a naturally occurring family of host molecules composed of α -*D*-glucose subunits, joined by α -1,4-glycosidic linkages.^{2,4,13} These hosts are formed by cyclodextrin glucanotransferase (CGTase), an enzyme that catalyzes the degradation of

starch to form both linear and cyclic oligosaccharides.^{2,4,14} While some early work was conducted on cyclodextrins in the late 19th and early 20th centuries, the first pure fractions were isolated by Freudenberg and his coworkers in 1936.¹⁵ His work was also the first to result in two individual homologues of cyclodextrin, which were distinguished from one another by the prefixes α and β .¹⁵ A third major homologue, γ , was discovered in the late 1940's.¹⁵ These homologues, α , β and γ -CD, were studied intensely in the mid-20th century and it was determined that they possessed 6, 7 and 8 α -D-glucose units, respectively (Figure 1.16).^{2,4,15}

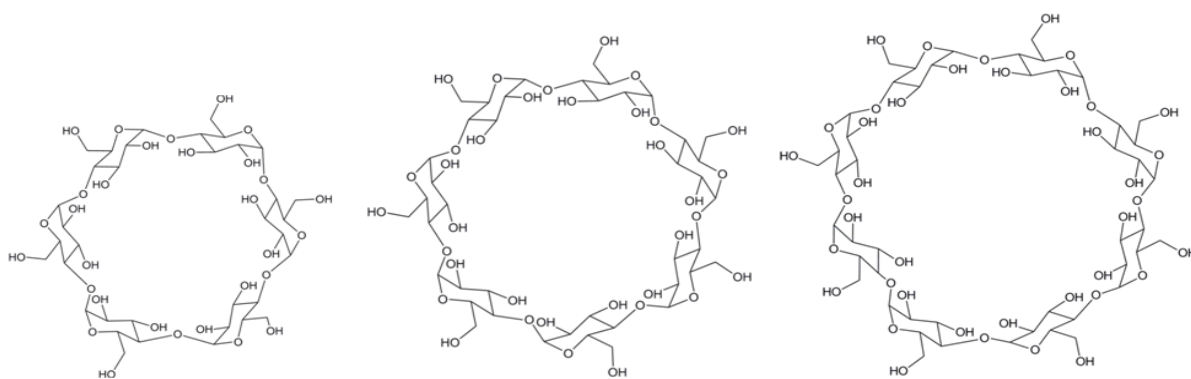


Figure 1.16 The structures of α , β and γ -Cyclodextrin, respectively.

In the 1950's, there were two major groups exploring the properties of cyclodextrins.¹⁵ One group, led by D. French, discovered several larger cyclodextrin homologues, while another group, led by F. Cramer, began to examine the host-guest properties of cyclodextrins. This research continued unabated until 1957, when the first review article on cyclodextrin chemistry was published by French.¹⁵ The article contained the details of a study, in which cyclodextrin was fed to rats as part of their diet. In this study, the (likely contaminated) cyclodextrin was found to be lethal for the rats and by extension

was thought to be lethal to humans. This misconception was later disproven, though it is thought to have set back cyclodextrin chemistry almost 25 years. Despite this set back, sporadic studies on cyclodextrins continued and by the late 1960's, most of the chemical, physical, and inclusion properties of cyclodextrin had been discovered. By the 1970's, several studies had been published that demonstrated pure fractions of cyclodextrins had no serious detriment to human health. Following this discovery, the use of cyclodextrins as novel host molecules increased drastically, driven by their low cost and beneficial host-guest properties.^{2,4,15}

In comparison to other host molecules, the structure, solubility, and binding properties of cyclodextrins are unique.^{2,4} Cyclodextrins possess a cone-like shape, with two polar rims lined with hydroxyl groups and a central non-polar cavity.^{2,4,13} Of the two polar rims, one is termed the primary rim because it is lined with primary hydroxyl groups, while the other, larger rim is termed the secondary rim because it is lined with secondary hydroxyl groups. These polar rims allow cyclodextrins to easily dissolve in polar solvents such as water and methanol.^{2,13} Once dissolved in a polar solvent, cyclodextrins are able to bind guests, not with their polar rims, as seen in previously described hosts, but with their central cavity.^{13,14} The walls of this cavity are lined with CH groups and glycosidic oxygens, making it very hydrophobic. Thus, the binding of cyclodextrins is driven by the replacement of high-energy polar solvent molecules with neutral guest molecules.^{13,15} Cyclodextrins are also very flexible, even hard plastic space filling models demonstrate a degree of flexibility.¹³

As a result of their high degree of flexibility, cyclodextrins can contort to bind any neutral guest that is a good steric fit to their central cavity.^{4,13,14} Of the three main

cyclodextrin homologues, α -CD will typically complex with aliphatic side chains, β -CD will complex with aromatic molecules, and γ -CD will complex with larger neutral guests, such as steroids.¹⁴ In addition to these broad series of guests, the hydroxyl rims of cyclodextrins can also be modified via aminations, esterifications, or etherifications. These modifications allow cyclodextrins to better accommodate a broader range of non-polar, polar, and ionic guests.¹⁴

A guest can benefit from cyclodextrin complexation in several ways. One well known benefit of complexation is improved solubility of the guests in polar solvents.¹⁵ As the non-polar regions of the guest are bound inside cyclodextrin's hydrophobic cavity, the concentration of dissolved guest increases significantly. Another common effect of cyclodextrin binding involves a change in the reactivity of the guest. This change often results in improved guest stability, making cyclodextrins ideal for long-term chemical storage, drug delivery, and food preservation.¹⁵ Occasionally, however, cyclodextrins can act as an artificial enzyme and increase the reactivity of certain guests. In these cases, cyclodextrins can be used to decompose toxic substances or increase the rate of chemical syntheses. Due to the properties described above, cyclodextrins have been used in food, cosmetics, packaging, textiles, catalysis, pharmaceuticals, and environmental protection.^{4,14}

1.3 Cucurbituril

In 1905, Behrand and coworkers conducted an acid-catalyzed condensation reaction between glycoluril and formaldehyde.¹⁶ The product formed by this reaction was a solid that was insoluble in most common solvents. However, if the product were dissolved in sulfuric acid, diluted with water and subsequently boiled, then another crystalline product was

obtained. An elemental analysis was conducted on this second product, and the results suggest that this was the first recorded cucurbituril synthesis (Figure 1.17).¹⁶

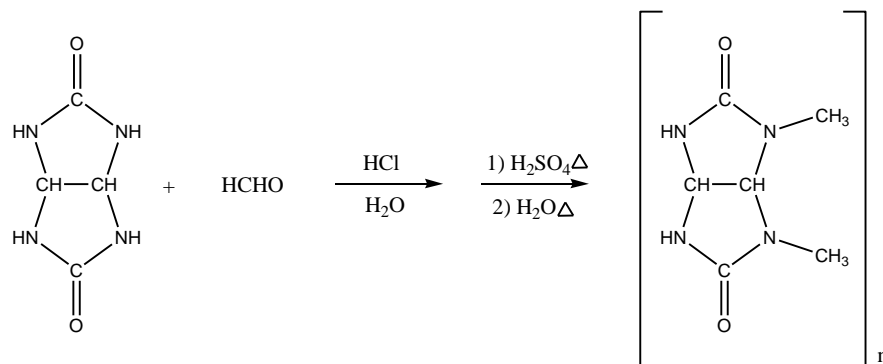


Figure 1.17 The reaction scheme for the synthesis of cucurbituril.¹⁶

More than 75 years later, Mock and coworkers began to characterize the final product of Behrand's synthesis by IR and NMR spectroscopy.^{17a} The results of these analyses suggested a highly symmetrical and non-aromatic structure. After conducting an X-ray crystallographic analysis on the product, it was determined that its structure was a macrocyclic hexamer of glycoluril, bound by methylene bridges (Figure 1.18).^{17a}

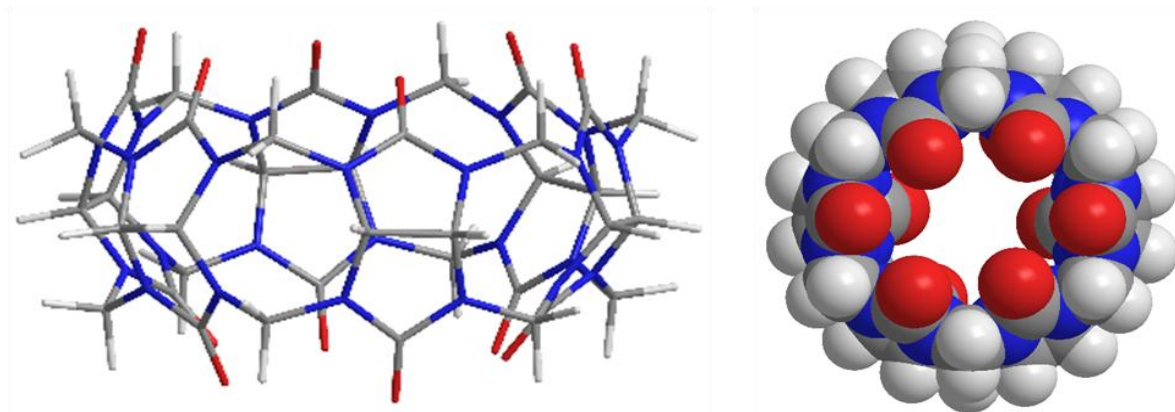


Figure 1.18 A stick side-view (left) and space-filling top-view (right) of the first synthesized cucurbituril molecule.

Once Mock's group determined the chemical structure of the product, they gave it the name cucurbituril, based on the similarity between the product's molecular structure and a pumpkin (a member of the *Cucurbitaceae* family).¹⁷

1.3.1 Properties of Cucurbiturils

After ascertaining the structure of cucurbituril (CB), Mock recognized its potential as a macrocyclic host and began to study its binding properties.¹⁷ Cucurbituril has a barrel-like structure, with a central hydrophobic cavity, and two sets of polar portals lined with ureido carbonyl groups. The original hexamer studied by Mock was shown to have portals that were $\sim 4\text{\AA}$ in diameter, and a slightly broader central cavity at $\sim 5.5\text{\AA}$ in diameter.¹⁷ The carbonyl lined portals were able to form strong ion-dipole interactions with cations, making cucurbituril an excellent cationic receptor.^{6,17} Also, like cyclodextrin, the central cavity of cucurbituril was able to bind neutral guests through the favourable expulsion of polar solvent molecules. In contrast to other macrocyclic hosts, such as calixarenes and cyclodextrins, cucurbiturils had two linkers holding each subunit together. This gave cucurbituril a unique structural rigidity that imparted a high degree of preorganization and allowed it to strongly and selectively bind guests.¹⁷ Initially, cucurbiturils were limited to binding metal cations and those small aliphatic and aromatic guests that could fit inside their hydrophobic cavities. This limitation was overcome, however, when several new homologues were discovered and characterized in the early 21st Century.^{18,19,20}

1.3.2 Homologues of Cucurbituril

In 2000, Kim *et al.* published a paper describing three new homologues of cucurbituril, which included a pentamer, a heptamer, and an octamer.¹⁸ In order to easily distinguish between these homologues, a naming system similar to the one employed for calixarenes was introduced. This system referred to cucurbit[*n*]uril (CB[*n*]), where *n* refers to the number of glycoluril residues found in the macrocycle.¹⁸ Thus, under this new system, the original hexamer was termed CB[6] and the new homologues were termed CB[5], CB[7], and CB[8], respectively. An additional homologue, CB[10], was also discovered in 2001 by Day and coworkers.¹⁹ Once each of these homologues had been discovered, Day and his group focused their efforts on optimizing the CB synthesis reaction conditions in order to improve the yields of each homologue. In order to accomplish this, Day's group varied the acid type, acid concentration, reactant concentrations and temperature of the reaction. Analysis of Day's data, enabled chemists studying cucurbituril to synthesize and isolate the various CB homologues in high yields, in contrast to the trace amounts that formed during Mock's synthesis.²⁰

Once procedures were available to produce each homologue in high yields, Kim and his group began to characterize the properties of the various homologues.^{18,20a} Each of these homologues was studied by electrospray ionization mass spectrometry (ESI-MS), infrared spectroscopy (IR), nuclear magnetic resonance spectroscopy (NMR), and X-ray crystallography.¹⁸ From these analyses, a number of key characteristics were determined, such as the dimensions and volume of each homologue. These characteristics are summarized in Table 1.1.

Table 1.1 The dimensions and volumes of cucurbit[*n*]urils.^{18,20,21}

	CB[5]	CB[6]	CB[7]	CB[8]	CB[10]
Portal Diameter (Å)	2.4	3.9	5.4	6.9	NA
Cavity Diameter (Å)	4.4	5.8	7.3	8.8	NA
Cavity Height (Å)	9.1	9.1	9.1	9.1	9.1
Cavity Volume (Å ³)	82	164	279	479	~870

Once the size of each homologue had been determined, the study of cucurbiturils shifted to their host-guest chemistry and potential applications.²⁰

1.3.3 Cucurbit[*n*]uril Host-Guest Complexes

In order to assess possible applications for cucurbit[*n*]urils, their potential as hosts must first be examined. For a host to form useful host-guest complexes, it must be soluble and capable of selectively binding to a wide variety of guests.⁴ Of the five cucurbituril homologues, CB[6], CB[8], and CB[10] all have very low solubilities (<0.01 mM in aqueous solution), while CB[5] and CB[7] have moderate solubilities (20-30 mM).^{20,21}

In terms of binding selectivity, CB[5] has the fewest uses.²⁰ This host can form complexes with alkali metals, ammonium, some transition metals, such as, Pb²⁺, and neutral gas molecules, such as, N₂, O₂, and argon.^{20,22} However, due to its small cavity size, CB[5] is limited to binding these sorts of small guest molecules.²⁰

Although it is only the next largest homologue, CB[6] has twice the cavity volume of CB[5], and, as a result, is able to bind a much broader range of guests.²⁰ This host can form complexes with most metals, including alkali, alkali earth, and some transition metals.^{20,23} Furthermore, it can complex many aliphatic guests including, ammonium and diammonium cations, amines, polypeptides, and tetrahydrofuran.^{20,23,24,25}

Although CB[6] can bind to some aromatic guests, such as toluene and *para*-substituted phenyl rings, it is unable to bind *ortho* and *meta*-substituted phenyl rings.²⁰ In order to bind those sorts of aromatic compounds, the next largest homologue, CB[7], is employed.^{20,26} As a host, CB[7] is able to bind a broad range of guests, including most aliphatic and aromatic compounds, ferrocenes, adamantanes, and metal cations.^{20,26} This high degree of variability makes CB[7] an excellent host.²⁶

CB[8] is also able to bind many of the same of guests as CB[7], but due its larger cavity size, it does so with less selectivity and lower binding constants.²⁰ However, CB[8] can also form complexes with larger guests that CB[7] is unable to bind to, such as fullerenes.²⁷ Furthermore, both CB[8] and CB[10] are capable of binding two or more guests in their central cavity.^{20,21} This feature could allow either host help catalyze intermolecular reactions between guest molecules.^{20,21} As the largest cucurbituril homologue, CB[10], has some unique properties, such as the ability to form complexes with smaller hosts, such as CB[5] and modified calix[4]arene.^{19,21} This feature could allow CB[10] to conduct some unique supramolecular interactions.²¹

In summary, CB[6], CB[8], and C[10] are each able to bind to a variety of guests, but have very low solubility.^{19,20,21} CB[5] has moderate solubility, but its small cavity size precludes binding to most guest molecules.²⁰ As a result, these four homologues are not ideal candidates for wide-spread applications. Thus, CB[7] is the best candidate for practical applications, due to its moderate solubility and the wide variety of guests that it can bind.^{20,26,28}

1.3.4 Applications of CB[7]

Supramolecular chemists have observed that the structural and chemical properties of CB[7] can exert a profound effect on the physical and chemical properties of a guest during complexation.²⁰ These binding effects can include changes in the guest's solubility, physical structure, pK_a values, chemical stability and reactivity, UV-vis absorption and emission spectra, and fluorescence intensities and lifetimes.²⁹ These effects open up a variety of uses for CB[7], including chemical sensing, self-sorting systems, molecular switches, molecular machines, drug delivery, controlled drug release, and molecular catalysis within and between guests.^{28,29} Although CB[7] has an important role in each of these applications, the research described in this thesis can be best applied to molecular catalysis, drug delivery, and chemical sensing. The uses of CB[7] in each of these applications is summarized below.

1.3.4.1 Molecular Catalysis

The application of CB[7] to molecular catalysis relies on CB[7]'s ability to shift the pK_a of a bound guest.²⁹ In previous studies, CB[7] has reportedly demonstrated average pK_a shifts of ~2-3, which is higher than those of other cationic hosts, such as cyclodextrin and sulfonatocalixarenes that have average pK_a shifts of ~1 and ~2, respectively.³⁰ Due to these pK_a shifts, regions of a guest's molecular structure can be stabilized or made more vulnerable to nucleophilic attack.^{29,30} Ultimately these shifts can either result in increased stability of the molecule's current electronic structure, or facilitate the conversion of the molecule to a new product with a new electronic structure. A beneficial example of this process was presented by Nau and his coworkers during their work on the proton pump inhibitor, omeprazole.³⁰

One limitation of omeprazole is that it undergoes slow conversion from its inactive linear form to its active cyclic form (Figure 1.19).

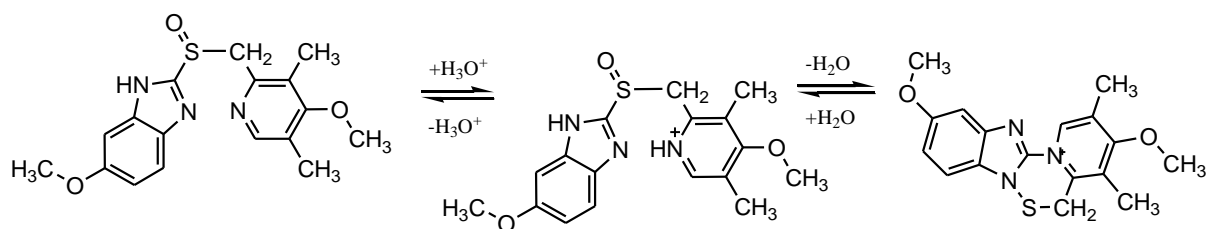


Figure 1.19 The cyclization of omeprazole from its in-active form to its active form.

Under ideal circumstances, the basicity of the benzimidazole group would be increased while maintaining the nucleophilicity of pyridine ring. CB[7] has been shown to bind to the benzimidazole ring and effectively increase its pK_a .³⁰ This pK_a increase improved the viability of the cyclization reaction in a number of ways. The half-life for the reaction, described above, in the absence of CB[7] was approximately five minutes, and its corresponding rate was measured to be about 0.2 min^{-1} . Once CB[7] was added, however, its half-life dropped to 20 seconds, and its rate increased 15-fold to 3.0 min^{-1} . A second limitation of omeprazole was that it underwent dimerization in acid, becoming inactive. At a pH of 2.9, the active form of omeprazole had a half-life of 60 minutes. However, once CB[7] was introduced, it stabilized the active form of omeprazole and increased its half-life by 500-fold to almost three weeks. This example demonstrates both the ability of CB[7] to catalyze a reaction and stabilize its product.

Although the aforementioned example involved an intramolecular reaction, intermolecular reactions, such as photodimerization and other biomolecular reactions, are

also possible.²⁹ Keinan and coworkers recently published a review summarizing a number of reactions catalyzed by CB[7].²⁹ This review demonstrates the growing use of CB[7] in the field of molecular catalysis.

1.3.4.2 Drug Delivery

Drug delivery is a process that involves the introduction of a drug into the body, the uptake of the drug by the blood stream, the ability of the drug to cross the cell membranes of the target tissue, and the interaction of the drug with the desired biochemical pathway.^{31,32} To be effective, a drug must be soluble, non-toxic, efficacious, and stable both *in-vivo* and *in-vitro*.^{28,31,32,33} Binding to CB[7] could improve any of these properties in a drug, helping to make it viable for pharmaceutical use.^{28,33} However, before the viability of a CB[7]·Drug complex can be examined, the effects of CB[7] itself on the body must be explored.

In a recent study, Day and coworkers attempted to determine what, if any, toxicological effects CB[7] had on the body.³² The preliminary results of their research described *in-vitro* and *in-vivo* studies on the effects of CB[7]. The *in-vitro* cell cultures revealed an IC₅₀ value of 0.53 ± 0.02 mM, which translates to ~620 mg of CB[7] per kg of cell material. The *in-vivo* studies on mice showed a maximum dosage of 250 mg/kg when administered intravenously and 600 mg/kg when administered orally. These values are similar to other water soluble hosts, such as *para*-sulfonatocalix[4]arene and some of the cyclodextrins homologues.³³ While these results do not conclusively prove that CB[7] is safe for human use, they do provide evidence to support the idea that CB[7] could one day be used for drug delivery system in humans.

The use of CB[7] as a drug carrier has been applied to a number of guests, including metallocenes, benzimidazoles, local anesthetics, choline derivatives, anti-tumor agents, and tuberculosis drugs.^{28,33} In many of these studies, CB[7] has demonstrated a number of useful characteristics for drug delivery. One example of this is how CB[7] has been shown to improve the solubility of most of the drugs discussed above, particularly the hydrophobic drugs, which can undergo self-aggregation in aqueous solution.²⁸ Several other beneficial properties of binding to CB[7] were recently demonstrated when CB[7] was bound to the anti-tumor drug complex, oxaliplatin.³⁴ In this study, binding to CB[7] was shown to not only improve drug stability, but also to reduce the undesired side-effects that resulted when oxaliplatin bound to a series of useful proteins.³⁴ Recently, two review articles were published, one by Macartney,²⁸ the other by Wheate and coworkers,³³ describing the benefits of binding CB[7] to a wide variety of drug molecules. These benefits include increased solubility, drug stability, reaction rates, uptake (both in the bloodstream and targeted tissues), and reduced side effects and cytotoxicity. It is beneficial properties such as these that promote the use of CB[7] as a potential drug carrier and slow-release agent.

1.3.4.3 Chemical Sensors

In previous sections, the ability of CB[7] to bind guests and alter their physical properties, such as pK_a and UV-visible spectra, were established. In a recent review article, Keinan and coworkers demonstrated that the spectral changes, which accompany binding with CB[7], can be useful in altering a guest to make it a more effective chemical sensor.²⁹ One example of this spectral shift was demonstrated by Macartney and coworkers when they bound CB[7] to vitamin B₁₂.³⁵ Vitamin B₁₂ is an inorganic complex, with a metal cobalt

center bound by a corrin ring. This corrin ring has an arm with a terminal α -axial 5,6-dimethylbenzimidazole (α -DMB) group, which can also bind to the cobalt center. In solution, this α -DMB group can be found either attached to the cobalt center in a “base-on” form, or unattached to the center and free in solution in a “base-off” form (Figure 1.20). Normally, this equilibrium is shifted to the base-on form, however, when CB[7] was introduced to the solution, it bound to the free α -DMB group and stabilized the base-off form (Figure 1.20).³⁵

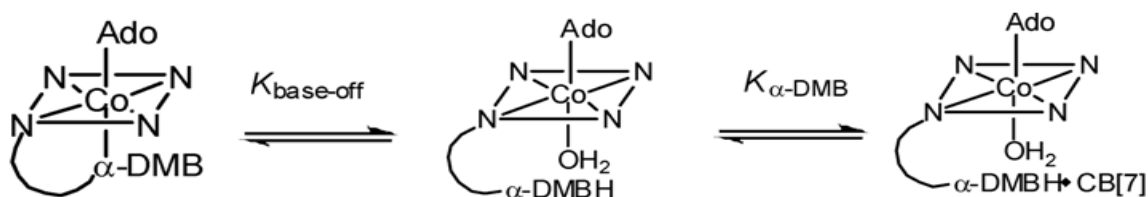


Figure 1.20 The base-on/base-off equilibrium of vitamin B₁₂ and the effect of CB[7] binding

In its base-on form vitamin B₁₂ emitted red light, but, as CB[7] was added to solution the equilibrium shifted from the base-on to the base-off form, and the emitted light shifted from red to yellow.³⁵ Also, by binding the α -DMB group, CB[7] indirectly opens up a binding site on the cobalt metal center. In a previous study by Zelder, it was shown that cyanide anions could bind to the open site on the cobalt center and change emitted light from red to purple.³⁶ This was a slow process, however, due to the slow release of the α -DMB group from the cobalt center. Also, since the reaction took several minutes to go to completion, it was difficult to determine if the slow transition from transparent red to transparent purple was indicative of a positive test for cyanide. However, an open binding site on the cobalt would allow the CN⁻ to bind almost instantly, with a noticeable colour change from yellow to

purple. Improvements, such as those described above, are what make CB[7] a potentially useful addition to chemical sensors.

1.4 Research Aims

The research described in this thesis focuses on the effects of CB[7] on several different families of guest molecules containing cationic groups such as tetraalkylammonium, biguanidium, amidinium, and oxonium. The effects of CB[7] on the properties of these guests will be characterized by ESI mass spectrometry, NMR and UV-visible spectroscopy, and computational calculations. The specific aims of this research include:

1. Examining the nature and strength of CB[7] binding and the effects of binding on the properties of a series of known cationic drugs, including salts containing the benzethonium, metformin, phenformin, chlorhexidine, alexidine, pentamidine, and berenil cations and dications.
2. Examining the catalytic effects of CB[7] as it degrades the berenil dication through the excision of its central azide group.
3. Synthesizing hexafluorophosphate salts of the 4'-methoxyflavylium, 6-methoxyflavylium, and 6,4'-dimethoxyflavylium cations, and studying the effects of CB[7] complexation on their molecular stabilities in aqueous solution.

References

1. J.-M. Lehn, *J. Incl. Phenom.*, **1988**, 6, 351.
2. P. D. Beer, P. A. Gale, and D. K. Smith, *Supramolecular Chemistry*, Oxford Chemistry Primers, 74, Oxford University Press: Oxford, 2003; pp. 1-30.
3. J. W. Steed, D. R. Turner and K. J. Wallace, *Core Concepts in Supramolecular Chemistry and Nanochemistry*, John Wiley & Sons, Ltd.: Chichester, 2007; pp. 1-27.
4. J. W. Steed and J. L. Atwood, *Supramolecular Chemistry*, John Wiley and Sons, Ltd.: Chichester, 2000; pp. 2-33.
5. C. A. Schalley, *Analytical Methods in Supramolecular Chemistry*, Wiley-VCH Verlag GmbH & Co. KGaA: Weinheim, 2007; pp 1-10.
6. G. V. Oshovsky, D. N. Reinhoudt and W. Verboom, *Angew. Chem. Int. Ed.*, **2007**, 46, 2366.
7. D. J. Cram, *Angew. Chem. Int. Ed.*, **1988**, 27, 1009.
8. F. M. Menger, *Proc. Natl. Acad. Sci. USA*, **2002**, 99, 4818.
9. D. J. Cram, *Angew. Chem. Int. Ed.*, **1986**, 25, 1039.
10. C. J. Pedersen, *Angew. Chem. Int. Ed.*, **1988**, 27, 1021.
11. B. G. Cox, H. Sneider, and J. Stroka, *J. Am. Chem. Soc.*, **1978**, 100, 4746.
12. V. Böhmer, *Angew. Chem. Int. Ed.*, **1995**, 34, 713.
13. K. A. Connors, *Chem. Rev.*, **1997**, 97, 1325.
14. E. M. M. Del Valle, *Proc. Biochem.*, **2004**, 39, 1033.
15. J. Szejtli, *Chem. Rev.*, **1998**, 98, 1743.
16. R. Behrend, E. Meyer, and F. Rusche, *Liebigs Ann. Chem.* **1905**, 339, 1.

17. (a) W. A. Freeman, W. L. Mock, N.-Y. Shih, *J. Am. Chem. Soc.*, **1981**, *103*, 7367.
(b) W. L. Mock, *Chapter 15: Cucurbituril*, In *Comprehensive Supramolecular Chemistry, Volume 2*, J. L. Atwood, J. E. D. Davies, D. D. MacNicol, F. Vogle, and J. M. Lehn (eds.), F. Vogtle (volume ed.), Pergamon: New York, 1996; pp. 477-493. (c) P. Cintas, *J. Incl. Phenom. Mol. Recognit. Chem.*, **1994**, *17*, 205.
18. J. Kim, I. Jung, S. Kim, E. Lee, J. Kang, S. Sakamoto, K. Yamaguchi, and K. Kim, *J. Am. Chem. Soc.*, **2000**, *122*, 540.
19. A. Day, A. P. Arnold, R. J. Blanch, and B. Snushall, *J. Org. Chem.*, **2001**, *66*, 8094.
20. (a) J. W. Lee, S. Samal, N. Selvapalam, H. Kim, and K. Kim, *Acc. Chem. Res.*, **2003**, *36*, 621. (b) J. Lagona, P. Mukhopadhyay, S. Chakrabarti, and L. Isaacs, *Angew. Chem. Int. Ed.*, **2005**, *44*, 4844; (c) K. Kim, N. Selvapalam, Y. H. Ko, K. M. Park, D. Kim and J. Kim, *Chem. Rev.*, **2007**, *36*, 267; (d) L. Isaacs, *Chem. Commun.*, **2009**, 619; (e) E. Masson, X. Ling, R. Joseph, L. Kyremeh-Mensah, and X. Lu, *RSC Adv.*, **2012**, *2*, 1213.
21. S. Liu, P. Y. Zavalij and L. Isaacs, *J. Am. Chem. Soc.*, **2005**, *127*, 16798.
22. K. A. Kellersberger, J. D. Anderson, S. M. Ward, K. E. Krakowiak, and D. V. Dearden, *J. Am. Chem. Soc.*, **2001**, *123*, 11316.
23. H. J. Buschmann, E. Cleve, K. Jansen, A. Wago, and E. Schollmeyer, *J. Incl. Phenom. Macrocycl. Chem.*, **2001**, *40*, 117.
24. H. J. Buschmann, L. Mutihac, and E. Schollmeyer, *J. Incl. Phenom. Macrocycl. Chem.*, **2008**, *61*, 343.
25. H. J. Buschmann, L. Mutihac, R. C. Mutihac, and E. Schollmeyer, *Thermochim. Acta.*, **2005**, *430*, 79.

26. S. Liu, C. Ruspic, P. Mukhopadhyay, S. Chakrabarti, P. Y. Zavalij, and L. Isaacs, *J. Am. Chem. Soc.*, **2005**, *127*, 15959.
27. G. Jiang and G. Li, *J. Photochem. Photobiol. B*, **2006**, *85*, 223.
28. D. H. Macartney, *Isr. J. Chem.*, **2011**, *51*, 600.
29. G. Parvari, O. Reany, and E. Keinan, *Isr. J. Chem.*, **2011**, *51*, 646.
30. N. Saleh, A. L. Koner, and W. M. Nau, *Angew. Chem. Int. Ed.*, **2008**, *47*, 5398.
31. G. Hettiarachchi, D. Nyugen, J. Wu, D. Lucas, D. Ma, L. Isaacs, and V. Briken, *PLoS ONE.*, **2010**, *5*, e10514.
32. V. D. Uzunova, C. Cullinane, K. Brix, W. M. Nau, and A. Day, *Org. Biomol. Chem.*, **2010**, *8*, 2037.
33. S. Walker, R. Oun, F.J. McInnes and N.J. Wheate, *Isr. J. Chem.*, **2011**, *51*, 616.
34. Y.J. Jeon, S.Y. Kim, Y.H. Ko, S. Sakamoto, K. Yamaguchi and K. Kim, *Org. Biomol. Chem.*, **2005**, *3*, 2122.
35. R. Wang, B.C. MacGillivray and D.H. Macartney, *Dalton Trans.*, **2009**, 3584.
36. F. H. Zelder, *Inorg. Chem.*, **2008**, *47*, 1264.

Chapter 2

EXPERIMENTAL

2.1 Preparation of Materials

2.1.1 Synthesis of the CB[7] Host Compound

The CB[7] host compound was prepared using the method described by Day and coworkers.¹ This acid-catalyzed reaction was conducted in a 250 mL round-bottom flask and used 42.6 mL of concentrated hydrochloric acid to start a polymerization reaction between 30.0 g of glycoluril and 12.7 g of paraformaldehyde (Figure 1.17).^{2,3,4,5} The solution was stirred as the reaction began, but after a few minutes the liquid solidified into a gel, which was allowed to stand for one hour. The gel was then heated to a temperature of 100 °C. This increase in temperature caused the gel to melt and form an orange solution, which was then refluxed at 100 °C for 18 hours. The cloudy orange solution was then cooled in an ice bath and filtered to remove the solid by-products which had formed. The filtrate was then allowed to stand for one hour to allow any additional by-products to precipitate. This precipitate was also removed from the filtrate by vacuum filtration. In order to remove any remaining impurities, the filtrate was placed in a rotary evaporator, reduced to one-third its original volume and added to 15 mL of pure water. The white precipitate that was formed during this process was once again removed by filtration. Next, 105 mL of methanol were added to the filtrate and left to stand for 18 hours. The solid precipitate that formed in this case was a mixture of CB[*n*] homologues, primarily CB[6]. This CB[*n*] precipitate was isolated by vacuum filtration and left to dry until all of the solvent had evaporated. Once dry, the solid CB[*n*] was added to a solution containing 60 mL of glycerol and 240 mL of distilled water.

The resulting mixture was heated to 85°C and stirred for half an hour in an attempt to dissolve most of the CB[*n*]. After the half hour, any undissolved solid was filtered until a clear, colourless filtrate remained. Once the clear solution was obtained, methanol was added until the solution turned cloudy as a white precipitate began to form. This solution was allowed to stand for 30 minutes and the resulting yellow-white, flaky solid was filtered. This precipitate contains mostly CB[6] and trace amounts of other CB[*n*] homologues, leaving a filtrate containing mostly dissolved CB[7]. From this point forward, the process of adding methanol and collecting the precipitate that formed was repeated until the filtrate stopped producing precipitate. This process usually led to approximately five fractions of useful product. Each of the fractions obtained were washed several times with methanol to remove any residual glycerol and then left to dry. The purity of each fraction and its effective molecular mass (including waters located in the cavity) was determined by ¹H NMR spectroscopy with a reference guest (tetracaine). Overall, the CB[*n*] synthesis process described above usually produces about 2 g of CB[7] (a 5.5% yield).

Cucurbit[7]uril

¹H NMR (400 MHz, D₂O at 4.75 ppm) δ 4.20 (d, 14H, *J* = 15.4 Hz), 5.49 (s, 14H), 5.76 (d, 14H, *J* = 15.4 Hz) ppm.

2.1.2 Synthesis of the Guest Compounds

Several guest compounds were used as received from the manufacturer. These guests included benzethonium chloride, 1,1-dimethylbiguanidine hydrochloride (metformin), phenformin hydrochloride, chlorhexidine dihydrochloride, pentamidine isoethionate, diminazene aceturate (berenil), and 4-aminobenzamidine dihydrochloride (Aldrich Chemical

Company); alexidine dihydrochloride from Toronto Research Chemicals; and 4-hydroxybenzamidine from Alfa Aesar Company.

The flavylum hexafluorophosphate guests (Chapter 6) were prepared using the method described by Goeldner and co-workers.⁶ This synthesis method involved 1.0 mmol of a 2-hydroxybenzaldehyde derivative and 1.0 mmol of an acetophenone derivative being dissolved in a minimum amount of acetic acid. To start the reaction, an excess of hexafluorophosphoric acid (50% in H₂O) was added to the solution, which immediately turned dark red. Next, the solution was stirred at room temperature for 48 hours. After this time, 20 mL of diethyl ether were added to the mixture, producing a coloured precipitate. This precipitate was then vacuum-filtered and washed several times with diethyl ether to remove any impurities. The final product, a flavylum hexafluorophosphate salt, was then dried and identified by ¹H NMR spectroscopy. The general mechanism of this flavylum synthesis reaction is depicted in Figure 2.1 below.

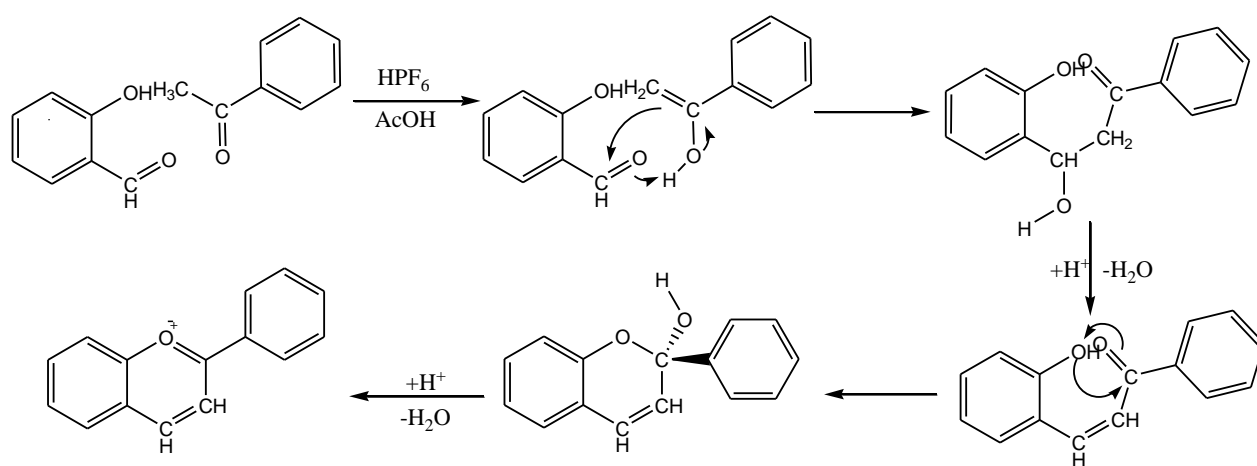


Figure 2.1 The mechanism used to convert 2-hydroxybenzaldehyde and acetophenone into a flavylum salt in the presence of hexafluorophosphoric acid and acetic acid.

This general mechanism described in Figure 2.1 was used to synthesize each of three different flavylium salts. The 6-methoxyflavylium, 4'-methoxyflavylium and 6,4'-dimethoxyflavylium hexafluorophosphate salts were each created using different combinations of 2-hydroxy-5-methoxybenzaldehyde, 4-hydroxybenzaldehyde, 4-methoxyacetophenone, and acetophenone as depicted in Figure 2.2 below. Each of the benzaldehyde and acetophenone derivatives were purchased from the Aldrich Chemical Company and used as received.

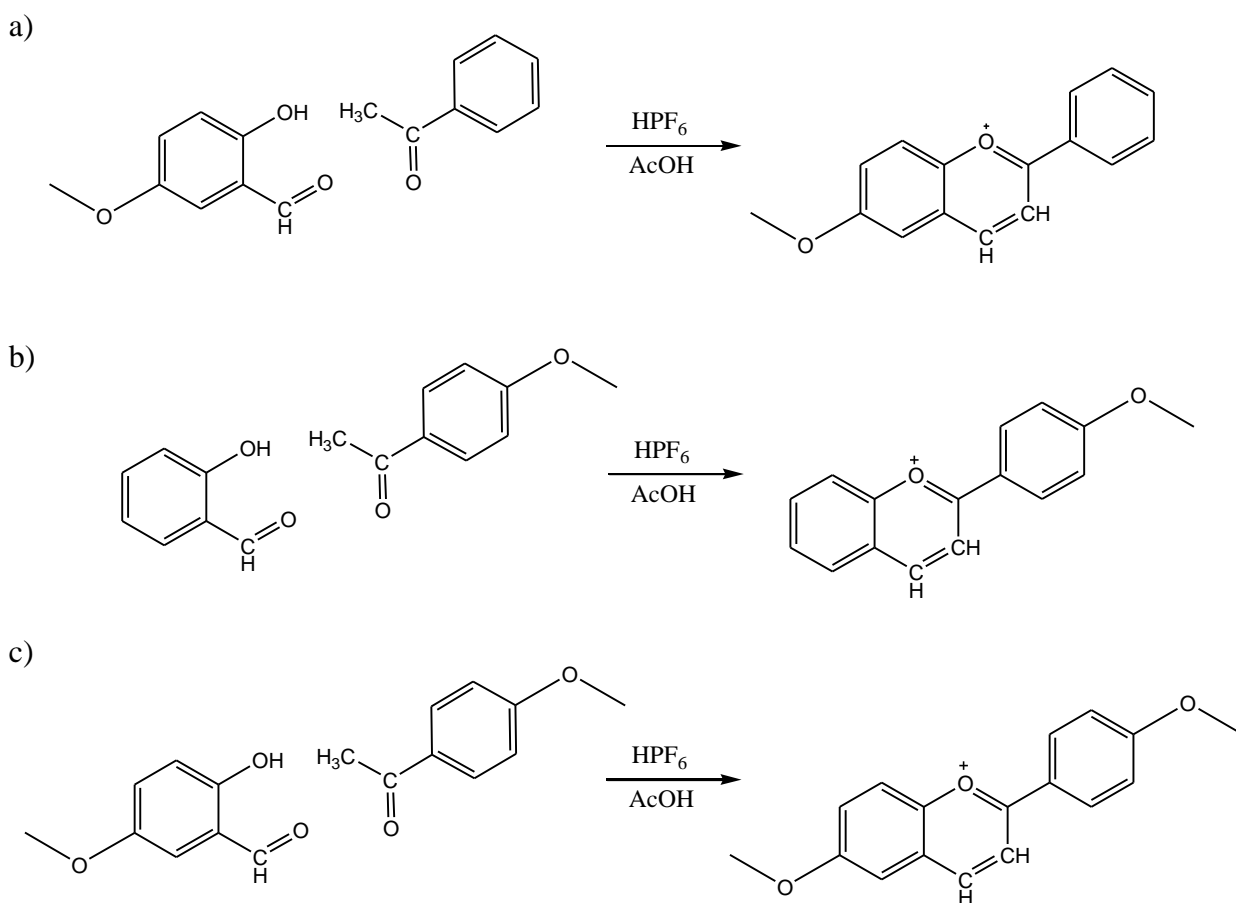


Figure 2.2 The acid-catalyzed formation of (a) 6-methoxyflavylium from 2-hydroxy-5-methoxybenzaldehyde and acetophenone (b) 4'-methoxyflavylium from 2-hydroxybenzaldehyde and 4-methoxyacetophenone (c) 6,4'-dimethoxyflavylium from 4-methoxyacetophenone and 2-hydroxy-5-methoxybenzaldehyde.

The synthesis of 6,4'-dimethoxyflavylium hexafluorophosphate produced an orange salt, while the syntheses of 6-methoxyflavylium hexafluorophosphate and 4'-methoxyflavylium hexafluorophosphate produced yellowish-green salts. Each of these three reactions produced high yields of approximately 90%.

6-methoxyflavylium hexafluorophosphate

^1H NMR (400 MHz, D_2O) δ 9.31 (d, 1H, $^3J_{2-3} = 11.0$ Hz, H_2), 8.65 (d, 1H, $^3J_{3-2} = 11.0$ Hz, H_3), 8.43 (d, 2H, $^3J_{2'-3'} = 10.5$ Hz, $\text{H}_{2'}$), 8.23 (d, 1H, $^3J_{8-7} = 11.5$ Hz, H_8), 7.91 (dd, 1H, $^3J_{7-8} = 11.5$ Hz, $^4J_{7-5} = 3.5$ Hz, H_7), 7.84 (t, 1H, $^3J_{4'-3'} = 9.5$ Hz, $\text{H}_{4'}$), 7.71 (t, 2H, $^3J_{3'-2' \& 4'} = 10.0$ Hz, $\text{H}_{3'}$) 7.64 (d, 1H, $^4J_{5-7} = 3.5$ Hz, H_5), 3.98 (s, 3H, H_{10}) ppm.

4'-methoxyflavylium hexafluorophosphate

^1H NMR (400 MHz, D_2O) δ 9.17 (d, 1H, $^3J_{2-3} = 11.5$ Hz, H_2), 8.51 (m, 3H, H_3 , $\text{H}_{2'}$), 8.17 (m, 3H, H_5 , H_7 , H_8), 7.86 (td, 1H, $^3J_{6-5 \& 7} = 10.0$ Hz, $^4J_{6-8} = 3.0$ Hz, H_6), 7.25 (d, 2H, $^3J_{3'-2'} = 11.5$ Hz, $\text{H}_{3'}$), 3.97 (s, 3H, $\text{H}_{5'}$) ppm.

6,4'-dimethoxyflavylium hexafluorophosphate

^1H NMR (400 MHz, D_2O) δ 9.05 (d, 1H, $^3J_{2-3} = 12.0$ Hz, H_2), 8.43 (d, 1H, $^3J_{3-2} = 11.5$ Hz, H_3), 8.39 (d, 2H, $^3J_{2'-3'} = 11.0$ Hz, $\text{H}_{2'}$), 8.08 (d, 1H, $^3J_{8-7} = 12.0$ Hz, H_8), 7.72 (dd, 1H, $^3J_{7-8} = 12.0$ Hz, $^4J_{7-5} = 4.0$ Hz, H_7), 7.53 (d, 1H, $^4J_{5-7} = 4.0$ Hz, H_5), 7.19 (d, 2H, $^3J_{3'-2'}$, $\text{H}_{3'}$), 3.95 (s, 3H, H_{10}), 3.93 (s, 3H, H_5) ppm.

The ^1H NMR spectrum of 6,4'-dimethoxyflavylium hexafluorophosphate was in good agreement with the data obtained by Goeldner and co-workers in $\text{DMSO}-d_6$.⁶ The ^1H NMR spectra of the 6-methoxyflavylium hexafluorophosphate and 4'-methoxyflavylium

hexafluorophosphate were consistent with spectra obtained using ^1H NMR Predicting Software (ACD Labs 7.0).

2.2 Experimental Methods and Apparatus

2.2.1 Mass Spectrometry

The electrospray mass spectra described herein were obtained using a QStar XL Qq TOF MS/MS system with an electrospray ionization (ESI) source. This method was selected because ESI-MS is an established soft ionization method that can ionize supramolecular complexes without breaking the non-covalent bonds that hold these complexes together.^{7,8} When the flavylium hexafluorophosphate salts were synthesized, their presence and purity were determined using ESI-MS. Since flavylium salt already contained an intramolecular cation, it could be easily identified by MS at a concentration of 1.0×10^{-3} M in a solution of distilled water.

ESI-MS was also used to determine whether a cationic guest formed a host-guest complex with the CB[7] host in aqueous solution. To determine if a complex had formed, an aqueous solution containing 1.0×10^{-3} M of guest and 5.0×10^{-3} M of CB[7] was prepared. Once this solution had been analyzed, the resulting spectrum was examined for evidence of peaks that matched the expected mass-to-charge ratio (m/z) of the host-guest complex. In addition to a peak for the guest complexing to CB[7], peaks are often observed which correspond to addition H^+ or Na^+ complexing to the guest or host, respectively, in the host-guest complex. When peaks of the correct m/z values were discovered in the spectrum, this was considered evidence of the existence of the host-guest complex in aqueous solution. While mass spectrometry can suggest that a host-guest complex exists in an aqueous

solution, it cannot provide information about where on a guest a host is binding, or how tightly bound the resulting complex is. To obtain this information, Nuclear Magnetic Resonance (NMR) spectroscopy was employed.

2.2.2 Nuclear Magnetic Resonance Spectroscopy

NMR spectroscopy is an important tool in the study of supramolecular chemistry because it can not only describe the structure and properties of a host and its guest, but also the structure and properties of the complex that forms between them.⁹ The research described herein uses NMR spectroscopy to confirm the structure of host and guest molecules (as described below), to determine where the CB[7] host is binding on the structure of a guest (Section 2.2.3), and determine how strongly the CB[7] host is binding to a guest (Section 2.3). The 1D ¹H NMR spectra described in this research were obtained using Bruker Avance 400 and 500 manual spectrometers, operating at frequencies of 400.14 and 499.12 MHz respectively. Each NMR sample was prepared in deuterium oxide, which was used as received from either the Aldrich Chemical Company or Cambridge Isotope Laboratories. The proton resonance for the residual, incompletely deuterated, HOD in the D₂O solvent appeared in each spectrum as a singlet and was set at 4.75 ppm as a reference peak. Kim *et al* demonstrated that the CB[7] host has three characteristic peaks that can be observed in NMR samples that contains more than 5.0 x 10⁻⁵ M CB[7].¹⁰ These three peaks were also used to confirm the identity of each newly synthesized fraction of CB[7] (Section 2.1.1). Although ¹H NMR spectroscopy has already proven to be a useful tool in confirming the structure of hosts and guests, it can also be applied to examine nature of the host-guest complex that forms between them.

2.2.3 NMR Chemical Shift Titrations

In the previous section, NMR spectroscopy proved to be highly effective in characterizing the structure of host and guest molecules. This section will draw on previous research conducted by Isaacs and coworkers, which has shown that NMR spectroscopy can be used to monitor the chemical shifts of the proton resonances of a guest as it undergoes titration with the CB[7] host.¹¹ To conduct each of the titrations, two solutions were prepared. The first solution was made up of 0.8 - 1.5 mM of the guest in D₂O. Approximately 0.7 mL of this solution was used to obtain an NMR spectrum of the guest solution in the absence of the CB[7] host. Next, a guest solution containing the same concentration of guest and ~5-10 times that concentration of the host was prepared. This second solution was then titrated into the NMR tube containing the first solution, such that each new scan contained an additional 0.2 equivalents of CB[7] and the guest was maintained at a constant concentration. The titration was discontinued once there were no further changes in the peak position for three consecutive spectra. The exact concentration of host and guest used in each titration is presented in Table 2.1, below.

As guest molecules began to bind with CB[7], the proton resonances of the guest were monitored to determine whether they exhibited upfield shifts or downfield shifts ($\Delta\delta$) corresponding to increased shielding or deshielding, respectively. The peaks which move upfield ($\Delta\delta < 0$) are identified as belonging to guest protons within the hydrophobic cavity of CB[7] and peaks that shifted downfield ($\Delta\delta > 0$) are identified as belonging to protons external to the cavity and involved in associations with the ureido oxygens of the polar portals of CB[7]. These effects of binding with CB[7] are summarized in Figure 2.3, below.

Table 2.1 The host and guest concentrations used to conduct each titration in this research.

Guest	[Guest]	[Host]
Benzethonium	1.0×10^{-3} M	5.0×10^{-3} M
Metformin	8.0×10^{-4} M	4.0×10^{-3} M
Phenformin	8.0×10^{-4} M	8.0×10^{-3} M
Chlorhexidine	8.0×10^{-4} M	8.0×10^{-3} M
Alexidine	8.0×10^{-4} M	8.0×10^{-3} M
Pentamidine	1.5×10^{-3} M	7.5×10^{-3} M
Berenil	1.5×10^{-3} M	7.5×10^{-3} M
4-aminobenzamidine	1.0×10^{-3} M	5.0×10^{-3} M
4-hydroxybenzamidine	1.0×10^{-3} M	5.0×10^{-3} M
6-methoxyflavylium	1.0×10^{-3} M	5.0×10^{-3} M
4'-methoxyflavylium	1.0×10^{-3} M	5.0×10^{-3} M
6,4'-dimethoxyflavylium	1.0×10^{-3} M	5.0×10^{-3} M

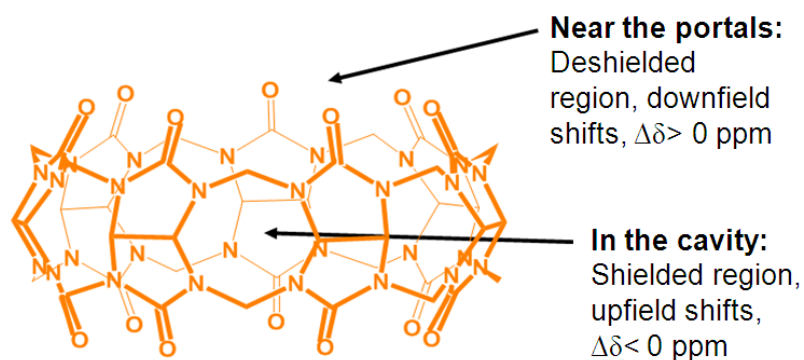


Figure 2.3 A summary of the effects exhibited by a guest, when binding to a CB[7] host.

From the results shown in Figure 2.3, it was possible to determine where the CB[7] was binding on the structure of the guest, based on the shifts in the guest's proton resonances. For a strongly bound complex, once a 1:1 host-guest ratio was achieved and each guest molecule became bound to a CB[7] host, the proton resonances on the guest molecule reached the limit of their chemical shift change. By calculating the change in peak position for each proton resonance ($\Delta\delta_{\text{lim}} = \delta_{\text{bound}} - \delta_{\text{free}}$), it became possible to determine which protons were located within the cavity of CB[7] ($\Delta\delta_{\text{lim}} < 0$) and which were located near the polar portals ($\Delta\delta_{\text{lim}} > 0$). Furthermore, by depicting the structure of each guest with its limiting chemical shifts placed beside the appropriate proton environment, it was possible to create a visual representation of exactly where CB[7] was binding to the guest.

In addition to describing where CB[7] was binding to a guest, chemical titrations monitored by NMR spectroscopy can also provide information on how strongly a host and guest are bound to one another. Once a titration is complete, several representative spectra at different host-guest concentrations are selected and combined to demonstrate the effects of host complexation on the guest protons. These summary figures, called stack plots, were prepared for the titration of CB[7] with each of the guests examined in this research. The appearance of these stack plots can vary, depending on how fast the exchange (dissociation) rate between the host-bound and free guest is, in comparison to the NMR timescale. As a result of this effect, the guest resonances in a titration between CB[7] and a guest can result in a stack plot exhibiting either fast exchange, intermediate, or slow exchange behaviour. Stack plots exhibiting fast exchange behaviour have guest peaks which gradually shift upfield or downfield as the host is titrated. This effect is observed because the guest is exchanging so quickly with the host that its resonances appear as a weighted average of the

free and bound resonances. By contrast, a guest undergoing slow exchange with a host can be observed in either their free or bound form. This effect results in two separate peaks for each proton environment per guest spectra; one peak represents the proton resonance of the free guest and the other represents that of the bound guest. As a titration between CB[7] and a slow exchange guest progresses, the peaks of the free guest will diminish until CB[7] has bound to all of the guest molecules and only the bound proton peaks remain in the NMR spectra. Although most guests can be classified as either fast exchange or slow exchange, there are a few guests which undergo exchange at an intermediate rate on the NMR timescale. Guests undergoing intermediate exchange display proton resonances that initially broaden at the position of the free guest at low host concentrations, and then sharpen at the position of the bound guest in the spectrum at high host concentrations. Based on this information, it is clear that different guests exhibit different properties and different exchange rates when forming host-guest complexes with CB[7]. Regardless of the differences in NMR spectra caused by different exchange rates, any stack plot can prove useful in determining how strongly a host is binding to a guest. The methods of determining a binding constant using the ^1H NMR spectral data are discussed in Chapter 2.3.1.

2.2.4 UV-Visible Spectroscopy

UV-visible spectroscopy has proven to be a highly useful analysis tool in the study of CB[7] and its host-guest chemistry.^{13,14} In this research, spectrophotometric analyses were conducted using a Hewlett Packard 8452A Diode Array UV-visible spectrophotometer and 1.00 cm quartz cells. Sample solutions were prepared in water at concentrations on the order of 10^{-5} – 10^{-4} M, depending on the molar extinction coefficient of the sample at

wavelength(s) monitored. The research described herein used a combination of UV-visible spectroscopy and pH titrations to monitor changes in the absorbance spectrum and thereby measure pK_a shifts (Chapter 2.4) and also to examine the reaction kinetics of a guest at a variety of host concentrations (Chapter 2.5).

2.2.5 Chemical Structures & Molecular Modeling Studies

The chemical structures and reaction mechanisms depicted in this work were created using ChemDraw Pro 12.0 (and earlier versions) from CambridgeSoft. The molecular modeling studies of the host-guest complexes were conducted through a MM2 energy minimization calculation that was run using ChemBio3D Ultra 12.0 (and earlier versions) from CambridgeSoft. These molecular modeling studies often provided evidence supporting the existence of a host-guest complex in the gas phase, however, the use of this technology is still limited when attempting to describe the behaviour of these complexes in aqueous solution.

2.3 Determination of Binding Constants

Once the existence of a host-guest complex (H·G) has been indicated by ESI mass spectrometry and/or ^1H NMR spectroscopy (Equation 2.1), the next step in its characterization involves determining how strongly the host (H) and guest (G) are bound to one another.^{15,16}



The thermodynamic stability of a host-guest complex is determined by the preorganization of the host, the size fit between the host and guest, and the complementarity of the non-covalent forces that hold the complex together. The stability of such a host-guest complex in solution is measured as a binding constant (also called stability or association constants), which can be expressed as described in Equation 2.2, where $[H_f]$ and $[G_f]$ are the concentrations of the free host and guest, respectively.

$$K = \frac{[H \cdot G]}{[H_f][G_f]} \quad (2.2)$$

It is also possible for the stoichiometry to vary beyond a simple 1:1 host-guest complex.^{15,16} In this research, host-guest complexes with 1:2, 2:1, and 3:1 stoichiometries have been observed. In the case where one host is bound to two guests, Equation 2.3 describes the formation of the complex and Equation 2.4 describes its binding constant.



$$K_{1:2} = \frac{[H \cdot G_2]}{[H \cdot G][G_f]} \quad (2.4)$$

For complexes which contain n hosts (where $n > 1$) and a single guest, Equation 2.5 describes the formation of the complex and Equation 2.6 describes its binding constant.



$$K_n = \frac{[H_n \cdot G]}{[H_{(n-1)} \cdot G][G_f]} \quad (2.6)$$

There are a number of different methods for determining the binding constant that occurs between a host and its guest. For example, if a guest has formed a weakly bound complex with its host ($K < 10^4 \text{ M}^{-1}$), then its binding constant can be measured by plotting a binding curve using the information obtained from a ^1H NMR chemical shift titration of the host into the guest (Chapter 2.3.1). However, if a guest is strongly bound to its host ($K > 10^4 \text{ M}^{-1}$) then plotting a binding curve using ^1H NMR data will not result in an accurate binding constant. In this situation, the binding constant of a host-guest complex must be determined using a ^1H NMR competition study (Chapter 2.3.2). The use of either a binding curve or a competition study will often result in an accurate binding constant. One complication that can arise when determining the binding constants of a guest is that the guest contains two or more identical binding sites, with similar binding constants anticipated. This circumstance is difficult to resolve because the use of either a binding curve or competition study will result in a single binding constant, which is an average of these two separate binding events. In order to account for this effect, the concept of statistical binding is applied (Chapter 2.3.3). Each host-guest binding constant described in this thesis was calculated using a binding curve, competition study, or statistical binding as indicated in the sections that follow.

2.3.1 Fitting a Binding Curve

In the study of host-guest complexes, fitting a binding curve is the most common method of determining a binding constant.¹⁶ In the present research, this is also one of the simplest methods, since it uses existing data from a ^1H NMR titration to calculate the binding constant. The exact means of determining the stability constant from the ^1H NMR spectra

can vary, depending on whether the complex is exhibiting fast, intermediate, or slow exchange behaviour with respect to the NMR timescale.

If the complex is undergoing fast exchange, then the guest proton resonances represent an average between the chemical shifts of the free and bound forms. The approach taken was to identify the resonance that showed the greatest shift in position ($\Delta\delta_{\text{lim}} = \delta_{\text{bound}} - \delta_{\text{free}}$) without overlapping other peaks. From each spectrum in the titration, the total concentration of the host (from the relative integrations of host and guest resonances) and the corresponding change in chemical shift of the resonance ($\Delta\delta_{\text{obs}}$) were determined. A binding curve, produced by plotting $\Delta\delta_{\text{obs}}$ versus the concentration of host present in solution, was subjected to a non-linear least-squares fit (using SigmaPlot 8.0, Systat Software) to equations 2.7, where $[\text{H}\cdot\text{G}]$ is determined using equations 2.8 and 2.9.¹⁷

$$\Delta\delta_{\text{obs}} = \Delta\delta_{\text{lim}}([\text{H}\cdot\text{G}]/[\text{G}]_{\text{total}}) \quad (2.7)$$

$$[\text{H}\cdot\text{G}] = \{b - (b^2 - 4[\text{G}]_{\text{total}}[\text{H}]_{\text{total}})^{1/2}\}/2 \quad (2.8)$$

$$\text{where } b = [\text{G}]_{\text{total}} + [\text{H}]_{\text{total}} + K^{-1} \quad (2.9)$$

This least-squares fit method was used successfully to determine the binding constants for the second and third stepwise stability constants for the 2:1 CB[7]·benzethonium and 3:1 CB[7]·chlorhexidine complexes, respectively.

For host-guest complexes which exhibit slow exchange behaviour on the NMR timescale, there are separate resonances for the free and bound forms of the guest. Using a pair of resonances representing the free and bound protons that do not overlap with other peaks, the integration of these peaks provided information on the concentration of free guest

[G_f] and bound guest [G_b]. Using this information it is possible to determine the fraction of bound guest as expressed in Equation 2.10 below.

$$\text{Fraction of Bound Guest} = \frac{[G_b]}{([G_f]+[G_b])} \quad (2.10)$$

The integration of the CB[7] peaks also provided information on the concentration of host present in the solution. Once these values had been determined, a binding curve was produced by plotting fraction of bound guest versus the concentration of host.

However, if a binding constant is too high, then this method cannot be used to determine an accurate binding constant. Under these conditions, a competitive binding study is required.

2.3.2 Competitive Binding Studies

Competitive binding studies were first used by Isaacs and coworkers to calculate binding constants between CB[7] and tightly bound guests.¹¹ These binding studies employ a guest with a known binding affinity for the CB[7] host, to help determine the unknown binding constant of a new guest. The guest with a known binding constant, hereafter referred to as the competitor, is selected based on its structural similarities to the new guest, in the hope that they will have similar binding constants. Isaacs and coworkers originally published a list of potential competitors and their binding constants.¹¹ This short list of two dozen guests has since been extended by our group and others to include several hundred guests with known CB[7] binding constants.^{18,19,20} The original binding studies, conducted by Isaacs, were carried out in D₂O at a pD of 4.75 using 50 mM of sodium acetate and 25 mM

of DCl as a buffer. Since binding constants are sensitive to both pH and salt concentrations, all subsequent competitive binding studies were also conducted under these conditions. Once a competitor had been selected, a buffered D₂O solution containing approximately 3:4:4 mM of CB[7], guest, and competitor respectively, was prepared and analyzed by ¹H NMR. Ideally, both the guest and competitor peaks would have show some evidence of binding with CB[7], indicating that both were competing for the limited amount of host. By examining the degree to which each set of peaks shifted, it becomes possible to calculate how strongly the new guest was binding to CB[7] in comparison to the competitor. The degree of difference between these two binding events was measured quantitatively as a relative binding constant (K_{rel}). The calculation of this relative binding constant is expressed in Equation 2.11 below.

$$K_{rel} = \frac{[H \cdot C][G_f]}{[H \cdot G][C_f]} \quad (2.11)$$

In Equation 2.11, $[G_f]$ and $[C_f]$ represent the concentrations of free guest and competitor, respectively, and $[H \cdot G]$ and $[H \cdot C]$ represent the respective concentrations of guest and competitor bound to the CB[7] host. Each of these concentration values were calculated as described in Equations 2.12 – 2.15 below.

$$[H \cdot C] = [C_{Tot}] \times (\Delta\delta_{obs}/\Delta\delta_{lim}) \quad (2.12)$$

$$[C_f] = [C_{Tot}] - [H \cdot C] \quad (2.13)$$

$$[H \cdot G] = [H_{Tot}] - [H \cdot C] \quad (2.14)$$

$$[G_f] = [G_{Tot}] - [H \cdot G] \quad (2.15)$$

In Equations 2.11 – 2.15 the total concentrations of host (H_{Tot}), guest (G_{Tot}), and competitor (C_{Tot}) were measured through peak integration. The observed chemical shift change of the competitor ($\Delta\delta_{\text{obs}}$) and the limit of the chemical shift change for the competitor ($\Delta\delta_{\text{lim}}$) were measured as expressed in Equation 2.16 and 2.17 below.

$$\Delta\delta_{\text{obs}} = \delta_{\text{obs}} - \delta_{\text{free}} \quad (2.16)$$

$$\Delta\delta_{\text{lim}} = \delta_{\text{bound}} - \delta_{\text{free}} \quad (2.17)$$

Since the peak positions of the competitor when free (δ_{free}) and bound (δ_{bound}) can often be found in the paper describing its binding constant, only the observed change in competitor peak position during the competition study is required to complete this series of calculations. Thus, by determining the observed peak position of the competitor (δ_{obs}) in the competition study, as well as the total concentration of host, guest, and competitor used, and by using the known peak positions of the competitor when free (δ_{free}) and bound (δ_{bound}), it became possible to determine a relative binding constant. In order to be considered useful, a relative binding constant needed to fall within the range of $0.1 \leq K_{\text{rel}} \leq 10$. Any relative binding constant outside of this range would produce an inaccurate binding constant, and the competition experiment would need to be repeated using a different competitor. Once a competitor produced a relative binding constant within the acceptable range, then it could be used to calculate the unknown binding constant of the guest as expressed in Equation 2.18 below.

$$K_{\text{CB}[7]\cdot\text{Guest}} = \frac{K_{\text{CB}[7]\cdot\text{Comp}}}{K_{\text{rel}}} \quad (2.18)$$

The competition method was used successfully to determine the 1:1 binding constants between CB[7] and benzethonium, phenformin, chlorhexidine, alexidine, berenil, 4-aminobenzamidine, 4-hydroxybenzamidine, 6-methoxyflavylium, 4'-methoxyflavylium, and 6,4'-dimethoxyflavylium. This method was also used to calculate a binding constant for pentamidine, however, the calculated binding constant represented a combination the 1:1 and 2:1 binding events on the identical termini of pentamidine. In order to correct for this effect, the statistical binding method needed to be applied.

2.3.3 Statistical Binding

Statistical binding was employed when a guest contained two or more identical binding sites.²¹ In theory, a host could bind to either of the available sites with equal probability, and their binding constants would be expressed as described in Equations 2.2 and 2.6. However, since the host was binding to identical binding sites, the binding constants for each binding event would be nearly identical. The only minor difference between the two binding constants might result from the second CB[7] being slightly repulsed by the polar portals of the first CB[7], if the binding sites were in sufficiently close proximity to each other. Overall, the binding events at these identical sites may exhibit spectroscopic changes (e.g. fast exchange behaviour in ¹H NMR) which would yield only a single, combined binding constant. To correct for this effect, it is necessary to consider exactly what each of these binding events entails. In principle, a binding constant (K) can be described as the rate at which the host binds to the guest (k_{on}) versus the rate at which the host releases from the guest (k_{off}). This relationship can be expressed as shown in Equation 2.19 below.

$$K = k_{\text{on}}/k_{\text{off}} \quad (2.19)$$

In the case of a guest with two identical binding sites, the first host can bind to either of the two available binding sites, but once bound can only release from that one site. The second host can bind to only the unbound site on the guest, but once its bound, either of the two hosts can release. The ratio of the binding and release rate constants would therefore be proportional to the probability based on the number of sites involved. These relationships are expressed in Equations 2.20 and 2.21 below.

$$K_{1:1} = k_{\text{on}}/k_{\text{off}} \propto 2/1 \quad (2.20)$$

$$K_{2:1} = k_{\text{on}}/k_{\text{off}} \propto 1/2 \quad (2.21)$$

Based on this information, the binding constants for the first and second binding events would be approximately double and half of the observed binding constant, respectively. The relationship of these binding constants is expressed in Equations 2.22 – 2.24 below.

$$K_{1:1} = 2K_{\text{obs}} \quad (2.22)$$

$$K_{2:1} = 0.5K_{\text{obs}} \quad (2.23)$$

$$K_{1:1} = 4K_{2:1} \quad (2.24)$$

This statistical binding method (Equation 2.24) was used successfully to determine the binding constants for the 2:1 CB[7]-chlorhexidine complex and the 1:1 and 2:1 CB[7]-pentamidine and CB[7]-alexidine complexes.

2.4 Complexation-Induced pK_a Shifts

In the field of supramolecular chemistry, there is a growing interest in the ability of macrocyclic hosts to induce shifts in the effective pK_a of included guests.¹⁴ Previous research, conducted by our group and others, has shown that CB[7] is capable of inducing significant pK_a shifts in bound guests.^{13,22,23} In order to determine if a pK_a shift had taken place, UV-visible spectra of the guest, at various pH values, were recorded in the absence and presence of CB[7]. Using the wavelength at which the absorbance change was the largest, a plot of absorbance vs pH was constructed and the pK_a was estimated based on the inflection point of each of the two resulting sigmoidal curves. The observed absorbance values can be subjected to a non-linear least-squares fit to Equation 2.25 to obtain the value of the pK_a .

$$A_{\text{obs}} = \frac{A_{\text{HG}^+} + A_{\text{G}}K_a/[\text{H}^+]}{1 + K_a/[\text{H}^+]} \quad (2.25)$$

The difference between the bound and unbound pK_a values describes the degree of the pK_a shift. Complexation-induced pK_a shifts, resulting from binding to CB[7], were successfully determined for the 4-aminobenzamidinium, 4-hydroxybenzamidinium, 6-methoxyflavylium, 4'-methoxyflavylium, and 6,4'-dimethoxyflavylium cations.

2.5 Complexation-Induced Changes in Rate Constant

The binding event between CB[7] and a guest can have a profound effect on the reactivity of that guest.^{13,23} In this research, UV-visible spectroscopy was used to determine what effect, if any, binding to CB[7] had on the reactivity of a guest. In order to determine

the extent of a change in the reactivity of a guest, its rate of reaction in the absence and presence of CB[7] needed to be determined through the use of Equation 2.26

$$\ln A_t = -kt + \ln A_0 \quad (2.26)$$

where t is the amount of time since the reaction began, A_t is the absorbance at time t , A_0 is the absorbance when the reaction began ($t = 0$) and k is the first-order rate constant of the reaction. When this equation is rearranged as shown,

$$\ln(A_t/A_0) = -kt \quad (2.27)$$

it is possible to plot a graph of $\ln(A_t/A_0)$ vs t and obtain lines of slope $-k$. If binding to CB[7] has resulted in a change in reactivity then there will be a noticeable difference in k_{bound} and k_{free} . This method of determining the change in rate constant was successfully applied when examining the acid-catalyzed degradation of berenil (Chapter 5) and the thermal isomerization of 2-hydroxychalcone in basic solution (Chapter 6).

References

1. A. Day, A. P. Arnold, R. J. Blanch, and B. Snushall, *J. Org. Chem.*, **2001**, *66*, 8094.
2. W. A. Freeman, W. L. Mock, and N.-Y. Shih, *J. Am. Chem. Soc.*, **1981**, *103*, 7367.
3. W. L. Mock and N.-Y. Shih, *J. Org. Chem.*, **1986**, *51*, 4440.
4. W. L. Mock, *Chapter 15: Cucurbituril*, In *Comprehensive Supramolecular Chemistry, Volume 2*, J.L. Atwood, J. E. D. Davies, D. D. MacNicol, F. Vogle, and J. M. Lehn (eds.), F. Vogtle (volume ed.), Pergamon: New York, 1996; pp. 477-493.
5. L. Isaacs, *Isr. J. Chem.*, **2011**, *51*, 578.
6. M. Kueny-Stotz, S. Chassaing, R. Brouillard, M. Nielsen, and M. Goeldner, *Bioorg. Med. Chem. Lett.*, **2008**, *18*, 4864.
7. I. Osaka, M. Kondou, N. Selvapalam, S. Samal, K. Kim, M. V. Rekharsky, Y. Inoue, and R. Arakawa, *J. Mass Spec.*, **2006**, *41*, 202.
8. C. A. Schalley, *Int. J. Mass Spec.*, **2000**, *194*, 11.
9. H.-J. Schneider and A. K. Yatsimirsky, *Principles and Methods in Supramolecular Chemistry*, John Wiley and Sons, Ltd.: Chichester, 2000; pp. 227-258.
10. J. Kim, I.-S. Jung, S.-Y. Kim, E. Lee, J.-K. Kang, S. Sakamoto, K. Yamaguchi, and K. Kim, *J. Am. Chem. Soc.*, **2000**, *122*, 540.
11. S. Liu, C. Ruspic, P. Mukhopadhyay, S. Chakrabarti, P. Y. Zavalij, and L. Isaacs, *J. Am. Chem. Soc.*, **2005**, *127*, 15959.
12. J. W. Steed and J. L. Atwood, *Supramolecular Chemistry*, John Wiley & Sons, Ltd.: Chichester, 2000; pp. 16-17.
13. G. Parvari, O. Reany, and E. Keinan, *Isr. J. Chem.*, **2011**, *51*, 646.
14. N. Saleh, A. L. Koner, and W. M. Nau, *Angew. Chem. Int. Ed.*, **2008**, *47*, 5398.

15. J. W. Steed, D. R. Turner, and K. J. Wallace, *Core Concepts in Supramolecular Chemistry and Nanochemistry*, John Wiley & Sons, Ltd.: Chichester, 2007; pp. 14-15.
16. C. A. Schalley, *Analytical Methods in Supramolecular Chemistry*, Wiley-VCH Verlag GmbH & Co. KGaA: Weinheim, 2007; pp 17-45.
17. R. S. Wylie and D. H. Macartney, *Inorg. Chem.*, **1993**, 32, 1830.
18. A. D. St-Jacques, I. W. Wyman, and D. H. Macartney, *Chem. Commun.*, **2008**, 4936.
19. I. W. Wyman and D. H. Macartney, *Org. Biomol. Chem.*, **2010**, 8, 253.
20. L. Yuan, R. Wang and D. H. Macartney, *Tetrahedron: Asymmetry*, **2007**, 18, 483.
21. G. Ercolani, *J. Am. Chem. Soc.*, **2003**, 125, 16097.
22. R. Wang, B. C. MacGillivray, and D. H. Macartney, *Dalton Trans.*, **2009**, 3584.
23. D. H. Macartney, *Isr. J. Chem.*, **2011**, 51, 600.

Chapter 3

HOST-GUEST COMPLEXATION BETWEEN CUCURBIT[7]URIL AND THE BENZETHONIUM CATION

3.1 Introduction

Alkylammonium guests were among the first organic guests to be used in binding studies with the original cucurbituril host, CB[6].¹⁻⁶ In these cases, binding was driven by strong ion-dipole interactions between the electronegative oxygen atoms of the host's portal carbonyl groups and the guest's cationic ammonium group.^{1,2,4} The result of these binding events was strong and selective host-guest complexes with high binding constants.^{4,5,6} As the range of guests being studied expanded, cationic ammonium groups with longer alkyl chains were found to bind even more strongly to CB[6].³⁻⁶ ¹H NMR studies of these complexes determined that the longer non-polar chains were being included in the hydrophobic cavity of CB[6], which demonstrated that binding to CB[6] can be strengthened through the use of the hydrophobic effect.^{3,5,6} Within the last decade, the focus of cucurbituril host-guest chemistry has shifted from the use of CB[6] towards CB[7].^{6,7} As with CB[6], CB[7] has been shown to strongly bind to alkylammonium guests with high binding constants.^{7,8,9} CB[7] has also been shown to have higher affinity for guests that contain both a cationic group, which can bind to the portals of CB[7], and a nearby hydrophobic group, which can reside within the non-polar cavity of CB[7].^{8,9} One such guest, the conjugate acid of amantadine (1-ammonioadamantane, Figure 3.1), used as an anti-viral drug (Symmetrel) and for the treatment of symptoms of Parkinson's disease, is able to take advantage of both the

electrostatic and hydrophobic binding forces of CB[7] and, as a result, has a host-guest binding constant of $K_{\text{CB}[7]} = (4.23 \pm 1.00) \times 10^{12} \text{ M}^{-1}$ with CB[7].⁷

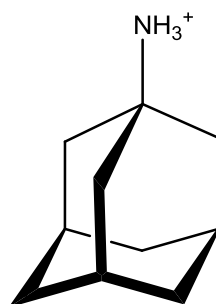


Figure 3.1 The structure of the conjugate acid of amantadine.

Binding constants of this strength are among the strongest seen in supramolecular chemistry and rival the binding constants of enzyme-substrate complexes found in Nature.⁷ It is this sort of tightly bound complex that underlines the potential for the use of CB[7] in a variety of applications and makes alkylammonium guests an ongoing source of attention in cucurbituril host-guest chemistry.

Benzethonium chloride is a synthetic compound, containing a quaternary tetraalkylammonium cation (Figure 3.2), used primarily as an anti-fungal preservative in the food and cosmetic industries.¹⁰ It also has moderate antiseptic and anti-infective properties, making it useful as a disinfectant and a viable alternative to alcohol-based hand sanitizers.^{10,11} Recently it was determined in a cell-based, small molecule screen that benzethonium is selectively toxic to human pharyngeal cancer cells, but not to normal human or mouse cells.¹²

When it is desirable to isolate organisms from solutions containing anti-microbial agents, such as benzethonium chloride, non-ionic detergents or phospholipids, which trap the

anti-microbial agents within micelles, are commonly employed. These molecules, however, can also be lethal to the microorganisms. Macrocyclic host molecules, such as β -cyclodextrin, have been shown to be effective as an alternative to detergents for neutralizing quaternary ammonium compounds, such as benzethonium chloride.¹³

It is these potential drug applications, both delivery and neutralization, that led us to study the benzethonium cation and its host-guest chemistry with CB[7].

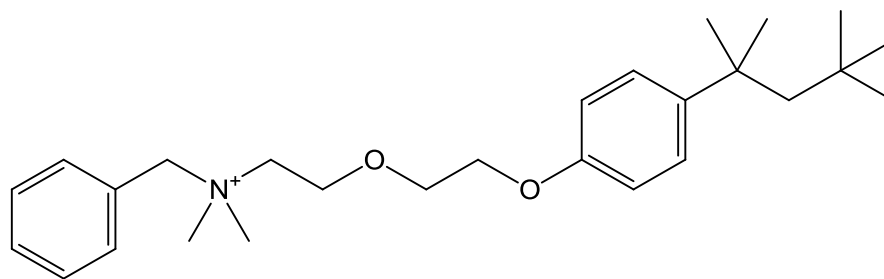


Figure 3.2 Structure of the benzethonium cation.

The benzethonium cation possesses a hydrophilic cationic benzyldimethylammonium fragment on one end and a hydrophobic 2-(2,4,4-trimethylpentyl)-substituted phenyl group on the other end, with a diethyleneglycol unit in the center. This would allow for the binding of two cucurbit[7]uril host molecules using different non-covalent interactions to stabilize the host-guest interactions. We have observed a similar phenomenon with coenzyme B₁₂, where the first CB[7] bound to the protonated α -axial 5,6-dimethylbenzimidazole base which had dissociated from the Co(III) center ($K^1_{\text{CB}[7]} = (3.02 \pm 0.35) \times 10^6 \text{ M}^{-1}$).¹⁴ This was followed by a second weaker binding to the neutral β -axial 5'-deoxyadenosyl ligand ($K^2_{\text{CB}[7]} = (1.1 \pm 0.2) \times 10^3 \text{ M}^{-1}$) without its detachment from the Co(III) center. The three orders of

magnitude difference in the binding constants allowed for the two processes to be observed separately in the ^1H NMR spectrum.

This chapter will describe the complexation between CB[7] and the benzethonium cation through the use of ESI mass spectrometry and ^1H NMR spectroscopy. The host-guest binding constants were also determined by ^1H NMR competition experiments for the 1:1 complex and by fitting the ^1H NMR titration binding curve for the 2:1 complex. The relative CB[7] complexations of the hydrophilic benzylammonium and hydrophobic alkyl termini of the guest will be discussed and compared with previous studies of similar guest binding moieties with CB[7].

3.2 Results and Discussion

3.2.1 ESI Mass Spectrometry and ^1H NMR Spectroscopy

In order to characterize the CB[7]·benzethonium host-guest complex(es), a number of analytical tools were used. Once an aqueous solution containing benzethonium and CB[7] had been prepared, high-resolution electrospray ionization mass spectrum (ESI-MS) was used to confirm the presence of the host-guest complex by the mass/charge ratio. The ESI mass spectrum of an aqueous solution of the benzethonium cation in the presence of a five-fold excess of CB[7] reveals peaks with $m/z = 1574.6675$ and 1380.0013 . The former peak corresponds to the 1:1 {CB[7]·benzethonium} $^+$ complex (calculated $m/z = 1574.6645$ for $\text{C}_{69}\text{H}_{84}\text{N}_{29}\text{O}_{16}^+$), while the second peak correspond to the 2:1 {CB[7]·benzethonium·CB[7]·Na} $^{2+}$ complex (calculated $m/z = 1379.9987$ for $\text{C}_{111}\text{H}_{126}\text{N}_{57}\text{O}_{30}\text{Na}^{2+}$). This data demonstrated that the benzethonium cation was able to form a complex with either one or two CB[7] hosts. Once the presence of the host-guest

complexes was confirmed by ESI-MS, ^1H NMR spectroscopy was then used to determine where on the guest the host molecules were binding and how the binding was affecting the chemical shifts of the guest proton resonances in the region where they bound. To examine how the guest protons were affected by binding with CB[7], it was necessary to first assign the proton resonances in the ^1H NMR spectrum. A complete set of NMR peak assignments for the benzethonium cation is shown in Figure 3.3.

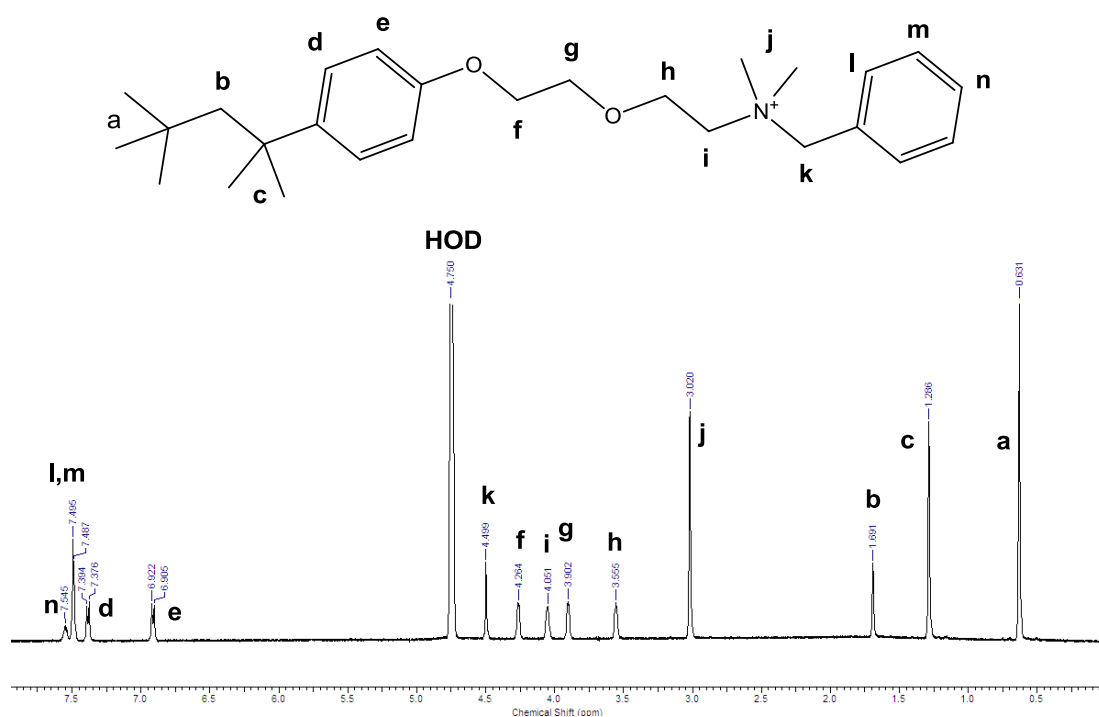


Figure 3.3 ^1H NMR proton resonance assignments for the benzethonium cation in D_2O .

Once the ^1H NMR resonances of the benzethonium cation had been identified, the guest was titrated with CB[7] and the upfield or downfield shifts ($\Delta\delta_{\text{lim}} = \delta_{\text{bound}} - \delta_{\text{free}}$) of the guest proton resonances were monitored. As the titration progressed, peaks that moved upfield were identified as belonging to protons involved in associations with the hydrophobic

cavity of CB[7]. Any peaks that moved downfield were identified as belonging to protons involved in associations with the polar portals of CB[7]. Once the titration was complete, several representative spectra at different host-guest concentrations were selected and combined to demonstrate the effects of host complexation on the guest protons. This summary figure, called a stack plot, was prepared for the titration of the benzethonium cation with CB[7], and is depicted in Figure 3.4.

By examining which proton peaks shifted and at what concentration of CB[7] they shifted at, it is possible to determine where and at what ratio the host became bound to the guest. The stack plot (Figure 3.4) and the summary of the complexation-induced chemical shift changes for the guest proton resonances, shown in Figure 3.5, indicate two sequential binding processes by CB[7] host molecules. The first process is the CB[7] binding of the more hydrophilic end of the molecule, over the benzyldimethylammonium group (protons H_j, H_k, H_l, H_m) to form a 1:1 host-guest complex. This is followed by the complexation of the more hydrophobic end, containing the 2-(2,4,4-trimethylpentyl) substituent on the aromatic ring (protons H_a, H_b, and H_c) to form a 2:1 host-guest complex.

The slight downfield shifts in the H_f, H_g, and H_h protons of the central linker indicate that this portion of the molecule is not complexed by the CB[7] host in either the 1:1 or 2:1 host-guest complexes. A gas-phase energy minimization calculation (MM2) for the structure of the 2:1 host-guest complex between CB[7] and the benzethonium cation, which is consistent with the complexation-induced chemical shift changes, is shown in Figure 3.6.

The limiting chemical shift changes for the aromatic and methylene protons of the benzyl group are upfield and are of comparable magnitude to other cationic guests molecules with benzyl end groups, such as the benzylammonium,¹⁵ benzyltrimethylammonium,⁸

benzylcholine,⁹ and N-benzyl-1-(1-naphthyl)ethylammonium¹⁶ cations (Figure 3.7). The magnitudes of the $\Delta\delta_{\text{lim}}$ values suggest that the complexation places the benzyl group within the cavity with the quaternary nitrogen center placed near the oxygens of the ureido carbonyl groups on the portals.

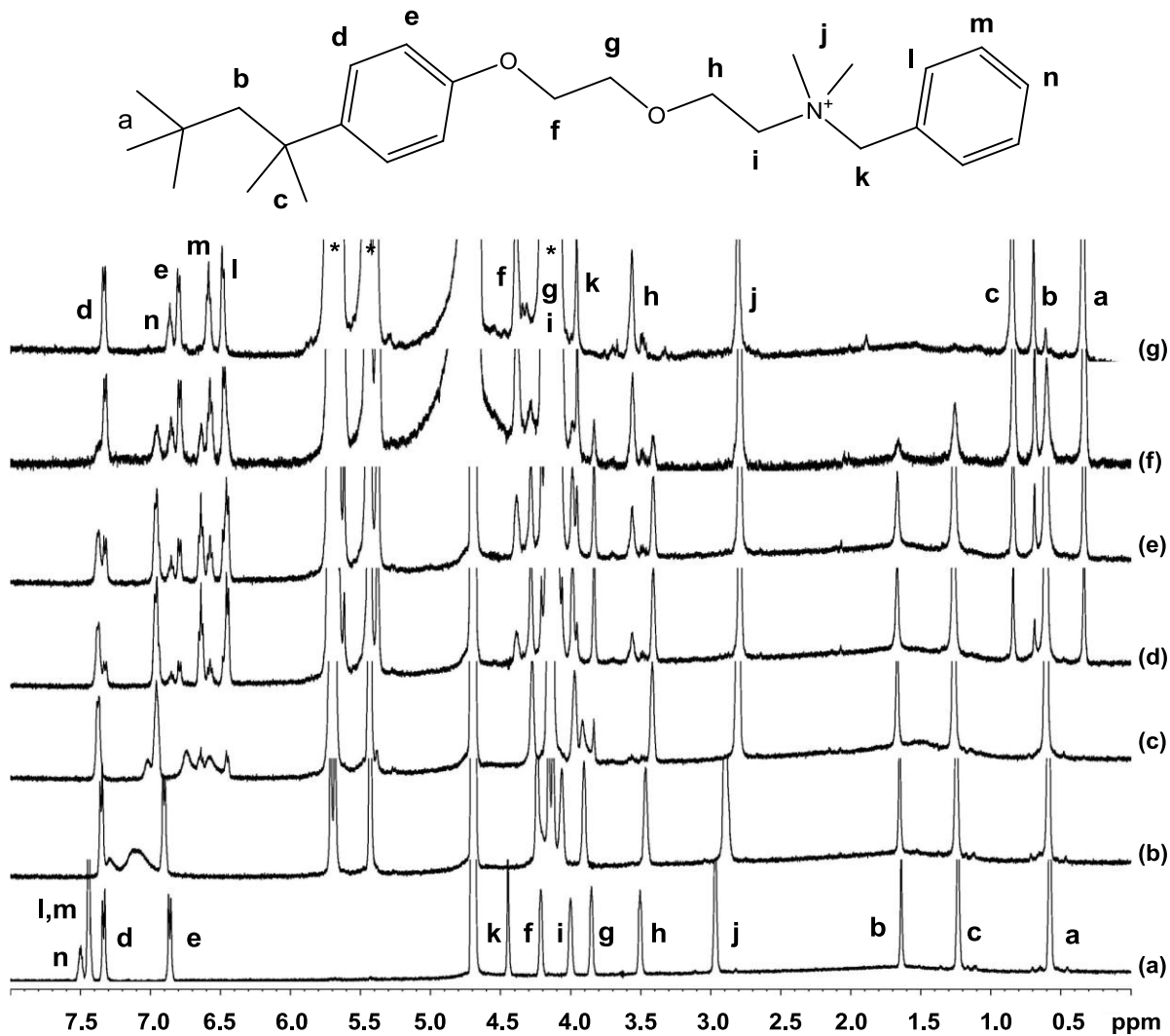


Figure 3.4 A stack plot of the ^1H NMR spectra of benzethonium in the presence of (a) 0.00, (b) 0.42, (c) 0.99, (d) 1.39, (e) 1.61, (f) 2.10, and (g) 3.52 equivalents of CB[7], titrated in D_2O .

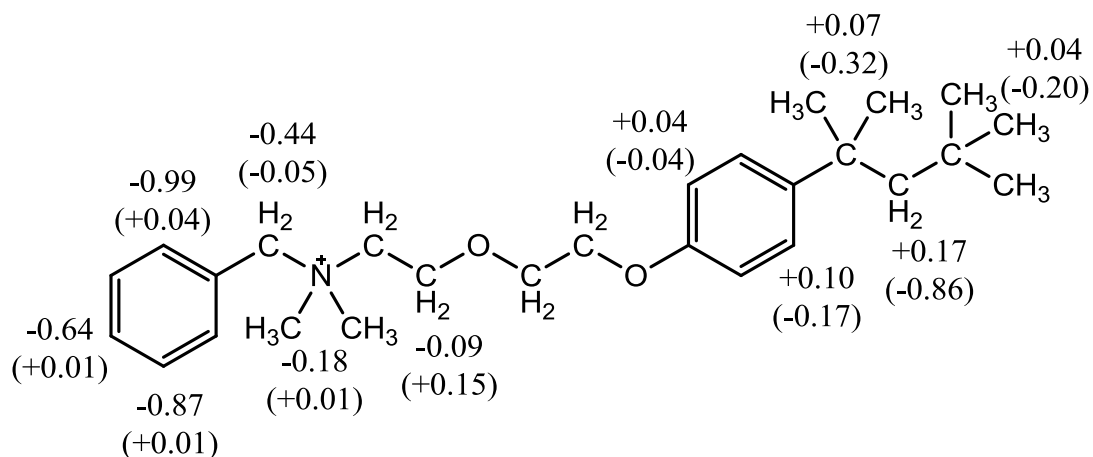


Figure 3.5 The ^1H NMR $\Delta\delta_{\text{lim}}$ values are shown for the titration of the benzethonium cation with CB[7]. The top numbers represent the shifts associated with the first host binding event and the bottom numbers in brackets represent shifts associated with the second binding event. The negative $\Delta\delta_{\text{lim}}$ values indicate upfield shifts and positive $\Delta\delta_{\text{lim}}$ values indicate downfield shifts. The shifts of some protons were obscured by the proton peaks of CB[7] and therefore could not be measured.

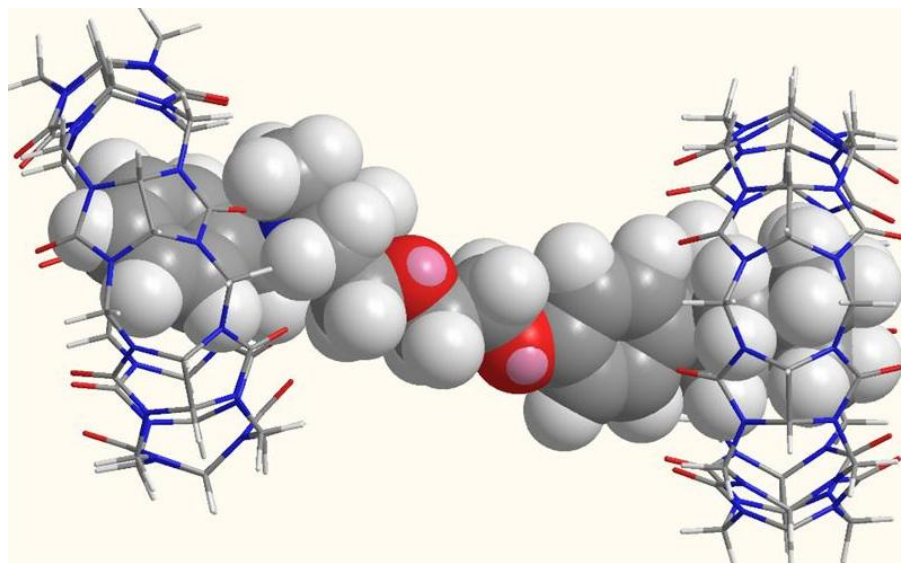


Figure 3.6 Energy-minimized gas-phase structure of the 2:1 host-guest complex of CB[7] and the benzethonium cation.

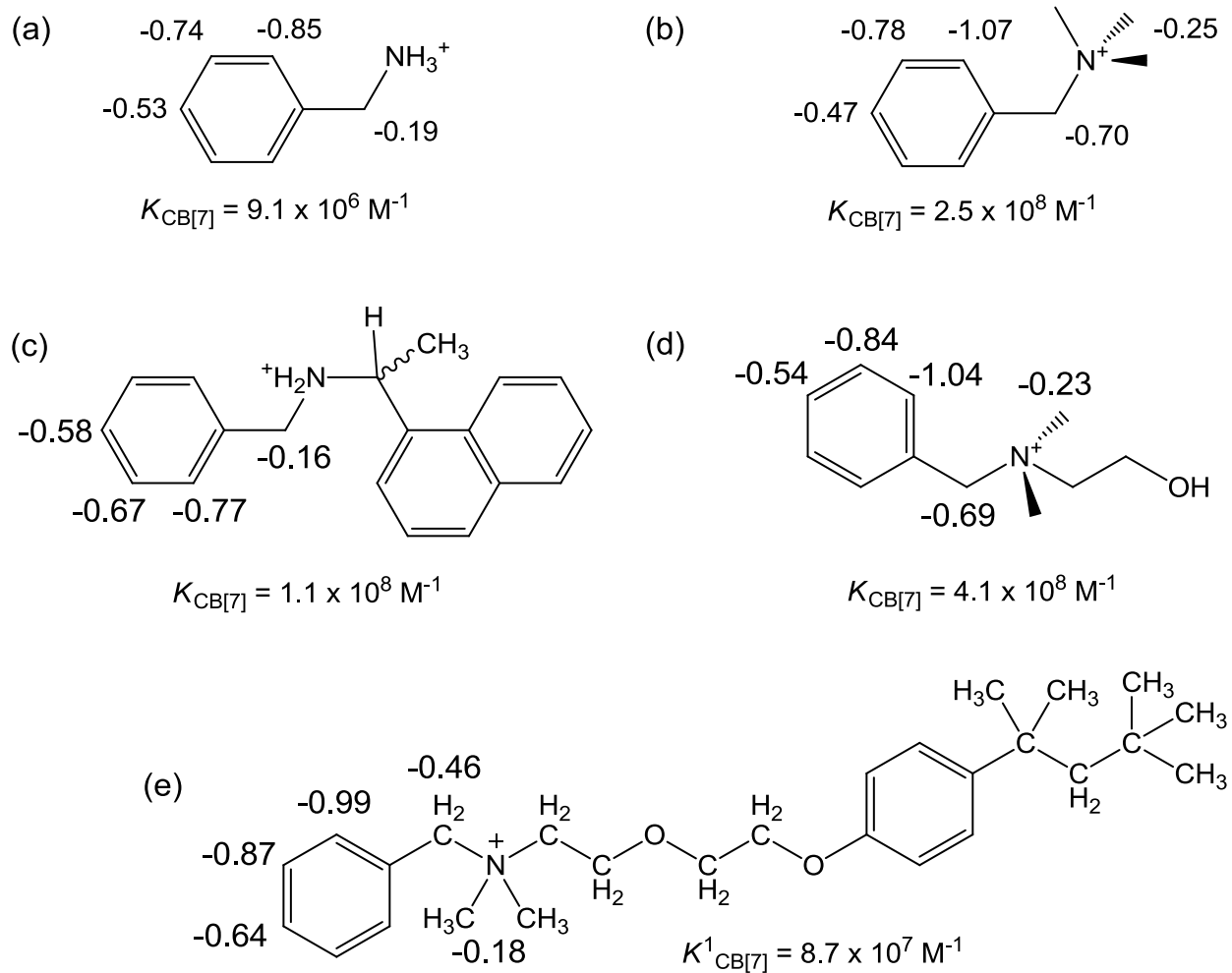


Figure 3.7 The CB[7] complexation-induced chemical shift changes ($\Delta\delta_{lim}$, ppm) for cationic guests containing benzylammonium and related binding sites: (a) benzylammonium,¹⁵ (b) benzyltrimethylammonium,⁸ (c) N-benzyl-1-(1-naphthyl)ethylammonium,¹⁶ (d) benzylcholine,⁹ and (e) benzethonium. The stability constants ($K_{CB[7]}$) for the 1:1 host-guest complexes with CB[7] are indicated below the guest.

3.2.2 Determination of Binding Constants

3.2.2.1 Binding of the Hydrophilic Moiety

Once the presence of the host-guest complex between CB[7] and the benzethonium cation had been confirmed, the binding constants of the 1:1 and 2:1 host-guest complexes were determined. The benzethonium cation is a unique guest because it contains two binding sites with different driving forces for complexation and, correspondingly, different binding strengths. Complexation at the first binding site is mainly driven by ion-dipole interactions between the cationic ammonium group of the benzethonium cation and the polar portals of CB[7]. This binding site is also stabilized by the hydrophobic effect, which results from the terminal phenyl group of benzethonium being encapsulated by the hydrophobic cavity of CB[7]. As a result of these two effects working in tandem, CB[7] is able to form a strong and tightly bound complex with benzethonium. In the case of these more tightly bound host-guest complexes ($K > 10^4 \text{ M}^{-1}$), the binding constant could not be determined accurately fitting the binding curve in Figure 3.8. Instead, the binding constant was determined by a competition study with a known competitor, as demonstrated by Isaacs and coworkers and described in Chapter 2.⁴ When choosing a competitor, it was best to select a molecule with similar properties to the guest with which it would compete. In the case of benzethonium, which contains a benzyldimethylammonium alkane group, benzyltrimethylammonium (Figure 3.7d) was chosen as the competitor. This tetraalkylammonium molecule is an excellent competitor because its structure is very similar to that of the 1:1 binding site on benzethonium. Studies conducted by St-Jacques *et al.* have found that benzyltrimethylammonium has a binding constant with CB[7] of $K = (2.5 \pm 0.6) \times 10^8 \text{ M}^{-1}$.⁸ Once the competition study was conducted, it was determined that benzethonium had a

relative binding constant (K_{rel}) that was 7.8 times lower than the binding constant of benzyltrimethylammonium. From this information, the binding constant of benzethonium was extrapolated to be $K = (8.7 \pm 1.1) \times 10^7 \text{ M}^{-1}$. This binding constant may also be compared with values for the benzylammonium cation ($K_{\text{CB}[7]} = (9.07 \pm 0.42) \times 10^6 \text{ M}^{-1}$)¹⁵ and the benzylguanidinium cation ($(1.43 \pm 0.18) \times 10^8 \text{ M}^{-1}$).¹⁵

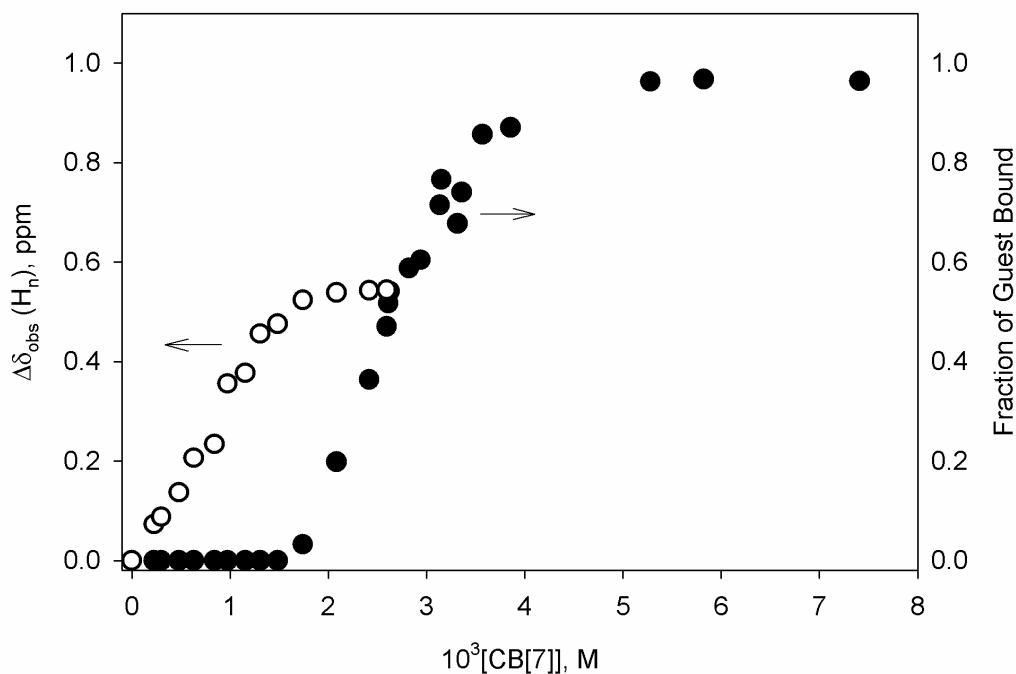


Figure 3.8 Plots of $\Delta\delta_{\text{obs}}$ for H_n (○, left ordinate) and the fraction of guest bound by a second CB[7] (●, right ordinate) against the total CB[7] concentration, from the ^1H NMR titration (see Figure 3.4 for partial data) of the benzethonium cation (1.5 mM) with CB[7] in D_2O .

3.2.2.2 Binding of the Hydrophobic Moiety

Once the first binding constant between benzethonium and CB[7] had been calculated, the focus shifted to examining the second binding event and its binding constant. The addition of further cucurbit[7]uril beyond one equivalent to the benzethonium guest results in a second weaker binding interaction with the more hydrophobic end of the molecule, the 2-(2,4,4-trimethylpentyl) substituent on the phenyl ring. The most notable

changes in the ^1H NMR spectra of the host-guest mixtures (Figure 3.4) are the upfield shifts of the alkyl protons of this substituent, with slow exchange behaviour (separate resonances for the free and bound guest protons) on the NMR timescale. The largest shift is found for the methylene protons (H_b), with $\Delta\delta_{\text{lim}} = -0.86$ ppm, while the methyl protons shift upfield to a smaller extent (-0.20 and -0.32 ppm for methyl protons, H_a and H_c , respectively). The stability constant for the binding of the second CB[7] to this hydrophobic region was determined to be $K^2_{\text{CB}[7]} = (4.0 \pm 1.9) \times 10^3 \text{ M}^{-1}$ by integrating the methyl proton resonances associated with the free and bound benzethonium cations. Recently, Yu *et al.* reported that the benzyl(dimethyl)hexadecylammonium cation (also an anti-microbial agent, like benzethonium) formed both 1:1 (encapsulating the benzyl group) and 2:1 (second CB[7] complexes the hexadecyl chain) host-guest complexes with CB[7], with stability constants (in D_2O , no added electrolyte) of $1.88 \times 10^8 \text{ M}^{-1}$ and $4.8 \times 10^4 \text{ M}^{-1}$, respectively.¹⁷

The value for complexing the hydrophobic 2-(2,4,4-trimethylpentyl) portion of the benzethonium cation, with 8 heavy atoms, is comparable in magnitude to those we determined previously for butan-2-one ($3.1 \times 10^3 \text{ M}^{-1}$)¹⁸ and 3,3-dimethylbutan-2-one ($6.74 \times 10^3 \text{ M}^{-1}$),¹⁸ which have 5 and 9 heavy atoms, respectively. Nau and co-workers^{19,20} have recently analyzed the properties of the inner cavity of cucurbiturils and have determined that the cavity of cucurbiturils, including CB[7], have a very low polarizability and are capable of tightly binding hydrophobic groups of a certain size, specified by either the number of heavy (non-hydrogen) atoms or by the molar volume. In the case of CB[7], the highest reported affinities for neutral guests are adamantanecarboxylic acid⁷ ($3.2 \times 10^5 \text{ M}^{-1}$) and hydroxymethylferrocene²¹ ($3.2 \times 10^6 \text{ M}^{-1}$), which have 9 and 11 heavy atoms, respectively, in the adamantyl and ferrocenyl fragments. The capacity of the CB[7] cavity appears to be 12

heavy atoms, as we have reported that the 2-aminopyridinium cation, bound to CB[7] in a 1:2 host-guest complex, can undergo a photodimerization²² to yield a product whose volume is 151 Å³ (PC = 62%),¹⁹ with all of the guest but the two amino substituents within the inner cavity. Mecozzi and Rebek,²³ based on host-guest binding in capsules, calculated that the optimum packing coefficient (PC), obtained by dividing the volume of the guest by the volume of the cavity of the host, is 55 ± 9 %, with the remaining void space necessary to retain some vibrational, rotational, and translational degrees of freedom of the guest, along with vibrational degrees of freedom for the host, to maximize entropy. Host-guest complexes with lower or higher PC values were associated with lower stability constants in solution. Nau has considered that Rebek's principle of 55% packing coefficient is ideal in host-guest complexes.¹⁹ The "expanded" cavity volume of CB[7], which includes the "bond dipole regions" near the portals, is calculated to be 279 Å³, compared with the "inner" cavity volume of 242 Å³.¹⁹ The latter is considered to be the more appropriate cavity volume when it comes to binding hydrophobic guests.

With the benzethonium guest, the uncharged hydrophobic 2-(2,4,4-trimethylpentyl) substituent has 8 heavy atoms and the upfield shifts of all of the protons within this substituent suggests that the inner cavity can accommodate them. The molar volume of 2,2,4-trimethylpentane has been calculated to be 147 Å³,²⁴ and using the inner cavity volume of CB[7], results in a packing coefficient of 61%, close to Rebek's ideal value of 55%. This accounts for the relatively strong binding of this neutral moiety on the benzethonium guest.

We have observed a similar phenomenon of distinct 1:1 and 2:1 host-guest complexes of CB[7] with coenzyme B₁₂, where the first CB[7] bound to the protonated α -axial 5,6-dimethylbenzimidazole base which had dissociated from the Co(III) center ($K^1_{\text{CB}[7]} = (3.02 \pm$

$0.35) \times 10^6 \text{ M}^{-1}$).¹⁴ This was followed by a second weaker binding to the neutral β -axial 5'-deoxyadenosyl ligand ($K^2_{\text{CB}[7]} = (1.1 \pm 0.2) \times 10^3 \text{ M}^{-1}$) without its detachment from the Co(III) center. The three orders of magnitude difference in the binding constants allowed for the two processes to be observed separately in the ^1H NMR spectrum.

3.2.3 Potential Applications of CB[7]•Benzethonium Host-Guest Complexes

The complexation of the benzethonium cation by β -cyclodextrin (10 mM) has been reported by Simpson to completely neutralize the effects of this compound as an anti-microbial agent. The smaller α -cyclodextrin had no effect on the benzethonium cation, but was effective against other anti-microbial quaternary ammonium cations, such as benzalkonium, with long linear aliphatic chains. The CB[7] may be useful at lower concentrations than the β -CD in neutralizing the anti-microbial effects of the benzethonium cation, because of its higher host-guest stability constants than observed for the β -CD host. Both the β -CD and CB[7] are more useful than detergents in neutralizing the quaternary ammonium anti-microbial agents because of their relatively non-toxicity with regards to cells.²⁵

Another feature of the effects on quaternary ammonium cations, such as benzethonium and benzalkonium, which is shared by β -CD¹³ and CB[7]¹⁷ is their ability to reduce the critical micelle concentrations (CMC) of the cations. This may be useful in maintaining the cations in a dispersed state, rather than a micelle at high concentrations, which would increase the effectiveness of the compound.

Finally, the observation of slow exchange behaviour in the ^1H NMR spectra of the titration of the benzethonium cation by the second equivalent of CB[7], suggests that release

of the hydrophobic 2-(2,4,4-trimethylpentyl) group may be relatively slow, and this could be used for controlled release of the compound. This feature may be useful in the compound's applications as a disinfectant^{10,11} or an anti-tumour agent.¹² An investigation of the kinetics of the release of the benzethonium cation from CB[7] would be a logical extension of the present work on this host-guest complex.

3.3 Conclusions

The formations of 1:1 and 2:1 host-guest complexes between CB[7] and the benzethonium cation have been monitored and analyzed through the use of ESI mass spectrometry and ¹H NMR spectroscopy. The results of these analyses indicate two binding events between the CB[7] host and the benzethonium guest. The first binding event was encapsulation of the benzyltrialkylammonium group, driven by ion-dipole interactions and hydrophobic forces between CB[7] and the benzylammonium terminus on the benzethonium cation. This binding event was found to have a high binding constant of $K_{\text{CB}[7]} = (8.7 \pm 1.1) \times 10^7 \text{ M}^{-1}$. The second binding event was driven exclusively by hydrophobic effects as the central hydrophobic cavity of CB[7] interacted with the 2,4,4-trimethylpentyl substituent on the other terminus of the benzethonium cation. This binding event was found to be weaker than the first, but still possessed a moderate binding constant of $K_{\text{CB}[7]} = (4.0 \pm 0.6) \times 10^3 \text{ M}^{-1}$ due to an efficient filling of the inner cavity of CB[7].

References

1. W. A. Freeman, W. L. Mock, and N. Y. Shih, *J. Am. Chem. Soc.*, **1981**, *103*, 7367.
2. W. L. Mock and N. Y. Shih, *J. Org. Chem.*, **1986**, *51*, 4440.
3. W. L. Mock, *Chapter 15: Cucurbituril*, In *Comprehensive Supramolecular Chemistry, Volume 2*, J. L. Atwood, J. E. D. Davies, D. D. MacNicol, F. Vogtle and J. M. Lehn (eds.), F. Vogtle (volume ed.), Pergamon: New York, 1996; pp. 477-493.
4. O. A. Gerasko, D. G. Samsonenko, and V. P. Fedin, *Russ. Chem. Rev.*, **2002**, *71*, 741.
5. C. Marquez, R. R. Hudgins, and W. M. Nau, *J. Am. Chem. Soc.*, **2004**, *126*, 5806.
6. J. Lagona, P. Mukhopadhyay, S. Chakrabarti, and L. Isaacs, *Angew. Chem. Int. Ed.*, **2005**, *44*, 4844.
7. S. Liu, C. Ruspic, P. Mukhopadhyay, S. Chakrabarti, P. Y. Zavalij, and L. Isaacs, *J. Am. Chem. Soc.*, **2005**, *127*, 15959.
8. A. D. St-Jacques, I. W. Wyman, and D. H. Macartney, *Chem. Commun.*, **2008**, 4936.
9. I. W. Wyman and D. H. Macartney, *Org. Biomol. Chem.*, **2010**, *8*, 253.
10. R. Tanaka and N. Hirayama, *Anal. Sci.*, **2008**, *24*, 163.
11. L. Jimenez and M. Chiang, *Am. J. Inf. Cont.*, **2005**, *33*, 41.
12. K. W. Yip, X. Mao, P. Y. B. Au, D. W. Hedley, S. Chow, S. Dalili, J. D. Mocanu, C. Bastianutto, A. Schimmer, and F. F. Liu, *Clin. Cancer Res.*, **2006**, *12*, 5557.
13. W. J. Simpson, *FEMS Microbiol. Lett.*, **1992**, *90*, 197.
14. R. Wang, MacGillivray, B. C. and D. H. Macartney, *Dalton Trans.*, **2009**, 3584.
15. D. S. N. Hettiarachchi and D. H. Macartney, unpublished results.
16. L. Yuan, R. Wang and D. H. Macartney, *Tetrahedron: Asymmetry*, **2007**, *18*, 483.

17. J.-S. Yu, F.-G. Wu, Y. Zhou, Y.-Z. Zheng and Z.-W. Yu, *Phys. Chem. Chem. Phys.*, **2012**, *14*, 8506.
18. I. W. Wyman and D. H. Macartney, *Org. Biomol. Chem.*, **2008**, *6*, 1796.
19. W. M. Nau, M. Florea and K. I. Assaf, *Isr. J. Chem.*, **2011**, *51*, 559.
20. M. Florea, M.; Nau, W. M. *Angew. Chem. Int. Ed.*, **2011**, *50*, 9338.
21. W. S. Jeon, K. Moon, S. H. Park, H. Chun, Y. H. Ko, J. Y. Lee, E. S. Lee, S. Samal, N. Selvapalam, M. V. Rekharsky, V. Sindelar, D. Sobransingh, Y. Inoue, A. E. Kaifer, K. Kim, *J. Am. Chem. Soc.*, **2005**, *127*, 12984.
22. R. Wang, L. Yuan and D. H. Macartney, *J. Org. Chem.*, **2006**, *71*, 1237.
23. S. Mecozzi and J. Rebek, Jr., *Chem. Eur. J.*, **1998**, *4*, 1016.
24. P. D. Huibers and A. R. Katritzky, *J. Chem. Inf. Comput. Sci.*, **1998**, *38*, 283.
25. G. Hettiarachchi, D. Nguyen, J. Wu, D. Lucas, D. Ma, L. Isaacs and V. Briken, *PLoS One*, **2010**, *5*, e10514.
26. F. Kopecky, B. Kopecka and P. Kaclik, *Ceska. Slov. Farm.*, **2006**, *55*, 175.

Chapter 4

HOST-GUEST COMPLEXATION BETWEEN CUCURBIT[7]URIL AND BIGUANIDIUM GUESTS

4.1 Introduction

The guanidine molecule can be easily protonated to form the guanidinium cation (Figure 4.1a), with a pK_a of 13.6, over a wide pH range.^{1,2} The guanidinium cation is stabilized by resonance structures and charge delocalization, making it three orders of magnitude more stable, with respect to deprotonation, than protonated alkyl amines ($pK_a = 10.5$).¹ In a recent study published by Yang and Dearden, it was determined that guanidinium cations were able to bind to the polar portals of CB[6] and CB[7] in the gas phase.³ This study used computational models and electrospray ionization mass spectrometry to prove that two guanidinium cations can act as capping structures with one binding to each CB[7] portal. The natural amino acid L-arginine contains a guanidinium group and Nau and co-workers have reported CB[7] binding constants of $3.1 \times 10^2 \text{ M}^{-1}$ and $1.1 \times 10^6 \text{ M}^{-1}$ for L-arginine and its enzymatic decarboxylation product agmatine, respectively, in aqueous solution.^{4a} In addition to this study, unpublished research by Hettiarachchi *et al.* using computational models, ESI mass spectrometry, and NMR spectroscopy, showed that a series of guests containing one or more guanidinium functional groups could form tightly bound complexes with CB[7] in water.^{4b} In a number of these cases, it was shown that CB[7] and guanidinium compounds could form complexes with equal or higher stability constants than ammonium compounds with similar chemical structures.



Figure 4.1 The structures of a) the guanidinium cation and b) the biguanidinium cation.^{4,5,6}

The work described in this Chapter builds on previous research involving complexes of guanidinium compounds, and extends these studies to include complexes that form between CB[7] and a series of guests containing biguanidinium groups (Figure 4.1b).⁴ The biguanidinium guests examined are the metformin and phenformin cations, and the chlorhexidine and alexidine dications. The applications of these guests are described below.

One of the earliest applications of biguanidinium was the use of *Galega officinalis* (also called French Lilac or Professor's Weed) as a treatment for diabetes in Europe during the middle ages.^{5,6} Guanidine is the active compound in *G. officinalis* and, in the 1920's, it was used to synthesize a series of biguanidinium drugs.⁵ In the 1950's, two of these drugs, metformin and phenformin (Figure 4.2), were patented and produced commercially.

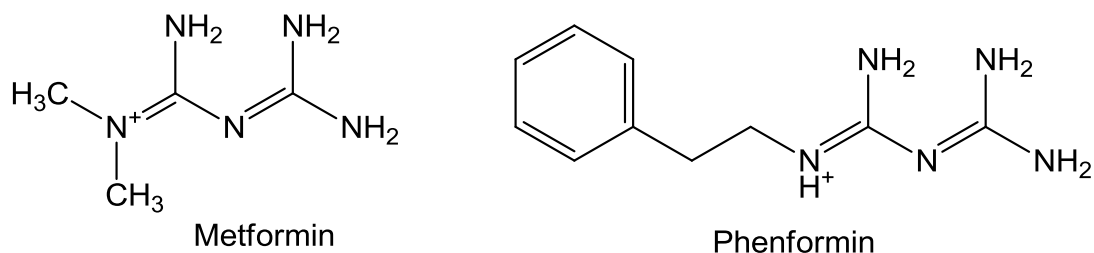


Figure 4.2 The chemical structures of a) metformin and b) phenformin.⁵

Metformin is an orally administered drug used to lower blood glucose levels in patients with Type 2 diabetes.^{5,6,7} It improves insulin sensitivity, decreases hepatic glucose output, and increases glucose uptake in peripheral tissues.⁵ The drug is not effective in the absence of insulin, and therefore cannot be used to treat Type 1 diabetes.⁵ As a drug, metformin is well established both on its own as a treatment in the early stages of Type 2 diabetes and as an adjunct treatment with other antihyperglycemic medicines.⁶ As a treatment, it helps maintain a steady weight, lowers the risk of hyperglycemia, counters insulin resistance, and has been shown to be safe for use during pregnancy.^{6,7} More recently, metformin has been shown to have anti-cancer potential by activating the pathway of liver kinase B1 (LKB1), a tumour suppressing protein, and its downstream target, adenine monophosphate-activated protein kinase (AMPK).⁸

Phenformin was also an orally administered drug that was known to be even more potent than metformin in the treatment of diabetes.^{5,6} Unfortunately, it was withdrawn from clinical use in the 1970's when it was found to be associated with a much higher risk of lactic acidosis than metformin. Lactic acidosis is characterized as a condition where the pH of blood and tissues drops, which is normally accompanied by a build-up of lactate in the body. Normally this condition is the result of low levels of oxygen reaching the tissues, but this did not appear to be caused directly by phenformin at the time it was withdrawn. After phenformin was withdrawn, it was determined that about 10% of the Caucasian population have a genetic defect that prevents them from adequately metabolizing this drug.⁵ The accumulation of phenformin in the blood stream and tissues is likely responsible for the increased incidence of lactic acidosis, but the exact mechanism involved is still unknown.

After biguanidinium drugs were proven successful in treating diabetes, chemists began creating and studying other forms of biguanidinium compounds with the goal of discovering a new series of drug molecules. The result of these analyses was the discovery of bis(biguanidinium) dications in the mid-20th century.^{9,10} Among the bis(biguanidinium) molecules discovered were chlorhexidine and alexidine (Figure 4.3). These two compounds demonstrated antiseptic properties, which made them the best candidates for novel drug development.⁹

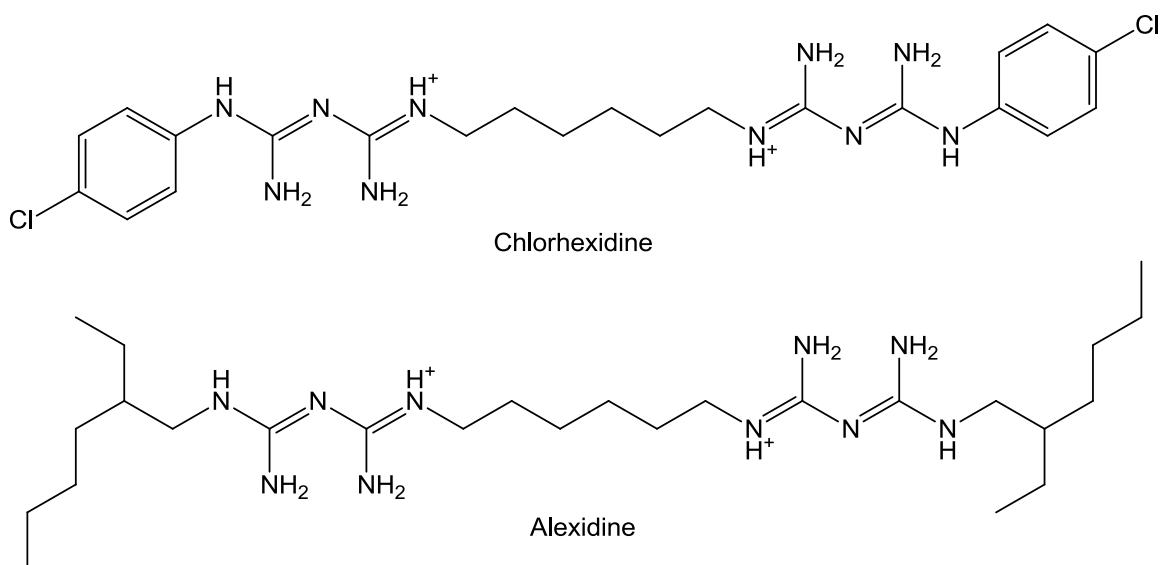


Figure 4.3 The chemical structures of chlorhexidine and alexidine.^{9,11}

Chlorhexidine is a multipurpose drug with bacteriostatic, bactericidal, fungicidal, fungistatic, and some virus killing properties.⁹ It is also an active ingredient in a variety of toothpastes, mouthwashes, oral sprays, hand disinfectants, and surgical hand antiseptics.^{9,12} The primary use of chlorhexidine is as an anti-plaque agent and is often used as a replacement when mechanical cleaning is not possible, such as after surgery.^{13,14} The mechanism of action of chlorhexidine involves disrupting the structure of the bacterial cell membrane, eventually resulting in cell death.^{9,12}

Alexidine, like chlorhexidine, is primarily used as an antiseptic drug in disinfectants, mouthwashes, and toothpastes.^{10,15} It interacts with the cell membranes of bacteria and disrupts their permeability, resulting in the release of cellular nutrients and, ultimately, cell death.¹⁰ Alexidine has also recently proven to be cytotoxic in malignant head and neck cancer cells.¹¹ Furthermore, it was shown that there was a difference between the dose required to produce apoptosis in the malignant cancer cells versus the normal head and neck cells.¹¹ These results could eventually be used to develop a drug regimen for alexidine in the treatment of these cancers.

Each of these biguanidinium and bis(biguanidinium) compounds have been proven effective in drug action, but several also have drawbacks, including poor solubility in aqueous solution and negative side effects, such as lactic acidosis. The goal of this work was the stoichiometries and binding constants of the biguanidinium and bis(biguanidinium) with CB[7] in aqueous solution, in the hope that the host molecule could be used to promote the solubility, bioavailability and controlled release of the drugs, and find applications in reversing the anti-bacterial activity of the bis(biguanidinium) dications. This chapter will describe the complexation between CB[7] and a series of guests containing one or more biguanidinium groups. These analyses were conducted through the use of ESI mass spectrometry and ¹H NMR spectroscopy. In addition, the host-guest binding constants were determined through the use of competition experiments and by fitting the host-guest binding curves, when appropriate, and are compared to the binding constants determined in our laboratory and elsewhere for other related guests with CB[7], as well for the bis(biguanidinium) dications with other hosts and physiological targets.

4.2 Results and Discussion

4.2.1 ESI Mass Spectrometry

The CB[7]-biguanidinium complexes were studied using a number of different analytical methods. Initially, a series of aqueous stock solutions were prepared, each one containing a biguanidinium guest and CB[7]. Next, high resolution ESI mass spectrometry was used to confirm the presence of the host-guest complex by mass/charge (m/z) ratio. The results of these analyses are presented in Table 4.1 below.

Table 4.1 High resolution ESI-MS data for the host-guest complexes of CB[7] with the metformin, phenformin, chlorhexidine, and alexidine guests (G^{n+}).

Guest	Host-Guest Stoichiometry	Observed (m/z)	Calculated (m/z)
Metformin	$\{CB[7] \cdot G\}^+$	1292.4528	1292.4547 for $C_{46}H_{54}N_{33}O_{14}^+$
	$\{CB[7] \cdot 2G\}^{2+}$	711.2825	711.2805 for $C_{50}H_{66}N_{38}O_{14}^{2+}$
Phenformin	$\{CB[7] \cdot G\}^+$	1368.4841	1368.4861 for $C_{52}H_{58}N_{33}O_{14}^+$
Chlorhexidine	$\{CB[7] \cdot G\}^{2+}$	834.2808	834.2806 for $C_{64}H_{74}N_{38}O_{14}Cl_2^{2+}$
	$\{2CB[7] \cdot G \cdot H\}^{3+}$	943.9748	943.9740 for $C_{106}H_{117}N_{66}O_{28}Cl_2^{3+}$
	$\{2CB[7] \cdot G\}^{2+}$	1415.4572	1415.4524 for $C_{106}H_{116}N_{66}O_{28}Cl_2^{2+}$
Alexidine	$\{CB[7] \cdot G\}^{2+}$	836.4143	836.4135 for $C_{68}H_{100}N_{38}O_{14}^{2+}$
	$\{2CB[7] \cdot G \cdot H\}^{3+}$	945.7331	945.7271 for $C_{110}H_{143}N_{66}O_{28}^{2+}$

The data in Table 4.1, with the ESI mass spectrum of chlorhexidine in the presence of an excess of CB[7] shown in Figure 4.4, demonstrate that each of the biguanidinium guests was able to form a complex with one or more CB[7] hosts in aqueous solution.

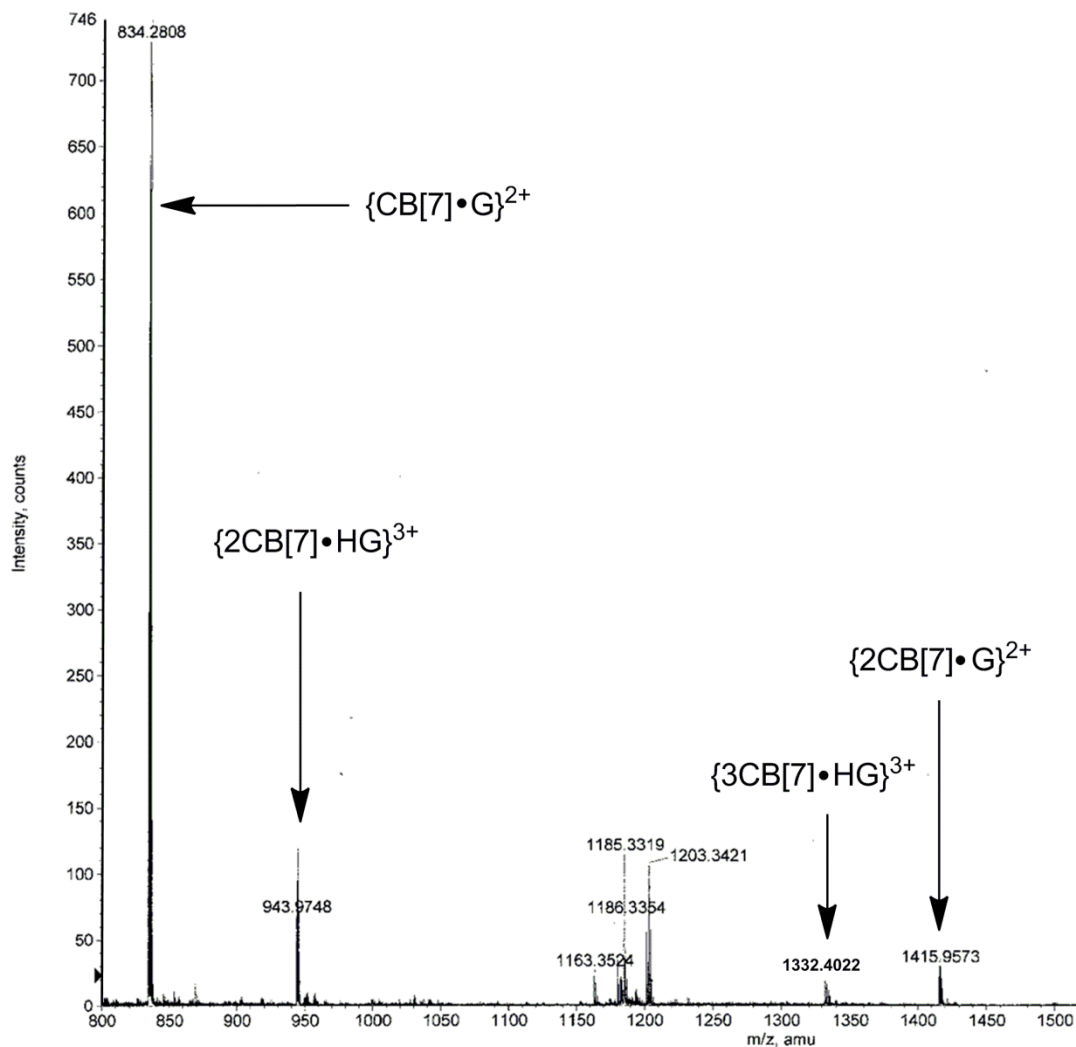


Figure 4.4 The ESI mass spectrum of chlorhexidine in the presence of a five-fold excess of CB[7], showing the 1:1, 2:1, and 3:1 host-guest complex stoichiometries. The peaks at m/z 1163, 1185, and 1203 represent H^+ , Na^+ , and $Na^+ + H_2O$ adducts of CB[7], respectively.

4.2.2 ^1H NMR Spectroscopy

With the presence of the host-guest complexes confirmed by ESI-MS data, ^1H NMR spectroscopy was then used to determine where the host was binding on the guest and how the host was affecting the chemical shifts of the guest proton resonances in the region where CB[7] bound.¹⁶ To examine how the guest protons were affected by binding with CB[7], it was necessary to assign the proton resonances in the ^1H NMR spectra of the guest dications. Once the proton resonances in the ^1H NMR spectrum of each biguanidinium guest had been assigned, each guest was titrated with CB[7] and the upfield or downfield shifts ($\Delta\delta_{\text{lim}} = \delta_{\text{bound}} - \delta_{\text{free}}$) of the guest proton resonances were monitored. As the titration progressed, resonances that moved upfield ($\Delta\delta_{\text{lim}} < 0$) were identified as belonging to guest protons within the hydrophobic cavity of CB[7]. Peaks that moved downfield ($\Delta\delta_{\text{lim}} > 0$) were identified as belonging to protons external to the cavity and involved in associations with the ureido oxygens of the polar portals of CB[7]. The values of the limiting chemical shifts for the host-guest complexes formed with each of the biguanidinium guests are presented in Figure 4.5.

Once each titration was complete, several representative spectra at different host-guest concentrations were selected and combined to demonstrate the effects of host complexation on the guest protons. These summary figures, called stack plots, were prepared for the titration of CB[7] with each of the biguanidinium guests. These stack plots are depicted in Figures 4.6 (metformin), 4.9 (phenformin), 4.11 (chlorhexidine), and 4.13 (alexidine).

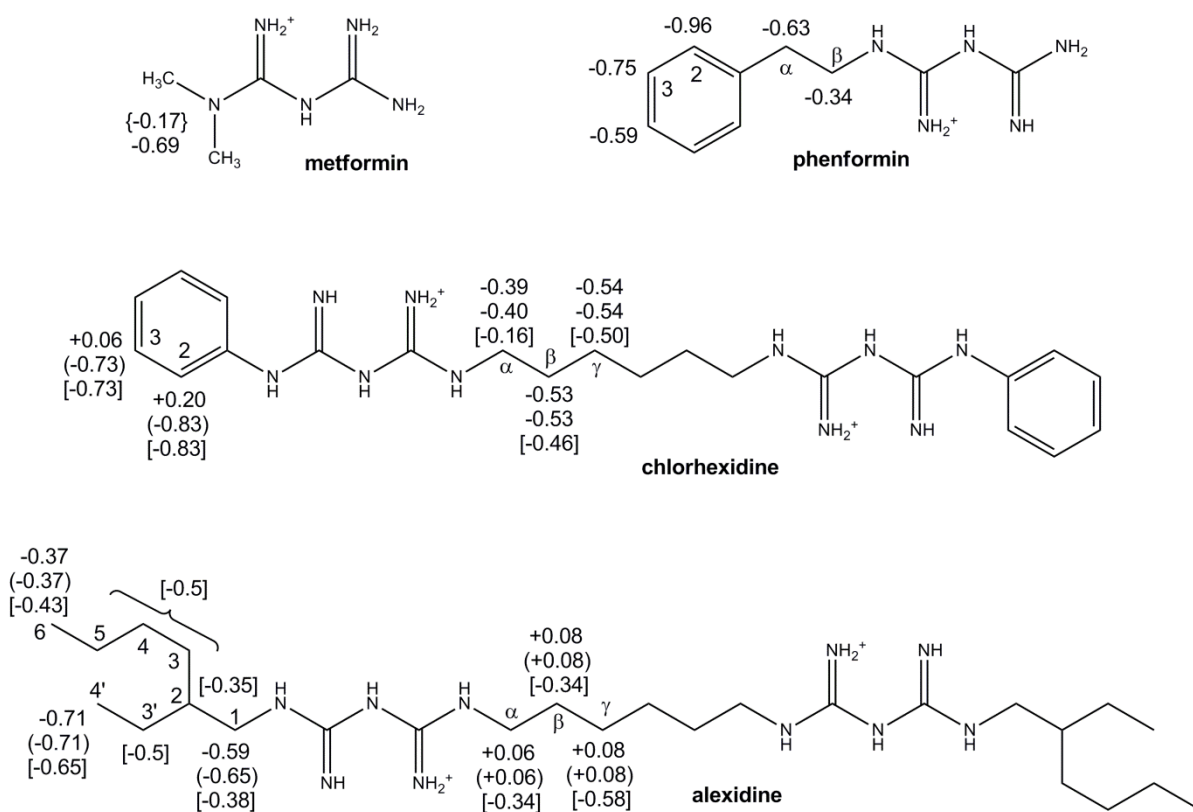


Figure 4.5 Structures of the biguanidinium and bis(biguanidinium) guests. The values listed adjacent to the guest proton positions are the CB[7] complexation-induced ^1H NMR chemical shift changes ($\Delta\delta_{\text{lim}}$) for the 1:2 (in { } brackets), 1:1 (non-bracketed values), 2:1 (in () brackets), and 3:1 (in [] brackets) host-guest complexes.

4.2.2.1 Metformin

The ^1H NMR chemical shift titration of the metformin cation with CB[7] in D_2O exhibits an upfield movement in the guest's methyl proton resonance with increasing concentrations of the host (Figure 4.6). The methyl resonance exhibits fast exchange behaviour, as the observed chemical shift represents an average between that of the free guest and bound guest species. The change in the chemical shift is not monotonic, as it is linear until a CB[7]/metformin ratio of 0.50, followed by a normal binding curve expected for a 1:1 complex (Figure 4.7).

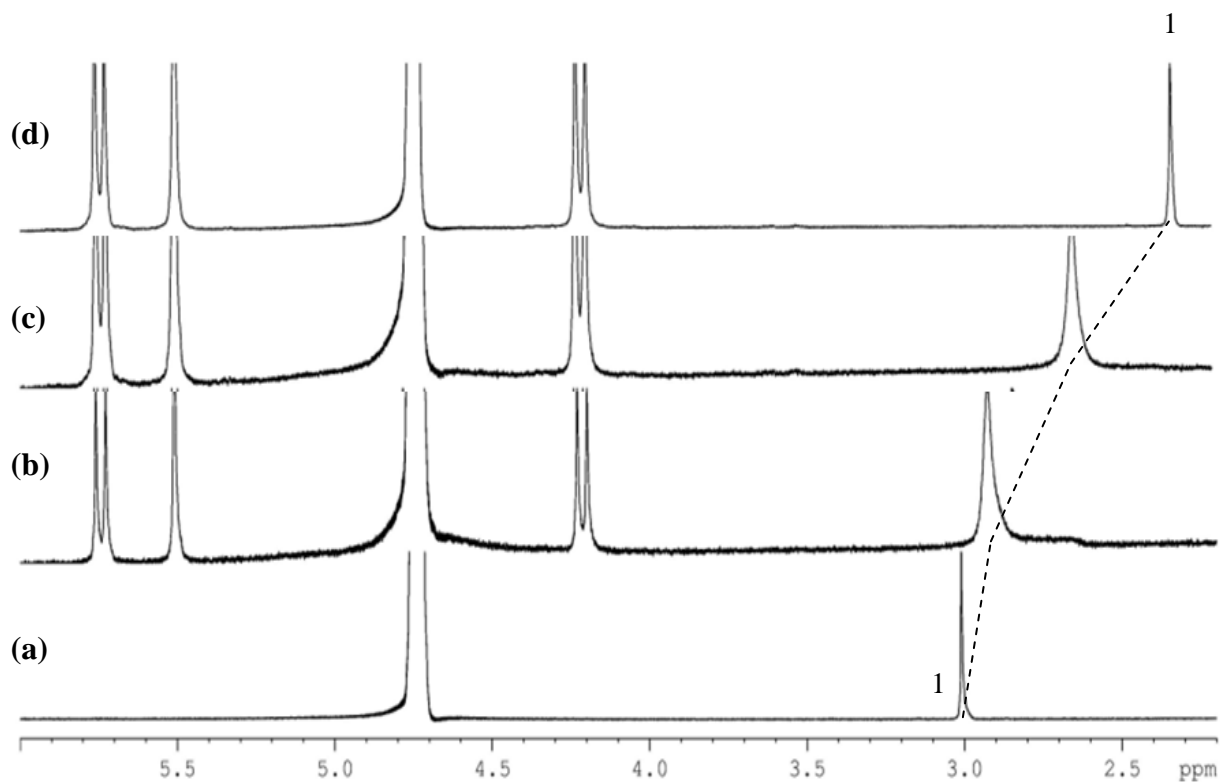
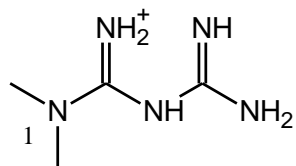


Figure 4.6 A stack plot of the ¹H NMR spectra of metformin in the presence of (a) 0.00, (b) 0.26, (c) 0.70, and (d) 1.39 equivalents of CB[7], titrated in D₂O. The dashed line indicates shifts in the peak positions of metformin. The numbered peak is matched with its numerically labeled protons on the chemical structure of metformin, above.

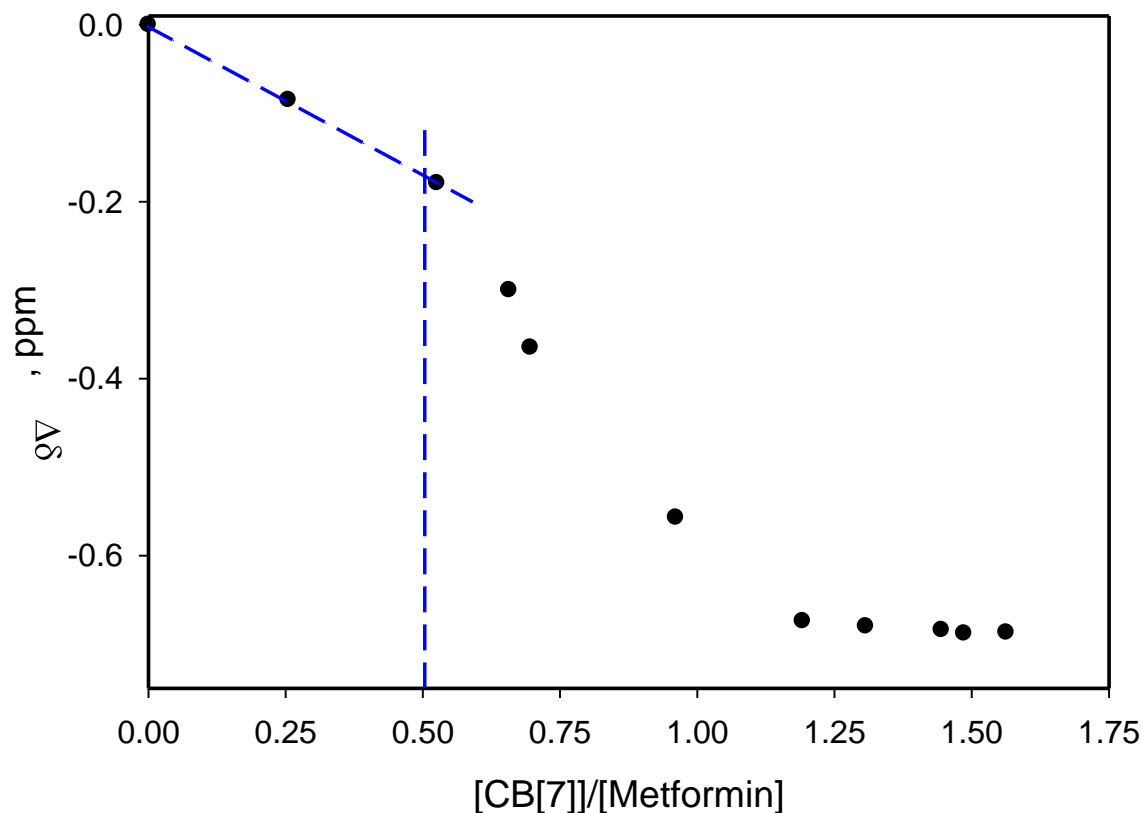


Figure 4.7 Chemical shift (methyl proton resonance) titration of metformin with CB[7]. The blue dashed line indicates the chemical shift change for the 1:2 host-guest complex formed at 0.50 equivalents of CB[7], followed by conversion to the 1:1 complex at higher ratios of CB[7]/metformin.

With this relatively small guest molecule, this behaviour is consistent with the initial formation of a 1:2 host-guest complex, followed by the formation of a 1:1 host-guest complex at higher CB[7] concentrations (Figure 4.8). These stoichiometries are supported by the observances of both species in the ESI mass spectrum of metformin in the presence of CB[7] (Table 1). The limiting chemical shift change ($\Delta\delta_{lim}$) for the methyl resonance in the 1:1 complex is -0.69 ppm, which is very similar to the values that we have observed for methylated quaternary ammonium centers in guests such as $N(CH_3)_4^+$ (-0.72 ppm),¹⁷ choline (-0.66 ppm),¹⁸ and trimethyllysine (-0.69 ppm),¹⁹ suggesting that the methyl group on the

metformin cation is well within the CB[7] cavity.

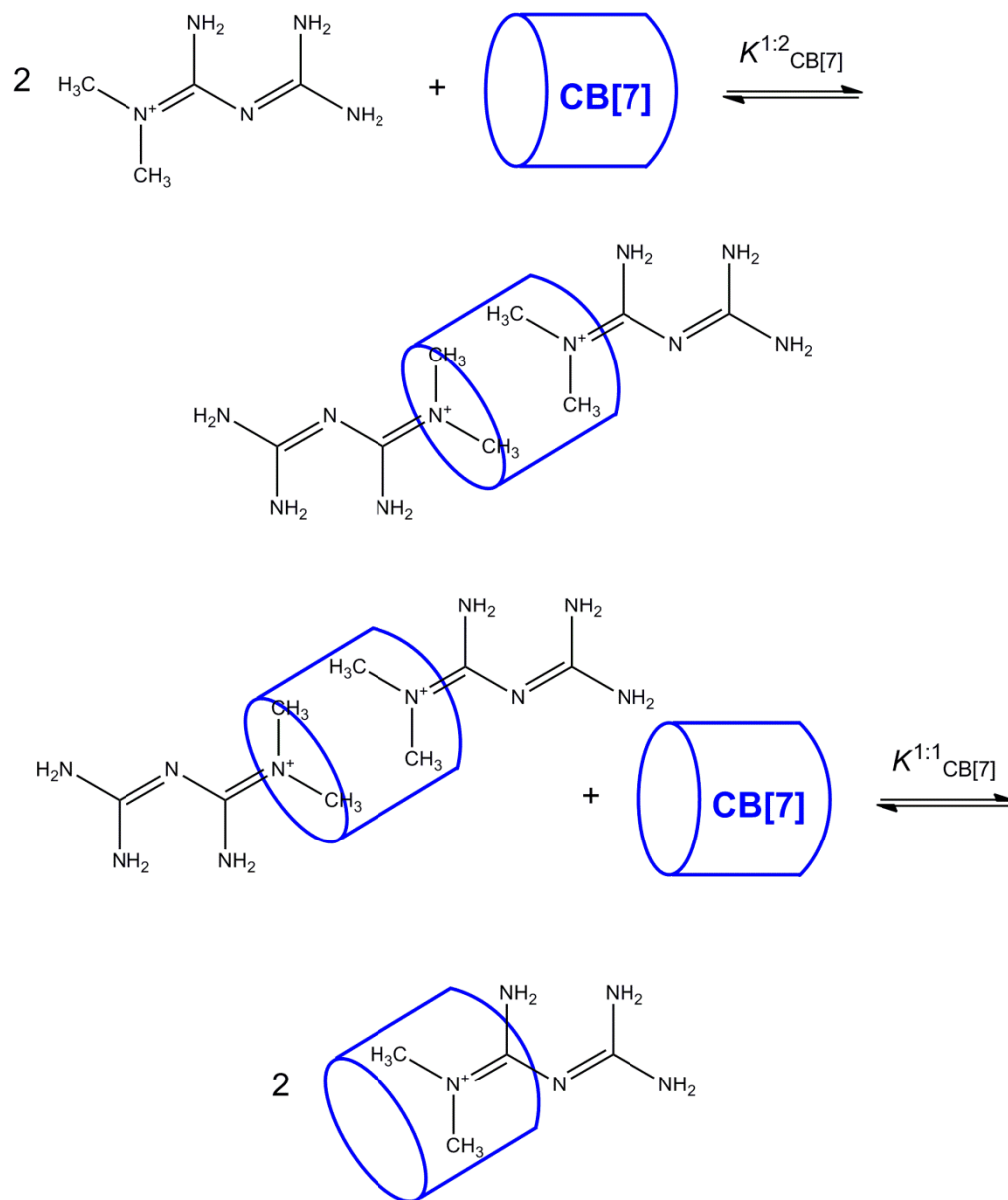


Figure 4.8 Host-guest equilibria between CB[7] and metformin.

For the 1:2 host-guest complex, the value of $\Delta\delta_{\text{obs}}$ at the CB[7]/metformin ratio of 0.50 is about -0.17 ppm, suggesting that the two metformin guests are both partially encapsulated,

with the methyl groups closer to the portals, or that one guest is fully encapsulated (as in the 1:1 complex), while the other is bound externally at the portal through hydrogen bonding and ion-dipole interactions. With the guest exchange being rapid on the NMR timescale, the observed chemical shift change in the latter case would be a combination of upfield shift for the encapsulated guest and a downfield shift for the portal bound guest. Dearden and co-workers have shown that in the gas-phase, the guanidinium cation can cap the portals of CB[7], with a better fit than in the case of CB[6].³ With the somewhat larger biguanidinium cation, it might not be expected to fit the portal as well as the guanidinium cation.

4.2.2.2 Phenformin

Unlike metformin, the ¹H NMR and ESI-MS data for phenformin show no evidence of a 1:2 host-guest complex, but the spectra do indicate the presence of a 1:1 complex between phenformin and CB[7] (Figure 4.9). The values of $\Delta\delta_{\text{lim}}$ for both the aromatic and methylene proton resonances in the phenylethyl portion of phenformin are similar in magnitude to the corresponding values determined previously in our group^{4b,17,18,20} for a series of cationic guest molecules containing the benzyl moiety (Figure 4.10). One interesting difference between the phenformin guest (containing the phenylethyl group) and the benzyl-containing cationic guests in Figure 4.10 is that the phenformin exhibits slow exchange behaviour in the ¹H NMR titration (separate resonances for the free and bound guests species), while all of the guests bearing benzyl groups exhibit fast exchange behaviour (single resonances for bound and free guests species at a weighted average chemical shift position). This may be due to the phenylethyl group being more hydrophobic than the benzyl group, and/or that the biguanidinium cation forms a stronger interaction at the portal than the cationic groups in the benzyl-bearing guests.

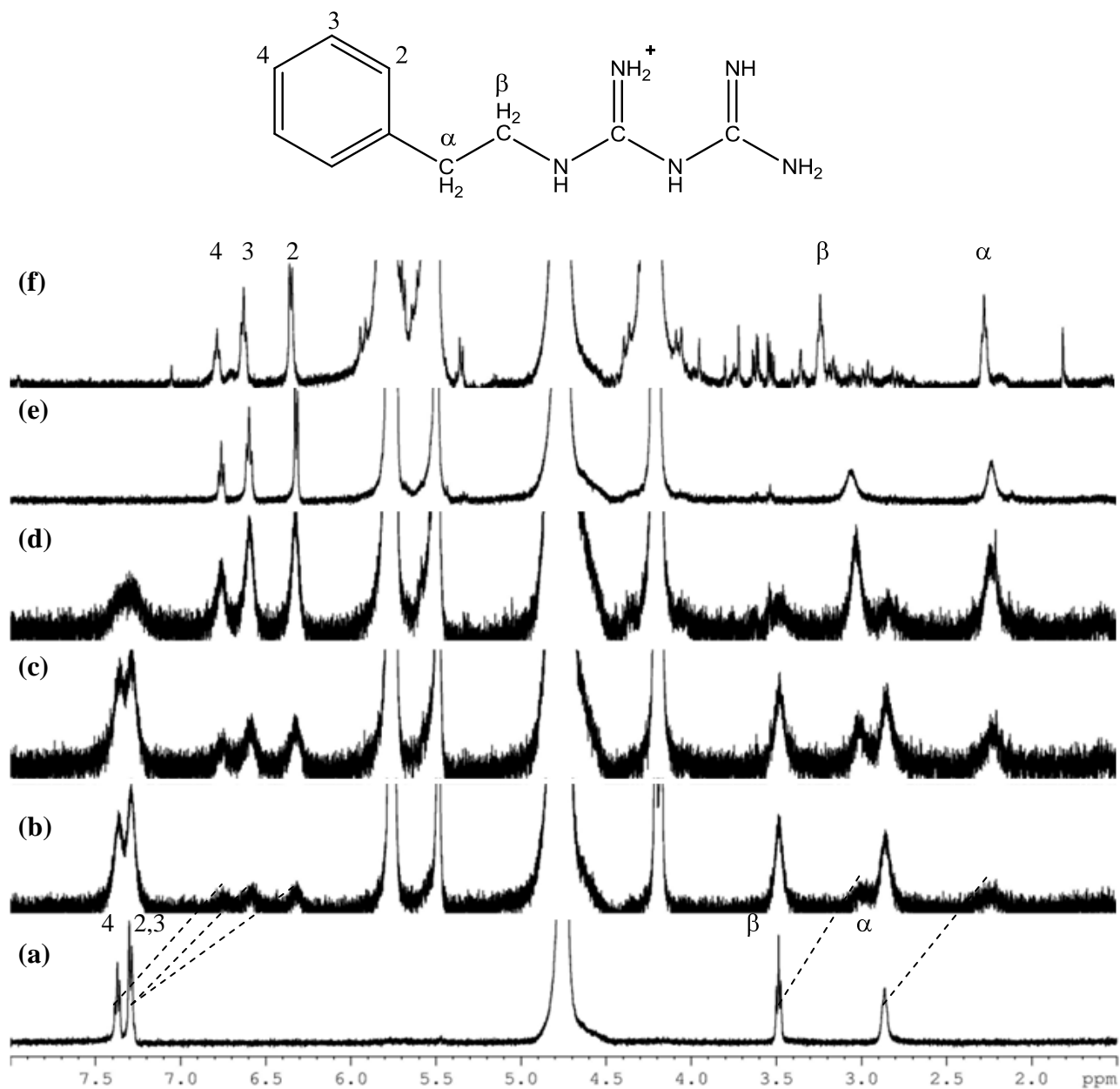


Figure 4.9 A stack plot of the ^1H NMR spectra of phenformin in the presence of (a) 0.00, (b) 0.35, (c) 0.48, (d) 0.94, (e) 1.37, and (f) 2.56 equivalents of CB[7], titrated in D_2O . The dashed line indicates shifts in the peak positions of phenformin. The numbered peaks are matched with their numerically labeled protons on the chemical structure of phenformin, above.

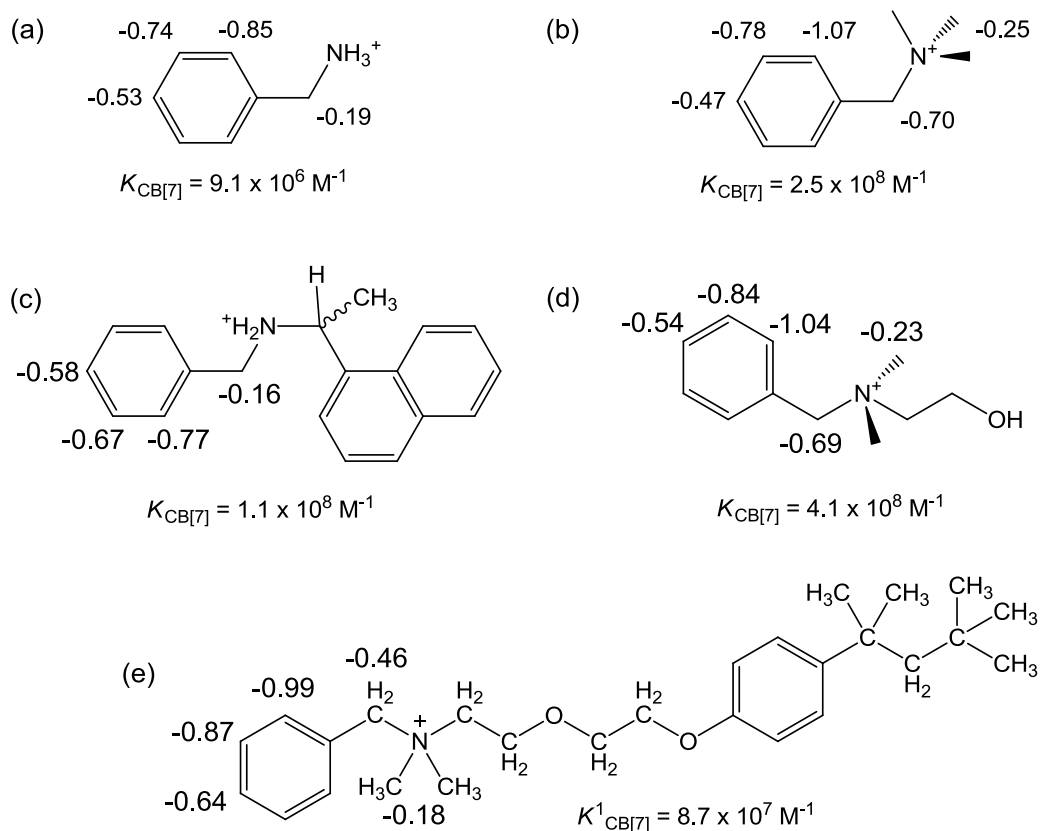


Figure 4.10 Host-guest stability constants and $\Delta\delta_{\text{lim}}$ values for the CB[7] complexations of the (a) benzylammonium,^{4b} (b) benzyltrimethylammonium,¹⁷ (c) N-benzyl-1-(1-naphthyl)ethylamine,²⁰ (d) benzylcholine,¹⁸ and (e) benzethonium (see Chapter 3) cations in aqueous solution.

4.2.2.3 Chlorhexidine

With the dicationic bis(biguanidinium) guests chlorhexidine and alexidine, the ESI-MS data, as well as ¹H NMR titrations with CB[7], revealed the different stoichiometries of the host-guest complexes, as well as the preferred sites of binding. The data for chlorhexidine indicated an initial 1:1 complex (Figure 4.11d) at low concentrations of CB[7] and a 3:1 complex (Figure 4.11e) at high concentrations of CB[7], with the first binding event being relatively distinct from the second and third binding events. The initial additions of CB[7] (up to about one equivalent) results a disappearance of the hexamethylene proton resonances

of the free dication and the appearance of the corresponding resonances of the bound guest at upfield positions ($\Delta\delta_{1:1} = -0.39, -0.52, \text{ and } -0.54$ ppm for the $H\alpha, H\beta, \text{ and } H\gamma$ methylene protons, respectively). This suggests that the first host molecule encapsulates the central hexamethylene chain. The aromatic protons also shift somewhat with the addition of the first equivalent of the host as the H2 proton resonance shifts downfield, becoming coincidental with the H3 proton. This shift is likely due to its proximity to the polar CB[7] portals. Upon the addition of two to three equivalents of the CB[7] host, the aromatic resonances undergo slow exchange upfield shifts from 7.35 ppm to resonances at 6.60 and 6.45 ppm, as the CB[7] binds to the two 4-chlorophenyl groups. While the methylene $H\beta$ and $H\gamma$ resonances move only slightly downfield as the end groups are bound, the resonance for the $H\alpha$ proton shifts downfield (slow exchange) by about 0.25 ppm as these protons are deshielded by the presence of the portals on the central and terminal CB[7] hosts. Beyond the additions of about three equivalents of CB[7], there are no further changes in the ^1H NMR spectrum. The host-guest complexation equilibria are depicted in Figure 4.12.

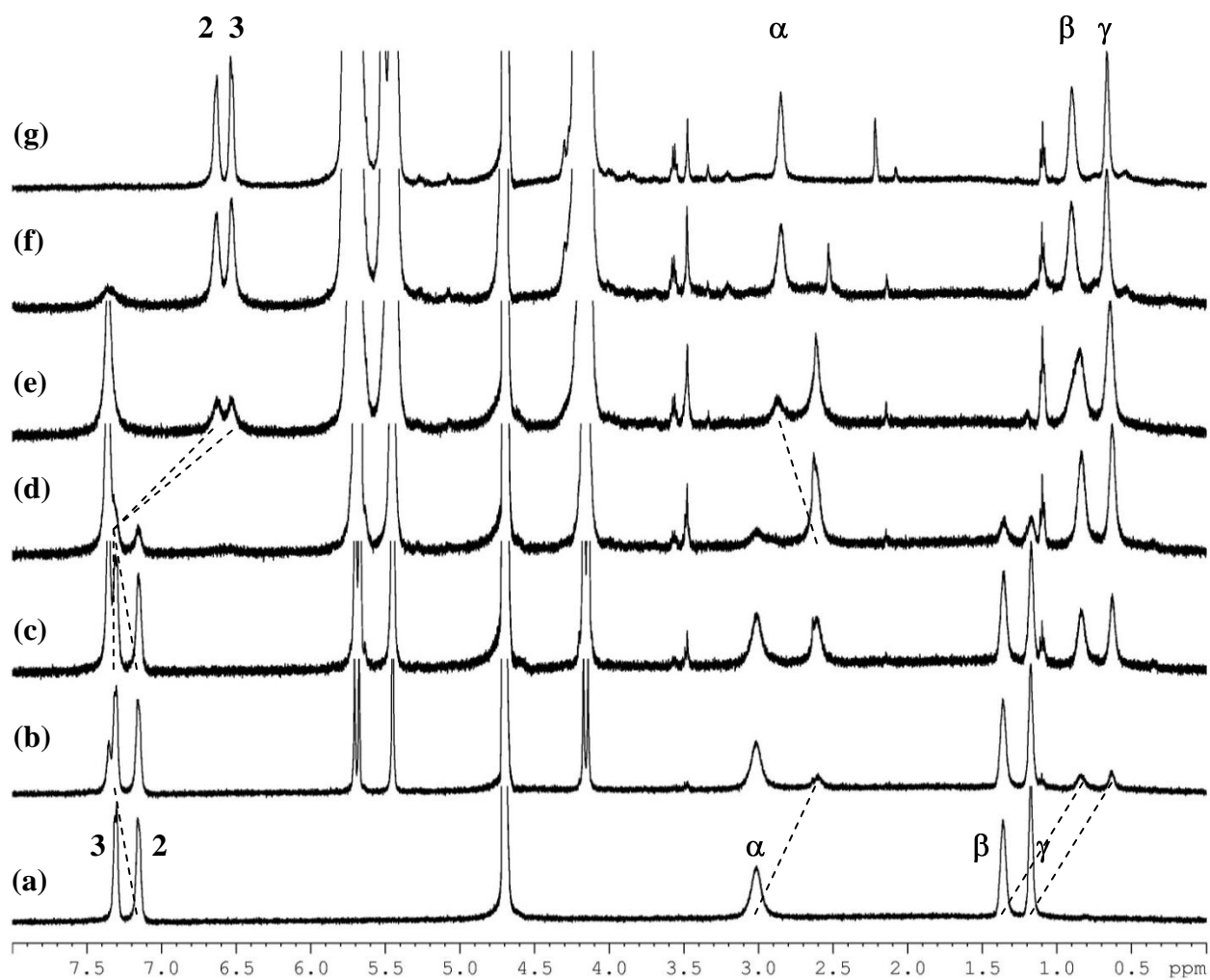
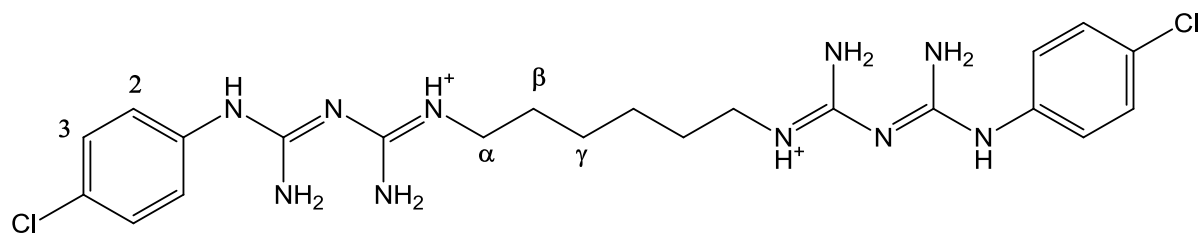


Figure 4.11 A stack plot of the ^1H NMR spectra of chlorhexidine in the presence of (a) 0.00, (b) 0.22, (c) 0.53, (d) 1.19, (e) 2.04, (f) 3.09, and (g) 3.98 equivalents of CB[7], titrated in D_2O . The dashed line indicates shifts in the peak positions of chlorhexidine. The numbered peaks are matched with their numerically labeled protons on the chemical structure of chlorhexidine, above.

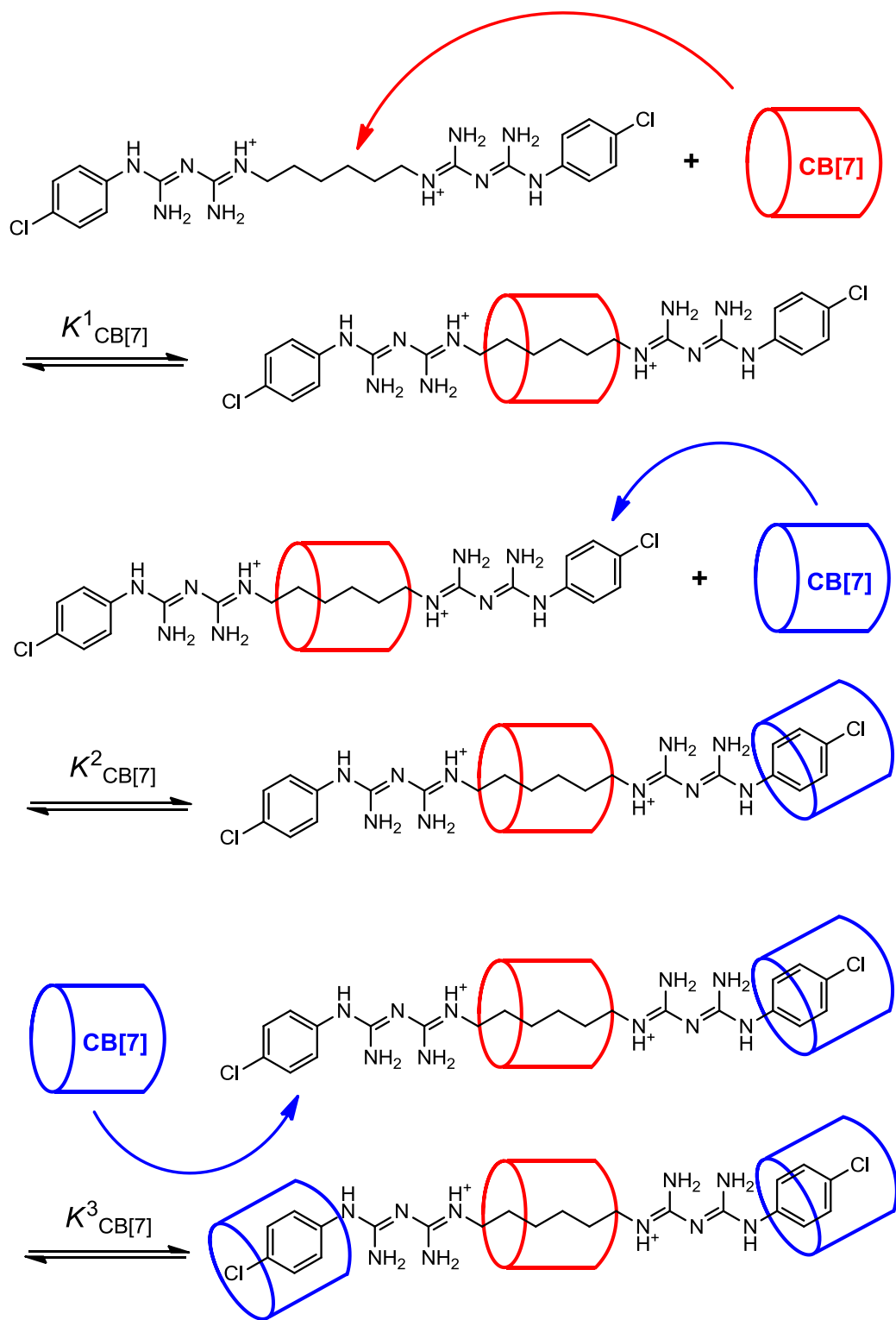


Figure 4.12 Stepwise formation of the 1:1, 2:1, and 3:1 host-guest complexes formed between CB[7] and chlorhexidine.

4.2.2.4 Alexidine

For alexidine, the two 4-chlorophenyl groups in chlorhexidine have been replaced by two 2-ethylhexyl groups. In the presence of a large excess of CB[7] (>7 equivalents), all of the guest resonances have shifted upfield, suggesting that three CB[7] host molecules are encapsulating the central hexamethylene chain and the two 2-ethylhexyl end groups (Figure 4.13). The titration of the alexidine with CB[7] would result in the initial formations of 1:1 host-guest and 2:1 host-guest intermediates, prior to complete encapsulation. There are two possible intermediates with a 1:1 stoichiometry, by placing the CB[7] over either the central hexamethylene chain, as observed with chlorhexidine, or over one of the terminal 2-ethylhexyl group. With a 2:1 host-guest stoichiometry, both CB[7] molecules could reside over the terminal groups, or one CB[7] could encapsulate each of the central chain or one terminal group. The changes in the ^1H NMR spectrum of the alexidine upon titration with CB[7] suggests that encapsulation of the terminal 2-ethylhexyl groups is favoured over central hexamethylene chain. Once both terminal groups have been bound, the formation of the 3:1 host-guest complex requires one of the CB[7] hosts binding a terminal site to move over the biguanide group to the central region, allowing another CB[7] to occupy the abandoned terminal group. It appears that all of the guest exchange processes between the host-guest complexes of different stoichiometry occur with slow exchange behaviour on the NMR timescale (Figure 4.13). This is also seen in the complexation of the hydrophobic 2-(2,2,4-trimethylpentyl) end of the benzethonium cation guest (Chapter 3). Both this moiety and the 2-ethylhexyl groups in alexidine are branched hydrocarbon groups with eight heavy (non-hydrogen) atoms. The volumes of these groups affords packing of the inner cavity of

CB[7] with close to the ideal (55%) packing coefficients to maximize the hydrophobic effect.²¹

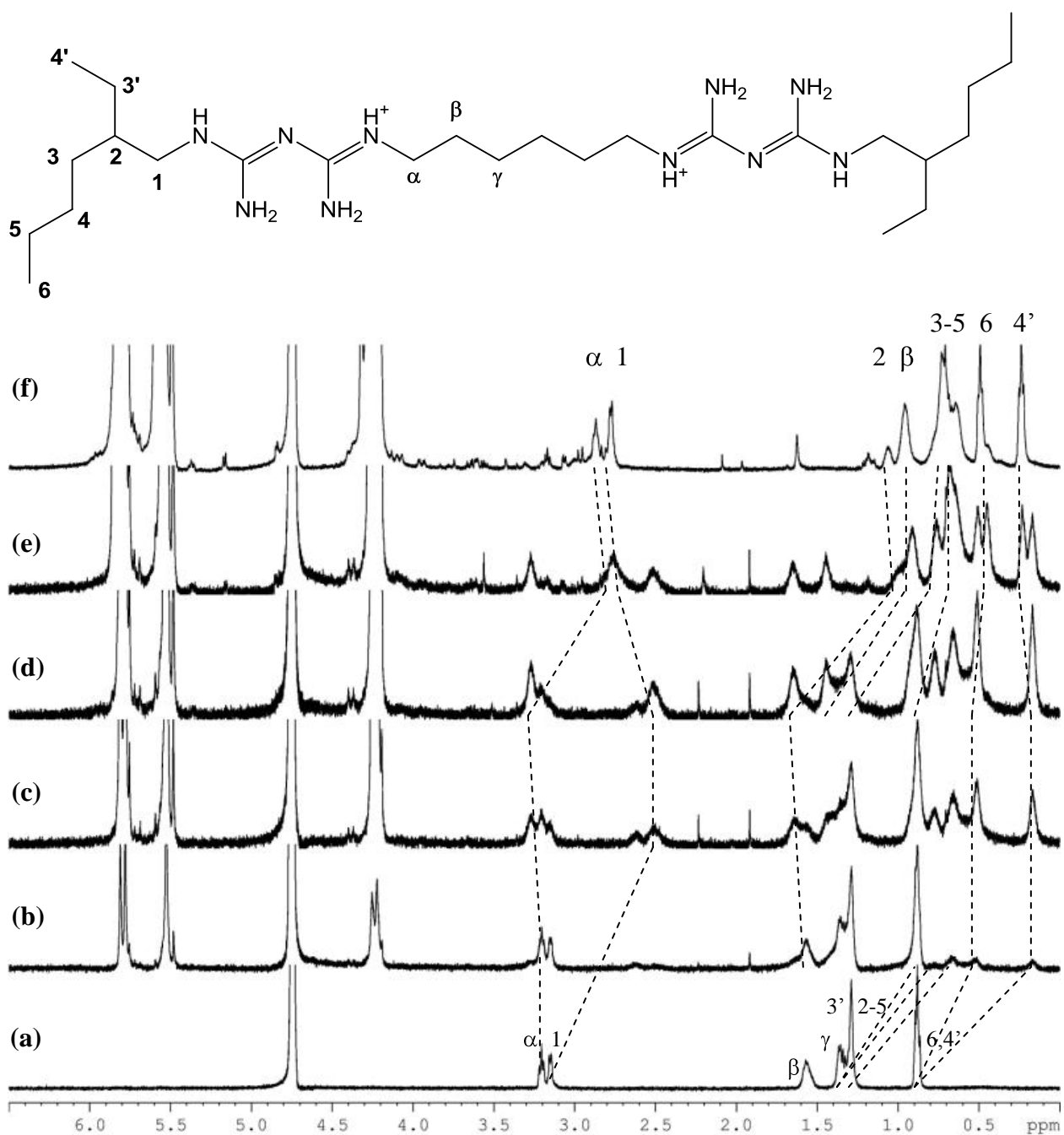


Figure 4.13 A stack plot of the ¹H NMR spectra of alexidine in the presence of (a) 0.00, (b) 0.72, (c) 1.77, (d) 2.28, (e) 3.60, and (f) 7.19 equivalents of CB[7], titrated in D₂O. The dashed line indicates shifts in the peak positions of alexidine. The numbered peaks are matched with their numerically labeled protons on the chemical structure of alexidine, above.

While there is considerably less distinction between the sequential binding processes for alexidine than observed for chlorhexidine, following the resonances for the two methyl group protons (H4' and H6) on the 2-ethylhexyl group allows for distinctions between binding on the terminal groups versus the central hexamethylene linker. The methyl resonances have essentially the same chemical shift in the free guest ($\delta_{\text{free}} = 0.88$ ppm), however upon complexation of this group by CB[7], one of the methyl environments experiences a considerably larger upfield chemical shift change ($\Delta\delta = -0.70$ ppm for H4') than the other ($\Delta\delta = -0.37$ ppm for H6). Above two equivalents of CB[7], the methyl resonances each exhibit a slight shift, with the H6 resonance moving upfield and the H4' proton resonance moving downfield. This may be as a result of the repulsions between the central CB[7] and the terminal host molecules, causing the terminal CB[7] hosts to move away from the center of the guest, such that the H6 methyl group is more inside the cavity and the H4' methyl protons closer to the deshielding portal region.

There are at least two possible routes (Figures 4.14 and 4.15) to the 3:1 host-guest product as CB[7] is added to the alexidine guest. The first CB[7] binds to the 2-ethylhexyl end group and this would be followed by complexation of the other 2-ethylhexyl end (Figure 4.14), or to the central hexamethylene chain (Figure 4.15). In the first route, the addition of the third CB[7] would require one of the two CB[7] hosts binding to the terminal 2-ethylhexyl to relocate to the central hexamethylene chain, prior to the third CB[7] occupying its original location. In the second route (Figure 4.15), one of the terminal binding sites would be vacant and the third CB[7] would simply bind in this position. The ^1H NMR titration favours the first process (Figure 4.14), as discussed above for the methyl resonances, but a minor involvement of the second route cannot be ruled out.

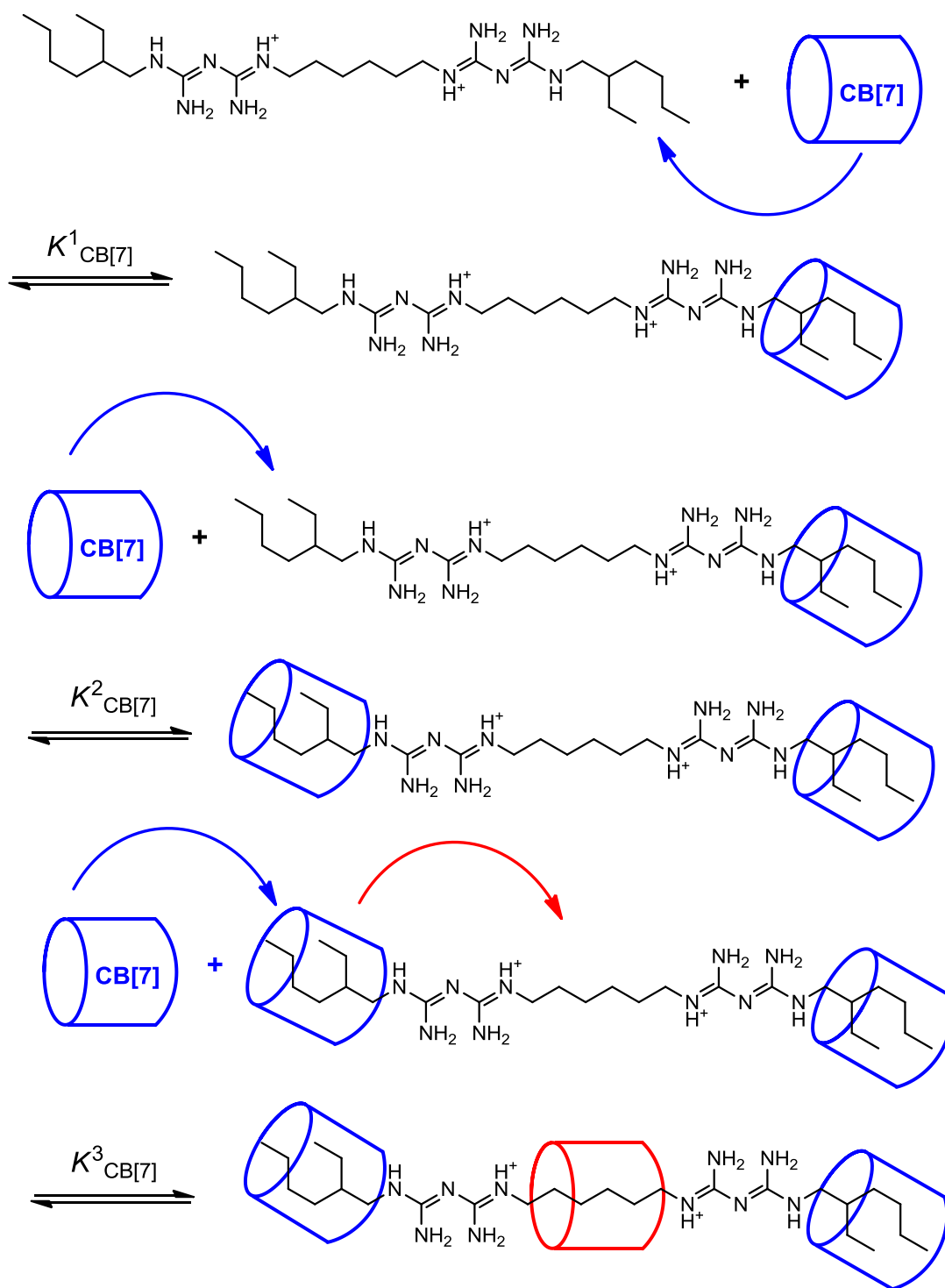


Figure 4.14 Stepwise formation of the 1:1, 2:1, and 3:1 host-guest complexes formed between CB[7] and alexidine.

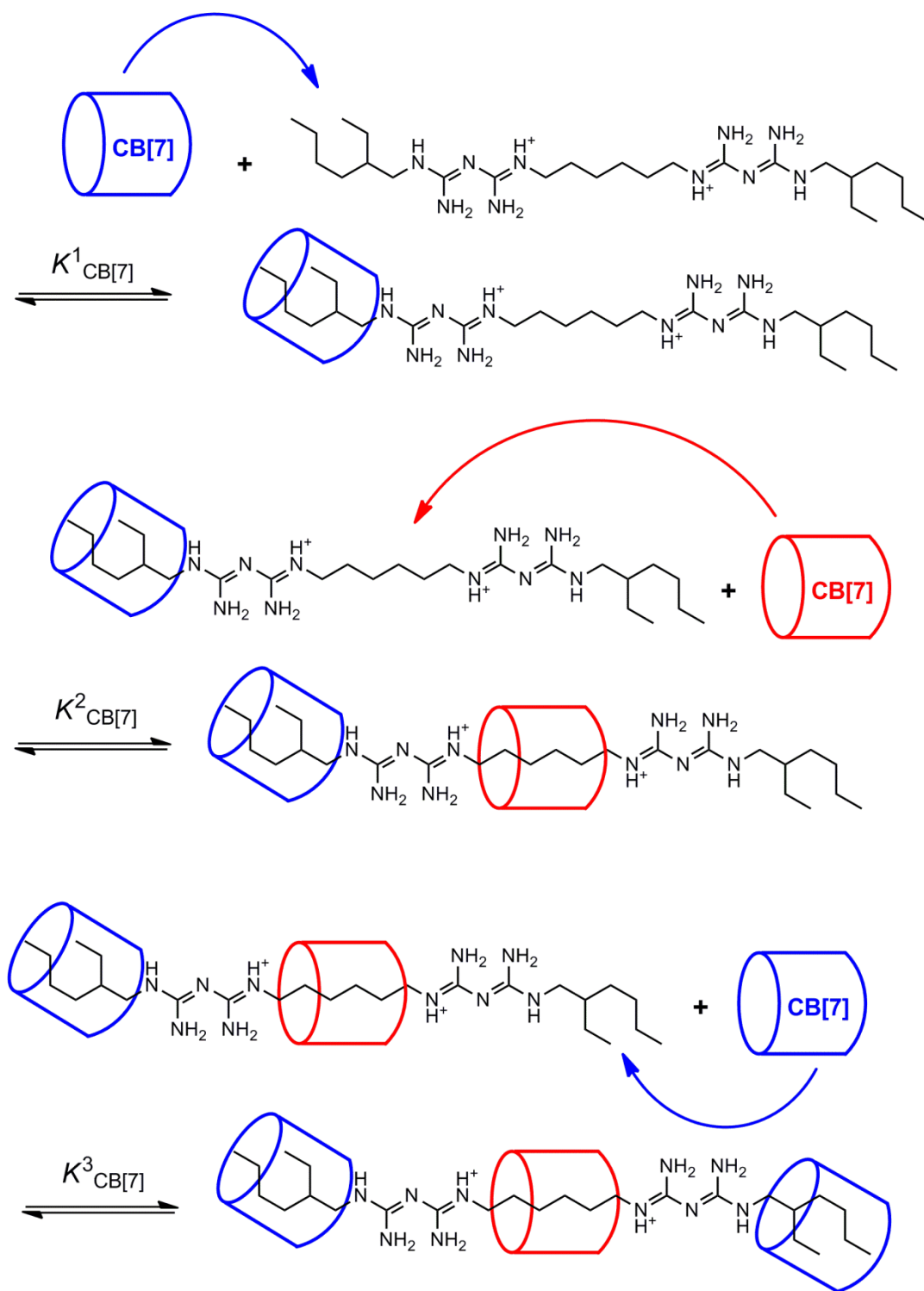


Figure 4.15 Alternative stepwise formation of the 1:1, 2:1, and 3:1 host-guest complexes formed between CB[7] and alexidine.

4.2.3 Determination of Binding Constants

Once the stoichiometries of the host-guest complexes formed between CB[7] and the biguanidinium guests had been determined by ESI mass spectrometry and ^1H NMR spectroscopy, determinations of the binding constants for the respective host-guest complexes were undertaken by means of ^1H NMR spectroscopy, using the dependences of the guest protons' chemical shifts on host concentration (for lower binding constants) or, in the case of more strongly binding guests, competitive binding experiments using guests of known affinity for CB[7].¹⁶

4.2.3.1 Metformin

The binding events that occur between the biguanidinium guests and CB[7] are driven by the interactions between the polar portals on CB[7] and the delocalized positive charge on the biguanidinium group. In the case of metformin, this ion-dipole interaction was the main driving force, since the two methyl groups attached to the biguanidinium group add only a modest degree of hydrophobic stability. The dependence of the ^1H NMR chemical shift change of the methyl proton resonance of the guest on the concentration of CB[7] (Figure 4.7) is interpreted as a sequence of binding equilibria involving the initial formation of a 1:2 host-guest complex, followed by the formation of the 1:1 host-guest complex at higher concentrations of the host (Figure 4.8). It is not possible to determine the value of $K_{\text{CB}[7]}^{1:2}$ from the linear dependence of $\Delta\delta_{\text{obs}}$ up to 0.5 equivalents of CB[7], however the chemical shift data beyond this point (Figure 4.7) provides for an estimate of the equilibrium constant $K^{1:2 \rightarrow 1:1}$ ($= [\text{H}\cdot\text{G}]^2/[\text{H}][\text{H}\cdot\text{G}_2]$). A value of 11 ± 5 was calculated for this equilibrium constant using $\Delta\delta_{\text{lim}}(\text{H}\cdot\text{G}_2) = -0.17$ ppm and $\Delta\delta_{\text{lim}}(\text{H}\cdot\text{G}) = -0.69$ ppm.

In addition, a ^1H NMR competition study was conducted with a known competitor guest, as outlined by Isaacs and coworkers,¹⁶ and described in Chapter 2. For metformin, the tetramethylammonium cation (Figure 4.16a) was chosen as a competitor, because like metformin, it contains a positively charged group and methyl substituents. Studies conducted by St-Jacques *et al.* have found that the tetramethylammonium cation has a binding constant with CB[7] of $K_{\text{CB}[7]} = (1.2 \pm 0.4) \times 10^5 \text{ M}^{-1}$.¹⁷

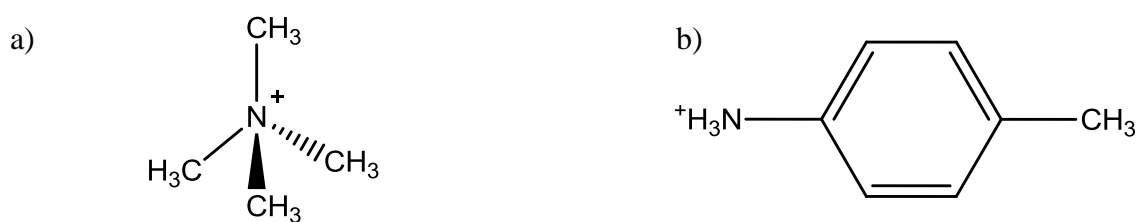
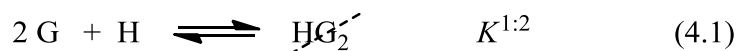


Figure 4.16 The chemical structures of a) the tetramethylammonium cation and b) *p*-toluidinium cation competitor guests.^{16,17}

A metformin:competitor:CB[7] ratio of 5.4 : 5.4 : 3.0 mM was employed and under these conditions, and with the competitor binding the majority of the CB[7], the 1:2 CB[7]-chlorhexidine complex would be the dominant species present involving this guest. This allowed for a calculation of $K^{1:2}_{\text{CB}[7]} = (3.2 \pm 1.0) \times 10^3 \text{ M}^{-2}$ to be made. Summing the equations for the two equilibria in Figure 4.8 results in the equilibrium for the formation of the 1:1 host-guest complex:



The product of the two equilibrium constants $K^{1:2 \rightarrow 1:1}$ (eq. 4.2) and $K^{1:2}$ (eq. 4.1), determined above, is equal to the square of the equilibrium constant for the formation of the 1:1 complex (eq. 4.3), and this gives a value of $K^{1:1} = 2 \times 10^2 \text{ M}^{-1}$. The binding constant between CB[7] and asymmetric dimethylarginine, which contains a structurally similar dimethylguanidinium group, was recently determined in our laboratory to be $2.0 \times 10^3 \text{ M}^{-1}$, while the binding constant for $\text{N}^\epsilon, \text{N}^\epsilon$ -dimethyllysine with CB[7] was found to be $6.7 \times 10^4 \text{ M}^{-1}$.¹⁹ The trend in the 1:1 binding constants of biguanidinium < guanidinium < ammonium is consistent with increase in the localization of the positive charge on the guest and therefore an increase in the ion-dipole interaction between the guest and the CB[7] host.

4.2.3.2 Phenformin

Phenformin, unlike metformin, has both a charged biguanidinium group and a bulky aromatic substituent, which can be used to bind to a polar portal of CB[7] and its hydrophobic cavity, respectively. Thus, it was expected that phenformin would have a higher binding constant than metformin due to the added stability of the hydrophobic effect that occurs when CB[7] encapsulates the aromatic functional group. A competition study was conducted with a competitor, the *p*-toluidinium cation (Figure 4.16b), whose binding constant was determined by Isaacs *et al.* to be $K = (8.4 \pm 1.3) \times 10^6 \text{ M}^{-1}$.¹⁶ Once the competition study had been conducted, the binding constant between phenformin and CB[7] was calculated to be $K = (2.7 \pm 0.5) \times 10^6 \text{ M}^{-1}$, which is several orders of magnitude stronger than the binding event between metformin and CB[7], as expected. The binding constant is slightly weaker than the series of cationic guests containing benzyl groups, depicted in Figure 4.10.

4.2.3.3 Chlorhexidine

Chlorhexidine and alexidine each contain two biguanidinium groups joined by a hexamethylene aliphatic chain. This hexamethylene group is an ideal site for CB[7] to bind to, due to the complementarity between this site on the guest and the CB[7] host cavity. The positively charged biguanidinium groups on the guest are ideally spaced to interact via ion-dipole interactions with both polar portals on CB[7]. Also, the non-polar hexamethylene linker on the guest can be encapsulated in the hydrophobic cavity of CB[7], reducing the enthalpically unfavourable interactions between the polar solvent and non-polar regions on the host and guest, in addition to displacing the high energy waters from the CB[7] cavity. As a result of this complementarity, this binding site on chlorhexidine and alexidine was expected to result in a higher binding constant with CB[7] than those of either metformin or phenformin with CB[7].

Since the binding constant of these 1:1 host-guest complexes was expected to be large, modified competition studies were conducted (as described in Chapter 2). In the case of chlorhexidine, the *p*-toluidinium cation was chosen as the competitor because they both possessed the same *para*-disubstituted benzene structure. From this study, the 1:1 binding constant between chlorhexidine and CB[7] was calculated to be $K = (9.3 \pm 1.7) \times 10^6 \text{ M}^{-1}$.

Chlorhexidine and alexidine also contain two terminal hydrophobic groups. On chlorhexidine, each terminus possesses a 4-chlorophenyl group joined to the charged biguanidinium group (Figure 4.3). Since each of these terminal groups is hydrophobic, a second and third equivalent of CB[7] can bind at these positions, however, the hydrophobic effect alone does not provide the driving force for binding. Each CB[7] would also be able engage in ion-dipole interaction with a biguanidinium group to improve binding, however

the interaction with a single resonance stabilized cationic center, would be expected to be weaker than the binding of the first CB[7] over the hexyl bridge. Additionally, the second and third equivalents of CB[7] would be affected somewhat by repulsions from the polar portals of the first CB[7] host. The combined results of these forces were weaker second and third binding events between CB[7] and either chlorhexidine or alexidine. Based on the integrations of the chlorhexidine proton resonances for the various host-guest species, as a function of the CB[7]/chlorhexidine ratio, a speciation diagram was constructed (Figure 4.17)

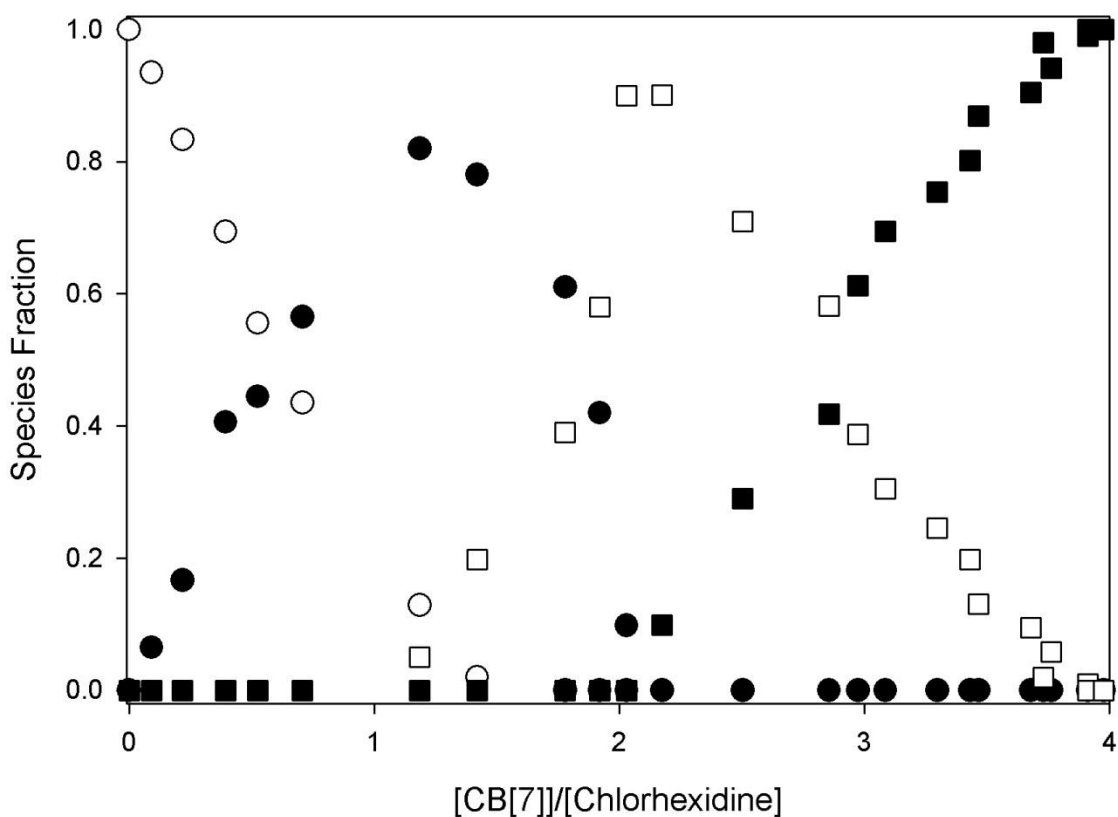


Figure 4.17 Speciation diagram for the host-guest complexes of chlorhexidine with CB[7] based on the ^1H NMR titration. (○) free chlorhexidine, (●) 1:1 chlorhexidine:CB[7] complex, (□) 1:2 chlorhexidine:CB[7] complex and the (■) 1:3 chlorhexidine:CB[7] complex.

The binding of the third CB[7] to the 2:1 host-guest complex with chlorhexidine was of sufficiently low strength ($K < 10^4 \text{ M}^{-1}$) for the binding constant to be determined by using the concentrations of the 2:1 and 3:1 host-guest species from the integrations of the aromatic resonances (as described in Chapter 2) using the spectral data (Figure 4.11) for the titration points in which the CB[7]/chlorhexidine was in the range of 2.5 to 3.5. From this, the 3:1 binding constant between CB[7] was found to be $(3.0 \pm 1.5) \times 10^3 \text{ M}^{-1}$. While it is not practical to directly determine the equilibrium constant for the 2:1 complex between CB[7] and chlorhexidine, because of the complex nature of the ^1H NMR spectra (Figure 4.11) and the corresponding mixture of species (Figure 4.17) in the vicinity of $[\text{CB}[7]]/[\text{chlorhexidine}] = 2$, the assumption of a statistical binding relationship²² between additions of the second and third CB[7] hosts may be used to determine reasonable approximations of this value. In Chapter 2, a host-guest binding constant was defined as $K_{\text{HG}} = k_{\text{on}}/k_{\text{off}}$, where k_{on} and k_{off} are the rates at which CB[7] binds to and releases from chlorhexidine, respectively. In the case of the second binding event, there are two terminal 4-chlorophenyl binding sites available on the chlorhexidine for CB[7] to bind to, but once bound there is only one binding site for it to be released from. As a result, $k_{\text{on}}/k_{\text{off}}$ is proportional to $2/1 = 2$. In the case of the third binding event, there is only one binding site available on the guest for CB[7] to bind to, but once bound, either terminal CB[7] can be released, returning the system to a 2:1 host-guest complex. As a result, $k_{\text{on}}/k_{\text{off}}$ is proportional to $1/2 = 0.5$, and the ratio of $K_{2:1}/K_{3:1} = 4$ in a statistical binding model. By multiplying the measured third binding constant determined above, a lower limit for the second binding constant was estimated to be $K_{2:1} = 1.2 \times 10^4 \text{ M}^{-1}$. It has been observed in our laboratory, using other dication guests with multiple binding sites (see discussion in Section 4.3 below), that binding constant ratios of > 4 (see Table 4.3) are

commonly observed, even when statistical binding behaviour might be anticipated. The most likely explanation for this lies in the repulsions between neighbouring host molecules when more than one host is present.

Chlorhexidine complexes with the β -cyclodextrin (β -CD) host molecule have been investigated,^{23a} with binding constants of $K_1 = 287 \pm 21 \text{ M}^{-1}$ and $K_2 = 268 \pm 23 \text{ M}^{-1}$ for the 1:1 and 2:1 host-guest complexes reported.²⁴ These complexes have been investigated for slow-release capabilities.²⁴ A subsequent study employing ESI-MS provided evidence for up to four β -CD hosts encapsulating the chlorhexidine, with the binding constant determined to be $K = 557 \pm 23 \text{ M}^{-1}$ from isothermal calorimetry.^{23b,c} The lower binding constants for β -CD versus CB[7] for chlorhexidine are likely due to the fact that the ion-dipole interactions between the biguanidinium center and the hydroxyl groups of the β -CD rims are weaker than with the ureido carbonyl groups on the portals of CB[7]. The higher stoichiometry with β -CD (up to 4:1 host-guest)^{23c} compared to CB[7] (up to 3:1 host-guest) would most likely be attributed to the favourable hydrogen bonding interactions between the rim hydroxyl groups on neighbouring β -CD molecules compared with the expected dipole-dipole repulsions between the carbonyl oxygens on the portals of adjacent CB[7] hosts.

4.2.3.4 Alexidine

Alexidine might be expected to have a very similar 1:1 host-guest binding constant to chlorhexidine, since they possess a common 1,6-bis(biguanidinium)hexane core. The ^1H NMR titration spectra and chemical shift change data (Figures 4.13 and 4.5) show, however, that the first CB[7] binds to a terminal 2-ethylhexyl group, rather than over the central hexamethylene group. To determine the 1:1 host-guest stability constant, the *p*-toluidinium

cation was once again chosen as the competitor, although in this case the choice was based on its success with chlorhexidine and not structural similarity to binding site on alexidine. The 1:1 binding constant between alexidine and CB[7] was determined to be $(6.6 \pm 1.2) \times 10^7 \text{ M}^{-1}$.

The process used above to determine the second and third binding constants between chlorhexidine and CB[7], based on a statistical relationship,²² can be applied to estimate an upper limit for the second binding constant between alexidine and CB[7], as the ^1H NMR data (Figures 4.13) suggest that the second CB[7] primarily binds to the other terminal 2-ethylhexyl site. Assuming the first binding mechanism (Figure 4.12) is in operation, the first and second binding processes would be expected to have a statistical relationship, as with second and third binding events of chlorhexidine. With a 1:1 binding constant of $(6.6 \pm 1.2) \times 10^7 \text{ M}^{-1}$, and the relationship of $K_{\text{CB[7]}^1}^1 = 4 K_{\text{CB[7]}^2}^2$, the 2:1 binding constant is estimated to be less than $1.7 \times 10^7 \text{ M}^{-1}$.

The third binding event, according to the mechanism in Figure 4.14, requires the relocation of a CB[7] from the terminal 2-ethylhexyl group to the central hexamethylene site. It was observed that upon a total of 3.60 equivalents of CB[7] (^1H NMR spectrum in Figure 4.13e), the sets of proton resonances associated with the 2:1 and 3:1 host-guest complexes were of approximately equal intensity. If it is assumed that at this stage in the titration, the spectrum represents solely an equilibrium between the 2:1 and 3:1 host-guest complexes, and that 2.0 equivalents of the total [CB[7]] are used to form the 2:1 complex, then are initially 1.6 equivalents remaining to complex the final position on the guest. This leads to a value of $K_3^{\text{CB[7]}}$ of approximately 900 M^{-1} . The much lower binding constant for the third CB[7] is likely associated with the need to relocate one of the CB[7] hosts over the biguanidinium

group from the terminal binding site to central binding site. In addition, the 3:1 complex would place the three host molecules relatively close to one another, maximizing the portal-portal electrostatic repulsions.

The binding constants for the 2:1 host-guest complexes of CB[7] with alexidine and chlorhexidine have been estimated on the basis of a statistical binding model. These binding constants, as well as the 1:1 host-guest complexes of CB[7] and metformin, phenformin, chlorhexidine, and alexidine, are summarized in Table 4.2.

Table 4.2 The host-guest stability constants for CB[7] complexes with metformin, phenformin, chlorhexidine and alexidine.

Guest	Host:Guest	Competitor (if applicable)	$K(\text{competitor})$ (M^{-1})	$K(\text{guest})$ (M^{-1})
Metformin	1:2	$\text{N}(\text{CH}_3)_4^+$ ¹⁷	$(1.2 \pm 0.4) \times 10^5$	$(3.2 \pm 0.8) \times 10^3$ ^a
	1:1	NA	NA	2×10^2 ^b
Phenformin	1:1	<i>p</i> -Toluidine ¹⁶	$(8.4 \pm 1.3) \times 10^6$	$(2.7 \pm 0.5) \times 10^6$
Chlorhexidine	1:1	<i>p</i> -Toluidine ¹⁶	$(8.4 \pm 1.3) \times 10^6$	$(9.3 \pm 1.7) \times 10^6$
	2:1	NA	NA	$> 1.2 \times 10^4$ ^c
	3:1	NA	NA	$(3.0 \pm 1.5) \times 10^3$
Alexidine	1:1	<i>p</i> -Toluidine ¹⁶	$(8.4 \pm 1.3) \times 10^6$	$(6.6 \pm 1.2) \times 10^7$
	2:1	NA	NA	$< 1.7 \times 10^7$ ^d
	3:1	NA	NA	$(9.0 \pm 2.0) \times 10^2$

^a Units of M^{-2} . ^b Calculated as described in Section 4.2.3.1. ^c Calculated using a statistical binding relationship between $K^1_{\text{CB}[7]}$ and $K^2_{\text{CB}[7]}$. ^d Calculated using a statistical binding relationship between $K^2_{\text{CB}[7]}$ and $K^3_{\text{CB}[7]}$.

From the information in Table 4.2, it was determined that CB[7] is able to bind to guests with one or more biguanidinium groups. Both metformin and phenformin were found to have 1:1 host-guest complexes that proved to be strongly bound to one another.

Chlorhexidine and alexidine were both shown to have tightly bound 1:1 CB[7] host-guest complexes, with very high binding constants. Additionally, chlorhexidine and alexidine were also both shown to have 2:1 and 3:1 host-guest complexes, with the attractive ion-dipole interactions between the biguanidinium group and the polar portals being offset somewhat by increases in repulsive dipole-dipole forces between portals of neighbouring host molecules.

In their antibacterial activity, chlorhexidine and alexidine bind at several anionic binding sites at the O-antigen of a lipopolysaccharide (LPS) molecule in the outer membrane of Gram-negative bacteria. Analyses of calorimetric titrations of LPS with the bis(biguanidinium) dications yielded association constants of 2.9×10^6 and $2.2 \times 10^5 \text{ M}^{-1}$ for alexidine and chlorhexidine, respectively.²⁵ The binding constants measured for chlorhexidine and alexidine with CB[7] in the present study, suggest that CB[7] should be effective in reversing the antibacterial effects of the bis(biguanidinium) dications.

4.3 Comparisons of Binding Modes of CB[7] with the Bis(biguanidinium) Guests and other Polycationic Guests

The ^1H NMR titrations of chlorhexidine and alexidine with CB[7] indicate that while both guests share the same 1,6-bis(biguanidinium)hexane core, they form 1:1, 2:1, and 3:1 host-guest complexes by different processes (Figures 4.12 and 4.14). In the case of chlorhexidine, the first CB[7] encapsulates the central hexamethylene group, followed by sequential bindings of the second and third CB[7] hosts to the terminal 4-chlorophenyl groups. With alexidine, the first two CB[7] host molecules sequentially bind the two terminal 2-ethylhexyl groups, with the addition of the third CB[7] requiring a relocation of the one of the first two CB[7] hosts from the terminal site to the central hexamethylene chain, prior to its binding of the vacated terminal site. The difference is the processes may

thus be attributed to the different binding affinities of the CB[7] for the terminal 4-chlorophenyl group on chlorhexidine versus the 2-ethylhexyl group on alexidine, with respect to the strength of binding to the common hexamethylene chain.

The preference of the initial CB[7] to bind to the central hexamethylene chain, thus positioning a cationic biguanidinium group adjacent to each polar portal of the CB[7], has been observed previously in our laboratory for dications bearing two terminal iminium (pyridinium and substituted pyridinium,²⁶ isoquinuclidinium,²⁷ imidazolium,²⁸ and bipyridinium²⁹) or quaternary ammonium or phosphonium groups³⁰ on polymethylene chains ($-\text{CH}_2-$, $n = 6, 8-10$). The addition of further equivalents of CB[7] to these dications has been observed to normally result in the formation of a 2:1 host-guest complex (of varying stabilities, depending on the nature of the terminal group and the length of the polymethylene chain) in which the initial CB[7] has abandoned the central binding site, with its relocation to one of the two terminal sites allowing for the second CB[7] to bind to the other terminal site. This process prevents electrostatic repulsions between neighbouring CB[7] hosts, if they were to be located on one terminal site and the polymethylene site, while maintaining an ion-dipole interaction between the cationic centers and one portal on each CB[7]. With guests such as the 1,6-bis(trimethylammonium)hexane dication,³⁰ however, the binding of the CB[7] to terminal trimethylammonium sites is so weak, compared to the central site, that no 2:1 host-guest complexes are observed by ^1H NMR spectroscopy nor ESI mass spectrometry.

With alexidine as the guest, the terminal 2-ethylhexyl groups are the sites of the binding of the first two CB[7] host molecules, rather than the central hexamethylene group. As discussed above, the molar volume of the hydrophobic 2-ethylhexyl group, with eight heavy atoms, is such that it provides very efficient filling of the inner CB[7] cavity (PC =

55%). The preference of CB[7] for terminal cationic binding sites over binding to a central hexamethylene chain have also been observed in our laboratory for dications bearing quinuclidinium and 4-*tert*-butylpyridinium groups.²⁶ In both of these cases, the addition further equivalents of CB[7] did not result in the formation of 3:1 host-guest complexes, because of the very strong affinity for these hydrophobic terminal moieties and because of the repulsive dipole-dipole interactions between neighbouring hosts that would result.

Table 4.3. Stability constants and $\Delta\delta_{\text{lim}}$ values for guest hexamethylene chain proton resonances for the 1:1 and 2:1 CB[7] host-guest complexes.

Guest	$K^1_{\text{CB}[7]}, \text{M}^{-1}$	$K^2_{\text{CB}[7]}, \text{M}^{-1}$	$\Delta\delta_{\text{lim}}, \text{ppm}$ H α , H β , H γ ^a	Ref.
chlorhexidine	9.3×10^6	$> 1.2 \times 10^4$	-0.40, -0.53, -0.54 -0.40, -0.53, -0.54	this work
alexidine	6.6×10^7	$< 1.7 \times 10^7$	+0.06, +0.08, +0.08 +0.06, +0.08, +0.08	this work
(Me ₃ N)(CH ₂) ₆ (NMe ₃) ²⁺	3.9×10^9	not observed	-0.68, -0.68, -0.88	30
(4-Mebpy)(CH ₂) ₆ (4-Mebpy) ⁴⁺	6×10^3	6.8×10^2	^b , -0.76, -0.76 ^b , -0.16, -0.15	29
pyr(CH ₂) ₆ pyr ²⁺	4.8×10^8	8.0×10^1	-0.68, -0.68, -0.64	26
(2-Mepyr)(CH ₂) ₆ (2-Mepyr) ²⁺	2.4×10^7	3.2×10^4	-0.51, -0.52, -0.58 -0.37, -0.17, +0.04	26
(3-Mepyr)(CH ₂) ₆ (3-Mepyr) ²⁺	1.6×10^8	2.3×10^4	-0.71, -0.63, -0.63 -0.03, -0.11, +0.21	26
(4- <i>t</i> -Bupyr)(CH ₂) ₆ (4- <i>t</i> -Bupyr) ²⁺	5.2×10^{10}	2.1×10^9	+0.03, +0.15, +0.17 +0.10, +0.34, +0.40	26
(imid)(CH ₂) ₆ (imid) ²⁺	4.0×10^7	not observed	-0.13, -0.71, -0.67	27
(isoquin)(CH ₂) ₆ (isoquin) ²⁺	1.2×10^9	1.6×10^8	-0.37, -0.26, -0.21 +0.36, +0.35, +0.52	28

^a First line of values for 1:1 complex, second line of values for 2:1 complex. ^b Resonance obscured by HOD solvent peak.

With chlorhexidine and alexidine, the extended biguanidinium groups provide a buffer region, which is both electrostatically attractive to the CB[7] host molecules, but at the same time keeps the hosts sufficiently far apart from one another even with three CB[7] bound simultaneously. In the case of alexidine, the binding of the third CB[7] requires a relocation of a CB[7] from the terminal 2-ethylhexyl group over the biguanidinium to the central hexamethylene group. The translocations of CB[n] host molecules between sites on multisite guest molecules can be accomplished by external stimuli such as pH,³¹ oxidation-reduction,³² heat,³³ and light,³⁴ in addition to the “stoichiometry-driven” process in this study and previous work from our laboratory.²⁶⁻³⁰

4.4 Effect of Complexation of Metformin by CB[7] on the Guest pK_a value

At neutral pH, the metformin guest is a biguanidinium cation, which can be deprotonated at pH 12.4.³⁵ In acidic media, the metformin cation can be further protonated, with a reported pK_a value of 2.8.³⁵ Complexations of acidic cationic guests by CB[7] have been shown to result in an increase in the pK_a value of the guest, provided the protonated (usually cationic) form of the guest has a higher stability constant with CB[7] than does the deprotonated (usually neutral) form of the guest.^{36,37} The increased stability of the protonated form is a result of the ion-dipole interactions between the positive charge on the guest and the oxygens of the polar portal carbonyl groups, plus any hydrogen-bonding interactions which may be present. In order to see if such an effect on the first pK_a would be observed with the doubly protonated metformin dication, a spectrophotometric pH titration (between pH 1 and 6) was performed with metformin in the absence and presence of CB[7] (Figure 4.18). The λ_{max} value for the metformin shifts from 232 nm in the absence of CB[7]

to 240 nm for the CB[7] host-guest complex with metformin. From plots of the absorbances at their respective λ_{\max} values against the pH of the solution, the pK_a values can be determined. In the absence of the CB[7] a value of $pK_a = 2.82$ was determined, in good agreement with the reported value of 2.8. For the host-guest complex, the pK_a of the complexed metformin dication actually decreased to 2.68, rather than exhibiting an increase as is observed with most acidic guests.

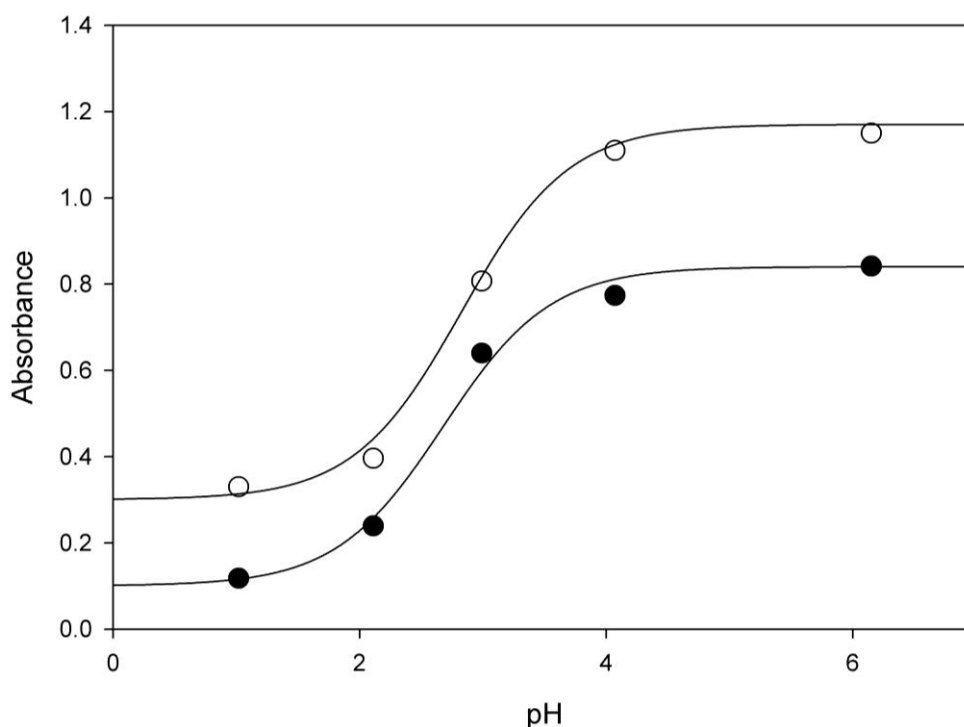


Figure 4.18 The pH dependences of the absorbances of metformin in the absence (○, 232 nm) and presence (●, 240 nm) of CB[7]. The solid curves are fit with pK_a values of 2.82 and 2.68, respectively.

This result suggests that the doubly protonated dication has a slightly lower affinity for the CB[7] than does the monocation. In both cases, the charges are likely to be delocalized over the biguanidinium framework as the result of resonance. It may be that the

dication has its charges too close together to allow each to interact with a different portal on CB[7], resulting in a smaller binding constant. A similar example has been observed in our laboratory in the case where the dication $\text{CH}_3^+\text{DABCO}^+\text{CH}_3$ (DABCO = 1,4-diazabicyclo[2.2.2]octane) bound to CB[7] with a stability constant of $(5.7 \pm 1.4) \times 10^9 \text{ M}^{-1}$, compared to a value of $(5.7 \pm 1.4) \times 10^9 \text{ M}^{-1}$ for the $\text{DABCO}^+\text{CH}_3$ cation.³⁸

4.5 Conclusions

The formations of host-guest complexes between CB[7] and several guests with biguanidinium groups have been investigated through the use of ESI mass spectrometry and ^1H NMR spectroscopy. The results of these analyses indicate that CB[7] was able to bind metformin, phenformin, chlorhexidine, and alexidine through ion-dipole interactions with their biguanidinium groups and hydrophobic interactions with the forming host-guest complexes with high binding constants. The two bisbiguanidinium guests, chlorhexidine and alexidine, demonstrated particularly high 1:1 binding complexes and more weakly bound 2:1 and 3:1 complexes. As a result of the ability of CB[7] to bind to these drugs molecules, it is possible CB[7] could be used to promote the solubility, controlled release, and drug delivery of these guests.

References

1. P. D. Beer, P. A. Gale, and D. K. Smith, *Supramolecular Chemistry*, Oxford Chemistry Primers, Vol. 74, Oxford University Press: Oxford, 2003; pp. 38-39.
2. J. W. Steed and J. L. Atwood, *Supramolecular Chemistry*, John Wiley and Sons, Ltd.: Chichester, 2000; pp. 220-223.
3. (a) F. Yang and D. V. Dearden, *Supramol. Chem.*, **2011**, 23, 53. (b) F. Yang and D. V. Dearden, *Isr. J. Chem.* **2011**, 51, 551.
4. a) A. Hennig, H. Bakirci, W. M. Nau, *Nat. Methods*, **2007**, 4, 629. b) D. S. N. Hettiarachchi, I. W. Wyman, and D. H. Macartney, manuscript in preparation.
5. C. J. Bailey and R. C. Turner, *New Engl. J. Med.*, **1996**, 334, 574.
6. T. Strack, *Drugs Today*, **2008**, 44, 303.
7. J. H. B. Scarpello and H. C. S. Howlett, *Diabetes Vasc. Dis. Res.*, **2008**, 5, 157.
8. T. V. Kourelis and R. D. Siegel, *Med. Oncol.* DOI 10.1007/s12032-011-9846-7 (published online February 8, 2011).
9. K. S. Lim and P. C. A. Kam, *Anaesth. Intensive Care*, **2008**, 36, 502.
10. J. A. Chawner and P. Gilbert, *Int. J. Pharm.*, **1989**, 55, 209.
11. K. W. Yip, E. Ito, X. Mao, P. Y. B. Au, D. W. Hedley, J. D. Mocanu, C. Bastianutti, A. Schimmer, and F. F. Liu, *Mol. Cancer Ther.*, **2006**, 5, 2234.
12. P. Sreenivasan, A. Gaffar, *J. Clin. Periodontol.*, **2002**, 29, 965.
13. M. Addy, *J. Clin. Periodontol.*, **1986**, 13, 957.
14. S. Jenkins, M. Addy, W. Wade, *J. Clin. Periodontol.*, **1988**, 15, 415.
15. V. W. Spolsky and A. B. Forsythe, *J. Dent. Res.*, **1977**, 56, 1349.

16. S. Liu, C. Ruspic, P. Mukhopadhyay, S. Chakrabarti, P. Y. Zavalij, and L. Isaacs, *J. Am. Chem. Soc.*, **2005**, *127*, 15959.
17. A. D. St-Jacques, I. W. Wyman, and D. H. Macartney, *Chem. Commun.*, **2008**, 4936.
18. I. W. Wyman and D. H. Macartney, *Org. Biomol. Chem.*, **2010**, *8*, 253.
19. M. A. Gamal-Eldin and D. H. Macartney, *Org. Biomol. Chem.*, submitted for publication.
20. L. Yuan, R. Wang and D. H. Macartney, *Tetrahedron: Asymmetry*, **2007**, *18*, 483.
21. (a) S. Mecozzi and J. Rebek, Jr. *Chem. Eur. J.*, **1998**, *4*, 1016. (b) W. M. Nau, M. Florea, and K. I. Assaf, *Isr. J. Chem.*, **2011**, *51*, 559.
22. G. Ercolani, *J. Am. Chem. Soc.*, **2003**, *125*, 16097.
23. (a) H. Qi, T. Nishihata and J. H. Rytting, *Pharm. Res.*, **1994**, *11*, 1207. (b) M. E. Cortés, R. D. Sinisterra, M. J. Avila-Campos, N. Tortamano, and R. G. Rocha, *J. Incl. Phenom. Macrocycl. Chem.*, **2001**, *40*, 297. (c) A. M. L. Denadai, K. I. Teixeira, M. M. Santoro, A. M. C. Pimenta, M. E. M. E. Cortés and R. D. Sinisterra, *Carbohydr. Res.*, **2007**, *342*, 2286.
24. C. F. Franco, A. L. Pataro, L. C. Ribeiro e Souza, V. R. Santos, M. E. Cortés and R. D. Sinisterra, *Artif. Organs*, **2003**, *27*, 486.
25. C. R. H. Raetz and C. Whitfield, *Annu. Rev. Biochem.*, **2002**, *71*, 635.
26. I. W. Wyman and D. H. Macartney, *Org. Biomol. Chem.*, **2009**, *7*, 4045.
27. R. Wang, Ph.D. Thesis, Queen's University, 2009.
28. J. Kwok, M.Sc. Thesis, Queen's University, 2011.
29. L. Yuan, R. Wang and D. H. Macartney, *J. Org. Chem.*, **2007**, *72*, 4539.
30. I. W. Wyman and D. H. Macartney, *J. Org. Chem.*, **2009**, *74*, 8031.

31. (a) D. Tuncel, O. Özsar, H. B. Tiftik and B. Salih, *Chem. Commun.*, **2007**, 1369. (b) D. Tuncel and M. Katterle, *Chem. Eur. J.*, **2008**, *14*, 4110. (c) D. Tuncel, O. Ünal and M. Artar, *Isr. J. Chem.*, **2011**, *51*, 525.
32. D. Sobransingh and A. E. Kaifer, *Org. Lett.*, **2006**, *8*, 3247.
33. (a) E. Masson, X. Lu, X. Ling and D. L. Patchell, *Org. Lett.*, **2009**, *11*, 3798. (b) X. Ling, E. L. Samuel, D. L. Patchell and E. Masson, *Org. Lett.*, **2010**, *12*, 2730.
34. W. S. Jeon, A. Y. Ziganshina, J. W. Lee, Y. H. Ko, J.-K. Kang, C. Lee and K. Kim, *Angew. Chem. Int. Ed.*, **2003**, *42*, 4097.
35. P. J. Pentikainen, *Int. J. Clin. Pharmacol. Ther. Toxicol.*, **1986**, *24*, 213.
36. D. H. Macartney, *Isr. J. Chem.*, **2011**, *51*, 600.
37. I. Ghosh and W. M. Nau, *Adv. Drug. Deliv. Rev.*, **2012**, *64*, 764.
38. I. W. Wyman, Ph.D. Thesis, Queen's University, 2010.

Chapter 5

HOST-GUEST COMPLEXATION BETWEEN CUCURBIT[7]URIL AND AMIDINIUM GUESTS

5.1 Introduction

Amidines, like guanidines, can become protonated over a broad pH range because of the high pK_a value of ~ 11 for their conjugate acids. The resulting amidinium cation (Figure 5.1) is stabilized by resonance and charge delocalization, but is less stable than its guanidinium and biguanidinium counterparts since there are fewer atoms involved in distributing the charge.¹

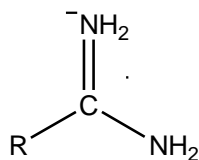


Figure 5.1 The structure of an amidinium cation.¹

In this chapter, my research will focus on the binding events that occurs between CB[7] and a series of amidinium guests. Of the guests considered for study, two bis(amidinium) drugs, pentamidine and berenil (Figure 5.2) were of particular interest. In addition, acid-catalyzed degradation of berenil in the presence of CB[7], and the complexations of the two degradation products,² 4-hydroxybenzamidine and 4-aminobenzamidine, with CB[7] were also examined. The results will be compared with a previous report of the complexation of the bis(amidinium) dication DAPI (4',6-diamidino-2-phenylindole, Figure 5.2), a blue-fluorescent dye for cell nuclei staining, by CB[7].³

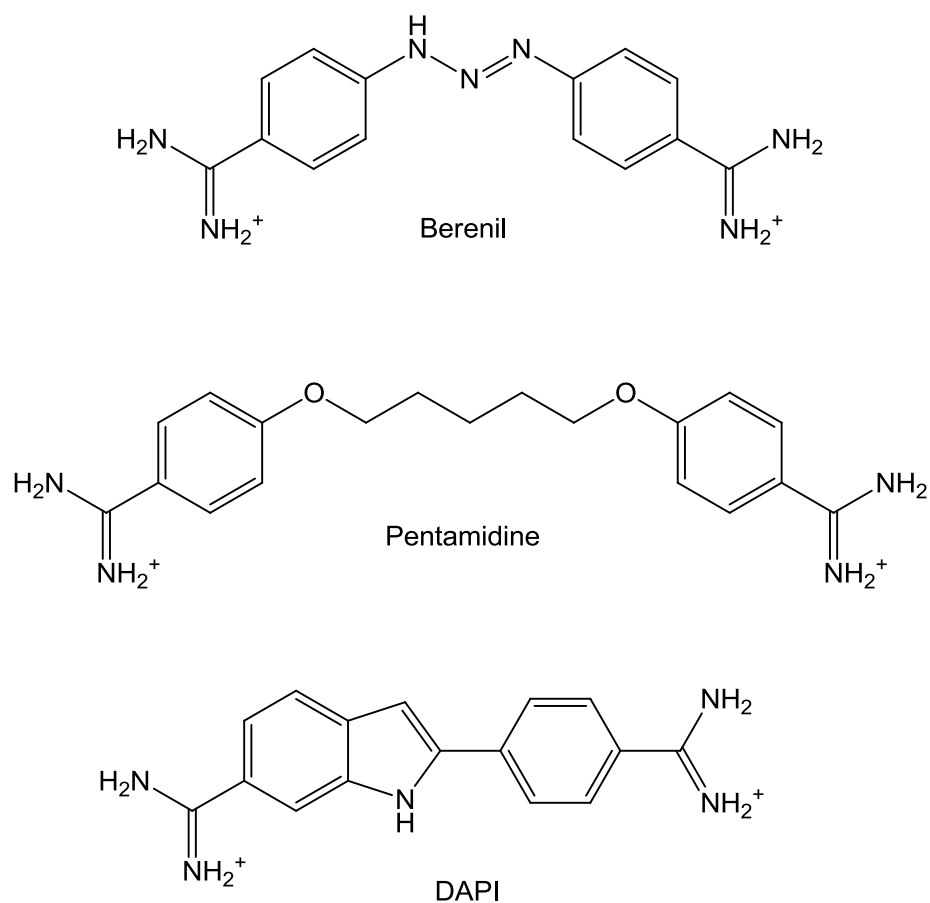


Figure 5.2 The chemical structures of berenil (top), pentamidine (middle), and DAPI (bottom).

The applications of these drugs are described briefly below. Pentamidine (4,4'-(pentamethylenedioxy)dibenzamide bis(2-hydroxyethanesulfonate)) was first synthesized in the 1930's and has been the established treatment for Human African Trypanosomiasis since 1967.¹ Human African Trypanosomiasis, or African sleeping sickness, as it is more commonly called, is characterized by headaches, fever, and joint pain. The most pronounced symptom, however, is extreme swelling of the lymph nodes, which can grow to several times their normal size. The disease eventually penetrates the blood brain barrier and can cause any number of neurological symptoms from disruption of the sleep cycle (hence the name of

the disease) to a comatose state, which is often followed quickly by death.^{1,4,5} African sleeping sickness is caused by two subspecies of bacteria: *Trypanosoma brucei gambiense* results in a chronic form of the disease, while *Trypanosoma brucei rhodesiense* results in an acute form.^{4,5} Pentamidine is the drug of choice in the early treatment of *T.b. gambiense*, which uptakes high concentrations of the drug via an amino-purine transporter. The build-up of pentamidine eventually results in cell death, but the exact mechanism of drug action has not yet been determined.⁵ One major difficulty that arises from use of pentamidine is that it has a very limited ability to penetrate the blood brain barrier and destroy any *T.b. gambiense* present in the cerebral spinal fluid. Thus, while pentamidine can slow the progress of the disease, once it reaches the neurological phase, it cannot cure the disease, and the patient eventually succumbs to neurological degradation, resulting in their death.^{1,4,5} It is hoped that a CB[7]-pentamidine host-guest complex may have greater success penetrating the blood barrier than pentamidine alone. If this were the case, it would improve the success of pentamidine as a treatment against the chronic form of sleeping sickness.

Berenil acetate (4,4'-diamidinodiazaminobenzene diacetate tetrahydrate), like pentamidine, was administered through intramuscular injections and was used as a front-line treatment against both the *gambiense* and *rhodesiense* strains of *Trypanosoma brucei*.^{1,2} As a drug, berenil was cheaper and had more acute effects against trypanosomiasis infections than pentamidine and other current treatment regimens.^{2,6} Berenil is still used today as the treatment of choice for livestock with trypanosomiasis infections, due to its shorter treatment period and lower cost.^{2,6} This treatment method fell out of use in humans, however, due to an intense burning sensation at the injection site during treatment.^{1,2} If this side effect could be overcome, then berenil could once again be used as the drug of choice against

Trypanosoma brucei.² If berenil were complexed with CB[7], then its slow release might temper the localized burning sensation.

It is also possible that berenil could be used to treat trypanomiasis infections if it could be administered orally. Presently, berenil cannot be administered orally because it is susceptible to cleavage at its central triazene group under acidic conditions,² such as those found in the stomach.

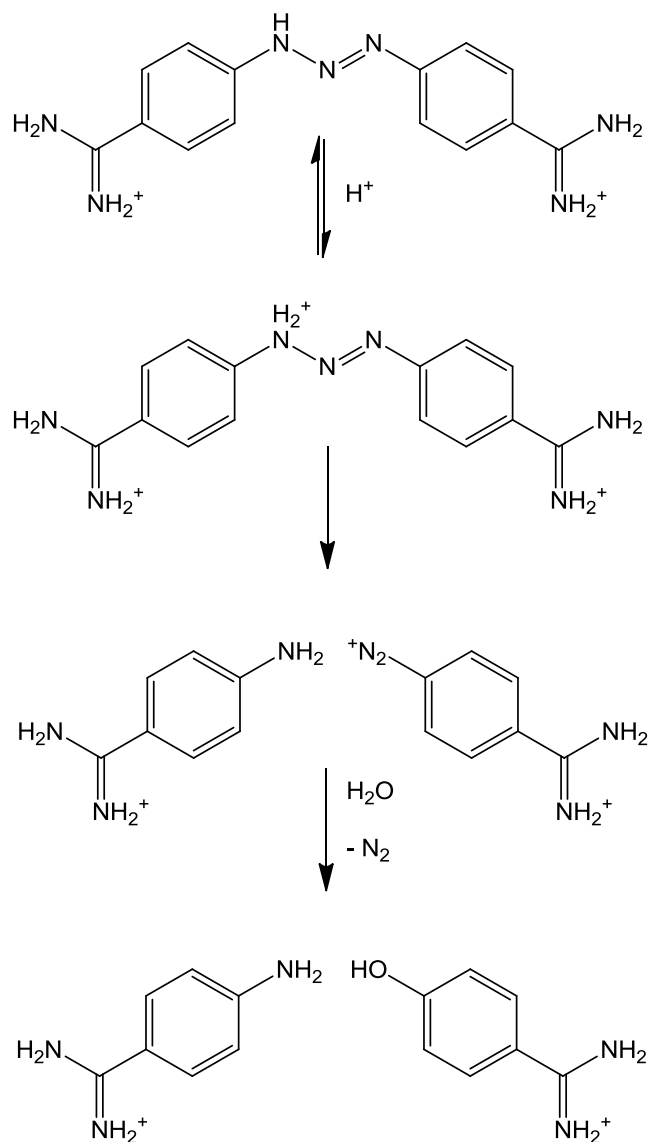


Figure 5.3 The acid-catalyzed cleavage of central triazene group of berenil.

This cleavage process is believed to result in two benzamidine degradation products.² The first product, 4-aminobenzamidine has been identified by NMR spectroscopy. The second product, 4-amidinophenyldiazonium has not been directly detected because it is believed to immediately decompose in aqueous solution to form 4-hydroxybenzamidine, which has been detected.

In addition to studying the CB[7]·berenil host-guest complex, the research described in this section will also employ UV-visible spectroscopy to examine the effects of CB[7] on the kinetics of the acid-catalyzed decomposition of berenil.

5.2 Results and Discussion

5.2.1 ESI Mass Spectrometry and ¹H NMR Spectroscopy

The complexes that formed between CB[7] and the amidinium guests were studied using a number of different analytical methods. Initially, a series of aqueous stock solutions were prepared, each one contained an amidinium guest and an excess of CB[7]. Next, high resolution ESI-MS was used to confirm the presence of the host-guest complex by mass/charge (m/z) ratio. The results of these analyses are presented in Table 5.1 below. The data in Table 5.1 demonstrated that each of the amidinium guests were able to form a complex with one or more CB[7] hosts. Once the presence of the host-guest complexes was confirmed by ESI-MS, ¹H NMR was then used to determine where the host was binding along the electronic structure of the guest and how the host was affecting the protons in the region where it bound. To examine how the guest protons were affected by binding with CB[7], it was necessary to identify the protons in the NMR spectrum (Figure 5.4 – 5.6).

Table 5.1 High resolution ESI-MS data for the host-guest complexes of CB[7] with pentamidine, berenil, 4-aminobenzamidine, and 4-hydroxybenzamidine.

Guest	Structure (Host:Guest)	Observed (m/z)	Calculated (m/z)
pentamidine	{CB[7]•pentamidine} ²⁺	752.2803	752.2821 for C ₆₁ H ₆₈ N ₃₂ O ₁₆ ²⁺
	{CB[7]•pentamidine•CB[7]} ²⁺	1333.4471	1333.4452 for C ₁₀₃ H ₁₁₀ N ₆₀ O ₃₀ ²⁺
berenil	{CB[7]•berenil} ²⁺	722.7469	722.7485 for C ₅₆ H ₅₉ N ₃₅ O ₁₄ ²⁺
4-NH ₂ benzamidine	{CB[7]•4-NH ₂ benzamidine•H} ²⁺	649.7201	649.7189 for C ₄₉ H ₅₂ N ₃₁ O ₁₄ ²⁺
4-OHbenzamidine	{CB[7]•4-OHbenzamidine•Na} ²⁺	661.2027	661.2018 for C ₄₉ H ₅₀ N ₃₀ O ₁₅ Na ²⁺

Once the ¹H NMR peaks of each amidinium guest had been identified, each guest was titrated with CB[7] and the upfield or downfield shifts ($\Delta\delta_{\text{lim}}$) of the guest proton resonances were monitored. As the titration progressed, peaks that moved upfield were identified as belonging to protons involved in associations with the hydrophobic cavity of CB[7]. Resonances that shifted downfield were identified as belonging to protons outside of the cavity and involved in associations with the polar portals of CB[7]. Once each titration was complete, several representative spectra at different host-guest concentrations were selected and combined to demonstrate the effects of host complexation on the guest protons. These stack plots were prepared for the titrations of CB[7] and each of the four amidinium guests. The stack plots are shown in Figures 5.4-5.6 below.

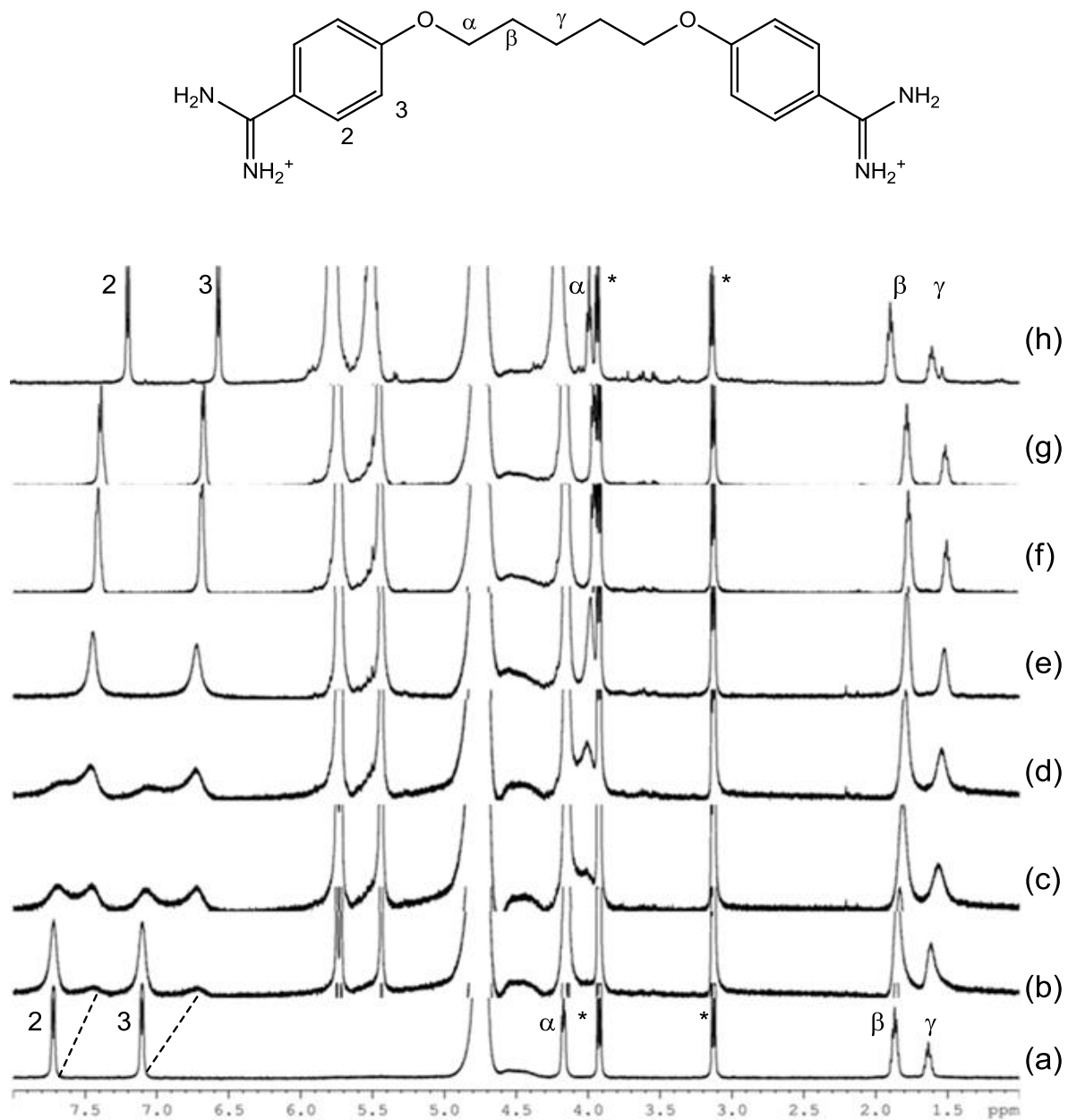


Figure 5.4 A stack plot of the ^1H NMR spectra of pentamidine in the presence of (a) 0.00, (b) 0.30, (c) 0.55, (d) 0.65, (e) 0.90, (f) 1.23, (g) 1.41, and (h) 2.10 equivalents of CB[7], titrated in D_2O . The dashed line indicates shifts in the peak positions of pentamidine. The numbered peaks are matched with their numerically labeled protons on the chemical structure of pentamidine, above. The proton resonances of the 2-hydroxyethanesulfonate counter anion are indicated by *.

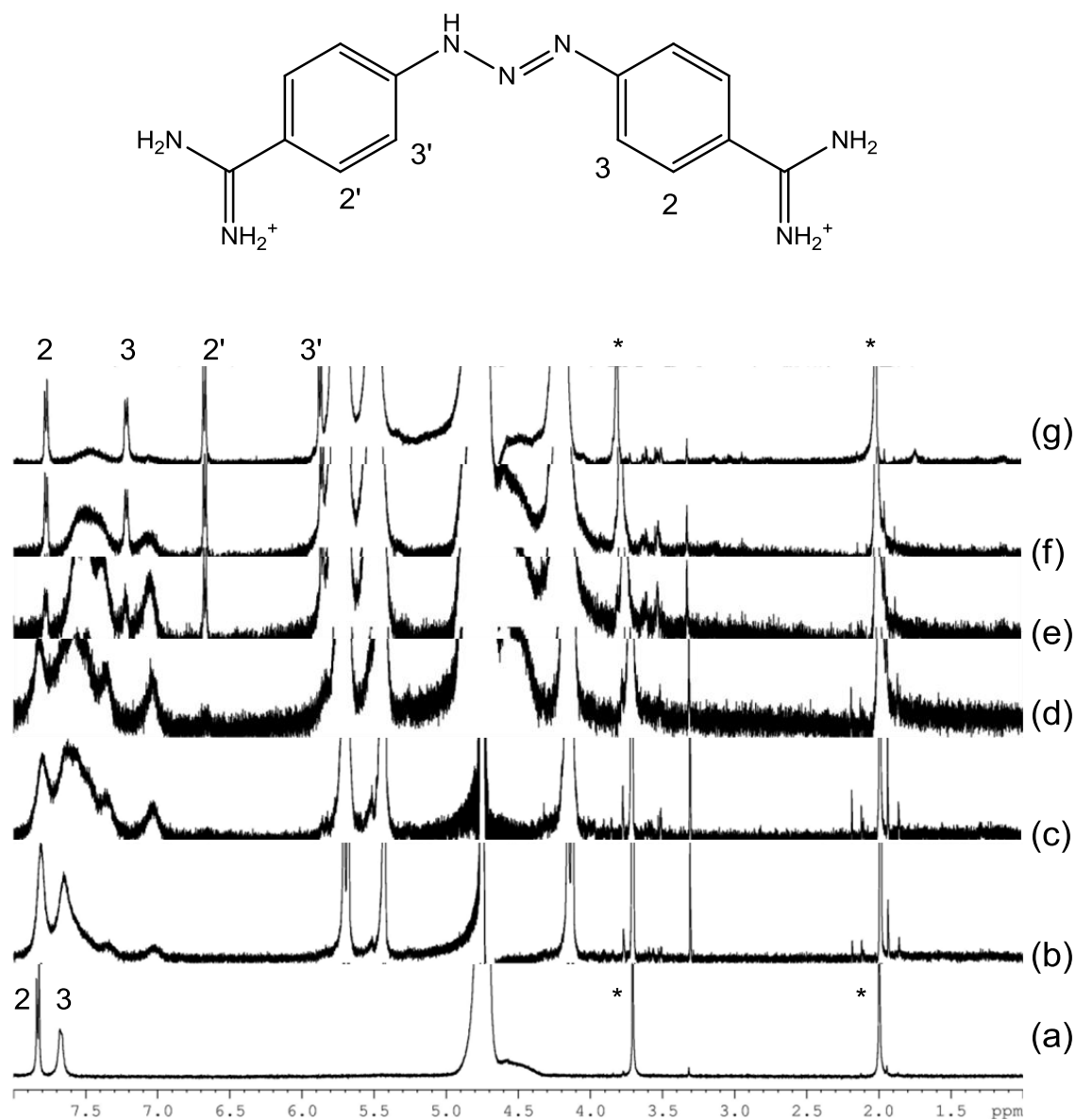


Figure 5.5 A stack plot of the ^1H NMR spectra of berenil in the presence of (a) 0.00, (b) 0.39, (c) 0.72, (d) 0.90, (e) 1.41, (f) 2.32, and (g) 3.88 equivalents of CB[7], titrated in D_2O . The dashed line indicates shifts in the peak positions of berenil. The numbered peaks are matched with their numerically labeled protons on the chemical structure of berenil, above. The proton resonances of the acetate counter anion are indicated by *.

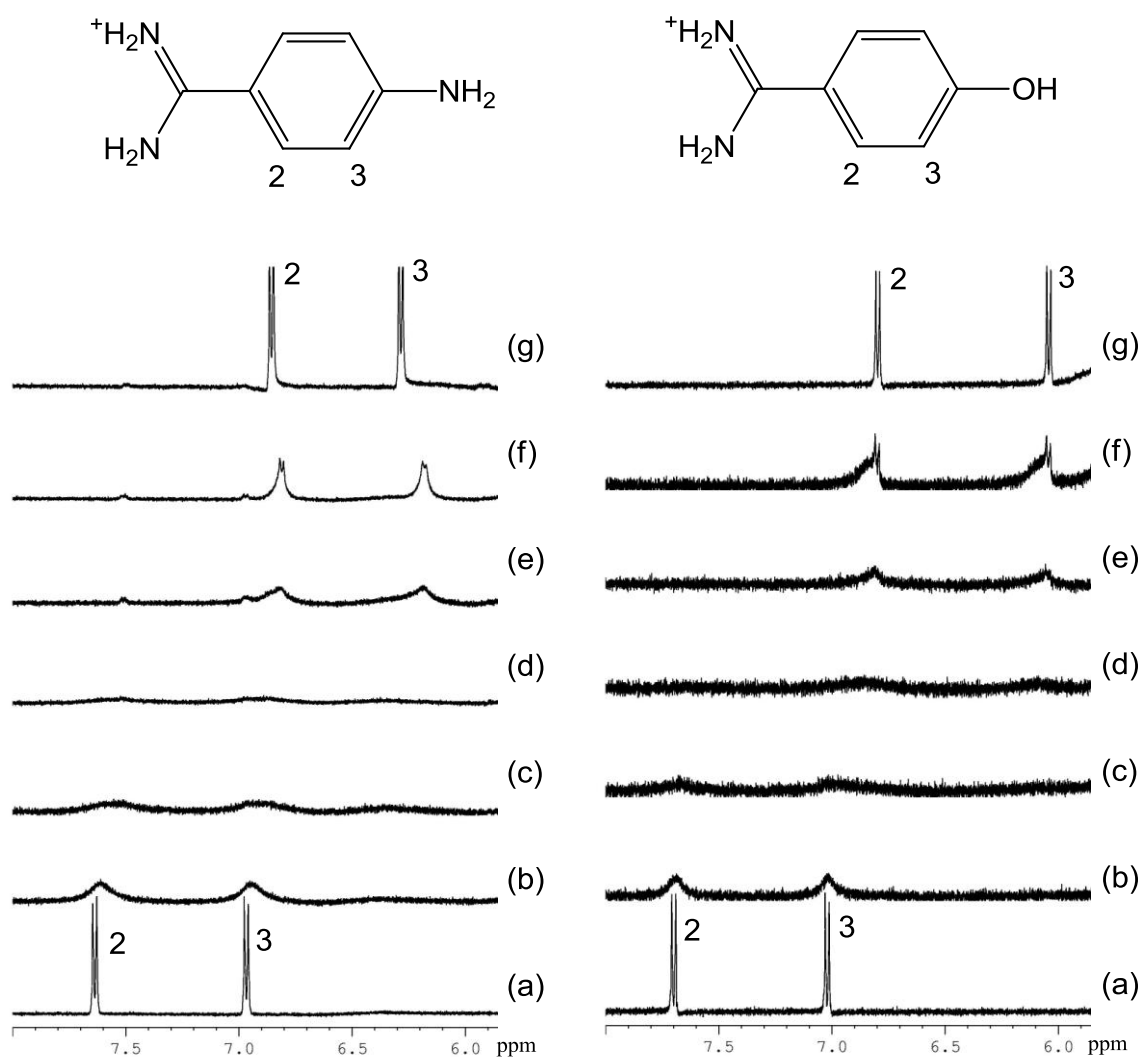


Figure 5.6 Stack plots of the ^1H NMR spectra of 4-aminobenzamidine (left) in the presence of (a) 0.00, (b) 0.11, (c) 0.22, (d) 0.27, (e) 0.81, (f) 1.08, and (g) 1.40 equivalents of CB[7], and 4-hydroxybenzamidine (right) in the presence of (a) 0.00, (b) 0.14, (c) 0.28, (d) 0.52, (e) 0.69, (f) 0.87, and (g) 1.04 equivalents of CB[7], in D_2O . The numbered resonances are matched with their numerically labeled protons on the chemical structures, above.

By examining which proton peaks shifted and at what concentration of CB[7] they shifted, it is possible to determine where and how the host became bound to the guest. A summary of these shifts is shown in Figure 5.7. Through the use of the data shown in Figure

5.7, it is possible to determine where upon the guests the CB[7] became bound and with what stoichiometries. When the amidinium guests were originally chosen for binding studies with CB[7], it was thought that they would likely form 1:1 host-guest complexes, and, in the cases of pentamidine and berenil, may have been capable of forming 2:1 host-guest complexes at higher concentrations of CB[7].

For pentamidine, both the ESI-MS (Table 5.1) and ^1H NMR spectra data indicate the presence of 1:1 and 2:1 host-guest complexes. The ^1H NMR spectra (Figure 5.4) indicate upfield shifts of 0.29 and 0.40 ppm for the aromatic H2 and H3 protons (slow exchange behaviour), respectively, when one CB[7] is complexing one of the two aromatic rings at a given time. The NMR spectra also indicate that there is a small degree of shielding of the H α , H β and H γ protons on the central pentamethylene group of pentamidine with binding of the CB[7] host. These shifts indicate that in the 1:1 CB[7]-pentamidine complex, the CB[7] host binds to either terminus of pentamidine, but occasionally exchanges across the pentamethylene group and binds to the opposite terminus. Once the 2:1 CB[7]-pentamidine complex forms (Figure 5.4h), with further upfield shifts in the aromatic H2 and H3 resonances and downfield shifts in the H β and H γ resonances of the pentamethylene chain, this exchange process ends due to the mutually repulsive negative ends of the dipoles on the carbonyl groups of the polar portals on CB[7]. The proton resonances of the 2-hydroxyethanesulfonate counter anions do not shift during the CB[7] titration, indicating, as expected, that they do not bind to the CB[7]. The energy-minimized gas-phase structures of the 1:1 and 2:1 CB[7]-pentamidine host-guest complexes are shown in Figure 5.8 below.

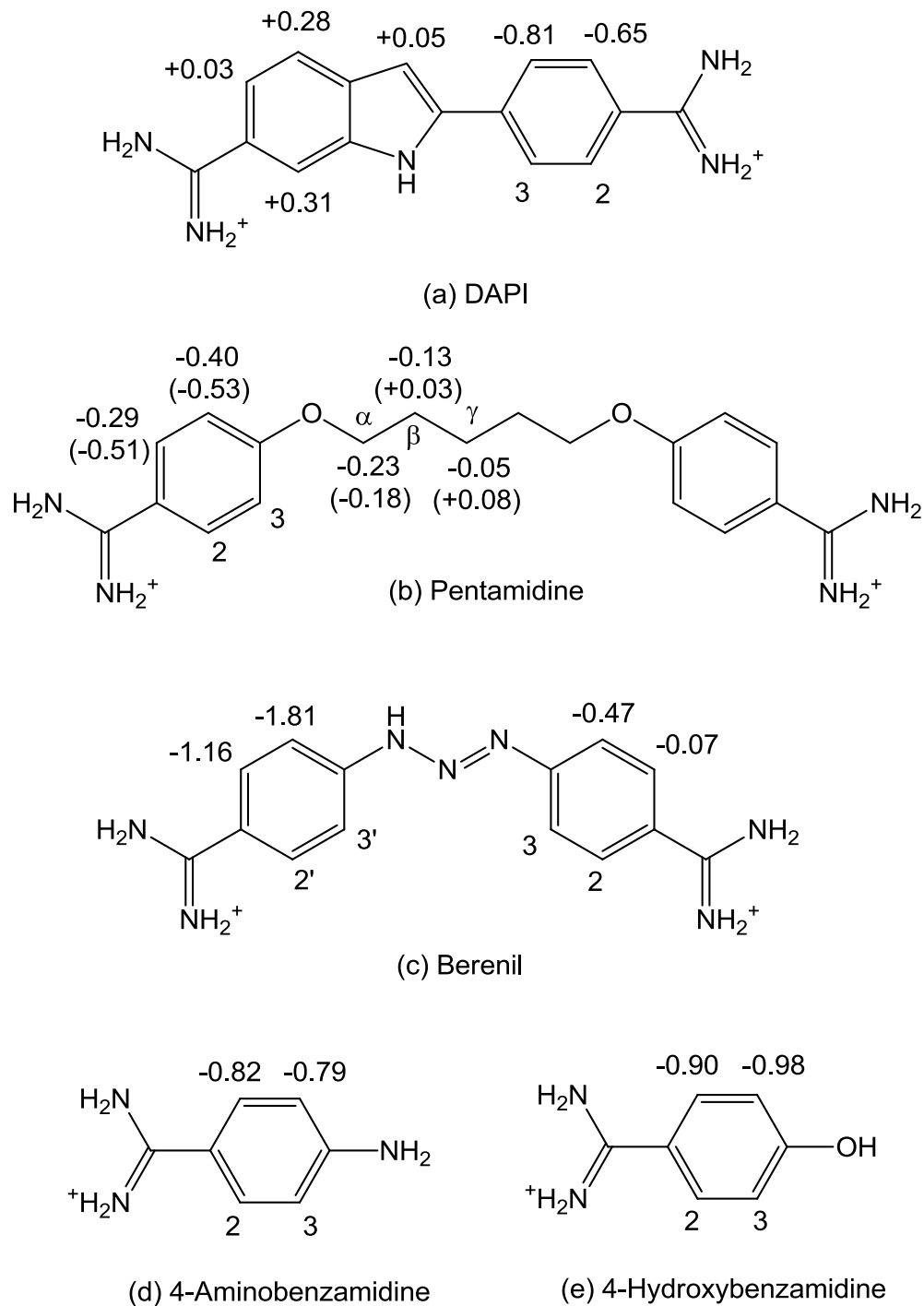


Figure 5.7 The ^1H NMR $\Delta\delta_{\text{lim}}$ values are shown for the titration of a) DAPI (data from Ref. 2), b) pentamidine, c) berenil, d) 4-aminobenzamidine, and e) 4-hydroxybenzamidine with CB[7]. For pentamidine, the top numbers represent the shifts associated with the first host binding event and the bottom numbers in brackets represent shifts associated with the second binding event. Negative $\Delta\delta_{\text{lim}}$ values indicate upfield shifts and positive $\Delta\delta_{\text{lim}}$ values indicate downfield shifts.

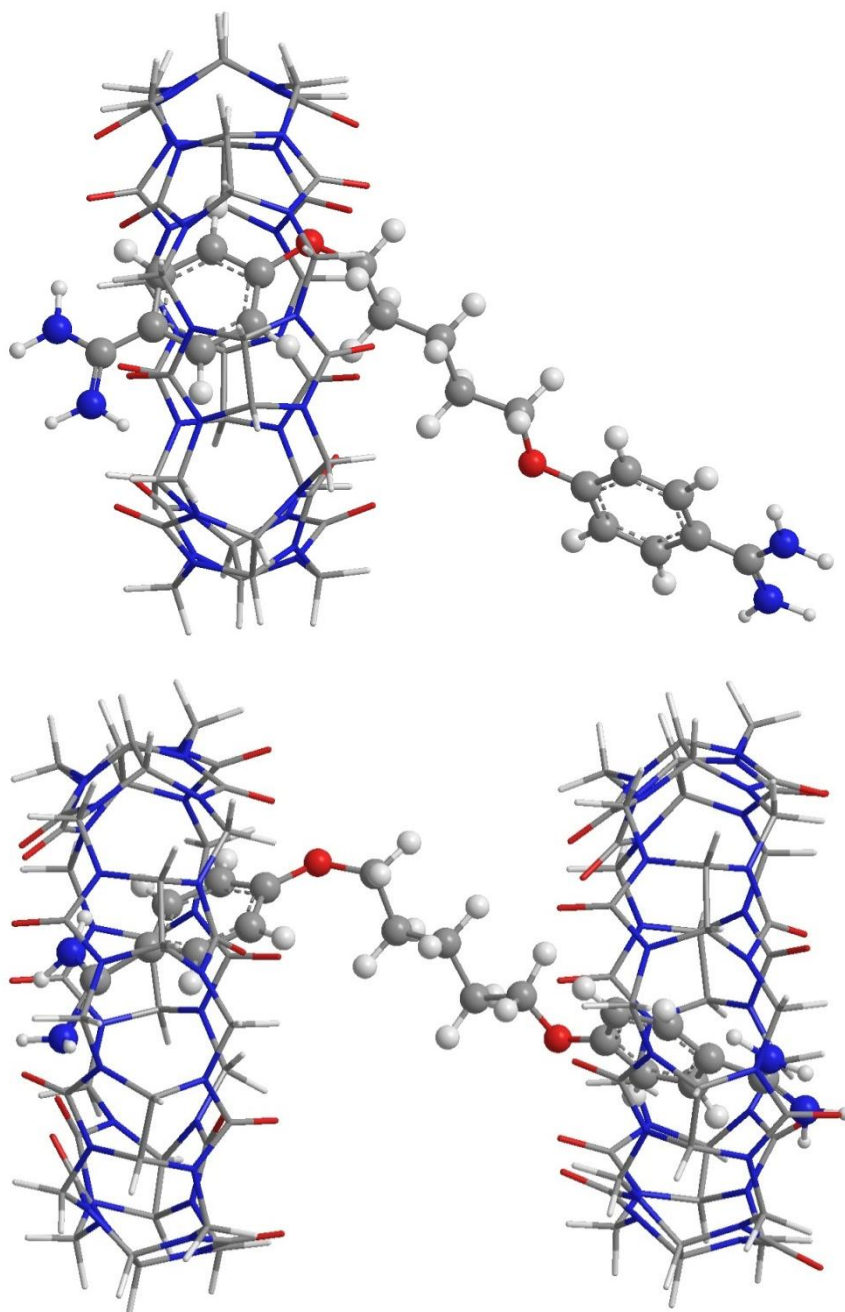


Figure 5.8 The energy-minimized gas-phase structures of the 1:1 (top) and 2:1 (bottom) host-guest complexes formed between CB[7] and pentamidine.

After examining pentamidine, it was thought that berenil, being similar in structure, could also form both 1:1 and 2:1 host-guest complexes with CB[7]. When the ESI-MS and ^1H NMR data were examined, however, they indicated only the existence of a 1:1 complex.

The absence of the 2:1 complex is likely due to the smaller triazene linker compared to the pentamethylene group found in pentamidine. Once the 1:1 complex is formed, a second CB[7] would likely be prevented from binding due to the close proximity of the repulsive dipoles of the carbonyl groups on polar portal of the first CB[7].

Berenil also differed from pentamidine due to the asymmetrical structure of its triazene group, which contains a secondary amine ($-\text{NH}-$) and two tertiary amines that are double bonded to one another. In the free guest (Figure 5.5a), only two aromatic resonances are observed, due to rapid exchange between two resonances structures, making the H2/H2' and H3/H3' positions equivalent on the NMR timescale. Upon addition of CB[7], the resonances shift upfield, indicating encapsulation of the aromatic rings of the guest. The proton resonances of the acetate counter anions do not shift during the CB[7] titration, indicating, as expected, that the anion does not bind to the CB[7]. According to the ^1H NMR data (Figure 5.5), and supported by the energy-minimized structure in the gas phase (Figure 5.9), the presence of an asymmetrical triazene group results in CB[7] preferentially binding to one terminus over the other.

The triazene secondary amine ($-\text{NH}-$), is capable of forming hydrogen bonds with the carbonyl portals of CB[7], which would result in CB[7] binding preferentially to one aromatic terminus over the other. The ^1H NMR spectrum at high [CB[7]] exhibits four aromatic proton resonances, indicating that the complexation of one aromatic ring preferentially has “frozen” the guest in one resonance structure on the NMR timescale. The $\Delta\delta_{\text{lim}}$ values in Figure 5.7 for berenil represent the difference between the free guest in the “symmetrical structure” and the complex guest in the “asymmetrical structure.” With the

asymmetric DAPI guest (Figure 5.7), a similar phenomenon was observed, with the CB[7] preferring the phenylamidinium end, rather than the indoleamidinium end of the guest.

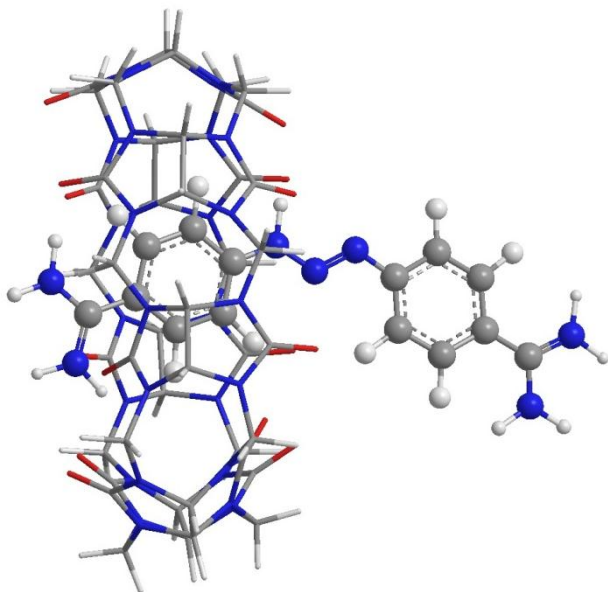


Figure 5.9 The energy-minimized gas-phase structure of the 1:1 host-guest complex formed between CB[7] and berenil.

The binding behaviour of berenil with CB[7] is different than with DNA,⁷ in which the berenil is believed to bind in the minor groove near an adenine-thymine base pair through hydrogen-bonding interactions.^{7a} The complexation results in downfield shifts of 0.19 and 0.11 ppm for the H2 and H3 proton resonances, with no localization of the resonance structures.^{7b}

The 4-aminobenzamidine and 4-hydroxybenzamidine guests, unlike bis(amidinium) pentamidine and berenil guests, would be only expected to form 1:1 complexes with CB[7]. Examination of the ESI-MS (Table 5.1) and ¹H NMR data (Figure 5.6) for these two mono(amidinium) guests indicated that this was in fact the case and that both guests underwent a simple 1:1 host-guest complexation process. Neither the ESI-MS nor NMR data

suggested the presence of any complex between CB[7] and these two guests, beyond their 1:1 host-guest complexes.

The H2 and H3 proton resonances of the two guests experience significant upfield chemical shifts (similar to the complexed phenylamidinium end of the DAPI guest (Figure 5.7)) as the complexation by CB[7] places both sets of protons within the host cavity and the amidinium and amino/hydroxo groups at the portals to participate in ion-dipole, dipole-dipole and hydrogen bonding interactions with the carbonyl groups. These non-covalent interactions, in addition to the hydrophobic effect, result in kinetically stable complexes, as indicated by the intermediate exchange behaviour in the ^1H NMR spectra (Figure 5.6). The structures of the CB[7]·4-aminobenzamidine complex and the CB[7]·4-hydroxybenzamidine complex are depicted in Figure 5.10, below.

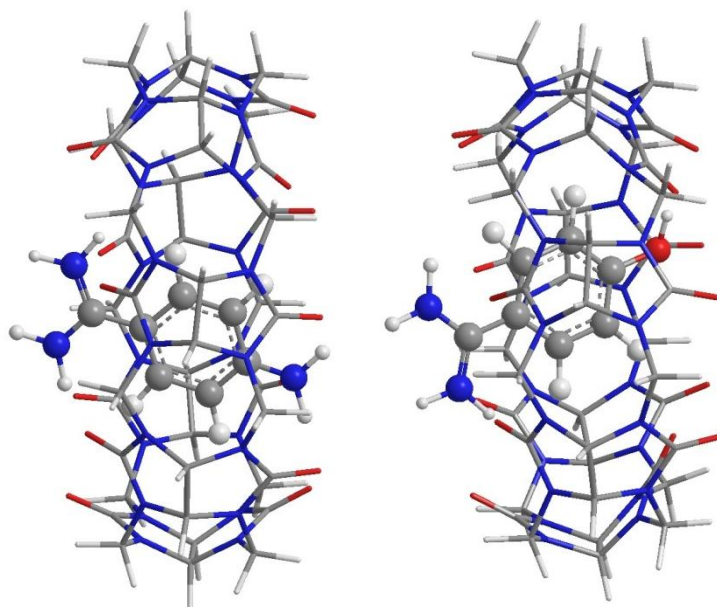


Figure 5.10 The energy minimized structures of the CB[7] host-guest complexes with 4-aminobenzamidine (left) and 4-hydroxybenzamidine (right).

Once the presence of host-guest complexes between CB[7] and the amidinium and bis(aminidinium) guests had been confirmed by ESI-MS and ^1H NMR spectral data, an examination of how strongly the CB[7] host bound to the guests was undertaken. In order to determine the affinity of CB[7] for an amidinium guest, their host-guest binding constants needed to be measured.

5.2.2 Determination of Binding Constants

The binding events that occurred between the amidinium guests and CB[7] were driven by the interaction between the polar portals on CB[7] and the delocalized positive charge on the amidinium group. This ion-dipole interaction was the main driving force for CB[7] binding, however the hydrophobic effect also imparted some entropic and enthalpic stability. CB[7] bound too tightly to each of the amidinium guests for a binding curve to produce an accurate measurement of its binding constant ($K > 10^4 \text{ M}^{-1}$), which resulted in the use of a competition study. This competition study was conducted with a known competitor, as demonstrated by Isaacs and coworkers, and described in Chapter 2.⁸ For the amidinium compounds, the *p*-toluidinium cation (Figure 5.12) was chosen as a competitor because, it contains similar structural elements, such as a cationic substituent bonded to a *para*-substituted aromatic ring. Studies conducted by Isaacs *et al.* have found that the *p*-toluidinium cation has a binding constant of $K = (8.4 \pm 1.3) \times 10^6 \text{ M}^{-1}$ with CB[7].⁸

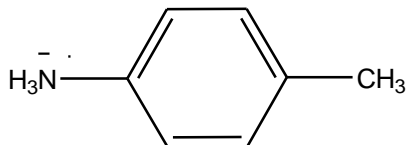


Figure 5.11 The chemical structure of the *p*-toluidinium cation.

Using berenil, 4-aminobenzamidine, and 4-hydroxybenzamidine as guests, and *p*-toluidinium as a competitor for the CB[7] host, provided the 1:1 host-guest binding constants shown in Table 5.2. In the case of pentamidine, a competition study with the *p*-toluidinium cation provided a 1:1 host binding constant of $(2.4 \pm 0.4) \times 10^6 \text{ M}^{-1}$ with CB[7]. However, since pentamidine possesses symmetrical binding sites on either terminus of its molecular structure it can also form a 2:1 host-guest complex at higher concentrations of CB[7].

As described for the bis(biguanidinium) guests, chlorhexidine and alexidine, in Chapter 4, a statistical binding relationship between the first and second binding events with CB[7] can be assumed, allowing for the estimation of an upper limit for the binding of the second CB[7] to pentamidine: $K_{\text{CB}[7]}^1 = 4 K_{\text{CB}[7]}^2$. This binding constant, $< 1.2 \times 10^4 \text{ M}^{-1}$, is also included in Table 5.2 below. The upper limit value assumes that it is four-fold lower than the first binding on the basis of the number of binding sites available in the forward and reverse processes. This is a reasonable assumption as the distance between the two binding sites would likely minimize any electrostatic dipole-dipole repulsions between the portals of the two host molecules in the 2:1 complex (Figure 5.8).

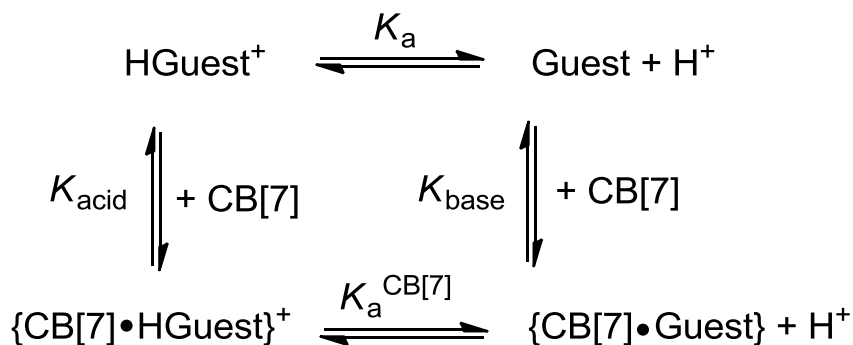
Table 5.2 The host-guest stability constants for CB[7] complexes with pentamidine, berenil, DAPI (data from Ref. 3), 4-aminobenzamidine, and 4-hydroxybenzamidine in D₂O (containing 50 mM sodium acetate buffer (pD = 4.7)), using *p*-toluidinium ($K = (8.4 \pm 1.3) \times 10^6 \text{ M}^{-1}$ from Ref. 8) as the competitor guest.

Guest	Host:Guest Stoichiometry	Host-Guest Binding Constant (M ⁻¹)
pentamidine	1:1	$(4.7 \pm 0.7) \times 10^6$
	2:1	$< 1.2 \times 10^6$
berenil	1:1	$(7.4 \pm 1.1) \times 10^6$
DAPI	1:1	1.1×10^7 (Ref. 3)
4-aminobenzamidine	1:1	$(8.9 \pm 1.4) \times 10^6$
4-hydroxybenzamidine	1:1	$(2.2 \pm 0.4) \times 10^6$

From the information summarized in Table 5.2, it is clear that each amidinium guest is bound by a CB[7] host, forming a tightly bound host-guest complex. In the case of CB[7] and pentamidine both a 1:1 and a 2:1 host-guest complex formed, while berenil, 4-aminobenzamidine, and 4-hydroxybenzamidine each formed 1:1 host-guest complexes with CB[7]. Each binding event between CB[7] and the amidinium guests proved to have a high binding constant of approximately 10^6 - 10^7 M^{-1} . The 4-aminobenzamidine cation can be viewed as a model for half of the berenil dication guest whereas 4-hydroxybenzamidine resembles each half of the pentamidine dication. The 1:1 host-guest binding constants of the dications match very well the binding constants of the respective monocations.

The amidinium groups in the 4-hydroxy- and 4-aminobenzamidine cations have pK_a values of 12.69 and 12.01, respectively.⁹ At lower pH values, hydroxyl and ammonium groups undergo deprotonation and the effects of complexations of the 4-hydroxy- and 4-

aminobenzamidines by CB[7] on their pK_a values have determined by spectrophotometric pH titrations in the absence and presence of the host molecule by A. Love and J. Rygus in our laboratory.¹⁰ In the absence of CB[7], the pK_a values were determined to be 7.5 and 9.4, respectively, for the 4-hydroxy- and 4-aminobenzamidines, which are close to the reported values of 7.8 and 9.2, respectively.¹¹ In the presence of an excess of CB[7], the $pK_a^{CB[7]}$ values increased to 9.2 and 11.8, respectively. The binding constants for the 4-hydroxy- and 4-aminobenzamidinium cations above the pK_a values were determined to be 5×10^4 and 4×10^4 M^{-1} , respectively. There have now been numerous examples of such pK_a shifts,¹² which arise because of the preferred binding of the protonated (and normally cationic) guest compared with the binding of the deprotonated (and normally neutral) guest (eq 5.3).



$$pK_a^{CB[7]} - pK_a = \log(K_{\text{acid}}/K_{\text{base}}) \quad (5.3)$$

The ΔpK_a shifts of 1.7 and 2.4 pK units for the 4-hydroxy- and 4-aminobenzamidines are consistent with the decreases of 44-fold ($\log(K_{\text{acid}}/K_{\text{base}}) = 1.64$) and 220-fold ($\log(K_{\text{acid}}/K_{\text{base}}) = 2.34$), respectively.

5.2.3 Kinetics of Berenil Decomposition

When berenil is introduced into an acidic solution, it undergoes a decomposition reaction to form 4-aminobenzamidine and 4-amidinophenyldiazonium, which immediately breaks down in aqueous solution to form 4-hydroxybenzamidine, as described in Figure 5.3.² This change in structure results in a change in the UV-visible spectrum and produces a colour change in aqueous solution from yellow to colourless. Previous studies have demonstrated that the complexation of an acidic guest by CB[7] can change (normally increase) the pK_a of that guest.¹² This sort of pK_a shift may lead to an increased tolerance for berenil in acid, or it could further catalyze the degradation of the drug. In order to determine the effects of CB[7] on this decomposition reaction, berenil was introduced into an aqueous solution at a pH of 2 in the absence and presence of CB[7]. The decomposition reaction that resulted was monitored by UV-vis spectroscopy until the solution reached a colourless state. The results of this study are presented in Figure 5.12 and 5.13 below. The data displayed in Figure 5.13 indicates that CB[7] is effecting the decomposition of berenil by increasing the rate of reaction. In order to determine the extent of the increase, the rate of reaction in the absence and presence of CB[7] needed to be determined by using the equation,

$$\ln A = -kt + \ln A_0 \quad (5.1)$$

where t is the amount of time since the reaction began, A is the absorbance at time t , A_0 is the absorbance when the reaction began ($t = 0$) and k is the first-order rate constant of the reaction. When this equation is rearranged as shown, it is possible to plot a graph of

$$\ln(A/A_0) = -kt \quad (5.2)$$

$\ln(A/A_0)$ vs t and obtain lines of slope $-k$ as shown in Figure 5.14 below.

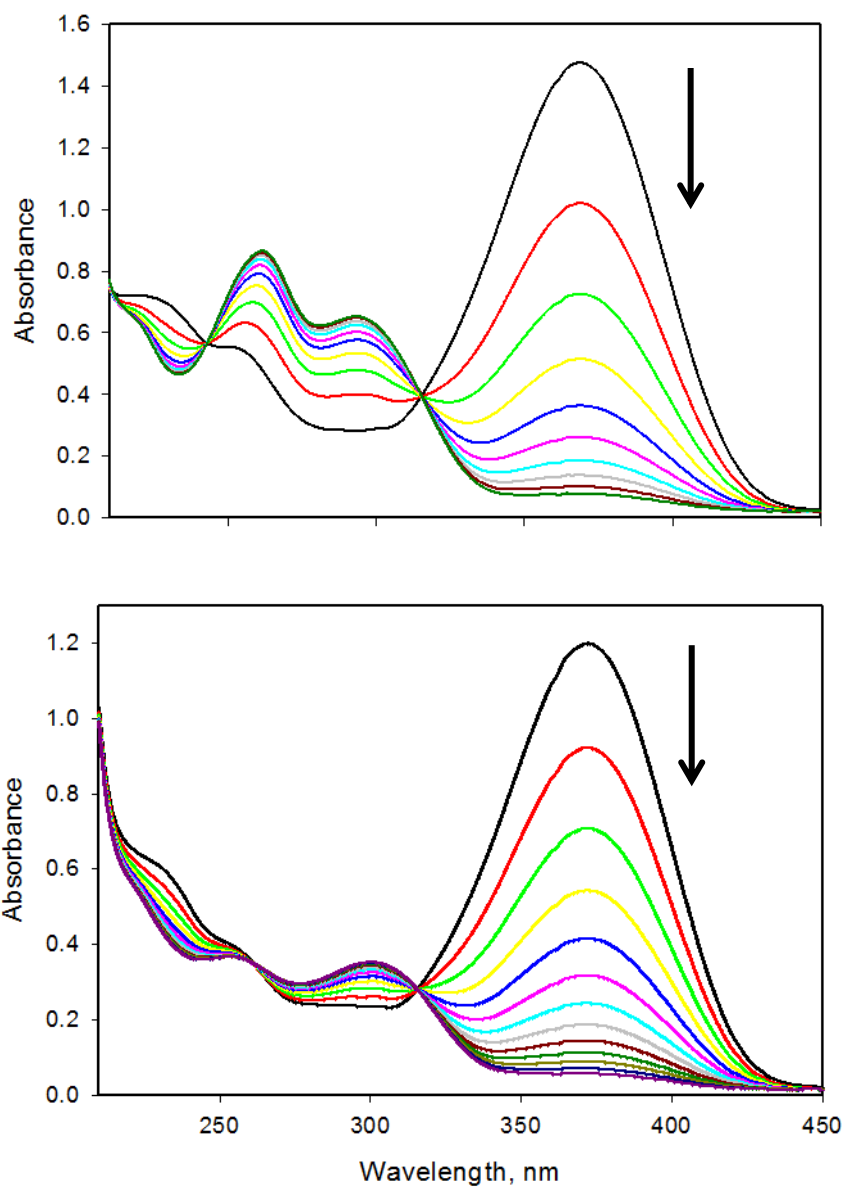


Figure 5.12 The absorbance spectra of berenil over time in an aqueous solution at pH 2.5 in the absence (top, 900 seconds between spectra, starting with black curve) and presence of CB[7] (bottom, 50 seconds between spectra, starting with black curve).

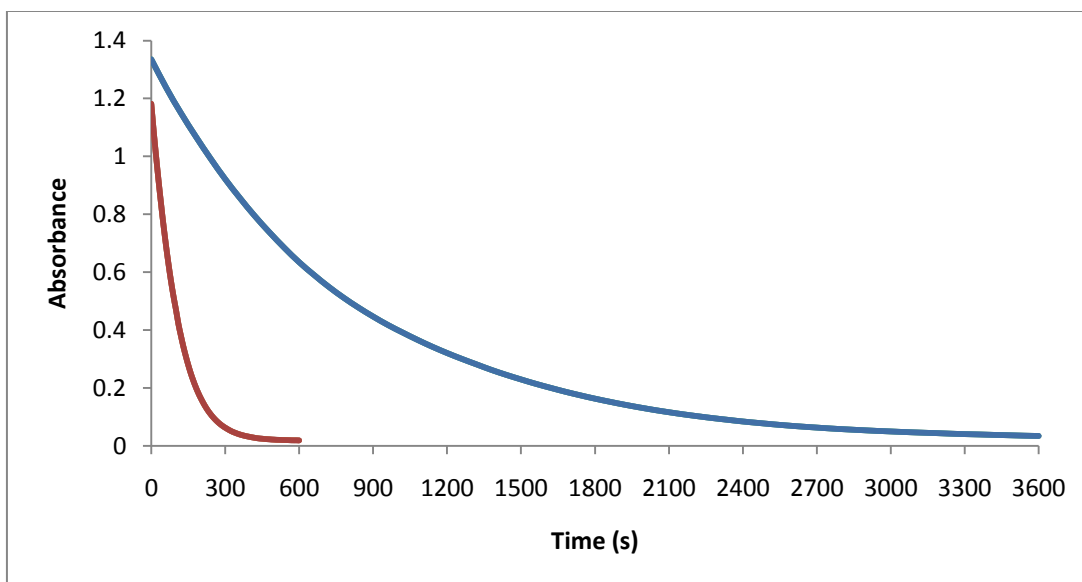


Figure 5.13 The time-dependent absorbance of berenil at 370 nm in an aqueous solution at pH 2.00 in the absence (top blue curve) and presence (bottom red curve) of CB[7].

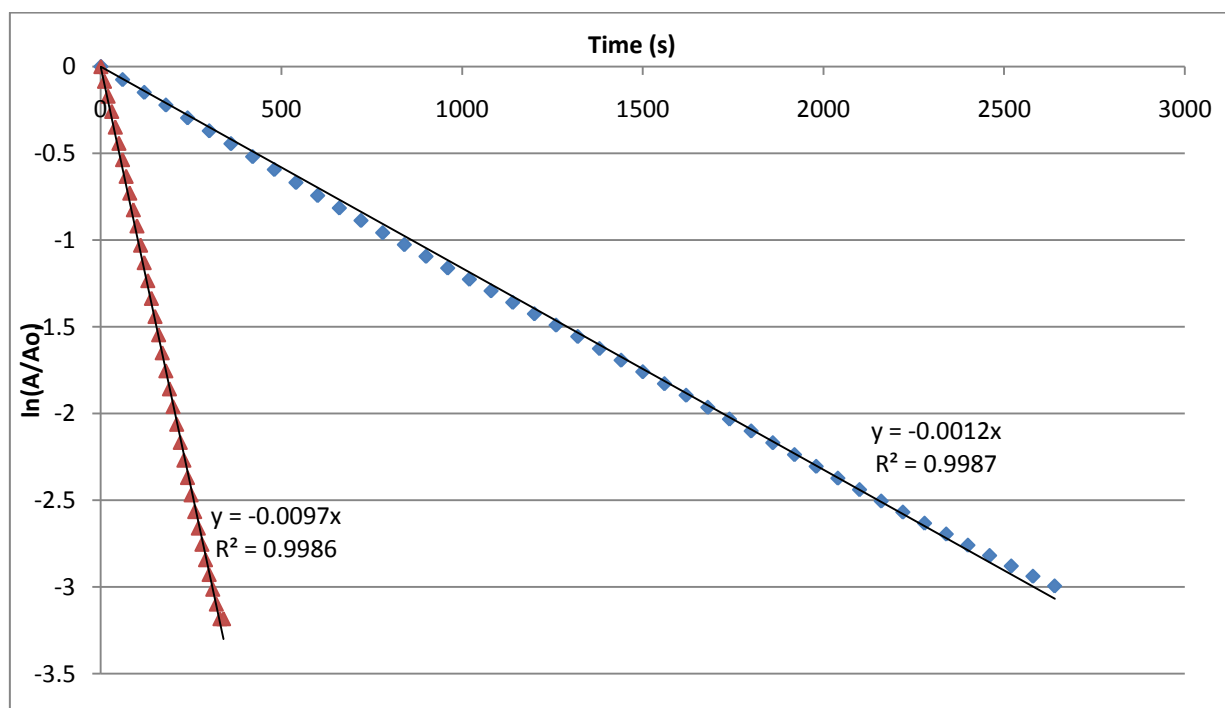


Figure 5.14 A first-order plot of the degradation of berenil in the absence (top blue line) and presence (bottom red line) of CB[7] at pH 2.00. A linear regression of these plots indicates that berenil decomposes at a rate of 0.0012 s^{-1} in the absence of CB[7] and 0.0097 s^{-1} in the presence of CB[7] at this pH.

The results depicted in Figure 5.14 indicate that CB[7] produces an 8-fold increase in the first-order rate constant for berenil decomposition in aqueous solution at pH 2.00. Although CB[7] did not act to stabilize the molecular structure of berenil as we had hoped it would, its catalytic effect on the degradation of berenil was still intriguing, and therefore we examined this effect at a variety of acidic pH values. The values of $\log k$ are plotted against pH in Figure 5.15 below.

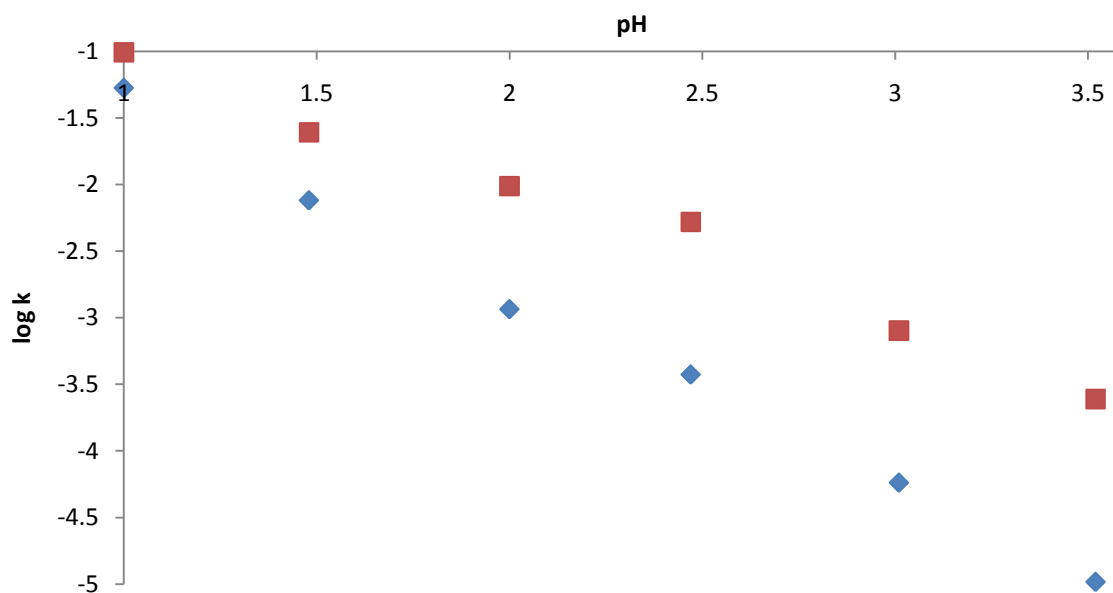


Figure 5.15 A plot of the log of the rate constants for the berenil degradation against pH in the absence (blue diamonds) and presence (red squares) of CB[7].

The data presented in Figure 5.15 indicates that the complexation of berenil by CB[7] increases the rate of the berenil degradation reaction over this range of acidic pH values. The relative rate acceleration in the presence of CB[7] is believed to result from an increase in the pK_a of the N3 protonated berenil, leading to a stabilization of the diazonium intermediate. Barra and co-workers have recently demonstrated that cyclodextrins, which are known to decrease the pK_a values of included guest molecules, inhibited the rate constants for the acid-

catalyzed decompositions of 1,3-diphenyltriazenes.¹³ The opposing behaviours of the host molecules toward their effects on acid-catalyzed diphenyltriene decomposition is consistent with normal effects of cucurbiturils and cyclodextrins on the pK_a values of basic guests, with increases and decreases, respectively, being reported for a variety of acidic guests.¹²

5.3 Conclusions

The formation of host-guest complexes between CB[7] and several guests with amidinium groups has been monitored and analyzed through the use of ESI mass spectrometry, ¹H NMR spectroscopy and UV-visible spectroscopy. The results of these analyses indicated that CB[7] is able to bind to pentamidine, berenil, 4-aminobenzamidine and 4-hydroxybenzamidine through ion-dipole interactions with their amidinium groups, forming 1:1 host-guest complexes with binding constants in the range of 10^6 - 10^7 M⁻¹, comparable to the value reported previously for the bis(amidinium) dication, DAPI.³ In addition to its 1:1 complex, pentamidine also demonstrated an ability to bind to a second CB[7], forming a 2:1 host-guest complex that also possessed a high binding constant. The formation of a CB[7]·berenil host-guest complex was observed to accelerate the rate of acid-catalyzed berenil degradation, by increasing the pK_a of the central triazene group.

References

1. M. Sands, M. A. Kron, and R. B. Brown, *Rev. Infect. Dis.*, **1985**, 7, 625.
2. M. Campbell, R. J. Pranker, A. S. Davie, and W. N. Charman, *J. Pharm. Pharmacol.*, **2004**, 56, 1327.
3. Z. Miskolczy, L. Biczok, M. Megyesi, and I. Jablonkai, *J. Phys. Chem. B*, **2009**, 113, 1645.
4. J. Pépin and H. Méda, *Antimicrob. Drug Resist.*, **2009**, 76, 1113.
5. H. Denise and M. P. Barrett, *Biochem. Pharmacol.*, **2001**, 61, 1.
6. H. P. de Koning, L. F. Anderson, M. Stewart, R. J. S. Burchmore, L. J. M. Wallace, and M.P. Barrett, *Antimicrob. Agents Ch.*, **2004**, 48, 1515.
7. (a) D. G. Brown, M. R. Sanderson, E. Garman and S. Niedle, *J. Mol. Biol.* **1992**, 226, 481. (b) S. Hu, K. Weisz, T. L. James and R. H. Shafer, *Eur. J. Biochem.*, **1992**, 204, 31.
8. S. Liu, C. Ruspic, P. Mukhopadhyay, S. Chakrabarti, P. Y. Zavalij, and L. Isaacs, *J. Am. Chem. Soc.*, **2005**, 127, 15959.
9. M. Mares-Guia, D. L. Nelson and E. Rogana, *J. Am. Chem. Soc.*, **1977**, 99, 2331.
10. (a) A. Love, B.Sc.(Hons.) Thesis, Queen's University, 2012. (b) J. Rygus, unpublished results.
11. S. Rumthao, O. Lee, Q. Sheng, W. T. Fu, D. C. Mulhearn, D. Crich, A. D. Mesecar and M. E. Johnson, *Bioorg. Med. Chem. Lett.*, **2004**, 14, 5165.
12. (a) D. H. Macartney, *Isr. J. Chem.*, **2011**, 51, 600. (b) I. Ghosh, W. M. Nau, *Adv. Drug. Deliv. Rev.*, **2012**, 64, 764.
13. T. Xu, A. V-Z. Asadi, and M. Barra, *Int. J. Chem. Kinet.*, **2010**, 42, 567.

Chapter 6

HOST-GUEST COMPLEXATION BETWEEN CUCURBIT[7]URIL AND FLAVYLIUM GUESTS

6.1 Introduction

Flavylium dyes (Figure 6.1) are water-soluble synthetic analogues of the naturally occurring anthocyanins, which are natural antioxidants responsible for the red, blue, and purple colours found in the petals, leaves and fruits of a variety of plants.^{1,2,3} There are a wide variety of flavylium derivatives found in Nature, including ones with functional groups such as -OH, -OMe and -NH₂ at positions 3, 5, 6, 7, 3', 4', and 5'.¹⁻⁴

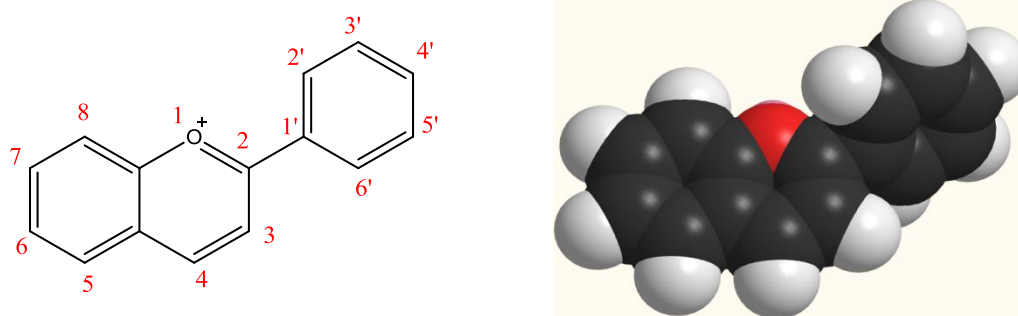


Figure 6.1 The chemical and space-filling structures of a flavylium cation.²

The research described in this chapter will examine complexes formed between CB[7] and flavylium derivatives to determine if CB[7] can bind to their central oxonium cation. In addition, three flavylium cations, possessing different combinations of terminal functional groups, were selected to determine the effect that their presence has on the binding position of CB[7] and the strength of the resulting complex. The three flavylium derivatives

studied were the hexafluorophosphate salts of the 4'-methoxyflavylium (Figure 6.2a), 6-methoxyflavylium (Figure 6.2b), and 6,4'-dimethoxyflavylium (Figure 6.2c) cations.⁴ These studies will include analyses by ESI mass spectrometry and NMR spectroscopy to confirm the presence of a host-guest complex and to determine where the host is binding to the guest.

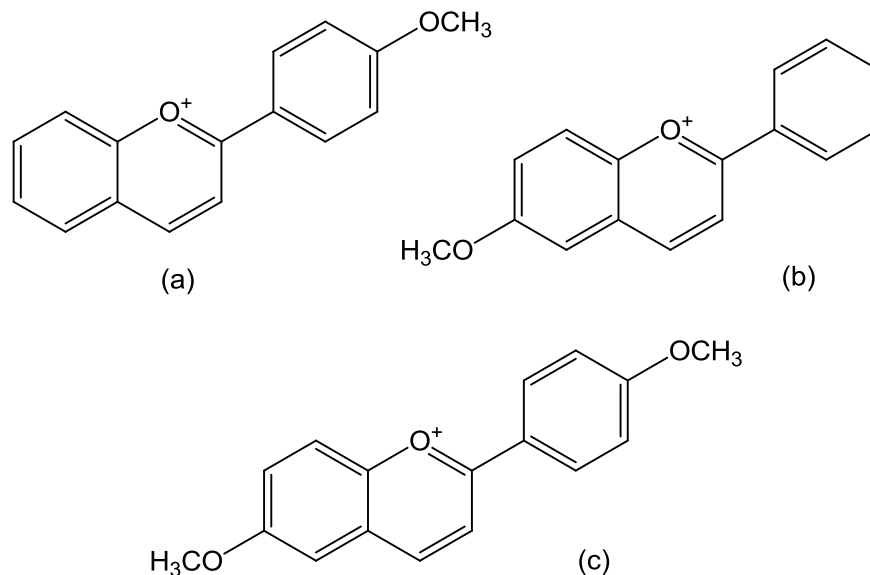


Figure 6.2 The chemical structures of the (a) 4'-methoxyflavylium, (b) 6-methoxyflavylium, and (c) 6,4'-dimethoxyflavylium cations.⁴

Each of the flavylium cations described above can undergo conversion to a chalcone species in the presence of light and hydroxide ions at neutral and basic pH values. This conversion occurs as shown in Figure 6.3.¹⁻⁴ The flavylium cation undergoes a hydrolysis (K_H) at the 2-position to yield a hemiketal, which then undergoes a rapid ring-opening tautomerization (K_T) to yield the *cis*-2-hydroxychalcone, followed by a rate-determining thermal or photochemical isomerization (K_I) to yield the thermodynamically favourable *trans*-2-hydroxychalcone.

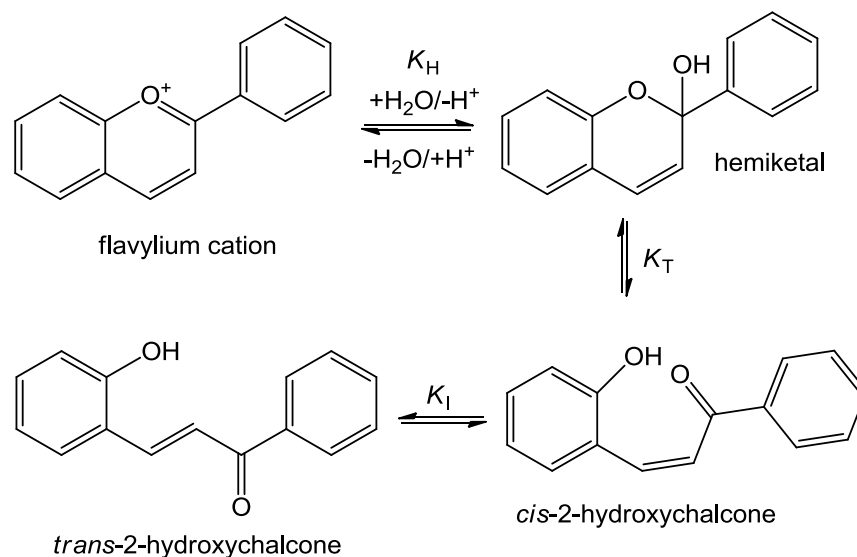


Figure 6.3 The base-catalyzed conversion of a flavylium cation to a *trans*-2-hydroxychalcone in aqueous solution.¹⁻⁴

The multistate character of the flavylium/chalcone system, whose equilibria can be modulated by external inputs, such as pH and light, has been investigated in terms of designing molecular scale electronic devices, such as optical memory devices. Several flavylium cations, in particular the 4'-methoxyflavylium, have been shown to have the requisite kinetic and thermodynamic properties to perform *write-lock-read-unlock-erase* cycles. The application of host-guest chemistry, in which the addition of the host system is a third external stimulus, has been investigated using anionic sodium dodecyl sulfate (SDS) micelles.

In addition to studying CB[7]·flavylium host-guest complexes, the research described in this section will also examine the effects of CB[7] on the flavylium-chalcone conversion reaction through the use of UV-visible spectroscopy. The behaviour in the presence of CB[7] will be compared with the reactions in the absence of the host molecule, and reported effects in the presence of the anionic SDS micelles.

6.2 Results and Discussion

6.2.1 ESI Mass Spectrometry and ^1H NMR Spectroscopy

The CB[7]-flavylium complexes were studied using a number of different analytical methods, including electrospray ionization mass spectrometry, and ^1H NMR and UV-visible spectroscopy. High-resolution ESI-MS was used to confirm the presence of the host-guest complex in an aqueous solution containing a flavylium guest and an excess of CB[7], by examining the mass/charge (m/z) ratio of peaks in the spectra. The results of these analyses are presented in Table 6.1 below.

Table 6.1 High resolution ESI-MS data for the host-guest complexes of CB[7] with the 4'-methoxyflavylium, 6-methoxyflavylium, and 6,4'-dimethoxyflavylium cations in aqueous solution.

Guest	Structure (Host:Guest)	Observed (m/z)	Calculated (m/z)
4'-methoxyflavylium (4'-OMeFV ⁺)	{CB[7]•4'-OMeFV} ⁺	1399.4340	1399.4351 for C ₅₈ H ₅₅ N ₂₈ O ₁₆ ⁺
6-methoxyflavylium (6-OMeFV ⁺)	{CB[7]•6-OMeFV} ⁺	1399.4320	1399.4351 for C ₅₈ H ₅₅ N ₂₈ O ₁₆ ⁺
6,4'-dimethoxy- flavylium (6,4'-(OMe) ₂ FV ⁺)	{CB[7]•6,4'-(OMe) ₂ FV} ⁺	1429.4475	1429.4456 for C ₅₉ H ₅₇ N ₂₈ O ₁₉ ⁺

The data in Table 4.1 demonstrated that each of the flavylium guests were able to form a complex with one or more CB[7] hosts. Once the presence of the host-guest complexes was confirmed by ESI-MS, ^1H NMR spectroscopy was then used to determine the location(s) of the host along the structure of the guest by examining how the host was

affecting the chemical shift of the guest proton resonances in the region(s) where it bound. To examine how the guest protons were affected by binding with CB[7], it was necessary to assign the guest proton resonances in the ^1H NMR spectra (Figure 6.4 – 6.6).

Once the ^1H NMR proton resonances of each flavylum guest had been identified, the guests was titrated with CB[7] and the upfield or downfield shifts ($\Delta\delta_{\text{lim}} = \delta_{\text{bound}} - \delta_{\text{free}}$) of the ^1H NMR guest proton resonances were monitored. As the titration progressed, peaks that moved upfield were identified as belonging to protons located within the inner hydrophobic cavity of CB[7]. Peaks that moved downfield were identified as belonging to protons involved in associations with carbonyl oxygens of the polar portals of CB[7]. For each titration, several representative spectra at different host-guest concentrations were selected and combined to demonstrate the effects of host complexation on the guest protons. These stack plots for each of the three flavylum guests are shown in Figures 6.4-6.6.

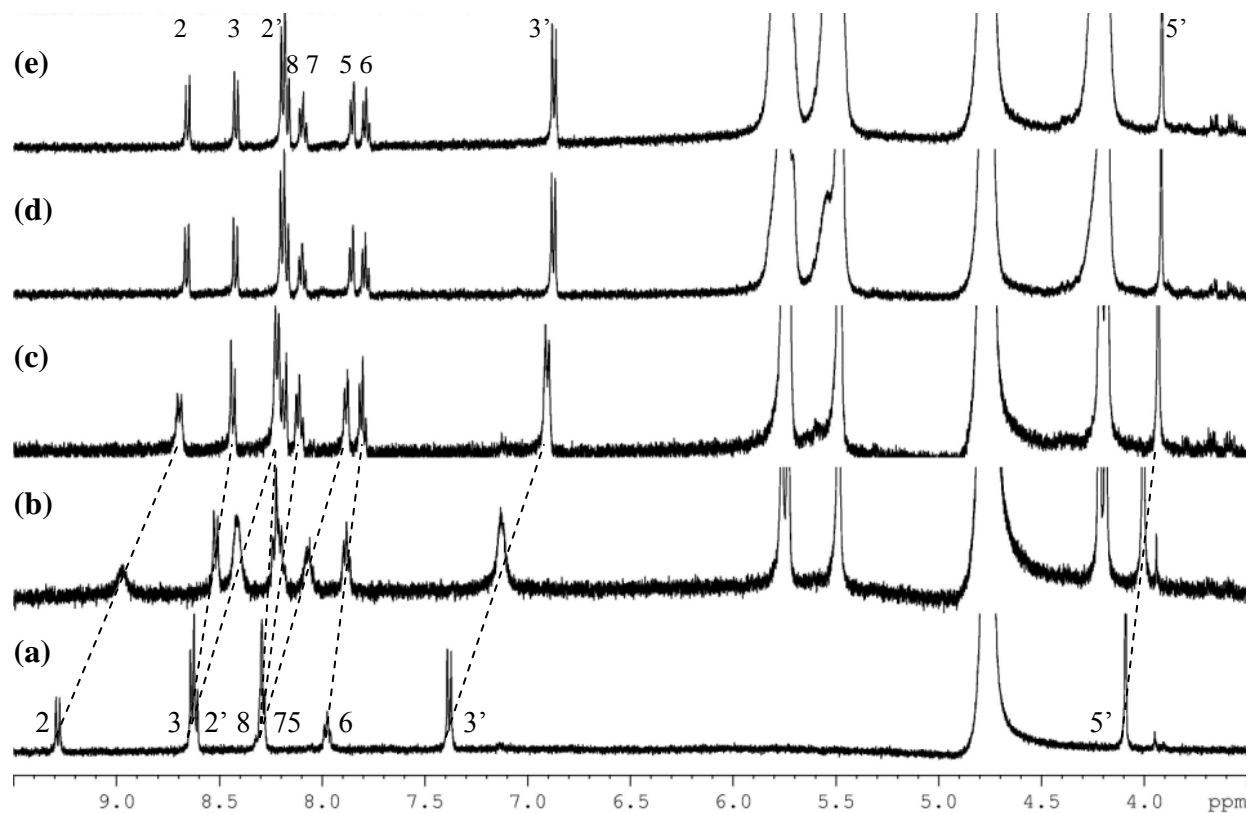
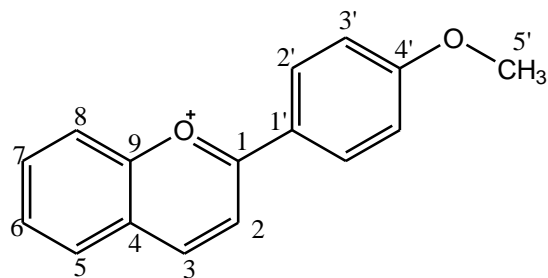


Figure 6.4 A stack plot of the ^1H NMR spectra of the 4'-methoxyflavylium cation in the presence of (a) 0.00, (b) 0.49, (c) 1.10, (d) 1.47, and (e) 2.05 equivalents of CB[7], titrated in D_2O . The dashed line indicates shifts in the peak positions of the 4'-methoxyflavylium cation. The numbered peak is matched with its numerically labeled protons on the chemical structure of the 4'-methoxyflavylium cation, above.

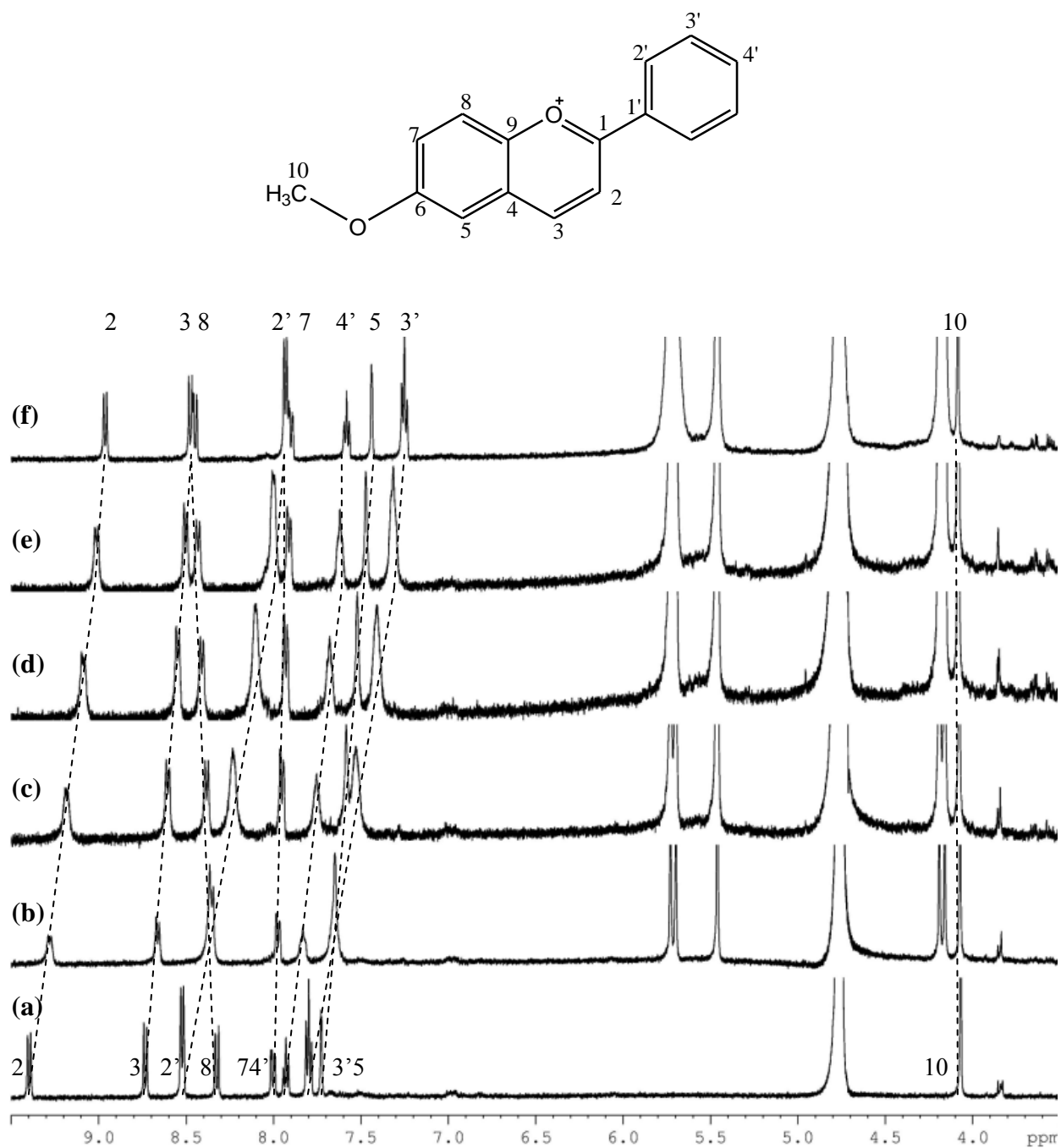


Figure 6.5 A stack plot of the ^1H NMR spectra of the 6-methoxyflavylium cation in the presence of (a) 0.00, (b) 0.31, (c) 0.55, (d) 1.01, (e) 1.27, and (f) 1.40 equivalents of CB[7], titrated in D_2O . The dashed line indicates shifts in the peak positions of the 6-methoxyflavylium cation. The numbered peak is matched with its numerically labeled protons on the chemical structure of the 6-methoxyflavylium cation, above.

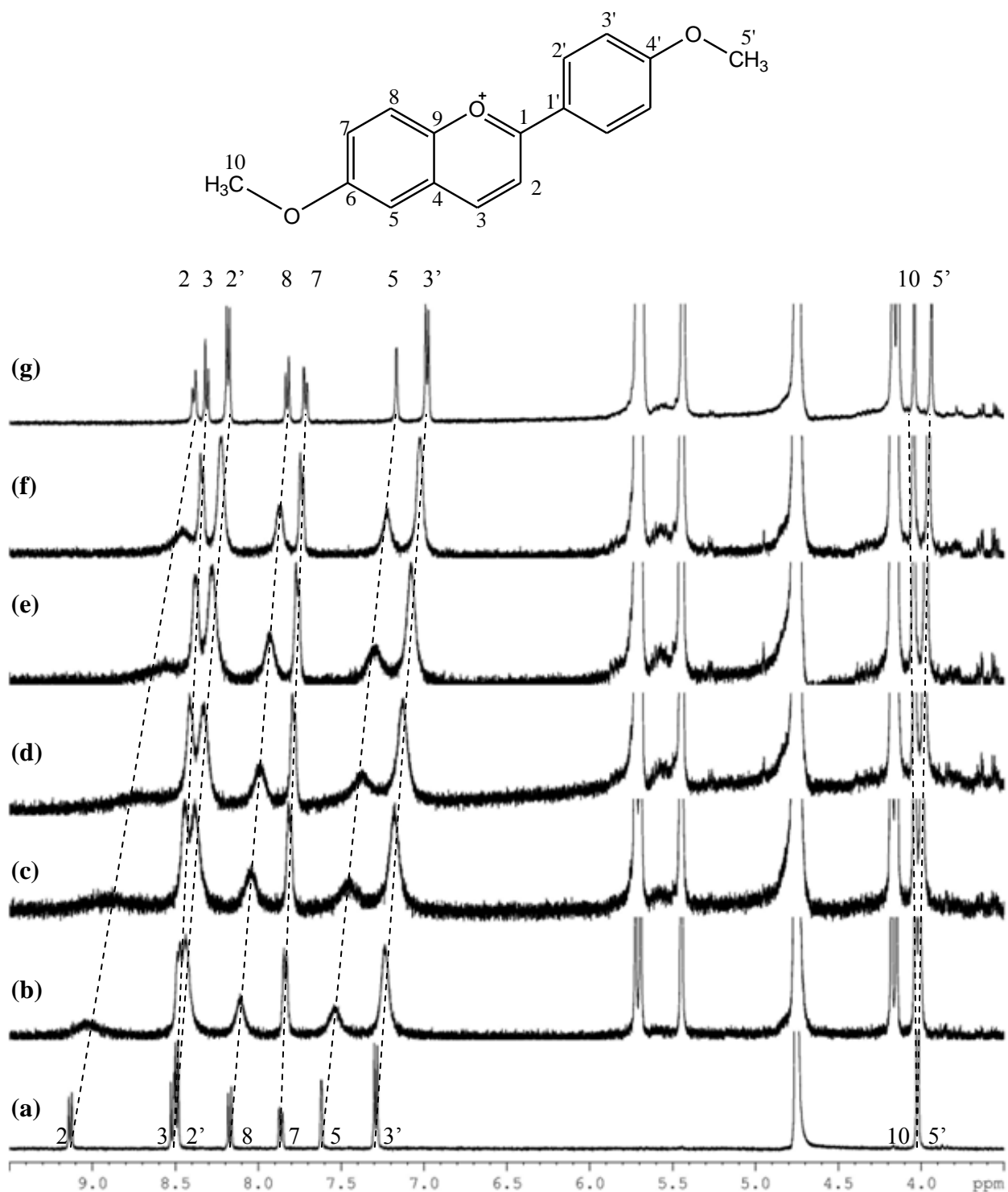


Figure 6.6 A stack plot of the ^1H NMR spectra of the 6,4'-dimethoxyflavylium cation in the presence of (a) 0.00, (b) 0.30, (c) 0.37, (d) 0.67, (e) 0.70, (f) 0.84, and (g) 1.01 equivalents of CB[7], titrated in D_2O . The dashed line indicates shifts in the peak positions of the 6,4'-dimethoxyflavylium cation. The numbered peak is matched with its numerically labeled protons on the chemical structure of the 6,4'-dimethoxyflavylium cation, above.

By examining which proton peaks shifted and at what concentration of CB[7] they shifted (Figure 6.7), it is possible to determine where and at what ratio the host became bound to the guest. The plots in Figure 6.7 indicate that the flavylium cations in this study form exclusively 1:1 host-guest complexes with the CB[7] host.

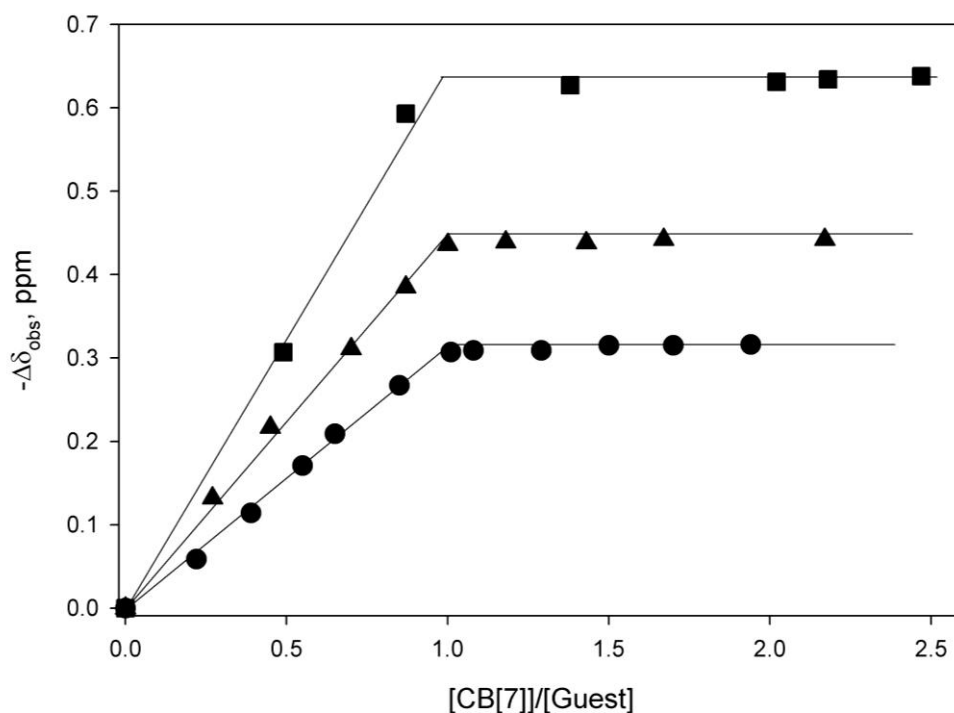


Figure 6.7 Plots of $-\Delta\delta_{\text{obs}}$ against $[\text{CB}[7]]/[\text{Guest}]$ for the titrations of the 4'-methoxyflavylium (■, H2), 6-methoxyflavylium (▲, H2), and 6,4'-dimethoxyflavylium (●, H3') cations in D_2O .

A summary of the limiting chemical shift changes induced by the formation of the 1:1 host-guest complexes is shown in Figure 6.8.

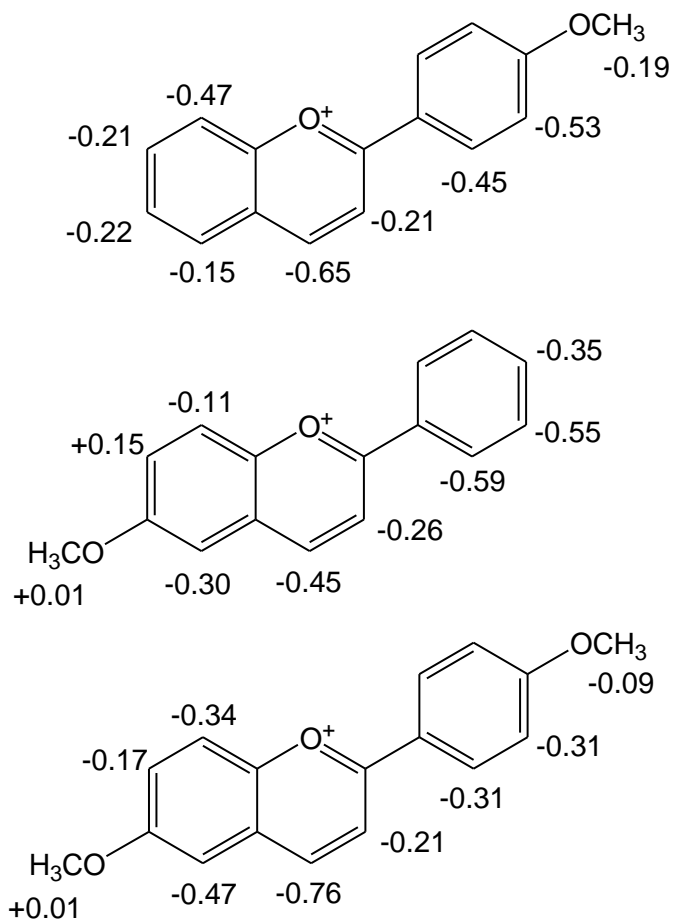


Figure 6.8 The ^1H NMR $\Delta\delta_{\text{lim}}$ values are shown for the titration of the 6-methoxyflavylium (top), b) 4'-methoxyflavylium (middle), and c) 6,4'-dimethoxyflavylium (bottom) cations with CB[7]. Negative $\Delta\delta_{\text{lim}}$ values indicate upfield shifts and positive $\Delta\delta_{\text{lim}}$ values indicate downfield shifts.

When the flavylium guests were originally chosen for binding studies with CB[7], it was thought that they would likely form 1:1 host-guest complexes with CB[7], and may have been capable of forming 2:1 host-guest complexes at high concentrations of CB[7], particularly in the case of 6,4'-dimethoxyflavylium (Figure 6.9).

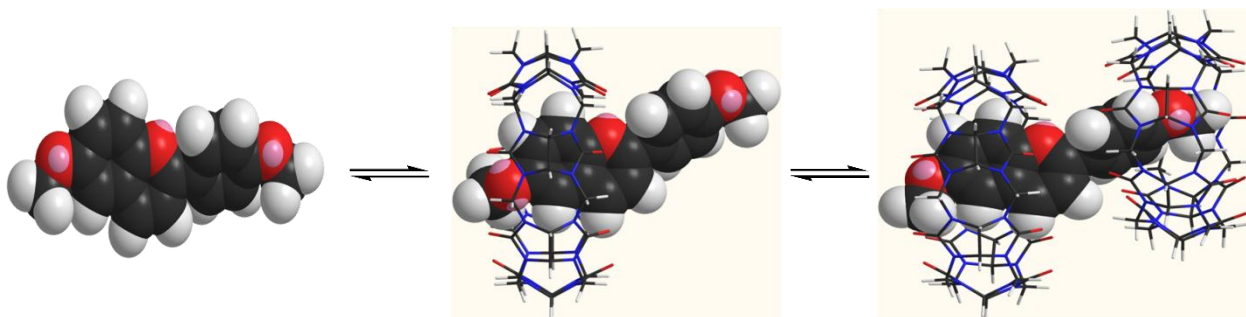


Figure 6.9 The possible structures of host-guest complexes of the 6,4'-dimethoxyflavylium cation with the CB[7] host.

However, the ESI-MS and ^1H NMR spectroscopy data indicated that a 1:1 complex was forming between each of the flavylium guests and CB[7], but they did not show evidence of the formation of a 2:1 complex. The upfield chemical shift changes in the ^1H NMR spectra indicate that the aromatic regions on either side of oxonium center undergo encapsulation by CB[7] (Figure 6.8). These observations are indicative of a rapid equilibrium between two possible positions of the host along the flavylium framework, as shown in Figure 6.10.

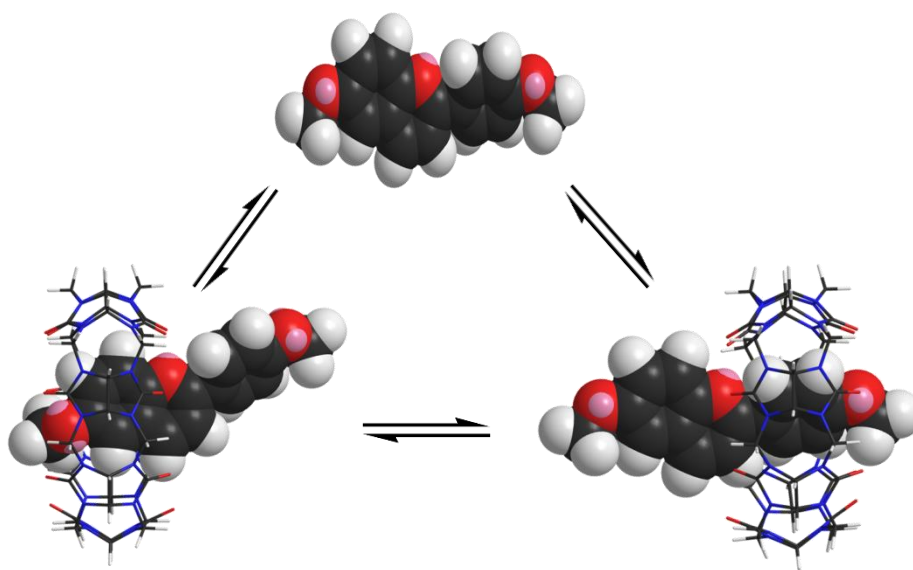


Figure 6.10 The energy-minimized gas phase structures of two potential 1:1 host-guest complexes formed between CB[7] and the 6,4'-dimethoxyflavylium cation.

The chemical shift changes for the guest protons in the 6-methoxyflavylium and 4'-methoxyflavylium cation in the presence of CB[7] indicate two possible host-guest complex structures, as illustrated for the 6,4'-dimethoxyflavylium cation above.

6.2.2 Determination of Binding Constants

With the presence of a host-guest complexes between CB[7] and the methoxyflavylium guests confirmed by ESI-MS and ^1H NMR spectroscopy, the strength of binding by CB[7] for each of the flavylium guests was measured. The binding events between CB[7] and the flavylium guests are driven by the ion-dipole interactions between the positively charged oxonium center of the flavylium cation and the carbonyl groups on the polar portals of CB[7]. While these interactions are the main driving force for CB[7] binding, the hydrophobic effect may also impart some entropic and enthalpic stability to the host-guest complex. The CB[7] bound too tightly to each of the flavylium guests for the fitting of binding curves (of $\Delta\delta_{\text{obs}}$ against [CB[7]]), Figure 6.7) to produce an accurate measurement of its binding constant ($K > 10^4 \text{ M}^{-1}$), which led to the use of competitive ^1H NMR binding experiments. This competition study was conducted with a known competitor, as demonstrated by Isaacs and coworkers, and described in Chapter 2.⁵ For the flavylium cations, the tetraethylammonium cation (Figure 6.11) was chosen as the competitor guest, because, similar to flavylium, it contains a positively charged central group, surrounded by non-polar substituents. Studies conducted by St-Jacques *et al.* have found that the tetraethylammonium cation has a binding constant with CB[7] of $K = (1.0 \pm 0.2) \times 10^6 \text{ M}^{-1}$.⁶

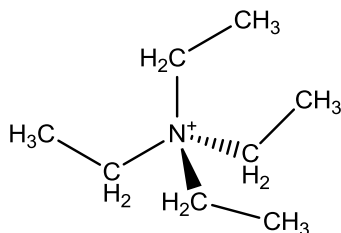


Figure 6.11 The chemical structure of the tetraethylammonium cation.

The stability constants for the 1:1 host-guest complexes formed between CB[7] and 4'-methoxyflavylium, 6-methoxyflavylium, and 6,4'-dimethoxyflavylium cations were determined from the competition experiments to be $(2.4 \pm 0.5) \times 10^6$, $(5.1 \pm 1.1) \times 10^6$, and $(3.8 \pm 0.9) \times 10^7 \text{ M}^{-1}$, respectively. The higher value of the binding constant for the dimethoxyflavylium cation, compared to the two methoxyflavylium cations, suggests that the methoxy groups provide some degree of stability to the host-guest complexes, even though the $\Delta\delta_{\text{lim}}$ values for the methyl proton resonances (Figure 6.8) indicate that these groups are not generally present in the cavity of the CB[7]. The flavylium host-guest complexes have similar stabilities to other 1:1 complexes between CB[7] and cationic quaternary ammonium, biguanidinium, and amidinium guests investigated in this thesis, indicating that the oxonium center is equally capable of providing for ion-dipole interactions with CB[7] as are the guests with various cation nitrogen-based functional groups.

6.2.3 UV-visible Spectroscopy

6.2.3.1 Flavylium/2-Hydroxychalcone Hydrolysis Equilibrium

Once the presence and stability of the CB[7]·flavylium complexes had been determined, the focus of the research shifted to describing what effects, if any, CB[7] had on

the conversion of flavylum cations to chalcones at various pH values. When a flavylum cation is introduced to a neutral or basic solution, it undergoes conversion to a neutral 2-hydroxychalcone molecule, as described in Figure 6.3. The change in the structure, involving a ring-opening process, results in a change in the UV-visible spectrum which is observed as a shift in solution colour from yellow to colourless, due to loss of aromaticity.

Previous studies have demonstrated that binding between CB[7] and an acidic guest can increase the pK_a of that guest.^{7,8} This pK_a shift can improve the stability of the cationic (protonated) form of the molecule. In the case of flavylum cations, the pH dependent equilibrium between the flavylum cation and the 2-hydroxychalcone ($K_a = K_H K_T$) should be modulated by the addition of CB[7]. The relative stabilities of these species can be monitored by UV-visible spectroscopy at various concentrations of CB[7], as shown in Figure 6.12.

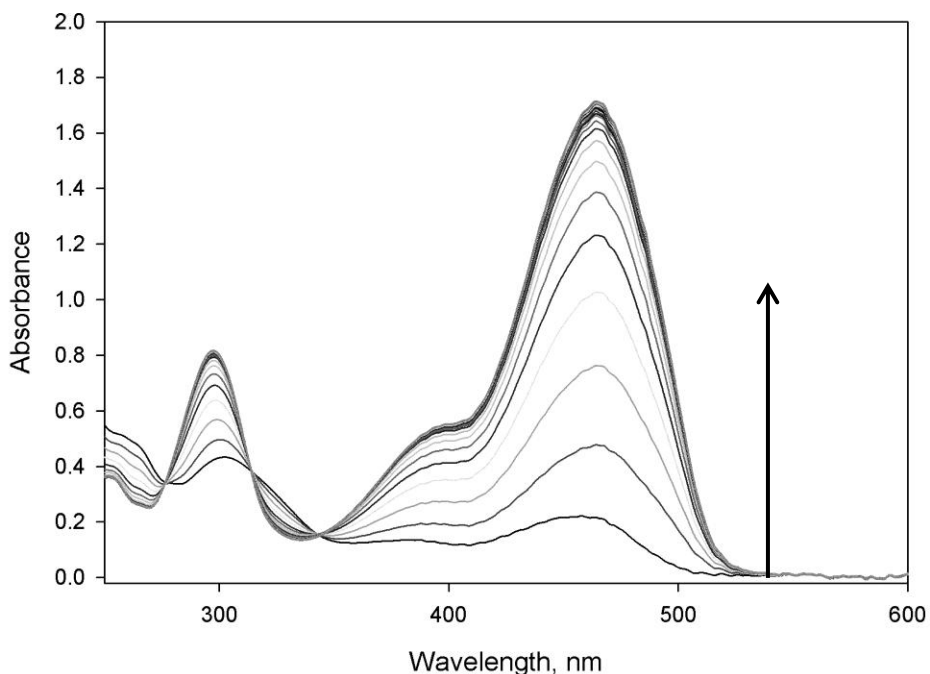


Figure 6.12 A UV-visible titration of 6,4'-dimethoxyflavylium (5.0×10^{-5} M in unbuffered aqueous solution) with 0 equivalents of CB[7] initially and 0.2 additional equivalents of CB[7] for each subsequent measurement.

The dependence of the absorbance on the concentration of CB[7] (Figure 6.13) was fit to a 1:1 host-guest binding model, yielding a value of $K = (3.3 \pm 0.2) \times 10^5 \text{ M}^{-1}$. This value would correspond to the binding of the 2-hydroxychalcone to CB[7].

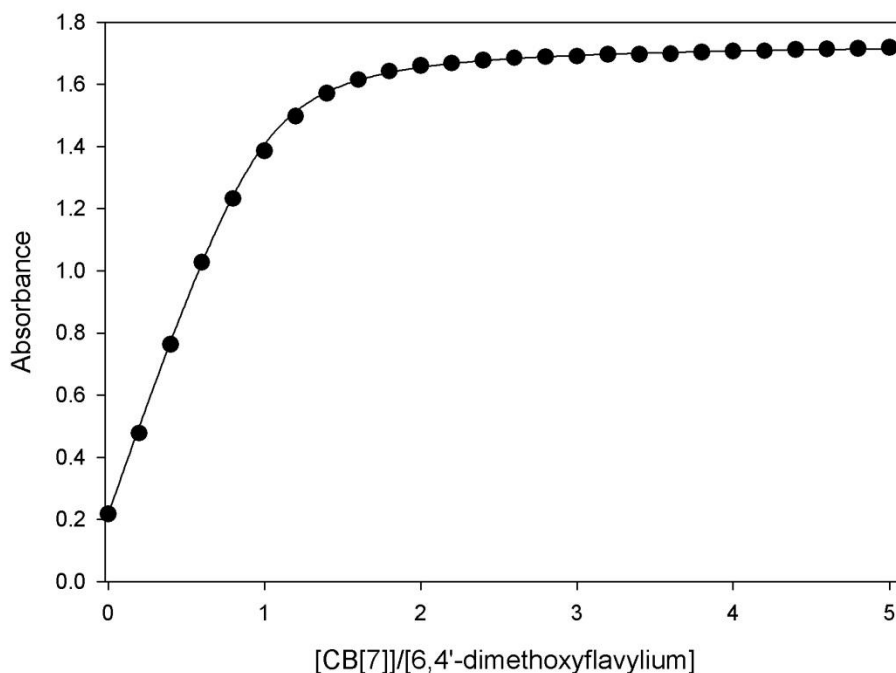


Figure 6.13 A plot of the absorbance at 464 nm as a function of the CB[7]/6,4'-dimethoxyflavylium ratio from the titration in Figure 6.12

Similar spectral changes, corresponding to the conversion of the 2-hydroxychalcone to the flavylium cation, were observed upon additions of CB[7] to the 4'-methoxyflavylium and 6-methoxyflavylium guests, with values of $K = (2.0 \pm 0.2) \times 10^5 \text{ M}^{-1}$ and $(6.7 \pm 0.5) \times 10^5 \text{ M}^{-1}$, respectively, were determined from fits of the data (as in Figure 6.13).

The data presented in Figure 6.12 indicated that CB[7] was influencing the flavylium-chalcone equilibrium at neutral pH. This change was likely a result of CB[7] stabilizing the flavylium cation and shifting its pK_a value. In order to determine the magnitude of this pK_a

shift, the absorbance spectra of flavylium was measured at a variety of pH values in the absence and presence of CB[7]. The results of these analyses are presented in Figure 6.14.

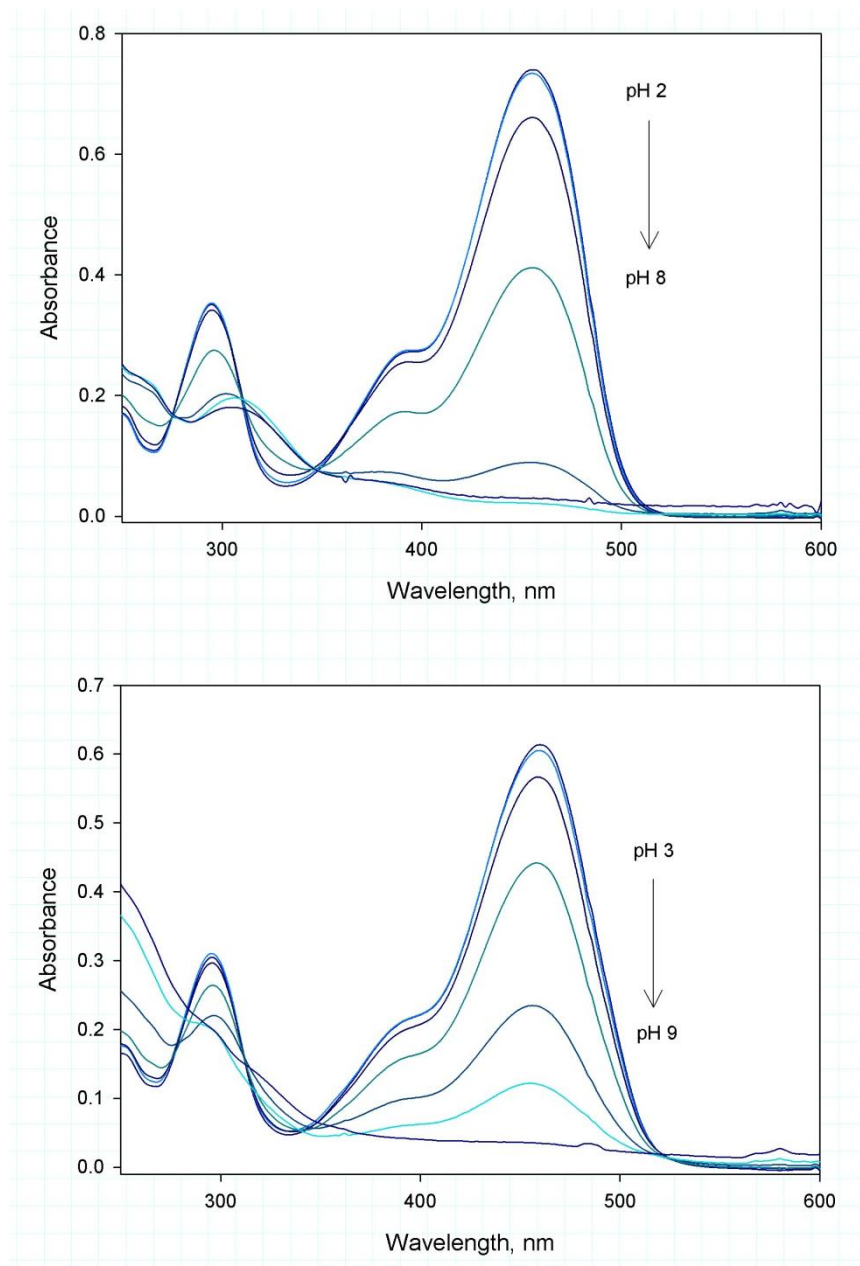


Figure 6.14 The pH dependent absorbance spectra of the 6,4'-dimethoxyflavylium cation at in the absence (top) and presence (bottom) of CB[7] (one pH unit increments over the ranges shown).

By plotting the change in absorbance shown in Figure 6.12 against pH, it is possible to determine the pK_a shift of 4'-methoxyflavylium in the absence and presence of CB[7], as shown in Figure 6.13.

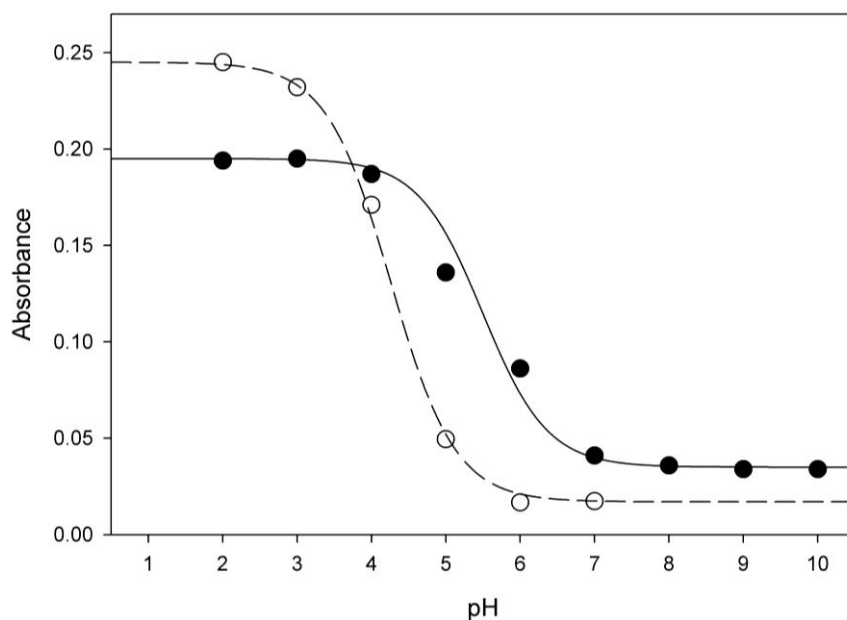


Figure 6.15 The absorbance spectra of the 4'-methoxyflavylium cation in the absence (○, 460 nm) and presence of CB[7] (●, 464 nm) as a function of pH.

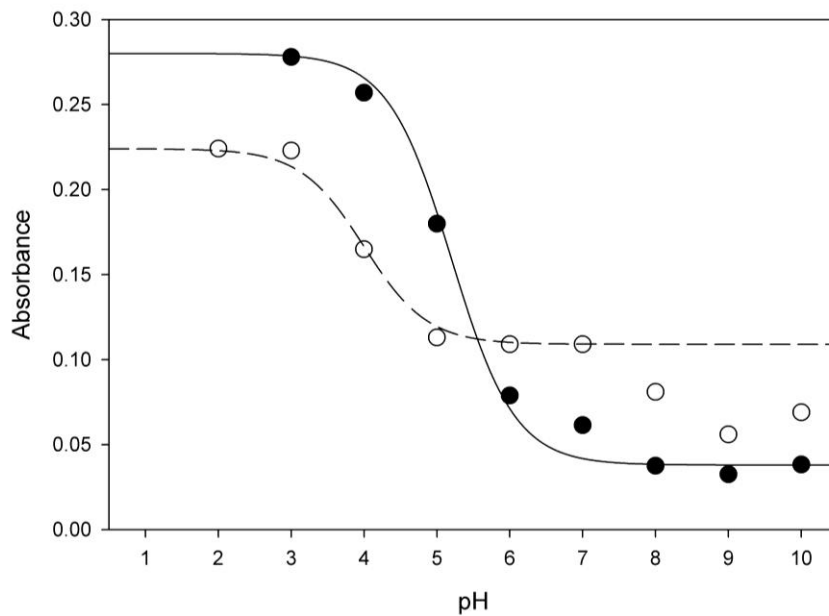


Figure 6.16 The absorbance spectra of the 6-methoxyflavylium cation in the absence (○, 460 nm) and presence of CB[7] (●, 464 nm) as a function of pH.

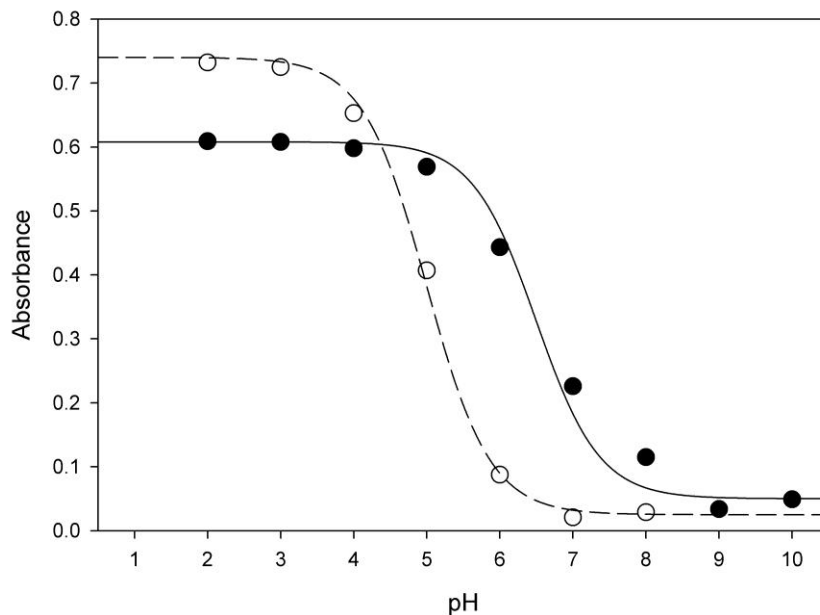


Figure 6.17 The absorbance spectra of the 6,4'-dimethoxyflavylium cation in the absence (○, 460 nm) and presence of CB[7] (●, 464 nm) as a function of pH.

The data from Figure 6.15-6.17 allow for the calculation of the pK_a value for the flavylium cations in the absence and presence of CB[7]. The results are summarized in Table 6.2. The pK_a value for the 4'-methoxyflavylium cation has previously been reported to be 4.26,⁹ in good agreement with the value in this study. The unsubstituted flavylium cation has a pK_a value of 2.98,⁹ indicating the additions of the methoxy groups in the 4'- and/or 6-positions stabilize the flavylium cation with respect to hydration.

Table 6.2 The calculated pK_H values (± 0.1) for the flavylium cations in the absence and presence of CB[7] in aqueous solution.

Guest	pK_a	$pK_a^{CB[7]}$	ΔpK_H
4'-methoxyflavylium	4.3	5.5	1.2
6-methoxyflavylium	4.0	5.2	1.2
6,4'-methoxyflavylium	5.0	6.5	1.5

The complexation of the flavylum cation by the CB[7] host increases the value of the pK_a value by 1.2 to 1.5 pK units. Cucurbit[n]urils are known to increase the pK_a values of acidic guest molecules as the result of preferential binding of the acid (normally cationic) species compared with the conjugate base (normally neutral). With the present guest molecules, the flavylum guests are cationic, while their hydrolysis products, the hemiketals and 2-hydroxychalcones (Figure 6.3) are neutral. As such, the equilibrium constant K_H would decrease if the CB[7] stabilized the flavylum species with respect to the hemiketal, resulting in an increase in the pK_a value. The value of pK_a for the 4'-methoxyflavylium in the presence of anionic SDS (sodium dodecyl sulphate) micelles also increases, to a value of 6.1,¹⁰ compared with the value of 4.3 in absence of SDS and 5.5 in the presence of CB[7].

The equilibrium constant between the flavylum cation and the 2-hydroxychalcone would be the product of K_H and K_T (Figure 6.3), which is equal to the observed K_a value (Table 6.2). The value of K_T for 4'-methoxyflavylium has been reported to be 0.5.⁹ As described for 4-hydroxy- and 4-aminobenzamidine guests in Chapter 5, the change in the pK_a value for the flavylum cations may be related to decrease in the CB[7] binding constant upon formation of the neutral 2-hydroxychalcone species. The values of $\log(K_{acid}/K_{base})$, where K_{acid} and K_{base} (see eq 5.3) are the binding constants for the flavylum and chalcone species, respectively, are 1.1, 1.9, and 2.1 for the 4'-methoxyflavylium, 6-methoxyflavylium, and 6,4'-dimethoxyflavylium guests, respectively, which are relatively close to the ΔpK_a values of 1.2, 1.2, and 1.5. The agreement is good considering that two different methods, 1H NMR and UV-visible spectroscopy, with different host and guest concentration ranges, were used to determine the binding constants.

6.2.3.2 Photochemical *Cis-* to *Trans*-2-hydroxychalcone Isomerization

The *cis*-2-hydroxychalcone to *trans*-2-hydroxychalcone equilibrium (Figure 6.3) can be manipulated by light as well as thermally in the dark. UV-visible spectra of neutral solutions of the three flavylum cations, in the absence and presence of excess CB[7] were recorded immediately after dissolution of the flavylum salts and then after 24 hours in the dark or after 24 hours exposed to light. The spectra are presented in Figure 6.18.

The spectra in Figure 6.18 indicate that in the absence of CB[7], the *cis*-2-hydroxychalcones isomerize to the *trans* species, with the solutions exposed to light proceeding somewhat more than those kept in the dark. With the solutions containing an excess of CB[7], the solutions kept in the dark had essentially the same spectra as the initial solutions, while considerable change was observed in the solutions exposed to light. These results indicated that the CB[7] host-guest complexes of the *cis*-2-hydroxychalcones prevent thermal isomerization to the *trans* species in neutral solution, while photochemical isomerization is possible for the CB[7] bound *cis*-2-hydroxychalcones.

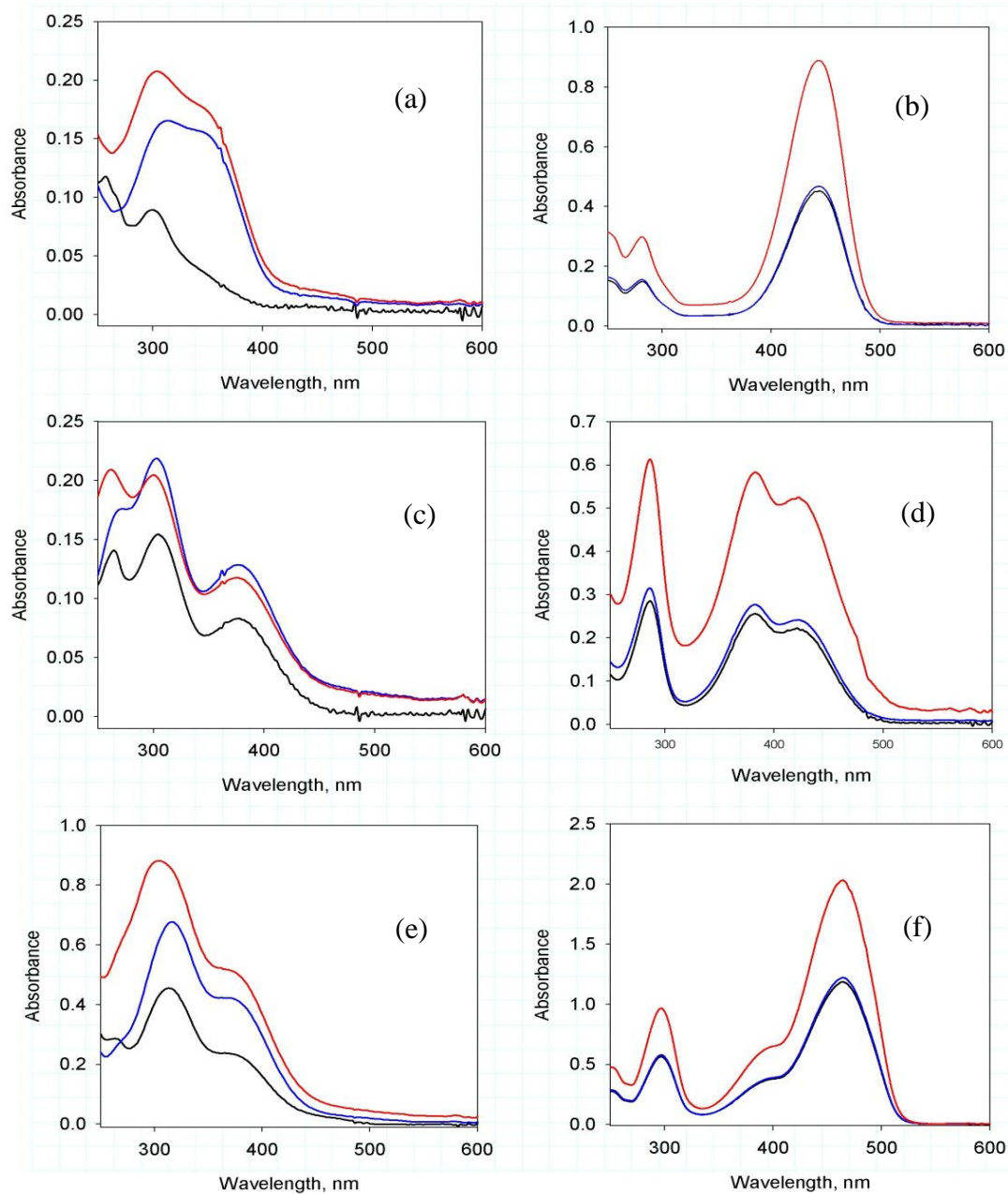


Figure 6.18 The UV-visible spectra of neutral solutions of the flavylium cations immediately after dissolution (black curves) and after 24 hours in the dark (blue curves) and after 24 hours under light (red curves) in the absence (left column) and presence (right column) of CB[7]: 4'-methoxyflavylium (top, (a) and (b)), 6-methoxyflavylium (middle, (c) and (d)), and 6,4'-dimethoxyflavylium (bottom, (e) and (f)).

6.2.3.3 Thermal *Cis*- to *Trans*-2-hydroxychalcone Isomerization in Basic Solution

In basic solution, the hemiketal species undergoes a rapid ring-opening process to yield the *cis*-2-hydroxychalcone which undergoes a rate-determining isomerization to the thermodynamically stable *trans*-2-hydroxychalcone species (Figure 6.3).⁹ The kinetics of the process in the absence and presence of CB[7] was carried out by adding base (0.3 mL of 0.10 M NaOH) to respective solutions of the 6,4'-dimethoxyflavylium cation (25 μ M) without and with CB[7] (125 μ M). The time-dependent changes of the solution from colourless (rapid change from original yellow flavylium to colourless hemiketal/*cis*-2-hydroxychalcone) to the yellow *trans*-2-hydroxychalcone was monitored by UV-visible spectroscopy (Figure 6.19). The plots of the absorbance as a function of time for the solutions without and with CB[7] are shown in Figure 6.20.

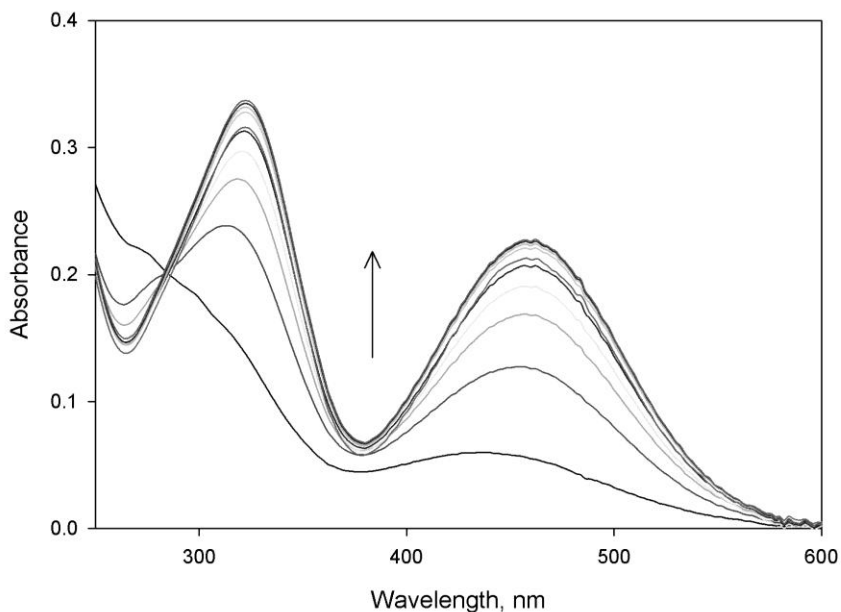


Figure 6.19 Time-dependent spectra of the reaction of a solution of the 6,4'-dimethoxyflavylium cation (25 μ M) containing CB[7] (125 μ M) upon addition of 0.10 M NaOH. Initial spectrum is 150 s after addition of base, and subsequent spectra shown are 900 s apart.

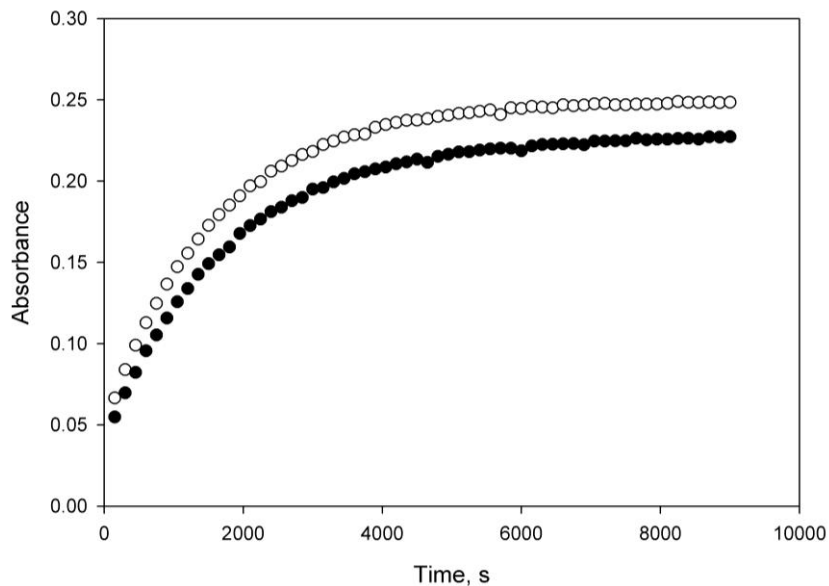


Figure 6.20 Plot of the absorbance (460 nm) as a function of time for the reaction of the 6,4'-dimethoxyflavyium cation ($25 \mu\text{M}$) without (\circ) and with (\bullet) CB[7] ($125 \mu\text{M}$) upon addition of 0.10 M NaOH .

From the slopes of plots of $\ln(A_{\text{inf}} - A_t)$ against time, the first-order rate constants for the ring-opening reaction was determined (Figure 6.21).

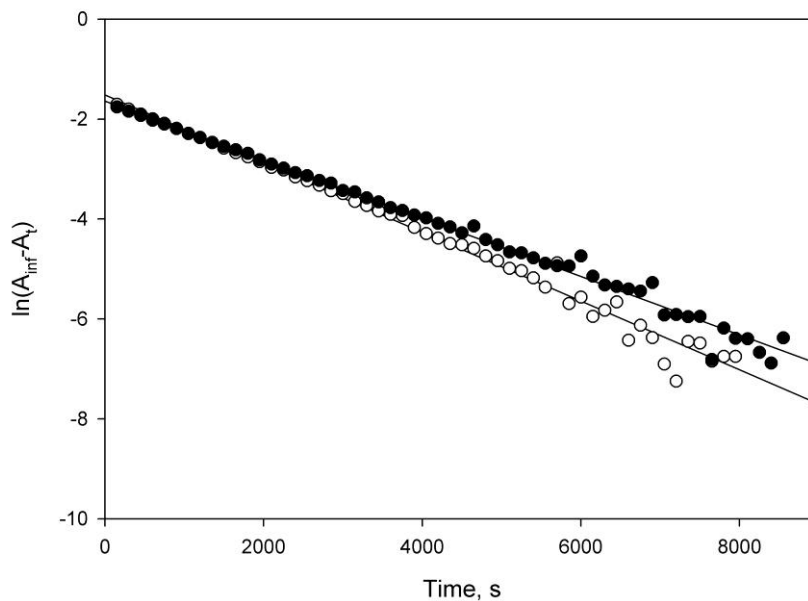


Figure 6.21 Plots of $\ln(A_{\text{inf}} - A_t)$ against time for the reaction of the 6,4'-dimethoxyflavyium cation ($25 \mu\text{M}$) without (\circ) and with (\bullet) CB[7] ($125 \mu\text{M}$) upon addition of 0.10 M NaOH .

The first-order rate constant for the ring-opening process is $6.9 \times 10^{-4} \text{ s}^{-1}$ in the absence of CB[7] and decreases slightly to $5.9 \times 10^{-4} \text{ s}^{-1}$ in the presence of CB[7]. The lack of a significant change in the rate constant is most likely due to the fact the CB[7] does not strongly bind to the deprotonated form of the *cis*-2-hydroxychalcone in basic solution. The rate constant for the 6,4'-methoxyflavylium cation in this study may be compared with a rate constant of $1.95 \times 10^{-5} \text{ s}^{-1}$ in neutral solution reported for the 4'-methoxyflavylium cation by McClelland and Sedge.⁹ It is of interest to note that the addition of SDS micelles only reduced this value by 50%, in line with the small effect that CB[7] had on the rate constant for the the 6,4'-methoxyflavylium cation.¹⁰

6.3 Conclusions

The formation of host-guest complexes between CB[7] and several methoxy-substituted flavylium guests has been monitored and analyzed through the use of ESI mass spectrometry, ¹H NMR spectroscopy and UV-visible spectroscopy. The results of these analyses indicated that CB[7] is able to bind 4'-methoxyflavylium, 6-methoxyflavylium and 4',6-dimethoxyflavylium through ion-dipole interactions with their oxonium groups, forming host-guest complexes with high binding constants. The formation of a CB[7]·flavylium host-guest complex resulted in p*K*_a shift values of 1.2-1.5, consistent with the stabilization of the flavylium cation, with respect to the neutral ring-opened 2-hydrochalcone, in neutral solutions. The complexations by CB[7] had only a small effect on the kinetics of the *cis* to *trans* isomerization of the chalcone following base-catalyzed ring-opening conversion from the hemiketal.

References

1. R. Gavara, V. Petrov, and F. Pina, *Photochem. Photobiol. Sci.*, **2010**, 9, 298.
2. L. Giestas, F. Folgosa, J. C. Lima, A. J. Parola, and F. Pina, *Eur. J. Org. Chem.*, **2005**, 4187.
3. F. Ito, N. Tanaka, A. Katsuki, and T. Fujii, *J. Photochem. Photobiol. A: Chem.*, **2002**, 150, 153.
4. M. Kueny-Stotz, S. Chassaing, R. Brouillard, M. Nielsen, and M. Goeldner, *Bioorg. Med. Chem. Lett.*, **2008**, 18, 4864.
5. S. Liu, C. Ruspic, P. Mukhopadhyay, S. Chakrabarti, P. Y. Zavalij, and L. Isaacs, *J. Am. Chem. Soc.*, **2005**, 127, 15959.
6. A. D. St-Jacques, I. W. Wyman, and D. H. Macartney, *Chem. Commun.*, **2008**, 4936.
7. D. H. Macartney, *Isr. J. Chem.*, **2011**, 51, 600.
8. G. Parvari, O. Reany, and E. Keinan, *Isr. J. Chem.*, **2011**, 51, 646.
9. R. A. McClelland and S. Gedge, *J. Am. Chem. Soc.*, **1980**, 102, 5838.
10. A. H. Parola, P. Pereira, F. Pina and M. Maestri, *J. Photochem. Photobiol. A: Chem.*, **2007**, 185, 383.

Chapter 7

CONCLUSIONS AND SUGGESTIONS FOR FUTURE WORK

7.1 Introduction

The research described herein used ESI mass spectrometry and ^1H NMR and UV-visible spectroscopy, along with molecular modeling studies, to characterize the host-guest complexes that formed between the cucurbit[7]uril host and a series of cationic alkylammonium, biguanidinium, amidinium, and flavylum guests in aqueous solution. These guests contain the aforementioned cationic nitrogen and oxygen (oxonium) which have received little or no previous study with respect to their host-guest complexes with CB[7]. The experimental results of the studies with each type of guest provide further insight into the importance of ion-dipole interactions and the hydrophobic effect in determining the strength and structure of host-guest complexes with cucurbiturils in aqueous solution. The sections below summarize the specific findings for each type of guest studied and suggest possible extensions of the research work and applications in which these host-guest complexes may play a role.

7.2 The Benzethonium Guest

The anti-fungal preservative, benzethonium chloride possessed two possible binding sites, an alkylammonium group on one terminus and a bulky hydrophobic group on the other terminus. Previous studies have shown that alkylammonium guests form tightly bound complexes with CB[7], owing to the strong ion-dipole interaction that occurs between the polar portals of CB[7] and the cationic nitrogen on the alkylammonium guest.¹⁻³ The

benzethonium cation proved to be no different, forming a tightly bound 1:1 host-guest complex between its benzyldimethylammonium group and CB[7]. The binding strength of this complex was shown to be consistent with other benzylammonium containing groups, such as, benzylammonium,⁴ benzyltrimethylammonium,² benzylguanidinium,⁴ benzylcholine,³ and N-benzyl-1-(1-naphthyl)ethylammonium.⁵ In each of the cases, the complexation placed the benzyl group within the CB[7] cavity and the quaternary nitrogen near the oxygens of the ureido carbonyl groups on the portals. However, unlike these other guests, the benzethonium cation was also able to form a moderately-strong 2:1 host-guest complex with its neutral 2,4,4-trimethylpentyl substituent in the presence of excess of CB[7]. Previous studies conducted by Nau and co-workers^{6,7} have determined that the cavity of cucurbiturils are capable of tightly binding hydrophobic groups of a certain size, specified by either the number of heavy (non-hydrogen) atoms or by the molar volume. With 8 heavy atoms, the 2,4,4-trimethylpentyl substituent is comparable in size and binding strength to the previously determined values for butan-2-one⁸ and 3,3-dimethylbutan-2-one⁸, which have 5 and 9 heavy atoms, respectively. The 2:1 binding site on benzethonium is also far enough away from the 1:1 binding site to minimize any repulsive effects from the polar portals of the CB[7] bound there. We have observed a similar phenomenon of distinct 1:1 and 2:1 host-guest complexes of CB[7] with coenzyme B₁₂, where the first CB[7] bound strongly to the protonated α -axial 5,6-dimethylbenzimidazole base and the second CB[7] bound more weakly to the β -axial 5'-deoxyadenosyl ligand.⁹

In a previous study by Simpson, β -cyclodextrin was shown to be more effective than micelle surfactants at neutralizing the antimicrobial effects of benzethonium.¹⁰ The results described above suggest that CB[7] binds more strongly to benzethonium than β -CD did,

and therefore may be better able to reduce the antimicrobial effects of benzethonium at lower host concentrations. A logical extension of this work would be to conduct biological studies on the antimicrobial effects of benzethonium in the absence and presence of CB[7].

Previous studies have proven that benzethonium has moderate antiseptic properties^{11,12} and a recent study by Yip and coworkers showed that it also has anti-tumour properties.¹³ These characteristics could one day result in benzethonium being selected for a drug regimen to treat infection of pharyngeal cancer. If this were the case, then CB[7] could be used to help deliver the drug.¹⁴ Based on this possibility, a kinetic study on the release of benzethonium from CB[7] (binding exhibited slow exchange behaviour on the NMR timescale) would be another logical extension of this work.

As with most molecules that possess a hydrophilic terminus and a hydrophobic terminus, benzethonium cations can form micelles when introduced into an aqueous solution at high concentrations. Previous studies have demonstrated that binding to CB[7] can help prevent amphipathic molecules from aggregating, thereby increasing their critical micelle concentrations (CMC).¹⁵ If CB[7] was able to keep the benzethonium cations dispersed, even at high concentrations, then it would greatly increase the effectiveness of the compound as an antifungal and anti-tumour agent. Thus a logical extension of this work would be to determine the CMC of benzethonium in the absence and presence of CB[7].

The hydrophobic 2,4,4-trimethylpentyl group found in benzethonium chloride is also used as a hydrophobic moiety in other drug molecules. An example of this is the anti-dandruff ingredient in some shampoos, 1-hydroxy-4-methyl-6-(2,4,4-trimethylpentyl)-2(1H)-pyridinone ethanolamine (Octopirox, Piroctone Olamine), shown in Figure 7.1.

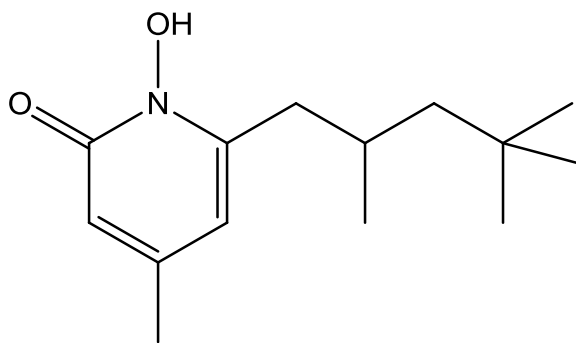


Figure 7.1 Structure of 1-hydroxy-4-methyl-6-(2,4,4-trimethylpentyl)-2(1H)-pyridinone.

There is an interest in controlled delivery of this drug that would result in a higher activity or allow for the use of a lower percentage of the drug in the shampoo.¹⁶ A CB[7] host-guest complex in which the 2,4,4-trimethylpentyl group is encapsulated might provide for improved delivery of this active ingredient.

7.3 The Biguanidinium Guests

Previous research in our group has shown that CB[7] can bind strongly to guests containing a delocalized positive charge, such as guanidinium cations.⁴ My research has further shown that guests containing cationic biguanidinium groups can also form strong complexes with CB[7]. The biguanidinium guests examined included metformin and phenformin, which have been used in the treatment of diabetes,^{17,18} as well as chlorhexidine and alexidine, which have been used as antiseptics in mouthwashes and toothpastes.^{19,20}

As smaller molecules, both metformin and phenformin were expected and shown to form strong 1:1 host-guest complexes with an excess of CB[7]. However, in the case of metformin, the guest was also shown to be capable of forming 1:2 host-guest complexes at low concentrations of CB[7]. These 1:2 host-guest complexes are believed to occur when a

metformin cation binds to each of the polar portals on CB[7]. Dearden and coworkers have recently shown that similar capping structures occur between CB[7] and guanidinium cations in the gas-phase.²¹ In addition to these properties, metformin has also been shown to deprotonate at a pH of 12.4, however in acidic media it can also undergo further protonation at a pK_a of 2.8 in the absence of CB[7].²² In the past, CB[7] has often been shown to increase the K_a of a guest by several orders of magnitude, however in this case the presence of CB[7] reduced the pK_a of the guest to 2.68. This result suggested that CB[7] had a lower affinity for doubly protonated dications than for monocations. This effect was also recently observed in mono- versus dimethylated DABCO (1,4-diazabicyclo[2.2.2]octane) cationic guests.²³

Chlorhexidine and alexidine were both larger guest molecules containing a central hexamethylene group, which was flanked on either side by a biguanidinium cation and a hydrophobic group. As a result of these extended molecular structures, both guests were expected to form host-guest complexes with higher stoichiometries. The results showed that both chlorhexidine and alexidine were capable of forming 3:1 host-guest complexes, but that they formed these complexes through different means. In the case of chlorhexidine, the first equivalent of CB[7] bound to the hexamethylene group, allowing each portal of CB[7] to interact with a biguanidinium group. The second and third equivalents of CB[7] bound over the 4-chlorophenyl groups on either terminus of the molecule. In the case of alexidine, similar behaviour to that of chlorhexidine was expected, however, the results showed that the first and second equivalents of CB[7] bound to the outer 2-ethyl-hexyl substituents and then a third equivalent took the place of a terminal CB[7] by pushing it onto the central hexamethylene group. This difference in binding mode was a result of the structure of the 2-ethylhexyl terminus on alexidine, which, like the neutral terminus on benzethonium,

contained 8 heavy atoms. The size of this 2-ethylhexyl group led to a tightly bound complex with CB[7] and required an additional CB[7] to bump the original host onto the central hexamethylene group. In both chlorhexidine and alexidine, it is interesting to note that each of the three binding events is driven, in part, by ion-dipole interactions that occur between CB[7] and the cationic biguanidinium groups. Although biguanidinium groups form weaker ion-dipole interactions with CB[7] than guanidinium or alkylammonium guests, they also have a charge that is distributed across seven heavy atoms. This broad charge distribution on the guest created a buffer region, which allowed two hosts to each interact with the cationic charge, but stay far enough apart to minimize the repulsive forces generated by their polar portals.

Each of the biguanidinium guests examined in this research has been used successfully as a medicinal drug.¹⁷⁻²⁰ Thus, a logical extension of this research would examine the kinetics of dissociation between each guest and CB[7] to determine if CB[7] could be used a slow-release drug delivery agent. It is also possible that CB[7] could be used to help mitigate some of the difficulties and side effects that arise with use of these drugs, such as the lactic acidosis caused by phenformin or the poor solubility of chlorhexidine and alexidine in aqueous solution. Further biological studies would be needed in each of these cases to determine if CB[7] could improve the efficacy of the drug or reduce any of its negative side effects.

7.4 The Amidinium Guests

Although amidinium guests contain a delocalized cationic charge, this charge is only distributed across three heavy atoms, unlike guanidinium and biguanidinium, whose charge

is spread across four and seven heavy atoms, respectively. This more centralized charge allows amidinium guests to form stronger complexes with CB[7], due to stronger ion-dipole interactions, however it also meant that any one amidinium cation was far less likely to form a complexes with two polar CB[7] portals, as a biguanidinium cation does. The amidinium guests examined included pentamidine, berenil, 4-aminobenzamidine and 4-hydroxybenzamidine. Pentamidine has been the drug of choice in the treatment of African sleeping sickness for more than 40 years.^{24,25} This drug was shown to form strong 1:1 and 2:1 complexes, with a CB[7] host binding to each cationic *para*-benzene termini. Berenil, like pentamidine, was once used in the treatment of African sleeping sickness, but fell out of use in humans due to a localized burning sensation at the site of injection.^{24,26} Oral administration of the drug was also not possible, due to the degradation of the drug under acidic conditions, such as those found in the stomach.²⁶ It was hoped that complexation with CB[7] could reduce one or both of these difficulties. The research results showed that CB[7] was able to form a tightly bound 1:1 host-guest complex with berenil, however this complex did not stabilize the molecular structure of berenil in acid, but instead, further catalyzed its degradation. The products of this degradation reaction, 4-aminobenzamidine and 4-hydroxybenzamidine, were each also shown to form strong 1:1 host guest complexes with CB[7]. Neither berenil nor either of its degradation products showed evidence a 2:1 host-guest complex. Recent work in our lab, conducted by A. Love and J. Rygus, has shown that the 4-hydroxy- and 4-aminobenzamidinium guests undergo pK_a shifts from 7.5 and 9.4, respectively, in the absence of CB[7], to 9.2 and 11.8, respectively, in the presence of CB[7]. Thus, complexation with CB[7] resulted in an overall pK_a shifts of 1.7 and 2.4 pK units for the 4-hydroxy- and 4-aminobenzamidines, respectively.

Since both pentamidine and berenil have been used as drugs, a logical extension of this research would examine the kinetics of dissociation between each of these guests and CB[7] to determine if it could be used successfully as a slow-release drug delivery agent.

The 4-aminobenzamidinium cation is a potent inhibitor of enzymes such as trypsin and thrombin,²⁷ with binding constants in the range of 10^5 - 10^6 M⁻¹.^{27,28} One feature of the binding is that it is accompanied by a significant enhancement of the intensity of the fluorescence of the 4-aminobenzamidinium cation.²⁹ Thus, another logical extension of this work would involve conducting a fluorescence titration with this guest and CB[7] to determine the effects of the host on the fluorescence spectrum of the guest. Because of its high affinity to serine protease enzymes, the 4-aminobenzamidinium group has been immobilized on a number of commercial solid supports, such as agarose (Figure 7.2), sepharose, and Celite, for use in enzyme isolation and purification.³⁰

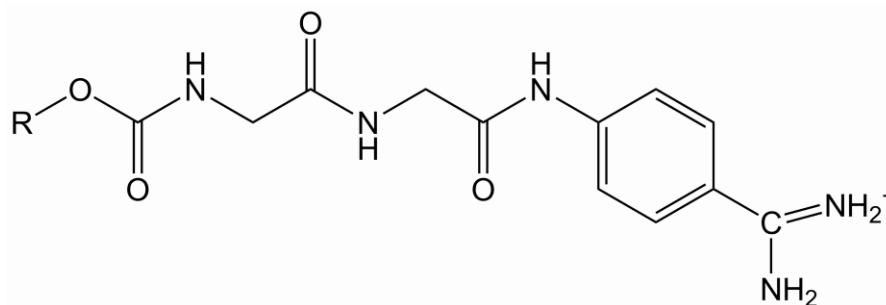


Figure 7.2 Structure of the 4-aminobenzamidinium cation appended to agarose beads (R) with a glycine-glycine spacer.

These commercially-available resins may also be useful in separating CB[7] from other members of the CB[n] family and aid in the synthesis and purification of novel CB[7] derivatives.

7.5 The Flavylium Guests

Flavylium dyes can be substituted by a wide variety of functional groups in a number of ring positions, making it a family of guests with hundreds of possible derivatives.^{31,32} As guests, flavylium molecules contain a cationic oxonium group at the center of their structures, which should provide a site for complexation with CB[7].^{31,32} For the present research, three derivatives, 4'-methoxyflavylium, 6-methoxyflavylium, and 6,4'-dimethoxyflavylium, were chosen to represent this family of guests.³³ The results showed that CB[7] was able to form strong 1:1 host-guest complexes with each of the three flavylium guests. Initially, the possibility of the flavylium cations being capable of forming 2:1 host-guest complexes was considered, however the results provided no evidence in support of this. Flavylium cations are also capable of undergoing a rapid ring-opening reaction, that forms a 2-hydroxychalcone in the presence of light and at either neutral or basic pH conditions.³¹⁻³³ It was hoped that CB[7] would act to stabilize the ring-closed, spectroscopically active, form of the dye. Through UV-visible studies, it was shown that CB[7] does stabilize the structure of the flavylium cations over the structure of the neutral chalcone. This change was believed to have been a result of CB[7] shifting the pK_a of the flavylium cation. When the absorbance spectra of each flavylium guest was plotted as a function of pH, we were able to show that CB[7] does increase the pK_a of each flavylium guest by 1.2 - 1.5 pK units. While CB[7] proved effective at stabilizing each of the flavylium cations in neutral solution, it proved far less effective at stabilizing the 6,4'-dimethoxyflavylium cation in basic solution. The lack of a significant change was likely due to the fact that CB[7] does not strongly bind to the deprotonated form of the *cis*-2-hydroxychalcone that forms when flavylium undergoes ring-opening in basic solution.

Future work could examine host-guest complexes between CB[7] and a broader range of flavylium derivatives to determine how complexation affects the ring-opening reaction and resulting spectrophotometric changes. By examining the effects of CB[7] on a wider range of derivatives, it would be possible to produce a series of flavylium dyes that could be tuned to create any desired colour in aqueous solution. One flavylium derivative, recently discovered by Diniz *et al.*, is of particular interest for future research.³⁴ This bis-(7-hydroxyflavylium) guest containing a methyl viologen bridge (Figure 7.3) is particularly interesting because CB[7] has been shown to bind to both the flavylium cation, in this study, and to methyl viologen cations in previous studies.³⁵ Thus, the concentration of CB[7] could have a profound ability to tune the spectrum of this guest, if it can be demonstrated that CB[7] can bind to several positions along the electronic structure of this guest.

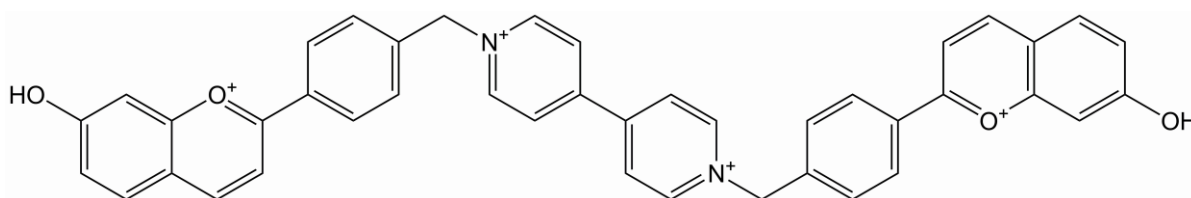


Figure 7.3 The structure of bis-(7-hydroxyflavylium) compound containing a methyl viologen bridge

Flavylium derivatives, particularly 4'-methoxyflavylium, have recently been shown to have the requisite kinetic and thermodynamic properties required to perform *write-lock-read-unlock-erase* cycles, with changes in pH and light being used to stimulate each change. In a previous study, the formation of SDS micelles was used as a third possible stimulus. The present research suggests that host-guest complexation with CB[7] could also be used to stimulate changes in the guests structure in order to perform *write-lock-read-unlock-erase* cycles, however further investigation would be required.

References

1. S. Liu, C. Ruspic, P. Mukhopadhyay, S. Chakrabarti, P. Y. Zavalij, and L. Isaacs, *J. Am. Chem. Soc.*, **2005**, *127*, 15959.
2. A. D. St-Jacques, I. W. Wyman, and D. H. Macartney, *Chem. Commun.*, **2008**, 4936.
3. I. W. Wyman and D. H. Macartney, *Org. Biomol. Chem.*, **2010**, *8*, 253.
4. D. S. N. Hettiarachchi and D. H. Macartney, unpublished results.
5. L. Yuan, R. Wang, and D. H. Macartney, *Tetrahedron: Asymmetry*, **2007**, *18*, 483.
6. W. M. Nau, M. Florea and K. I. Assaf, *Isr. J. Chem.*, **2011**, *51*, 559.
7. M. Florea and W. M. Nau, *Angew. Chem. Int. Ed.*, **2011**, *50*, 9338.
8. I. W. Wyman and D. H. Macartney, *Org. Biomol. Chem.* **2008**, *6*, 1796.
9. R. Wang, B. C. MacGillivray, and D. H. Macartney, *Dalton Trans.*, **2009**, 3584.
10. W. J. Simpson, *FEMS Microbiol. Lett.*, **1992**, *90*, 197.
11. R. Tanaka and N. Hirayama, *Anal. Sci.*, **2008**, *24*, 163.
12. L. Jimenez and M. Chiang, *Am. J. Inf. Cont.*, **2005**, *33*, 41.
13. K. W. Yip, X. Mao, P. Y. B. Au, D. W. Hedley, S. Chow, S. Dalili, J. D. Mocanu, C. Bastianutto, A. Schimmer, and F. F. Liu, *Clin. Cancer Res.*, **2006**, *12*, 5557.
14. D. H. Macartney, *Isr. J. Chem.*, **2011**, *51*, 600.
15. J.-S. Yu, F.-G. Wu, Y. Zhou, Y.-Z. Zheng and Z.-W. Yu, *Phys. Chem. Chem. Phys.*, **2012**, *14*, 8506.
16. A. Georgalas, *J. Cosmet. Sci.*, **2004**, *55*, S207.
17. A.J. J. Wood, *New Engl. J. Med.*, **1996**, *334*, 575.
18. T. Strack, *Drugs Today*, **2008**, *44*, 303.
19. K. S. Lim and P. C. A. Kam, *Anaesth. Intensive Care*, **2008**, *36*, 502.

20. J. A. Chawner and P. Gilbert, *Int. J. Pharm.*, **1989**, 55, 209.
21. (a) F. Yang and D. V. Dearden, *Supramol. Chem.*, **2011**, 23, 53. (b) F. Yang and D. V. Dearden, *Isr. J. Chem.*, **2011**, 51, 551.
22. P.J. Pentikainen, *Int. J. Clin. Pharmacol. Ther. Toxicol.*, **1986**, 24, 213.
23. I. W. Wyman, Ph.D. Thesis, Queen's University, 2010.
24. M. Sands, M. A. Kron and R. B. Brown, *Rev. Infect. Dis.*, **1985**, 7, 625.
25. J. Pépin and H. Méda, *Antimicrob. Drug Resist.*, **2009**, 76, 1113.
26. M. Campbell, R. J. Prankerd, A. S. Davie, and W. N. Charman, *J. Pharm. Pharmacol.*, **2004**, 56, 1327.
27. M. Mares-Guia and E. Shaw, *J. Biol. Chem.*, **1965**, 240, 1579.
28. R. Talhout and J. B. F. N. Engberts, *Eur. J. Biochem.*, **2001**, 268, 1554.
29. S. A. Evans, S. T. Olson and J. D. Shore, *J. Biol. Chem.*, **1982**, 257, 3014.
30. S. G. De-Simone, C. Correa-Netto, O. A. C. Antunes, R. B. De-Alencastro and F. P. Silva, Jr. *J. Chromatography B.*, **2005**, 822, 1.
31. R. Gavara, V. Petrov and F. Pina, *Photochem. Photobiol. Sci.*, **2010**, 9, 298.
32. L. Giestas, F. Folgosa, J. C. Lima, A. J. Parola and F. Pina, *Eur. J. Org. Chem.*, **2005**, 4187.
33. M. Kueny-Stotz, S. Chassaing, R. Brouillard, M. Nielsen and M. Goeldner, *Bioorg. Med. Chem. Lett.*, **2008**, 18, 4864.
34. A.M. Diniz, C. Pinheiro, V. Petrov, A.J. Parola and F. Pina, *Chem. Eur. J.*, **2011**, 17, 6359.
35. V. Sindelar, S. Silvi and A. E. Kaifer, *Chem. Commun.*, **2006**, 2185.